

**TECTONIC EVOLUTION OF THE
SOUTHERN PART OF
THE SERGIPANO FOLD BELT,
NORTHEASTERN BRAZIL**

by

Luiz Jose Homem D'el-Rey Silva

A thesis submitted for the degree
of Doctor of Philosophy
of the University of London

September, 1992

Royal Holloway and Bedford New College,
Department of Geology,
Egham Hill, Egham-Surrey,
TW20 OEX, UK

Abstract

This thesis is a stratigraphic and structural analysis of the Itabaiana Dome Area in the southern part of the Sergipano Fold Belt, northeastern Brasil. The ESE-WNW trending Sergipano Fold Belt is a subgreenschist to amphibolite grade metavolcano-sedimentary wedge polydeformed during the 700-600Ma Brasiliano-Pan-African orogeny. Crystalline basement gneiss domes mantled by metasediments are found within the fold belt which lies between the Sao Francisco Craton in the south and the Pernambuco-Alagoas Massif to the north. An area of 4000km² surrounding the Itabaiana and Simao Dias gneiss domes was mapped at 1:50,000 scale.

A new stratigraphy has been established for this part of the Sergipano Fold Belt. Two major Middle to Late Proterozoic sedimentary cycles have been recognised, each with a basal siliciclastic megasequence overlain by a carbonate megasequence. Four main stratigraphic groups have been established. The ≈330m thick Estancia Group consisting of metasandstones, pelites, and metacarbonates unconformably overlies the crystalline rocks of the craton and is laterally equivalent to the ≈200-1100m thick Miaba Group which consists of the Itabaiana quartzites; the Ribeirópolis phyllites, pebbly phyllites, diamictites and metavolcanics; and the Jacoca metacarbonates. The Miaba Group is unconformably deposited around the gneiss domes. The ≈700m thick Lagarto Group has been identified as a new lithotectonic element in the southern part of the Sergipano Fold Belt. This group is a coarsening-upward siliciclastic sequence that overlies the older rocks of both the craton and the fold belt. It consists of the Lagarto-Palmares mud stones, silts tones, sandstones and lithic wackes together with the Jacare metasiltites and the Frei Paulo phyllites, metarhythmites, metagreywackes, minor metacarbonates and metavolcanics. The ≈200-2000m thick Vaza Barns Group, consisting of the Palestina diamictites and the Olhos D'água metacarbonates, unconformably overlies the older rocks to the north of the Itaporanga fault.

The thickest Palestina diamictites occur in a WNW-ESE trending, fault-bounded depocentre which also received relatively deep water accumulations of the other formations. The siliciclastics generally thin towards the basement gneiss domes, whereas the carbonates thin away from the domes into the diamictite trough. The thickness and facies distributions of these units indicate tectonically controlled sedimentation, with basement highs supplying sediments from both the southern and northern margins of an asymmetric basin.

The structure of the Itabaiana Dome Area is dominated by shallowly plunging, SSW vergent F₁ and F₂ recumbent to inclined folds and steep D₂ thrust faults. D₁ is characterised by WNW-ESE trending, SW vergent, nappe-like folds associated with a penetrative layer-parallel foliation. D₂ is characterised by co-axial, up-right, tight and WNW-ESE trending folds, associated with penetrative axial surface foliations, lineations and high-angle, SSW vergent, oblique slip thrust faults. These regional thrust faults are probably inverted extensional faults. Late-stage, orogen-parallel movement generated transverse F₃ kink-style folding and rotation of fault bounded domains.

Regional lithostructural correlations between the southern and northern parts of the Sergipano Fold Belt indicate that the Sergipano Basin may be interpreted to have

been a WNW-ESE striking half graben that deepened towards the ENE. It was infilled by miogeoclinal-eugeoclinal sediments and evolved axially into a small oceanic basin, termed the Caninde sea, in its northeastern part. The preferred tectonic model for the evolution of the Sergipano Basin is that of a linked system of listric extensional faults that merged into a basal detachment with a ramp-flat geometry. Inversion of this extensional fault system due to oblique collision of the Borborema Province to the north with the São Francisco Craton to the south, produced sinistral transpression of the sedimentary wedge of the Sergipano Basin and resulted in the Sergipano Fold Belt.

The tectonic and stratigraphic evolution of the Sergipano Fold Belt is similar to that found in other Brasiliano and Pan-African mobile belts. In particular the correlation of stratigraphy from the craton into the fold belt, the interpretation of sedimentation controlled by extensional tectonics suggest a model of basin formation by extension of the craton margins, development of pericratonic and small ocean basins which were then deformed by collision of continental fragments against the craton margins. This model agrees with those postulated of a supercontinent that evolved by fragmentation and amalgamation along long-lived zones of lithosphere weakness throughout the Proterozoic.

Dedication

I dedicate this PhD thesis to my family, my wife Irene, my daughter Manuela, and to my sons Alexandre and Henrique. The support and criticism that I received from my family were fundamental in enabling me to complete this thesis. In particular the loyal and unfailing support of my wife Irene was the pillar upon which I leant throughout this research programme. For them, and for everyone who helped me in ways large and small I ask God's blessing.

Acknowledgements

This thesis has only been made possible because of the financial help I have been given from different funding agencies and people, and because of the fundamental assistance that I have received from many persons, both in Brazil and in Britain. To all of those listed below (and to those I may have inadvertently omitted from the list), I would like to express my most sincere and heartfelt thanks.

Thanks go to -

The Conselho Nacional de Desenvolvimento Científico e Tecnológico (CNPq, Brazil), for the financial support since the beginning of the field work, including the payment of part of the geophysical work, through the grants 402636/87.2/GL/FV, 200525/88-3GL, and 400865/90-4/GL/FV/PQ;

Caraíba Mineração, Departamento Nacional da Produção Mineral (DNPM, Brazil) and CPRM for the aid with the geophysical work and additional support for the field work;

The Busk-Howell Scholarship Fund (England) for additional financial help at the beginning of my work in Britain.

I must particularly emphasise my very special thanks to:

My wife Irene and my family for their support.

Professor Ken McClay, who acted as a real supervisor up to the end. His supervision throughout the research and patient correction of the English, together with his international level persistent criticism were fundamental for the completion of this PhD thesis. I always will be proud to have been his student.

Professor. A.J. Smith and D. Blundell, heads of the Geology Department of Royal Holloway and Bedford New College, University of London during my research, for their moral support in critical moments.

Dr. Ian Davison (RHBNC) for his advice in the choice of such an exciting area for a PhD dissertation, and for his advice since the very early beginning in Brazil.

Dr. Emanuel Ferraz Jardim de Sá (UFRN, Brazil) who introduced me to the geology of the Sergipano Fold Belt.

Dr. Antonio Carlos Motta (CPRM) for his detailed analysis of the geophysical data of the Itabaiana Dome Area, and for many fruitful discussions.

Dr. Hideo Takagi (WASEDA University, Japan) for his very teaching, and for discussions about my many thin sections, under the pressure of my enthusiasm.

Mr. Marcio Afonso Lima de Brito and his wife, Mrs. Giolanda Muniz, my solicitors in Brazil, for their support and assistance with my affairs in Brazil.

Geologist Jose Genario de Oliveira and mining engineer José Tarcisio de Mattos Menezes (Mineração Caraíba, Brazil) for their help in dealing with early drawings and particularly for their permanent friendship.

Geologist Jose Julio Carneiro and mining engineer Orlando Generoso (Brazil) for providing a car for field work in Brazil, in 1990, and for their friendship.

Prof. Gilles O. Allard (Georgia University, USA) for the letters, comments and key references.

My brother and second father Jose Homem D'El-Rey Silva, who gave me support so that I could get my degree in geology (1967-1971), and gave me his love and attention in my hardest moments here in Britain, through many and expensive international phone calls. My sister-in-law Ilma O.Lopes, who helped in the corrections of some of the chapters and also gave me her moral support.

My sincere thanks are also due to:

Drs. J. Alvarez-Marron, G.J. Nichols, C. Parkinson, Gu Lianxing, geologists T. Dooley, R. Symms, T. Liverton, D. Brown, W. Wilks and M. White, for providing literature and/or very fruitful discussions during my research. Special thanks are also due to all of the support staff at RHBNC and in particular Mrs. A. Harper, Mr. K.D'Souza, Ms. S. Muir, Mr. M Longbottom, Mr. N. Holloway, Mr. I. Gill, Mr. K.W. Stephens, Ms. J. Brown, Ms. J. Pickard and Ms. A. Lyon, for their assistance throughout my time at RHBNC. Dr. J.R. Keller, Dr. I. Fitzsimons, Mr. R. Symms, Mr.T.Liverton, and Dr. Peter Thomas, my neighbour in Egham, are thanked for their patient correction of various parts of the thesis.

Mr. Pedro Dias dos Santos and his terrific family who run the Hotel Irmaos Vasconcelos, Lagarto-Sergipe, Brazil, where I was extremely well treated, are thanked for their generosity and hospitahty. Mr. Gilson Pimenta, driver from Caraiba Mineraçãõ shared as a friend many moments during field work in Brazil.

Thanks are also due to:

Geologist J.A.R. Mello (CVRD), Dr. J. Karfunkel (UFMG), Dr. E.F. Jardim de Sa (UFRN), Dr. B.B. de Brito Neves (USP), Prof. R.A. Fuck (UNB), Drs. J. Barbosa, A. Misi, S. Fujimori, I. McReath, P. Sabate (UFBa), geologists J. Mascarenhas and R.Wilson (CBPM), geologists R.A. dos Santos and M.A. da Silva Filho (CPRM), Dr. I. Castro (Petrobras), all in Brazil, for providing literature.

Geologists G. Bacelar, J.C. Goncalves, CO. Berbet, J.C. Santana, and J.D. de Souza (DNPM-CPRM) for help in Brazil, and Drs. A. Pope, N. Way, Dr. J. Dobson, Dr. C. Dart for help in the first days in Britain.

C O N T E N T S

Abstract	ii
Dedication	iv
Acknowledgments	v
List of Figures	xj
List of Tables	xv
List of Appendices	xv
Chapter 1 - Introduction and the area of study	1
1.1 -Introduction	1
1.2-Regional geology of the Sergipano Fold Belt	1
1.3 -Aims of this thesis	6
1.4 -Methodology	6
1.5-Previous research	8
1.6-Structure of this thesis	9
Chapter 2. Regional geology of the Sergipano Fold Belt	10
2.1 -Aims	10
2.2 -Introduction	10
2.2.1 -Regional setting	10
2.2.2 - The Sergipano Fold Belt	10
2.3 -Litho-stratigraphic units of the northern part of the Sergipano Fold Belt	14
2.4 -Stratigraphy of the southern part of the Sergipano Fold Belt	17
2.4.1 -The Estância Group	17
2.4.2 - The Miaba Group.....	17
2.4.3 - The Vaza Barris Group	20
2.5-Structures and metamorphism	21
2.5.1 -Introduction	21
2.5.2 - Structural and metamorphic partitioning	22
2.6 -Geochronology	24
2.6.1 -Age of sedimentation	24
2.6.2 - Age of deformation and metamorphism	24
2.7-Geophysics of the Sergipano Fold Belt	25
2.8-Tectonic evolution	25
2.9 - Plate Tectonic setting of the Sergipano Fold Belt	29
2.10- Discussion	32
2.11- Conclusions	34
Chapter 3 - Stratigraphy of the southern part of the Sergipano Fold Belt	35
3.1 -Aims	35

3.2 -Introduction	35
3.3 - Stratigraphy of the Itabaiana Dome Area	37
3.3.1-The crystalline basement	45
3.3.2 - The basement-cover contact	45
3.3.3 - The Miaba Group	47
The Itabaiana Formation (P€ I)	47
The Ribeirópolis Formation (P€ R)	49
The Jacoca Formation (P€ Ja)	52
3.3.4-The Lagarto Group	55
The Lagarto-Palmares Formation (P€ LP)	55
The Jacaré Formation (P€ JeJ)	55
The Frei Paulo Formation (P€FP, FP1, FP3)	62
3.3.5 - The Vaza Barris Group	64
The Palestina Formation (P€P)	64
The Olhos D'agua Formation (P€ OA)	69
3.4 - Lithofacies and depositional environments	69
3.4.1 - Lithofacies distribution and paleogeography	69
3.4.2 - The Itabaiana-Ribeirópolis sedimentation	71
3.4.3 - The Lagarto Group sedimentation	72
3.4.4 - The diamictites	73
3.4.5 - The carbonate sedimentation	73
3.5 - Stratigraphy of the southern part of the Sergipano Fold Belt	77
3.6-Discussion: tectonic controls of sedimentation	77
3.7 -The origin of the Lagarto Group	70
3.8 -Conclusions	70

Chapter 4 - Structures and metamorphism of the Itabaiana Dome

Area	81
4.1 -Introduction	81
4.2 - The structures of the Itabaiana Dome Area - introduction	81
4.2.1 - Basement structures	83
4.2.2 - Summary of the deformational events and structural domains	83
4.3 -The D ₁ deformation	85
4.4 -The D ₂ deformation	89
4.4.1 - F ₂ folds and structural elements	89
4.4.2 - The regional faults	92
4.4.3 - D ₂ deformation fabrics	98
4.4.4 - Strain analyses	100
4.4.5 - Syn-D ₂ vein systems	104
4.4.6 - Interfoliation slip far from the fault zones	108
4.5 -The D ₃ deformation	108
4.6-The structural domains	116
4.6.1 -The cratonic domain	117

4.6.2 -The regional and Simão Dias domains	117
4.6.3 - The Itabaiana domain	121
4.6.4 - The west and east domains	123
4.7 -The Capitão farm outcrop	125
4.8 - Metamorphism in the Itabaiana Dome Area	12§
4.9 -Discussion and conclusions	129
Chapter 5 - Geophysics of the Itabaiana Dome Area	133
5.1 -Introduction	133
5.2 - Summary of the geophysical and density data of the Itabaiana Dome Area .	133
5.2.1 - Geophysical data	133
5.2.2 - Density data	135
5.3 -Geophysical domains in the southeastern Sergipano Fold Belt	135
5.3.1 -Domain A	137
5.3.2 - Domain B	137
5.3.3 - Domain C	137
5.3.4 - Domain D.....	138
5.3.5 - Domain E	138
5.3.6 - Domain F	139
5.3.7 - The basement domains and the radiometric data	139
5.4 - Aeromagnetic signature of the regional faults in the Itabaiana Dome Area ..	139
5.5 -Geophysical sections in the Itabaiana Dome Area	141
5.5.1 -The geophysical section XX'	141
5.5.2 - The geophysical section YY'	142
5.5.3-The geophysical section ZZ'Z"	142
5.6 -Conclusions	143
Chapter 6 - Geological evolution of the southern part of the	
Sergipano Fold Belt	145
6.1 -Introduction	145
6.2 -Geological evolution of the Itabaiana Dome Area	145
6.2.1 - Introduction	145
6.2.2 - Stratigraphy of the Itabaiana Dome Area	145
6.2.3 - Depositional environments, facies and thickness distribution	150
Siliciclastic sedimentation	150
Carbonate sedimentation	151
Thickness variations	151
6.2.4 - Basin evolution: A model for the Itabaiana Dome Area	152
6.2.5 - Structural and metamorphic evolution of the Itabaiana Dome Area	156
Structural evolution	156
<i>Dj Deformation</i>	157

<i>Dj Deformation</i>	157
<i>D3 Deformation</i>	157
<i>Evolution of the basement domes-</i>	159
Metamorphic evolution	161
6.3 - Tectonic evolution of the southern part of the Sergipano Fold Belt, and of the whole Sergipano Fold Belt	161
6.3.1 -Introduction	161
6.3.2 - Lithostratigraphy of the southern part of the Sergipano Fold Belt	162
6.3.3 - Structure of the southern part of the Sergipano Fold Belt	164
6.3.4 - Structural and lithostratigraphic interpretations	164
6.3.5 - Lithostructural continuity in the Sergipano Fold Belt	167
6.3.6 -Tectonic evolution of the Sergipano Fold Belt	170
Tectonic Domains	170
Thrust belt and foreland basin models	172
Tectonic model	172
The São Francisco Craton and the Sergipano Fold Belt	175
The opening and closure of the Sergipano Basin	177
6.4 - Implications for Proterozoic Crustal Evolution	180
6.4.1 -Introduction	180
6.4.2 - Late Proterozoic sequence stratigraphy	181
Palestina Diamictites	185
6.4.3 -Late Proterozoic tectonic evolution	188
6.4.4 - Craton-Mobile Belt evolution	191
6.4.5 - Implications for Proterozoic orogens and Plate Tectonics	191
Chapter 7 - Conclusions	198
References	202
Appendix	226

LIST OF FIGURES

Figure 1.1 - The Sergipano Fold Belt and the main structural provinces of Brazil	2
Figure 1.2 - Simplified geological map with the Sergipano Fold Belt, the São Francisco Craton and the Borborema Province	4
Figure 1.3 - Simplified geological map of the Sergipano Fold Belt. Introduces the main lithotectonic units and the thesis area	5
Figure 1.4 - The main features of the study area	7
Figure 2.1 - Geological map of northeastern Brazil	11
Figure 2.2 - The main tectonic units firstly described in the Sergipano Fold Belt (the Propria geosyncline)	13
Figure 2.3 - Geological map of the Sergipano Fold Belt. Highlights the area of this thesis	15
Figure 2.4 - Simplified geological map of the southern part of the Sergipano Fold Belt, including this thesis area	18
Figure 2.5 - Summary of stratigraphic columns of the Estância, Miaba and Vaza Barris Groups of the southern part of the Sergipano Fold Belt,	19
Figure 2.6 - The main structural interpretations published for the Sergipano Fold Belt	23
Figure 2.7 - The first analysis of geophysical data of the Sergipano Fold Belt	26
Figure 2.8 - Interpretations of more detailed gravity and magnetic data of the Sergipano Fold Belt	27
Figure 2.9 - Diagrammatic interpretation of the undeformed Sergipano basin and its sedimentary infilling	28
Figure 2.10 - The published models of tectonic evolution of the Sergipano Fold Belt	30
Figure 2.11 - Plate tectonic setting of the Sergipano Fold Belt	31
Figure 2.12 - Cartoons summarising the geology and models for tectonic evolution of the Sergipano Fold Belt	33
Figure 3.1 - 1:100,000 scale geological map of the Itabaiana Dome Area. Contains the geological data collected during this research (enclosure)	
Figure 3.1 - Summary geological map of the Itabaiana Dome Area	36
Figure 3.2 - Panoramic view of the Miaba range, one of the most impressive quartzitic ranges that surround the Itabaiana dome	38
Figure 3.3 - Summary stratigraphy of the Itabaiana Dome Area. Stratigraphic column erected for the study area	39
Figure 3.4 - Summary of the stratigraphic columns. Location and summary of the 12 stratigraphic columns constructed in the study area	40
Figure 3.5 - Stratigraphic section AA', across the western margin of the Simão Dias dome	41
Figure 3.6 - Stratigraphic section EE' across the Miaba Range and Vaza Barris river valley.	42

Figure 3.7 - Strati graphic section GG' across the northern part of the Itabaiana dome	43
Figure 3.8 - Strati graphic section JJ' across the eastern part of the Itabaiana dome	44
Figure 3.9 - The crystalline basement. Photographs of the Itabaiana gneiss, and the basement-cover contact.....	46
Figure 3.10 - The Itabaiana Formation. Photographs of the main lithofacies and sedimentary structures	48
Figure 3.11 - The Ribeirópolis Formation. Photographs of the main lithofacies and sedimentary structures	51
Figure 3.12 - The Jacoca Formation. Photograph with the main lithofacies of this carbonate formation	53
Figure 3.13 - Photograph of the main sedimentary structure in the Jacoca Formation.....	54
Figure 3.14 - Stratigraphic section of the upper part of the Lagarto Group at its type locality.	56
Figure 3.15 - The Lagarto-Palmares Formation. Photographs of the lithofacies and sedimentary structures	57
Figure 3.16 - The Jacaré and Frei Paulo Formations. Photographs of the Jacaré metasilts and the main lithologies of the Frei Paulo Formation.....	63
Figure 3.17 - Photographs of more lithofacies of the Frei Paulo Formation.....	65
Figure 3.18 - The Palestina Formation. Photographs of the main aspects of this diamictite formation.....	67
Figure 3.19 - The Olhos D'agua Formation. Photographs of the main lithofacies and sedimentary structures	68
Figure 3.20 - Summary map of distribution of facies and thicknesses in the Itabaiana Dome Area, and interpretative block diagram of the undeformed basin.....	70
Figure 3.21 - New tectono-stratigraphic framework of the southern part of the Sergipano Fold Belt, erected as result of this research	75
Figure 3.22 - Photomontage to show a probably tectonically controlled thickness variation in a small basin to the south of the mapped area	76
Figure 4.1 - Summary lithostructural map of the Itabaiana Dome Area, with location of the structural cross section lines of Figure 4.20.....	82
Figure 4.2 -Stereographic plot of the D_1, D_2 structures for the deformed structural domains of the study area	86
Figure 4.3 -Summary map showing the six structural domains, and the summary of D_2 linear structures of the Itabaiana Dome Area	87
Figure 4.4 - Photographs and line drawing of D_j deformation structures in the Itabaiana Dome area	88
Figure 4.5 - Photographs of F_2 folds in metasediments and gneisses	91
Figure 4.6 - Photographs showing the S_2 pressure solution and slaty cleavage foliations	93

Figure 4.7 - Photographs of the Lj intersection, pencil, and mylonitic lineations associated with F ₂ folds.....	94
Figure 4.8 - Photographs of the structural relationships along the regional faults in the Itabaiana Dome Area	96
Figure 4.9 - Photographs showing syn-D ₂ deformation fabrics.....	99
Figure 4.10 - Photographs of elongated clasts in the XZ, XY and YZ planes in outcrops of the Palestina diamictites	101
Figure 4.11 - Photograph of thin sections parallel to XZ and YZ illustrating the clasts and clast+tail systems in Palestina diamictites.....	102
Figure 4.12 - Plot of the finite strain ellipsoids calculated for several outcrops of the Palestina diamictites in Flinn and Hsu diagrams	103
Figure 4.13 - Photographs of syn-D ₂ veins and synthetic shear fractures and shear bands in the Itabaiana Dome Area.....	107
Figure 4.14 - 3-D diagram and photographs illustrating the inter-foliation slip in metasediments far from the fault zones	109
Figure 4.15 - Subvertical, synthetic extensional shear bands indicating local dextral strike-slip movements in the study area.....	110
Figure 4.16 - Photographs of the D ₃ structures in the study Area.....	111
Figure 4.17 - Stereographic plot of the D ₃ structural elements for the deformed structural domains in the study area	112
Figure 4.18 - F ₁ x F ₂ x F ₃ interference pattern. Photographs showing the interference pattern, and the S ₁ /S ₂ interfoliation slip	113
Figure 4.19 - Photographs and line drawings of late-stage thrusts in the regional structural domain	115
Figure 4.20 - AB, CD, EF structural cross sections across the regional domain, and the Simão Dias and Itabaiana domes..... (enclosure)	
Figure 4.21 - Summary of the AB and EF (Fig. 4.20), with detailed structural relationships in the northern and southern margins of the Itabaiana dome	118
Figure 4.22 - Photographs of the structural relationships in the southern margin of the Itabaiana dome	122
Figure 4.23 - Photographs of the sheared Itabaiana/Ribeirópolis contact, in the western side of the Itabaiana dome	124
Figure 4.24 - Detailed structural relationships in the Capitão farm outcrop.	126
Figure 5.1 - Geological map of the Itabaiana Dome Area with the location of the geophysical section lines..... (enclosure)	
Figure 5.2 - Location of the geophysical section lines in the study area and in the area of the Carira Project	134
Figure 5.3 - Aeromagnetic map and geophysical domains in the southeastern pan of the Sergipano Fold Belt	(enclosure)
Figure 5.4 - Radiometric map and geophysical domains for the southeastern part of the Sergipano Fold Belt	(enclosure)

Figure 5.5 - Geophysical signature of the regional faults in the southeastern part of the Sergipano Fold Belt	140
Figure 5.6 - Geophysical section XX'(enclosure)	
Figure 5.7 - Geophysical section YY' (enclosure)	
Figure 5.8 - Geophysical section ZZ'Z"(enclosure)	
Figure 6.1 - Summary lithostructural map of the Itabaiana Dome Area with more detailed lithofacies.....	146
Figure 6.2 -Summary map displaying the major tectonic elements in the Itabaiana Dome Area.....	147
Figure 6.3 - Sequence stratigraphy of the southern part of the Sergipano Fold Belt, resulting from this research	149
Figure 6.4 - Basin opening and infilling. A model for the deposition of Cycle I in the Itabaiana Dome Area.....	153
Figure 6.5 - Basin opening and infilling. A model for the deposition of Cycle II in the Itabaiana Dome Area	154
Figure 6.6 - Summary of the D ₁ D ₃ deformational and metamorphic events in the Itabaiana Dome Area.....	158
Figure 6.7 - Sequence of diagrams to explain the evolution of the Itabaiana gneissic dome.....	160
Figure 6.8 - Geological map of the Itabaiana-Carira area to the east of the 38°W meridian. Combines this study with previously published maps.....	163
Figure 6.9 - Structural cross sections ABB' and EFF' across the Itabaiana-Carira area. Combines the cross sections of Figure 4.20 with data from the literature	165
Figure 6.10 - Diagrams to explain structurally the new lithostratigraphic interpretations in the Itabaiana-Carira area	168
Figure 6.11 - Summary map displaying the Precambrian Uthotectonic units of the Sergipano Fold Belt.....	171
Figure 6.12 - Model for the structural evolution of the Sergipano Fold Belt with no foreland basin.....	174
Figure 6.13 - Sketch map of the São Francisco Craton, showing the surrounding fold belts and areas of pre Brasiliano syndepositional extension.....	176
Figure 6.14 - A model for the opening and closure of the asymmetric Sergipano Basin.....	178
Figure 6.15 - Craton-belt system and the Late Proterozoic Bambui Group sedimentation of the African and South American.....	182
Figure 6.16 - Geological map of the São Francisco Craton indicating the progradation of siliciclastic sequences from the centre of the craton onto lower carbonate megasequences of the craton margins.....	183
Figure 6.17 - Sketch map showing the diamictite formations around the São Francisco, West Congo and Kalahari Cratons.....	187
Figure 6.18 - Cartoon illustrating the opening of a narrow oceanic basin in the eastern part of the Sergipano Basin	190

Figure 6.19- Late Proterozoic and Mesozoic rift systems, with triple junctions, aulachogen-like grabens and internal cratonic fragments.....	194
Figure 6.20- The relevant tectonic elements around the São Francisco Craton, for discussion of the implications on Plate Tectonics theory.	195

LIST OF TABLES

Table 3.1 -Petrography of the Lagarto group sandstones	61
Table 4.1 - Symbols and the summary meaning of the main structures in the Itabaiana Dome Area.....	84
Table 4.2 -Summary of the harmonic means and the parametres used for the plot of the Flinn diagrams of Figures 4.12 C and D.....	105
Table 5.1 -Summary of the density of rocks in the Itabaiana Dome Area.....	136
Table 6.1 -Comparative stratigraphies of the cratonic sediments of the fold belts around the São Francisco Craton.....	184
Table 6.2 -Comparative stratigraphies of the Sergipano, West Congo and Damara Fold Belts.....	186
Table 6.3 - Summary of the tectonic evolution of the Sergipano Fold Belt.	192

LIST OF APPENDICES

Appendix A1.1 - Reduced geological map of the Itabaiana area with the location of the 12 stratigraphic sections.....	227
Appendix A1.2 - Stratigraphic section BB' across the west of the Simão Dias dome	228
Appendix A1.3 - Stratigraphic section CC across the west of the Simão Dias dome	229
Appendix A1.4 - Stratigraphic section DD' across the southwestern margin of the Itabaiana dome	230
Appendix A1.5 - Stratigraphic section FF across the western margin of the Itabaiana dome	231
Appendix A1.6 - Stratigraphic section HH' across the northeast of the Itabaiana dome with description of the lithologies and sedimentary structures. ...	232
Appendix A1.7 - Stratigraphic section II' across the northeast of the Itabaiana dome	233
Appendix A1.8 - Stratigraphic section KK' across the southern margin of the Itabaiana dome	234
Appendix A2.1 - Measurement of axis of clasts of the Palestina diamictites in surfaces nearly parallel to XY and YZ for strain analysis	235
Appendix A2.2 - Axial ratio of clasts and clast+tail of Palestina diamictites in surfaces nearly parallel to XZ and YZ for strain analysis	237

Appendix A2.3 - Axial ratio of clasts and clast+tail of Palestina pebbly phyllites in 38 thin sections parallel to XZ and YZ for strain analysis	241
Appendix A3.1 - Observed and calculated gravity and magnetic data along the XX' section line.....	254
Appendix A3.2 - Observed and calculated gravity and magnetic data along the YY' section line.	255
Appendix A3.3 - Observed and calculated gravity and magnetic data along the ZZ' section line.	256
Appendix A3.4 - Density of the rocks in the Itabaiana Dome Area	257

Chapter 1 - Introduction and the area of study

1.1 - Introduction

This thesis is an analysis of the tectonic and stratigraphic evolution of the southern part of the Sergipano Fold Belt, located in the Sergipe and Bahia States, northeastern Brazil. The Sergipano Fold Belt forms part of the Borborema Province, at its southern border with the Sao Francisco Craton (Fig. 1.1; Almeida et al. 1977).

The polydeformed and poly metamorphosed Late Proterozoic Sergipano Fold Belt trends ESE-WNW and its tectonic evolution is ascribed to the 900-600Ma old Brasiliano orogeny (Brito Neves & Cordani 1973; Brito Neves et al. 1977a). The southern part of this belt consists of folded and thrust faulted low- to mid-green schist facies metasediments (quartzites, phyllites, diamictites and carbonates) overlying a 2100-1800Ma old granite-gneiss basement. This basement crops out in two structural domes, the Itabaiana and Simão Dias domes, which are mantled by the metasediments.

This thesis is principally concerned with the structural and stratigraphic relationships and Brasiliano-age geological evolution of these cover and basement rocks.

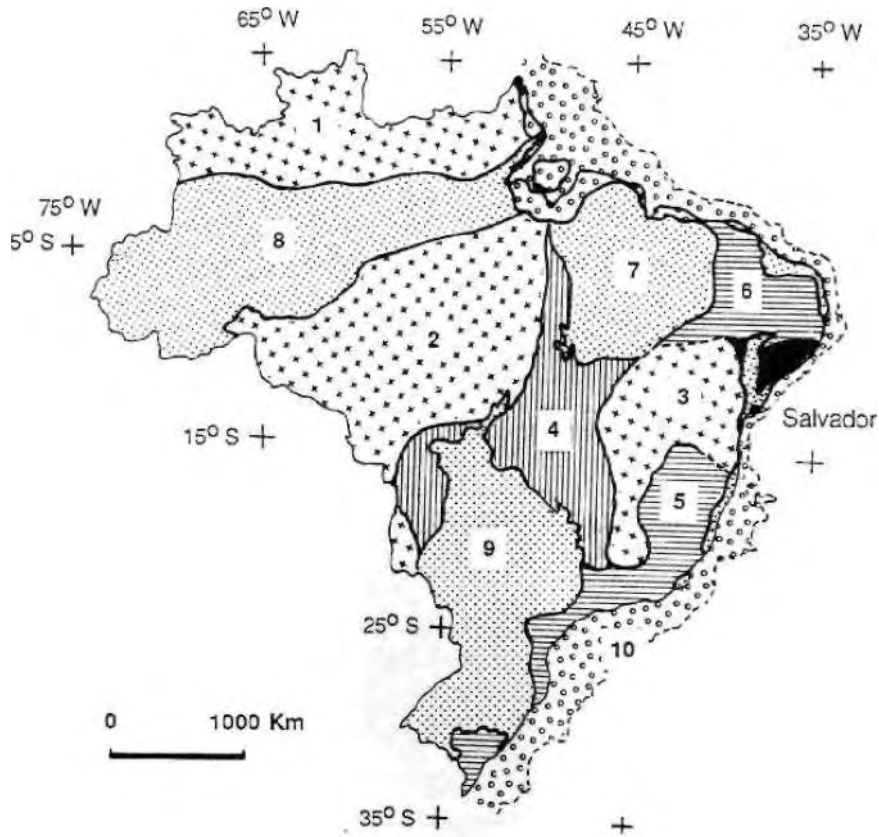
1.2 - Regional geology of the Sergipano Fold Belt

The Borborema Province (Fig. 1.2) is a mosaic of Archean to Early Proterozoic granitic, gneissic and migmatitic terranes with several NE-SW, E-W and WNW-ESE striking mobile belts. The province was consolidated during the 900-600 Ma Brasiliano thermo-tectonic cycle, which was also characterised by intense granite emplacement (Brito Neves 1975; Santos & Brito Neves 1984).

The structural grain of the Borborema Province is cross-cut by two E-W striking shear zones known as the Patos and Pernambuco lineaments. The age of these crustal-scale lineaments is not fully determined, but the Patos Shear Zone has been associated with the 700-500Ma old Brasiliano tectonic evolution of the Serido Fold Belt (Corsini et al. 1991) and the Pernambuco Shear Zone has been associated with Brasiliano cycle reactivation of the Transamazonian-age Riacho do Pontal Fold Belt (Fig. 1.2; Gomes 1990).

The Pernambuco-Alagoas Massif lies to the south of the Pernambuco Shear Zone. The Sergipano Fold Belt lies further south, between this massif and the Sao Francisco Craton.

The Sao Francisco Craton was fully consolidated by the end of the 2100-1800 Ma old Transamazonian tectonic cycle and is the largest surface extent of Archean rocks in Brazil (Mascarenhas et al. 1984; Teixeira & Figueiredo 1991). It consists largely of upper amphibolite to granulite facies metamorphic terranes, subsequently affected by granite emplacement and large-scale fracturing during the Brasiliano event. The Sao Francisco Craton is surrounded by five fold belts which display a centreward convergence of tectonic transport direction (Fig. 1.2; Mascarenhas et al. 1984).



Structural Provinces of Brazil



Figure 1.1 - The Sergipano Fold Belt (in black) and the main structural provinces of Brazil. (modified from Almeida et al. 1977).

The triangular-shaped Sergipano Fold Belt is transected by several ESE-WNW trending thrust and strike-slip faults (Fig. 1.3). The belt is 200km wide along its boundary with the Sergipe-Alagoas Mesozoic Basin, and stretches for about 400km to its western extremity (Brito Neves et al. 1977 a). It is cross-cut by the N-S to SW-NE trending Tucano-Jatoba Mesozoic basin, and is limited to the north by the Pernambuco Shear Zone.

The Sergipano Fold Belt is comprised of three main domains that define three major lithotectonic assemblages: the Estância, Miaba-Vaza Barris and Macururê Groups (from south to north in Fig. 1.3). These groups were interpreted by Silva Filho et al. (1978 a & b) as cratonic cover, and the fault-bounded miogeocline and eugeocline, respectively, whereas Santos et al. (1988) and Davison & Santos (1989) considered them to represent cratonic, supra, and mid- to infra-crustal structural levels. The Sao Miguel do Ateixo fault separates the southern and northern parts of the Sergipano Fold Belt (Davison & Santos 1989).

The northern part of the belt corresponds to the Macurure Group and comprises polydeformed, greenschist to upper amphibolite facies siliciclastic and carbonate metasediments, migmatites, acid and basic volcanics, and basic-ultrabasic intrusive rocks, all intruded by a series of 850-600Ma syn- and post-tectonic granites.

The southern part of the belt consists of the polydeformed, greenschist facies siliciclastic and carbonate metasediments of the Miaba and Vaza Barris Groups, and the almost undeformed and non-metamorphosed cratonic sediments situated to the south of the Itaporanga fault (Estancia Group).

The crystalline basement occurs as inliers in both the southern and northern parts of the belt. The inliers in the southern part are the Itabaiana and Simao Dias domes (within the Itabaiana Dome Area, Fig. 1.3), and a gneissic structure which is enclosed in the western corner of the belt (Brito Neves & Cordani 1973; Brito Neves et al. 1977 a; Gava et al. 1983).

The structure of the Sergipano Fold Belt is characterised by penetrative fold and foliation development, with associated WNW-ESE striking thrust and strike-slip faults. Metamorphism ranges from sub-greenschist to greenschist facies in the southern domain, and from greenschist to amphibolite facies in the northern part of the belt (Jardim de Sa' et al. 1981, 1986; Brito Neves et al. 1987a & b; Santos et al. 1988; Davison & Santos 1989).

The Sergipano Fold Belt has been mapped at 1:250,000 scale (Gava et al. 1983). In addition, its central area has been mapped at 1:100,000 scale (see the Carira Project, Fig. 1.4 A), and part of Itabaiana Dome Area has been mapped at 1:40,000 scale (Humphrey & Allard 1967, 1969).

The detailed sedimentary, stratigraphic and structural relationships, and the tectonic evolution of the Sergipano Fold Belt are poorly understood. These problems are addressed in this thesis.

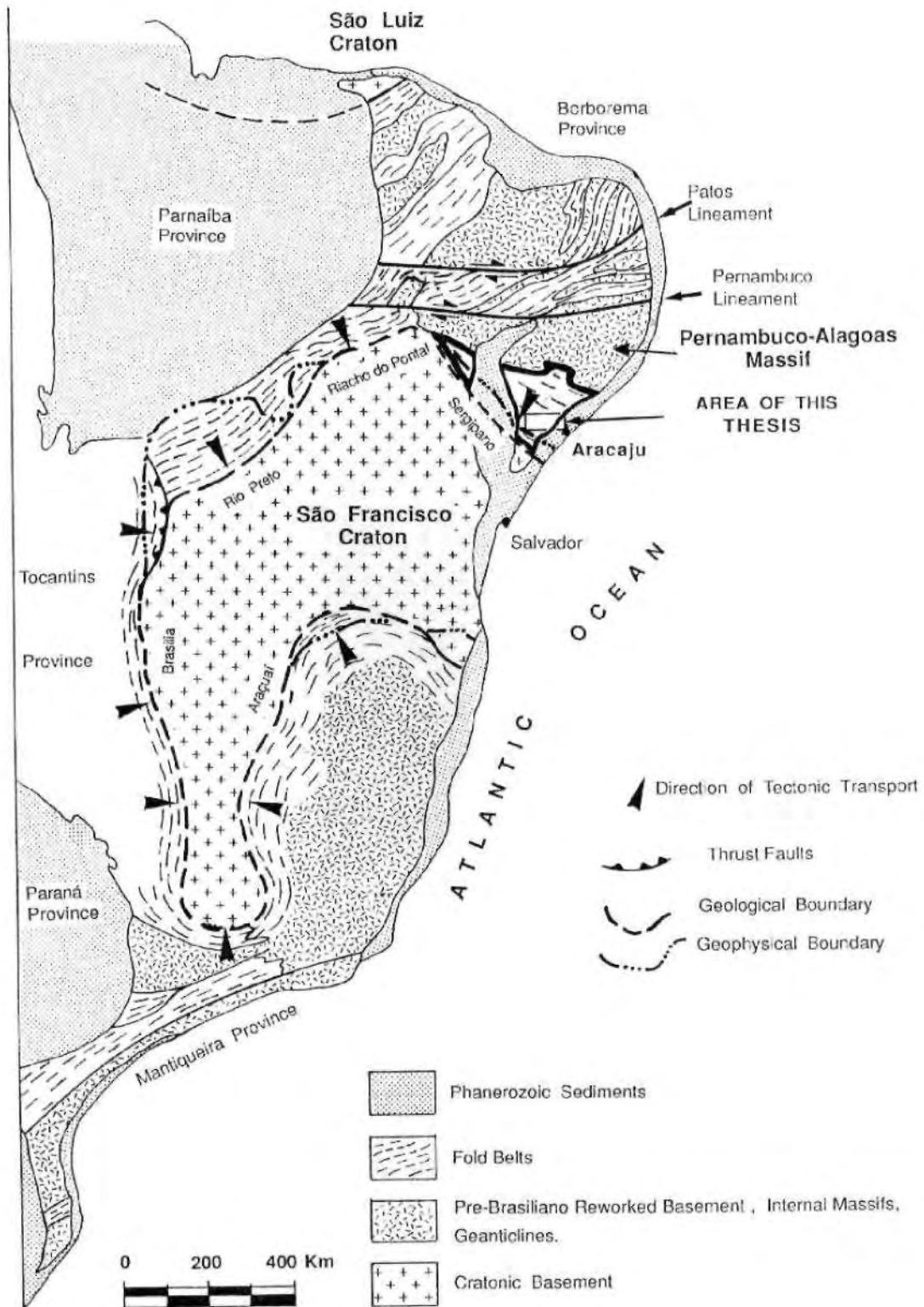
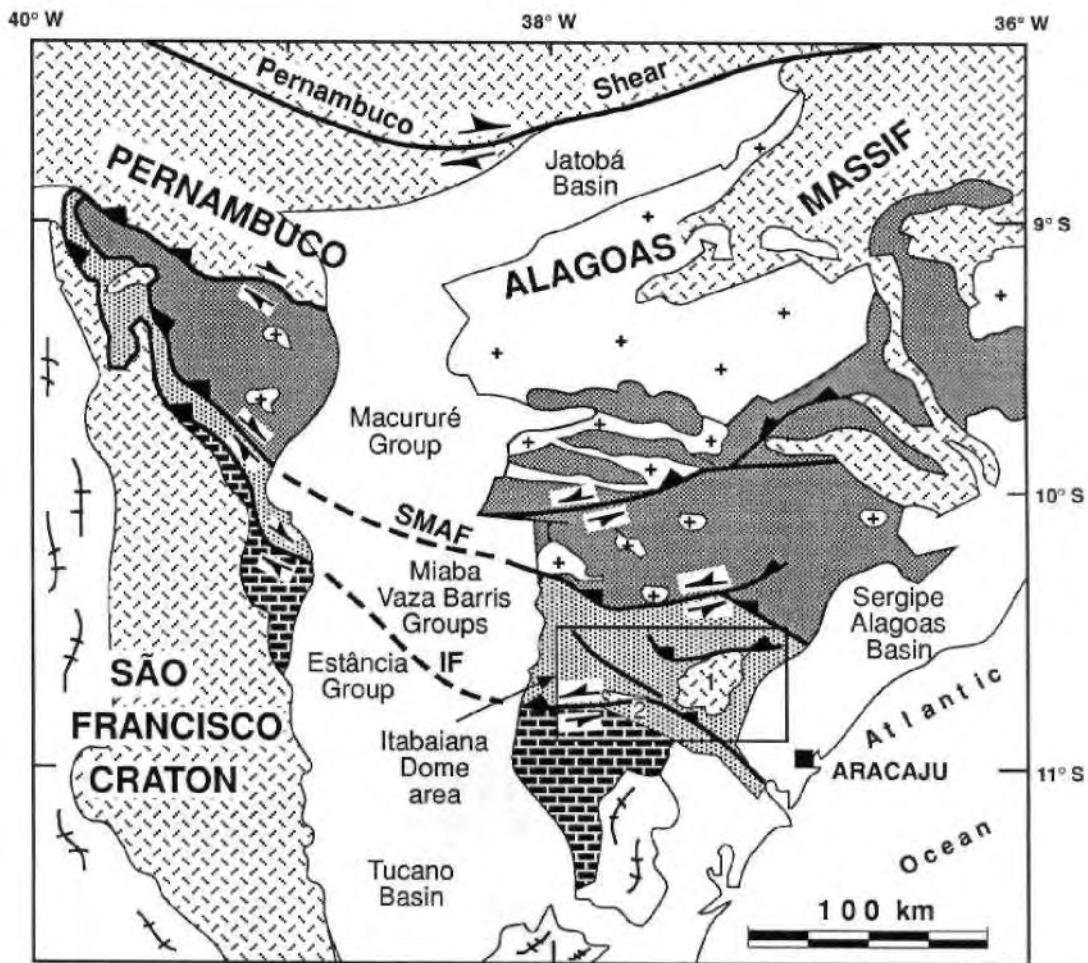



Figure 1.2 - Simplified geological map of eastern Brazil to show the São Francisco craton and the surrounding Pan-African-Brasiliano fold belts. The centraward convergences of the fold and thrust belts are shown (arrows). The geological and geophysical boundaries of the São Francisco craton are shown. The Sergipano Fold Belt is outlined in black (based on Wernick et al. 1978; and on Mascarenhas et al. 1984).





PHANEROZOIC

 Sediments

UPPER PROTEROZOIC

SOUTHERN BELT

 Polydeformed low-grade metasediments


 Cratonic sediments

1 = Itabaiana dome
2 = Simão Dias dome


IF = Itaporanga fault
SMAF = São Miguel do Aleixo fault

NORTHERN BELT

 Granites

 Polydeformed, up to amphibolite grade metasediments, migmatites, and igneous rocks

ARCHEAN to LOWER PROTEROZOIC

 Granulites

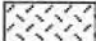
 Amphibolite grade gneisses

Figure 1.3 - Simplified geological map of the Sergipano Fold Belt (compiled from Gava et al. 1983, Jardim de Sa et. 1986, Santos et al. 1988, and Davison & Santos 1989).

1.3 - Aims of this thesis

This thesis details the results of research based on geological mapping in the area outlined in Figure 1.4, which covers approximately 4000km².

The aims of this research programme were:

1 - To undertake a detailed analysis of the sedimentological and stratigraphic evolution of the Itabaiana Dome Area (Fig. 1.3).

2 - To undertake a detailed analysis of mesoscopic and microscopic structures, and to determine the tectonic evolution of the area.

3 - To present an analysis of the stratigraphic and structural evolution of the entire southern part of the Sergipano Fold Belt, by combining the data collected in the field area with data obtained from the literature,

4 - To develop a model for the tectonic evolution of the southern part of the Sergipano Fold Belt, from basin formation and sediment deposition to its subsequent closure and incorporation in the Sergipano Fold Belt during the Brasiliano orogeny

1.4 - Methodology

This research programme involved both detailed and regional geological mapping, together with stratigraphic and structural analysis. Thin section petrographic analysis of selected samples and integration of the geophysical data from the study area were also carried out.

Field work

A total of 180 days were spent in the field during 1987, 1988, and 1990. Approximately 1200 outcrops were studied in detail. The outcrops were located on 1:100,000 scale topographic maps (IBGE - Brazilian Institute for Geography and Statistics) enlarged to 1:50,000 scale.

A detailed study was made of the large Capitaó farm outcrop, at the junction of the Salgado and Vaza Barris rivers (Fig. 1.4). This outcrop was mapped at 1:100 scale.

About eighty aerial photographs (SACS, Brazil, 1971, 1:70,000 scale) were studied in detail, to determine the continuity of the units within the area, the nature of contacts, the trends of foliations and other structures. The results were also incorporated in the geological map of the Itabaiana Dome Area.

Laboratory work

3,200 structural measurements were made in the Field, including the orientation of bedding, foliations, lineations and fold axes. About 140 rock samples were cut into 220 thin sections, which form the basis of detailed petrographic, sedimentary and structural studies. The majority of the thin sections were oriented for structural analysis. The length of about 1890 axes of clasts from diamictites and pebbly phyllites were determined; 750 measured directly from outcrops, and 1140 measured from 38 oriented thin sections.

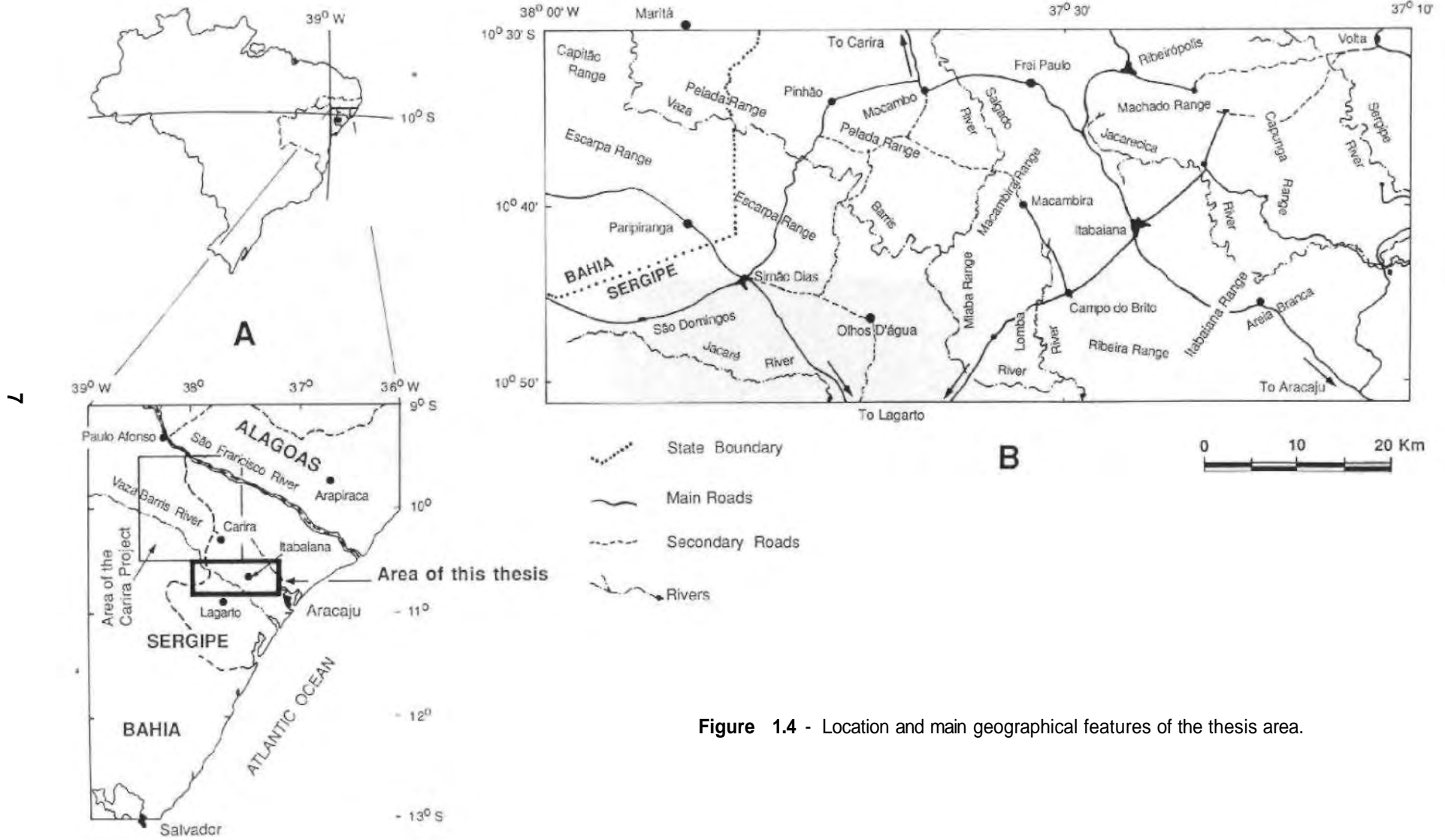


Figure 1.4 - Location and main geographical features of the thesis area.

Geophysical work

The geophysical data used in this study includes gravity, magnetic and scintillometer data. These data were collected by the Companhia de Pesquisas e Recursos Minerals (CPRM, Salvador-Bahia, Brazil) and were compiled by the geophysicist Dr. A.C. Motta, of the same company. Geophysical maps and sections were produced and the data integrated with cross-sections. Topographic data used for gravity interpretations were collected by Mr. Marcio Afonso Lima de Brito, from the Caraiba Mineracao company (CM, Salvador-Bahia, Brazil).

1.5 - Previous research

The geological knowledge of the Sergipano Fold Belt is based upon work done by the universities of UFBA, UFRN, UFPe, USP, as well as federal and state companies such as Petrobras, CPRM, EDRN, CODISE, CBPM, and Caraiba Mineracao). The comprehensive and systematic geological mapping of the belt was completed in 1977 (Brito Neves et al. 1977a).

Humphrey & Allard (1962, 1967, 1969) described the main lithostratigraphic units and established the basic elements of the geology of the area. They postulated that the area evolved as an intracratonic basin in accordance with the geosyncline theory of Auboin (1965). Previous geological studies concerned primarily with regional geology (summarised by Brito Neves et al. 1977a).

Santos & Silva Filho (1975), Silva Filho et al. (1978 a & b), Silva Filho & Brito Neves (1979), and Silva Filho (1982) established the basic stratigraphy of the area, and divided the Sergipano Fold Belt into the cratonic, miogeocline and eugeocline components.

Jardim de Sá & Calheiros (1981), Jardim de Sa et al. (1981, 1986) gathered much data on the metamorphic and structural evolution. They disputed previous geological models involving B-subduction zones and proposed an alternative model involving the collision of two cratonic blocks. A similar interpretation has been adopted by Brito Neves et al. (1977 b), Brito Neves et al. (1987) and Campos & Brito Neves (1987).

Davison (1987), Santos et al. (1988) and Davison & Santos (1989) also studied the area and interpreted the Sergipano Fold Belt as a collage of possibly exotic terranes produced by an oblique collision event.

The geochronology of the belt is based on scattered Rb-Sr and K-Ar determinations (Hurley 1966; Brito Neves & Coidani 1973; Brito Neves et al. 1977c; Gava et al. 1983; Santos et al. 1988). Geophysical data from the Sergipano Fold Belt were presented and interpreted by Rand et al. (1980), Santos et al. (1988), and Motta (1990).

The geology and geochemistry of the basic-ultrabasic Caninde' Complex, in the northern part of the Sergipano Fold Belt (Silva Filho 1976), has been subject of increasing interest and diverging interpretations in the recent years (Blais et al. 1989; Oliveira & Tarney 1990; Bezerra et al. 1990).

The metallogenic potential of the southern part of the Sergipano Fold Belt has been a subject of interest for companies such as Caraiba Mineração and Companhia Baiana de Pesquisas Minerais (Moraes et al. 1987; Conceição Filho & Sales 1988; Guimarães et al. 1991). Jardim de Sá (1986) analysed the economic geology of the whole Sergipano Fold Belt, and Santos et al. (1988) presented a 1:100,000 scale provisional metallogenic map of the Carira project area, based on geochemical, sedimentological, structural and geophysical data.

1.6 - Structure of this thesis

This thesis consists of seven chapters:

Chapter 1 introduces the Sergipano Fold Belt and the research area.

Chapter 2 reviews the geology of the Sergipano Fold Belt, and places the thesis study area in its tectonic context.

Chapter 3 describes the geology of the research area and focuses on the stratigraphic record. A new stratigraphy for the southern part of the Sergipano Fold Belt is presented.

Chapter 4 describes the structural and metamorphic evolution of the mapped area and relates this to the evolution of the southern part of the Sergipano Fold Belt.

Chapter 5 presents an analysis of geophysical data from the southern part of the Sergipano Fold Belt, and integrates this with the geological data.

Chapter 6 describes the geological evolution of the research area, and develops a model for the tectonic and stratigraphic evolution of the southern part of the Sergipano Fold Belt. This is integrated with the geology of the northern part of the Sergipano Fold Belt, and implications for the evolution of other Proterozoic fold belts are discussed.

Chapter 7 presents the conclusions of this research and recommendations for future research.

Chapter 2. Regional Geology of the Sergipano Fold Belt

2.1 - Aims

This chapter aims:

1 - To present an up-to-date review of the regional geology of the Sergipano Fold Belt, based on the current literature, with emphasis on the geology of the southern part of the Sergipano Fold Belt.

3 - To emphasise the importance of the area of this thesis in the understanding of the southern part of the Sergipano Fold Belt.

4 - To highlight the problems that will be addressed in the body of this thesis.

2.2 - Introduction

2.2.1 - Regional setting

The Sergipano Fold Belt (Fig. 2.1) lies between the granulites and the amphibolite-grade gneisses of the northern part of the Sao Francisco Craton to the south, and the Pernambuco-Alagoas Massif to the north (Mascarenhas et al. 1984; Santos & Brito Neves 1984).

The Borborema Province consists of SW-NE trending Archean to Early Proterozoic granite-gneiss migmatitic regions (originally named massif by Brito Neves 1975). The massifs have been reworked by the 900-600 Ma Brasiliano thermo tectonic events responsible for the ultimate evolution of the mobile zones (Santos & Brito Neves 1984; Brito Neves 1986). Some of the mobile belts, however, also show evidence of an early evolution starting in the 2100-1800 Ma Transamazonian cycle (Jardim de Sa et al. 1988; Jardim de Sá 1988).

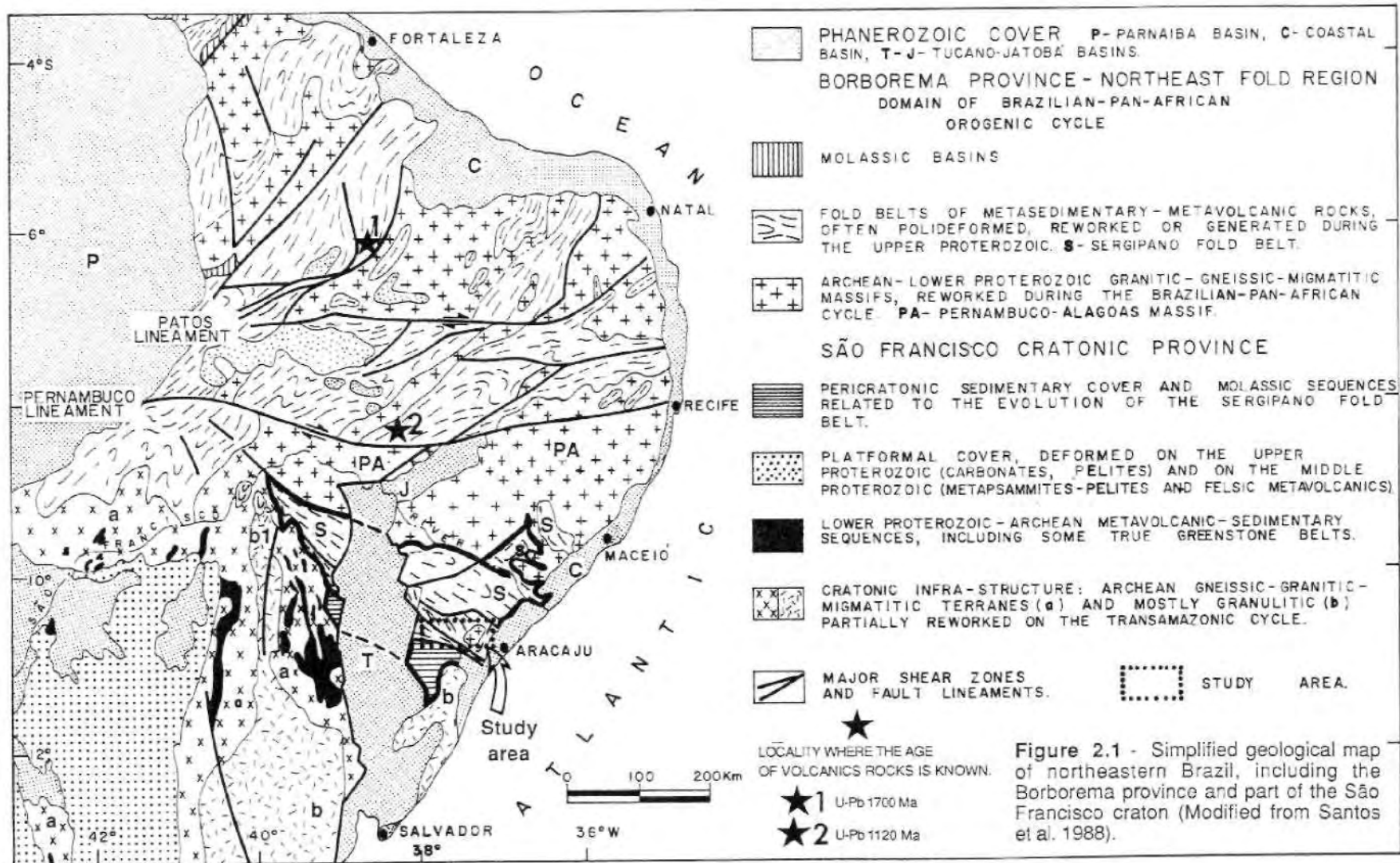
The northern part of the Sao Francisco Craton (Fig. 2.1) is comprised of Archean to Early Proterozoic high-grade gneisses and Early Proterozoic mobile belts, which include high-grade metamorphic rocks, low-grade supra-crustal rocks and granite-greenstone sequences (Inda & Barbosa 1982).

2.2.2 - The Sergipano Fold Belt

Humphrey & Allard (1962, 1967, 1968, 1969), Allard & Hurst (1969), and Allard (1969) first described the Sergipano Fold Belt, at that time named the Propria geosyncline (Fig. 2.2).

It consisted of a horst of Late Proterozoic, WNW-ESE trending, metavolcanic-sedimentary rocks separated from the Tucano and Sergipe-Alagoas Mesozoic basins, by the Tobias Barreto and Propria normal faults. These authors also described the basic lithostratigraphy, based on detailed studies carried out mainly around the Itabaiana dome.

Humphrey & Allard (1967, 1969) characterised five main structural elements within the Sergipano Fold Belt (Fig. 2.2):



1- The crystalline basement cropping out mainly in the Itabaiana and Simão Dias domes.

2- The metavolcano-sedimentary wedge comprising two laterally-equivalent groups (the miogeoclinal Miaba Group, unconformably deposited around the basement domes, and the eugeoclinal Vaza Barris Group).

3- The Glória batholith: a suite of granodioritic to quartz-monzonitic plutons surrounded by biotite-garnet hornfelses derived from the Vaza Barris Group.

4- Thrusts and small- to large-scale, overturned, nappe-like folds, both indicating a southward tectonic transport.

5- The Estância Formation (siliciclastic and carbonate sediments), unconformably deposited in the craton.

Barbosa (1970) studied the Sergipano Fold Belt to the west of the Tucano basin, and described a Precambrian to Ordovician lithostratigraphy consisting of the Macururé, Canudos and Bambui Groups (shown together in Fig. 2.2). The Macururé Group (paragneisses, micaschists and quartzites) is unconformably overlain by the Canudos Group (phyllites, metacarbonates and carbonaceous schists), which is in turn unconformably overlain by the Bambui Group (metacarbonates).

However, Jordan (1971) showed that the Bambui and Canudos Groups are laterally equivalent, and proposed that the Macururé group consists of two parts, one underlying and the other overlying these two equivalent groups.

The >900Ma old Bambui sediments (Misi 1976) form an extensive blanket of carbonate and siliciclastic sediments that covers large part of the surface of the São Francisco Craton (see heavy dotted pattern, Fig. 2.1). These sediments form a Late Proterozoic platformal sequence which has been partially deformed during the Brasiliano orogeny (Mascarenhas et al. 1984; Inda & Barbosa 1982; Teixeira & Figueiredo 1991)

Humphrey & Allard (1967, 1969) also mapped part of the belt situated to the west of the Tucano basin, analysed data from oil wells, and demonstrated the continuity of the metasediments underneath the Tucano and Sergipe-Alagoas Mesozoic basins, and correlated the metasediments to the east and west of the Tucano basin (Fig. 2.2).

Allard (1969) and Allard & Hurst (1969) carried out geological mapping in part of the western side of Gabon, in Africa, and correlated the Vaza Barris group, defined in the horst of the Sergipano Fold Belt, with the Nadjolé schists in the African continent.

After three decades of regional and detailed studies, the geological map (Fig. 2.3) of the Sergipano Fold Belt shows a substantially improved geology consisting of a much more complex distribution of lithologies dominated by an array of regional faults starting in the western apex of the belt (the Macururé, Canudos and Bendengó faults) and extending to the east of the Tucano-Jatobá basins (the Itaporanga, São Miguel do Aleixo, Belo Monte-Jeremoabo, and Jacaré dos Homens faults).

Apart from the Bendengó and Canudos faults (names adopted here), all the fault names have been taken from Gava et al. (1983), Santos et al. (1988) and Davison & Santos (1989).

Santos & Silva Filho (1975), Silva Filho et al.(1978 a & b), Silva Filho & Brito Neves (1979), and Silva Filho (1982), defined the basic stratigraphy of the belt (see

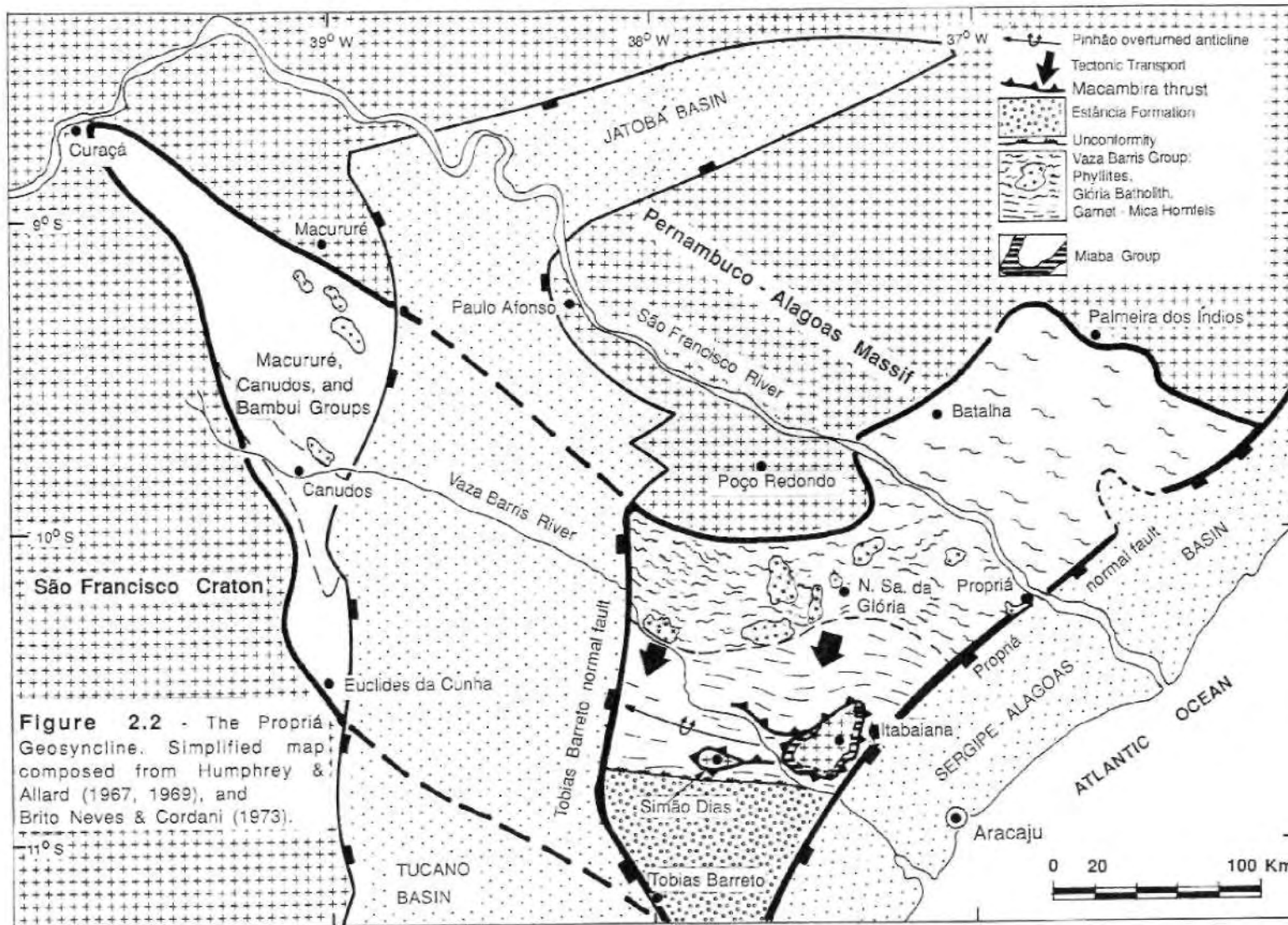


Figure 2.2 - The Propriá Geosyncline. Simplified map composed from Humphrey & Allard (1967, 1969), and Brito Neves & Cordani (1973).

legend of Fig. 2.3), consisting of the laterally continuous, Estância Group, the miogeoclinal Miaba and Vaza Barris Groups, and the eugeoclinal Macururé Group (including slices of basement rocks, and the mafic-ultramafic, volcanic and intrusive Canindé Complex of Silva Filho 1976).

These authors also defined two younger formations: the Palmares sandstones overlying the cratonic Estância Group, and the Juá conglomerates and sandstones which infill a small graben within the Macururé Group.

Following their regional synthesis, the Estância, Miaba and Vaza Barris Groups have been considered equivalent to the Bambuí Group (Misi 1976; Silva Filho et al. 1978 a & b), a correlation widely accepted in the literature, at least between the cratonic Estância and Bambuí Groups (Inda & Barbosa 1982; Gava et al. 1983; Mascarenhas et al. 1984; Teixeira & Figueiredo 1991).

Many other authors argued for the lateral continuity within the cratonic, miogeocline and eugeocline domains, and adopted models of a tectonic evolution mainly based upon a frontal collision between the Pernambuco-Alagoas Massif and the São Francisco Craton (Rand et al. 1980; Jardim de Sá et al. 1981; Jardim de Sá et al. 1986; Campos Neto & Brito Neves 1987).

Davison (1987) proposed a model of transpressional and oblique collision, and with more detailed studies by Santos et al. (1988), which resulted in the mapping of areas of high grade gneisses and acid-intermediary metavolcanics within the northern domain (Fig. 2.3), Davison & Santos (1989) proposed to divide the Sergipano Fold Belt into the northern and southern parts, separated by the São Miguel do Aleixo fault, and that the belt could be the result of the collage of possible allochthonous, fault-bounded domains (possibly terranes).

The tectonic evolution of the whole Sergipano Fold Belt is attributed to a Brasiliano (600Ma old) collisional event between the Pernambuco-Alagoas Massif and the São Francisco Craton (Davison & Santos 1989).

2.3 - Litho-stratigraphic units of the northern part of the Sergipano Fold Belt

The northern part of the Sergipano Fold Belt is comprised of the Macururé, Canindé, Poço Redondo and Marancó Domains (Santos et al. 1988; Davison & Santos 1989).

The Macururé Domain contains metasedimentary and metavolcanic rocks of the Macururé Group, and also the sediments of the Juá Formation and intrusive granites.

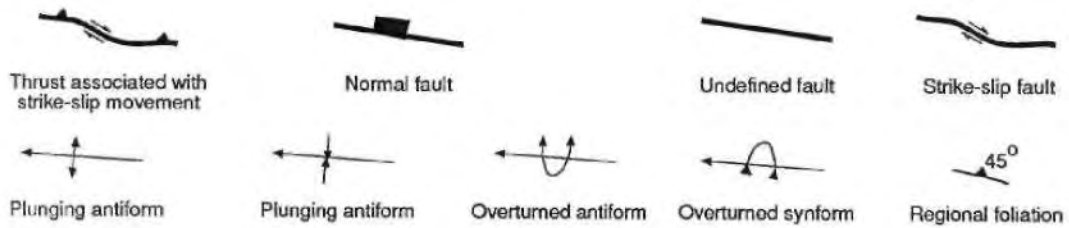
The Canindé and the Marancó Domains contain rocks of mid- to infra-crustal affinities, and correspond to the Canindé and Marancó Complexes (Fig. 2.3).

The Canindé Domain lies to the north of the Canindé village and is cut by the São Francisco river. The Marancó Domain lies to the south of the Poço Redondo village, and is bounded to the south by the Belo Monte-Jeremoabo fault (Fig. 2.3).

Overleaf: Legend of the geological map of the Sergipano Fold Belt (Fig. 2.3).

L E G E N D - Figure 2.3

Data from Silva Filho et al. (1978 a & b); Silva Filho & Brito Neves (1979); Gava et al. (1983); Jardim de Sá et al. (1986); Santos et al. (1988) and Davison & Santos (1989). The relative positions of the Canindé and Marancó Complexes do not mean any age relationship.



Foreland basin



Intramontane basin

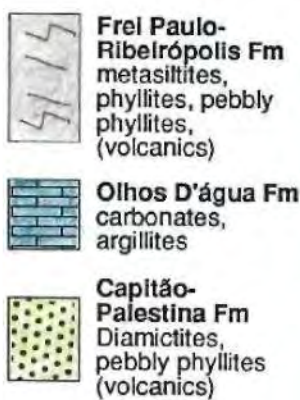


Craton Estância Group (undiferenciated)



Miogeoclinal Miaba and Vaza Barris Groups

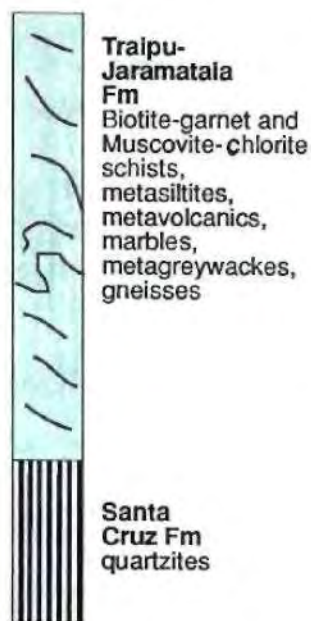
Vaza Barris Gr



Miaba Gr



Eugeoclinal Macururé Group



Magmatism



SFC= São Francisco Craton

Pam = Pernambuco-Alagoas Massif

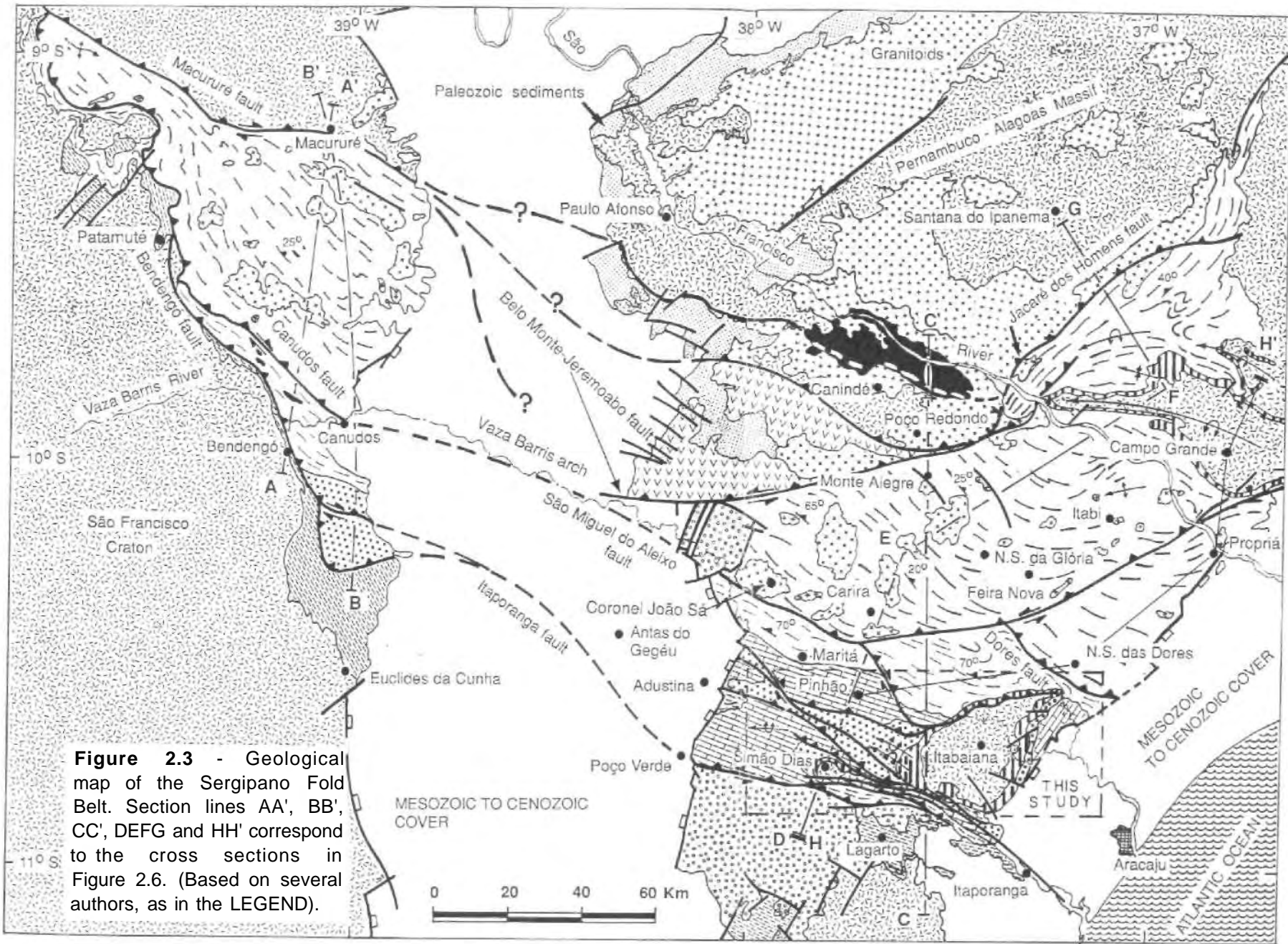


Figure 2.3 - Geological map of the Sergipano Fold Belt. Section lines AA', BB', CC', DEFG and HH' correspond to the cross sections in Figure 2.6. (Based on several authors, as in the LEGEND).

The Poço Redondo Domain occupies the faulted bounded area between the Canindé and Poço Redondo villages and the border with the Tucano basin (Fig. 2.3).

The Macucuré Group is comprised of the Santa Cruz and the Traipu-Jaramataia formations. The Santa Cruz Formation consists of white micaceous quartzites (Leite 1969) that surround a basement dome in the northern part of the belt (Fig. 2.3) and are conformably overlain by the Traipu-Jaramataia Formation.

The Traipu-Jaramataia Formation consists of mica schists, metagreywackes, phyllites, lenses of quartzites and marbles, especially in the western side of the northern part of the belt (Silva Filho et al. 1978a; Silva Filho & Brito Neves 1979).

Intercalations of calc-silicatic rocks, amphibolites and basic metavolcanics are described to the northeastern end of the belt (Jardim de Sá et al. 1981), whereas in the central area, Santos et al. (1988) identified phyllites, metasiltites, metagreywackes, mylonitic quartzites, mylonitic chlorite-quartz, biotite-garnet and staurolite-garnet schists, metadacites and porphyry metadacites.

The Juá Formation consists of conglomerates, greywackes, and arkoses with clasts derived from rocks situated to the north of the Juá graben (Santos et al. 1988).

The Canindé Complex (Silva Filho 1976) consists of gabbros, basalts, ultrabasic schists, felsic lavas intercalated with lenses of the Santa Cruz quartzites, and also with Traipu-Jaramataia marbles, meta-arkoses and graphite phyllites.

The **Marancó Domain** (metarhyolitic and metadacitic lavas, interleaved with two sub-concordant serpentinised ultramafic bodies and minor metasediments of the Macucuré Group). The Canindé and Marancó Domains are intruded by syn and post-tectonic granites.

The **Poço Redondo Domain** consists of migmatitic gneisses intruded by syn and post-tectonic granites.

The **Granites** form a calc-alkaline series of late- to post-tectonic intrusions relative to the F_2 folding phase (Santos et al. 1988). They consist of granodiorites, diorite-monzonites and granites (Humphrey & Allard 1967, 1969; Silva Filho et al. 1978a; Gava et al. 1983; Giuliani & Santos 1988; Fujimori 1989).

The geochemistry of the rare earth and major elements of the main plutons (e.g. those surrounding the Carira town, Fig. 2.3) suggests that the magmas are co-genetic, and were intruded at depths of 9 -10 km (Giuliani & Santos 1988; Santos et al. 1988) under pressures around 5 kbar (Fujimori 1989).

Giuliani & Santos (1988) discussed the origin of these granites, and interpreted the magmas as probably originated from the partial melt of the upper mantle (eclogites) with strong contribution of the lower continental crust (granulites).

Fujimori (1989) argue that the granodiorites of the Sergipano Fold Belt have a mantle origin and geochemical signature of volcanic arcs, whereas the alkaline granites probably represent the syn-collisional stage.

Other Brasiliano-age granitic bodies intruded in the Pernambuco-Alagoas Massif (Brito Neves et al. 1977 a & b) have a syenitic to quartz-monzonitic composition and commonly contain xenoliths of basic rocks (Gava et al. 1983; Jardim de Sá et al. 1986).

2.4 - Stratigraphy of the southern part of the Sergipano Fold Belt

The southern part of the Sergipano Fold Belt (Fig. 2.4) is comprised of the cratonic Domain, where the Estância Group is deposited, and the supra-crustal Domain, where the Miaba and Vaza Barris Groups are deposited.

2.4.1 - The Estância Group

The Estância Group in the region to the south of Itabaiana (Silva Filho et al. 1975 b; Silva Filho 1982) consists of a 1km-thick sequence of continental to shallow marine siliciclastic and carbonates, divided into the Jueté, Acauã and Lagarto Formations. This is unconformably overlain by the Palmares sandstones.

In an area 100 km to the south of Itabaiana, Saes (1984) documented in detail a gradual passage between the Lagarto and Palmares formations and described a 3km-thick Estância Group (Fig. 2.5 A).

The Jueté Formation consists of laminated sandstones, with conglomeratic lenses of basement derived clasts, and brown to red argillites. The top is marked by red-brown to purple, fine to medium grained feldspathic sandstones with clasts of red argillites.

The Acauã Formation is conformably deposited on the Jueté Formation, and unconformably overlies the basement gneisses. It is comprised of basal limestones and dolomites, calcitic argillites with lenses of limestones, overlain by limestones and dolomites with thin intercalations of fine grained, cross bedded, red sandstones and green argillites.

The Lagarto Formation generally conformably overlies the Acauã Formation, the basal contact is locally erosive with the Acauã carbonates, or it is even in fault contact with the crystalline basement.

This formation consists of conglomeratic basal sandstones with intercalations of red argillites and siltites, passing upward to green and brown siltites and to calcite cemented, fine sandstones and wackes with small- to meso-scale tabular cross stratification.

The Palmares Formation is typically green, mostly medium grained, well-cemented arkosic sandstones with intercalations of locally pebbly lithic greywackes, which have fragments of quartz, feldspars, quartzites and phyllites.

The contact with the Lagarto sandstones is generally gradual, although a breccia with fragments of carbonates, and lenses of polyimictic conglomerates are found locally along this contact.

2.4.2 - The Miaba Group

The Miaba Group (Fig. 2.5 B) is comprised of the Itabaiana, Jacarecica, and Jacoca Formations. The Miaba Group is probably as thick as 1 km (Humphrey & Allard 1969; Silva Filho et al. 1978 a & b; Davison & Santos 1989)

The Itabaiana Formation (200-600m thick) unconformably overlies the crystalline basement, and consists of arkosic basal quartzites (locally conglomeratic) passing upward to quartzites with small- to meso-scale cross bedding.

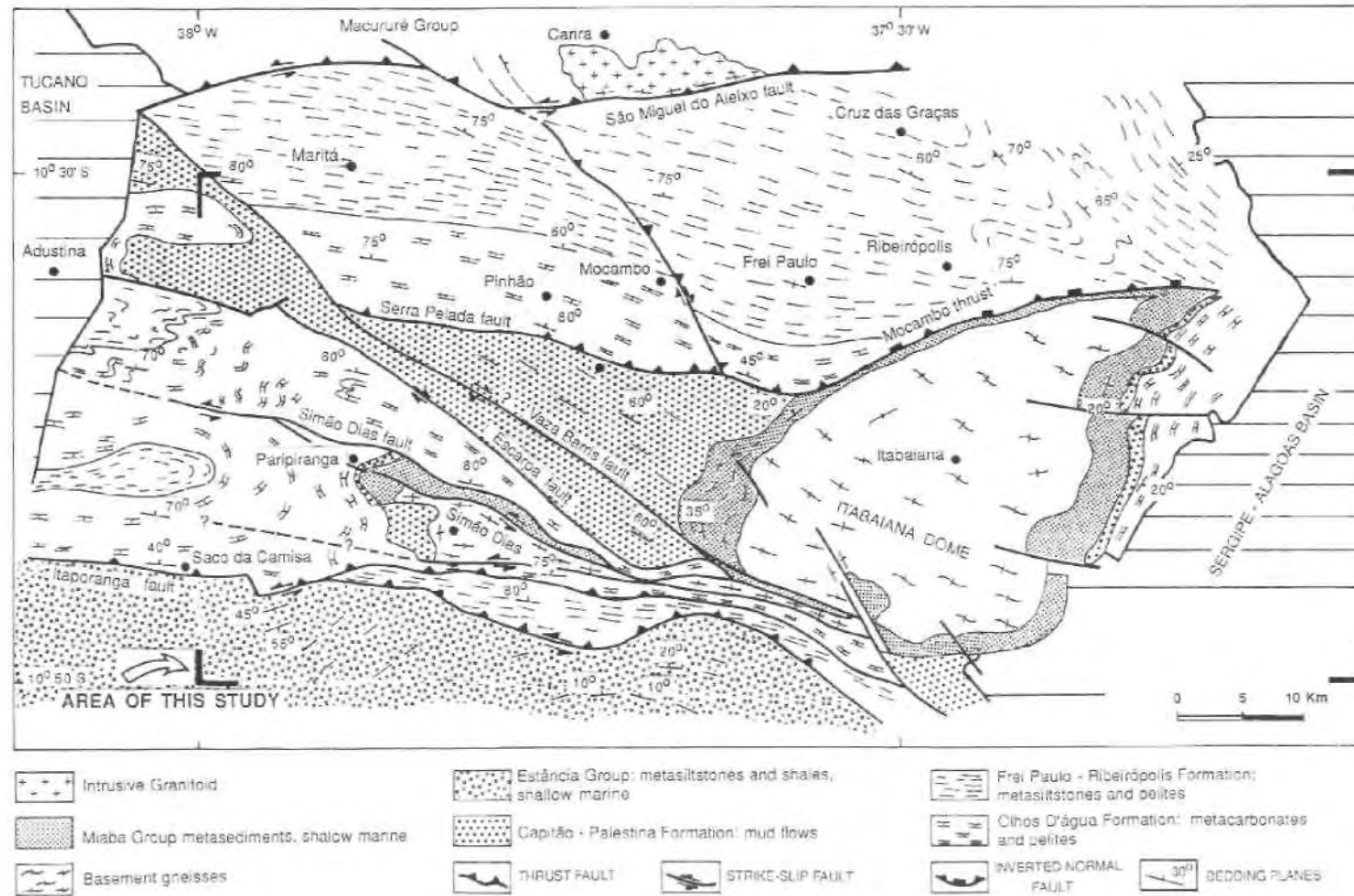


Figure 2.4 - Simplified geological map of the southeastern Sergipano Fold Belt (Modified from Silva Filho et al. 1979; Davison a Santos 1939).

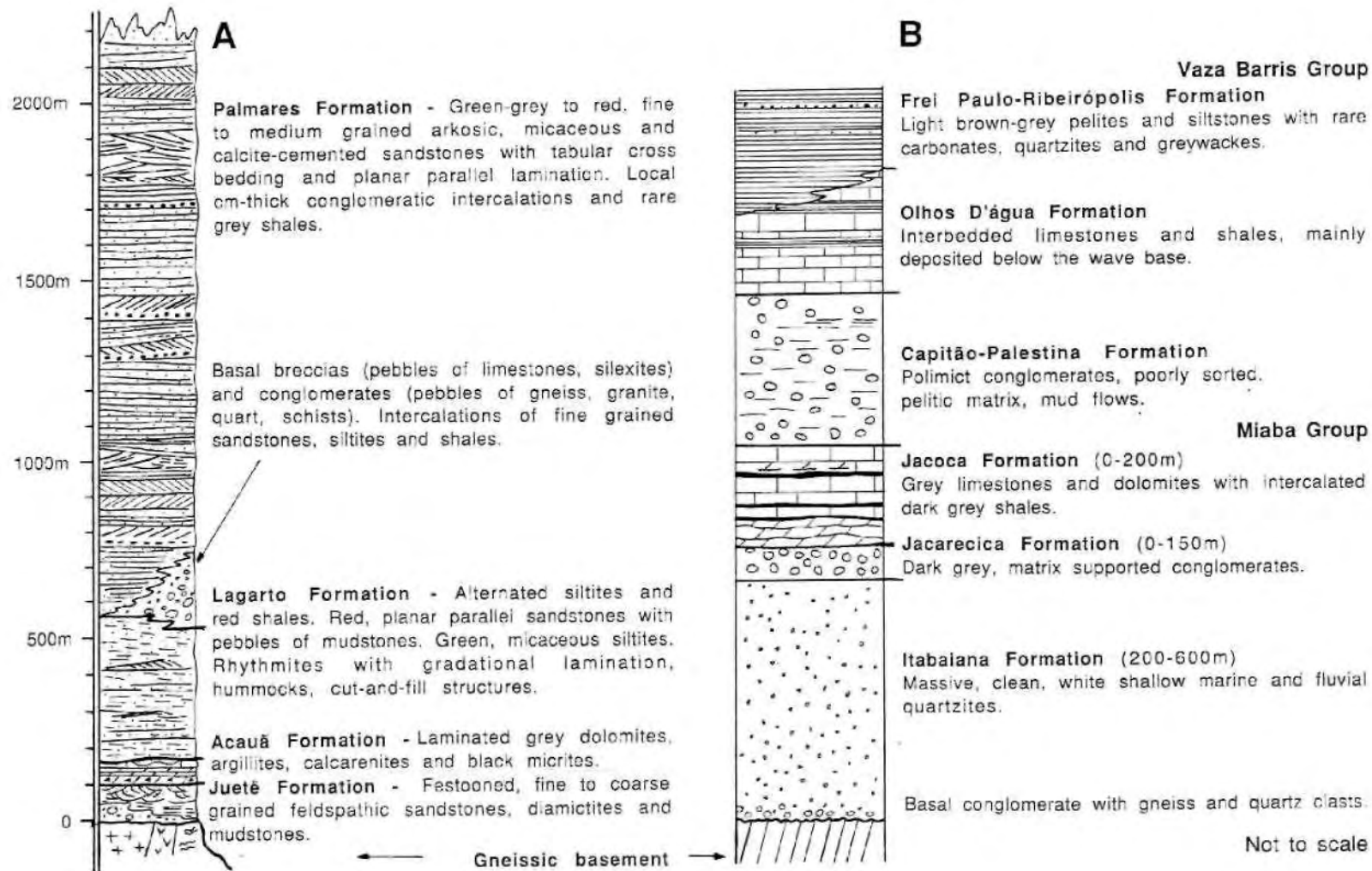


Figure 2.5 - Stratigraphic columns of (A): the Estância Group, and (B): the Miaba and Vaza Barris Groups. Slightly modified from (A) : Saes (1984), and (B): Davison & Santos (1939).

The **Jacarecica Formation** (0-150m thick) unconformably overlies the Itabaiana Formation, and consists of grey to reddish, locally conglomeratic metagreywackes, white to grey metaargillites, and reddish phyllites. Some pyroclastic rocks may also occur in this formation. The clasts in the conglomeratic bodies are from basement rocks and from the Itabaiana quartzites. In the northeastern border of the Itabaiana dome, Humphrey & Allard (1969) clasts of gneiss of up to 120cm in size.

The **Jacoca Formation** (200m thick, Humphrey & Allard 1967, 1969) conformably overlies the Jacarecica Formation and unconformably overlies the Itabaiana Formation, specially around the eastern and western Itabaiana dome. It consists of marbles, metadolomites, metacherts, metaargillites, limestones, marls, dark grey phyllites and calcitic quartz-chlorite schists. The basal part of the column locally contains syn-sedimentary copper sulphide occurrences.

2.4.3 - The Vaza Barris Group

The Vaza Barris Group is comprised of the Capitão-Palestina, Olhos D'água and Frei Paulo-Ribeirópolis Formations. Generally the thicknesses are highly variable, and are barely estimated because of the deformation. However, it is normally accepted that this group could be as thick as 3km, on the eastern side of the itabaiana dome (Davison & Santos 1989).

The **Capitão-Palestina Formation** unconformably overlies either the Jacarecica or Jacoca Formations, and in places the crystalline basement. It shows marked variations in thickness, and comprises two lithofacies: grey to green phyllites with lenses of metacarbonates, impure metarenites, local metabasalts and pyroclastic rocks (the Capitão facies) and a second lithofacies of diamictites containing granules to boulders of basement rocks, quartzites, quartz veins, carbonates and phyllites, with intercalated lenses of quartzites (the Palestina facies).

The **Olhos D'água Formation** is a sequence of dark grey to black, metalimestones, metadolomites, and intercalated variegated argillites. The carbonates are commonly parallel laminated, cross bedded and probably indicate a shallow marine depositional environment. Stratifera Undata stromatolites were described by Cassedane & Silva Filho (1982), close to the Saco da Camisa locality (Fig. 2.4).

The **Frei Paulo-Ribeirópolis Formation** merges the original Frei Paulo and Ribeirópolis formations of Humphrey & Allard (1967, 1969) into two lithofacies.

The Frei Paulo lithofacies consists of well-foliated metasiltites and sandy metasiltites passing to silty phyllites. The Ribeirópolis lithofacies consists of locally conglomeratic metagreywackes, meta-argillites, phyllites, metavolcanics, and lenses of metarenites and metacarbonates.

The Frei Paulo lithofacies was described as having a gradual transition from the Lagarto sandstones, close to the southern margin of the Itabaiana dome (Silva Filho et al. 1978 a & b; Silva Filho 1982), whereas in the northern part of the area (Fig. 2.4) they were described as having a gradual transition from the Olhos D'água carbonates (Santos et al. 1988).

Despite the lateral continuity of the major formations for 350km along the WNW-ESE strike, stratigraphic analysis by Gava et al. (1983), Moraes et al. (1987) and Conceição Filho & Sales (1988) have shown that the sedimentary units are reduced in thickness, or in some cases even absent in the Sergipano Fold Belt to the west of the Tucano basin.

In the cratonic area to the west of the Tucano basin, the Jueté Formation is almost absent, and consists of local conglomeratic bodies. The Acauã Formation is generally continuous, but the Lagarto and Palmares Formations are absent.

In the western miogeocline the Miaba Group cannot be mapped on a regional scale, although Humphrey & Allard (1969) described thin Itabaiana quartzites and lacocarnetacarbonates. The Vaza Barris Group is represented only by the Frei Paulo-Ribeirópolis and Capitão-Palestina Formations.

2.5 - Structures and metamorphism

2.5.1 - Introduction

The Sergipano Fold Belt records a polyphase history of ductile to brittle-ductile deformations (D_1 - D_3), with involvement of the crystalline basement.

The deformation history is summarised in terms of two major co-axial folding phases (F_1 - F_2) associated with metamorphism (M_1 and M_2) together with generally southward thrusting. F_2 folds are associated with the regional thrust faults, which generally have a late-stage E-W strike-slip movement. A minor, non-metamorphic, transversal folding event is associated with the late-stage strike-slip movement along the regional faults (Jardim de Sá et al. 1981, Jardim de Sá et al. 1986, Davison & Santos 1989).

The two main folding events are locally followed by a third phase of co-axial, open, non penetrative and non-metamorphic folding (Campos Neto & Brito Neves 1987).

D_1 structures are a layer-parallel foliation (S_1), and local, isoclinal to recumbent, generally rootless, and south verging F_1 folds. These are co-axially refolded by the F_2 folds which are WNW-ESE trending, subhorizontal to gentle plunging, open to tight, commonly upright to overturned folds. There is generally a NNE dipping axial planar foliation (S_2) associated with these folds.

D_2 and D_3 structures are locally (particularly in the northern part of the Sergipano Fold Belt) and co-axially refolded by kink-style or cylindrical, generally open, up-right F_3 folds. There is generally a spaced cleavage axial planar foliation (S_3) associated with these folds.

The F_2 folds and the regional faults are the main mappable structures. The strike-slip movement is dextral along the faults to the west of the Tucano-Jatobá basin, and sinistral in those faults to the east (Fig. 2.3; Jardim de Sá et al. 1986; Moraes et al. 1987; Davison & Santos 1989).

2.5.2 - Structural and metamorphic partitioning

In the cratonic (Estância) Domain, the sediments are mostly undeformed and unmetamorphosed, whereas the intensity of deformation increases toward the Bendengó-Itaporanga fault (Fig. 2.6 A & E). Jardim de Sá et al. (1986) described important F_1 folds associated with low-angle, southward thrusts and amphibolite facies metamorphism, 20km southward onto the São Francisco Craton, in the Patamuté area, to the west of the Tucano basin (Fig. 2.3).

In the Vaza Barris Domain, limited by the Bendengó-Itaporanga and the Canudos-São Miguel do Aleixo faults, F_2 and S_2 are the main observed structures. S_2 is either a spaced cleavage, or a slaty cleavage, or a quartz-sericite or chlorite-biotite foliation, or a pressure solution foliation, dipping at intermediate to high angles to NNE (Figs. 2.6 A & E).

Although F_1 folds have been identified, or inferred from structural relationships by Jardim de Sá et al. (1986) and Santos et al. (1988), Davison & Santos (1989) argued for a monophasic deformation consisting generally of upright folds and thrusts in the southern Vaza Barris Domain (Figs. 2.6 B & C).

Jardim de Sá et al. (1981) reports that from the cratonic to the Vaza Barris Domain, the metamorphism generally shows a gradual northward increase under sub-greenchist to greenschist conditions, probably reaching temperatures of 300° to 400°C, and pressures of 1-3 kbar, and that on the basis of mineral paragenesis of sericite, chlorite and biotite in the metasediments, it has not been possible to distinguish the metamorphism associated with F_1 and F_2 folding events.

A sharp metamorphic contrast is described across the central part of the São Miguel do Aleixo fault (Santos et al. 1988), but the passage is more gradual elsewhere between the southern and northern parts of the belt (Jardim de Sá et al. 1986; Campos Neto & Brito Neves 1987),

Within the northern part of the Sergipano Fold Belt, the bedding (S_0), the S_1 and S_2 foliations (generally defined by the preferred orientation of biotite, garnet, quartz and minor staurolite and kyanite) are generally shallow-angle dipping (Figs. 2.6 a & B,C & E), and are affected by gentle to open F_3 folds (Brito Neves et al. 1987; Campos Neto & Brito Neves 1987), but approaching the Belo Monte-Jeremoabo fault all the planar features turn to near vertical or dip at high angles to NNE (Fig. 2.6 C).

The metamorphic evolution of the northern part of the belt is much more complex than the southern part, and is generally described in terms of amphibolite facies, although greenschist facies mineral paragenesis dominate in the northern boundary (Brito Neves et al. 1987; Santos et al. 1988).

Jardim de Sá et al. (1981) described a greenschist to high-amphibolite facies metamorphism, which probably reached silimanite and anatexis isograds, but probably in a low pressure regime (M_1) in the northern end of the belt. M_1 was superimposed by a new recrystallisation event under greenschist to amphibolite facies, with kyanite or andalusite present, indicating M_2 metamorphism of probably higher pressures than M_1

Particularly in the area surrounding the Carira town (Fig. 2.3) the M_1 metamorphism reaches a peak of high greenschist to amphibolite facies of intermediate

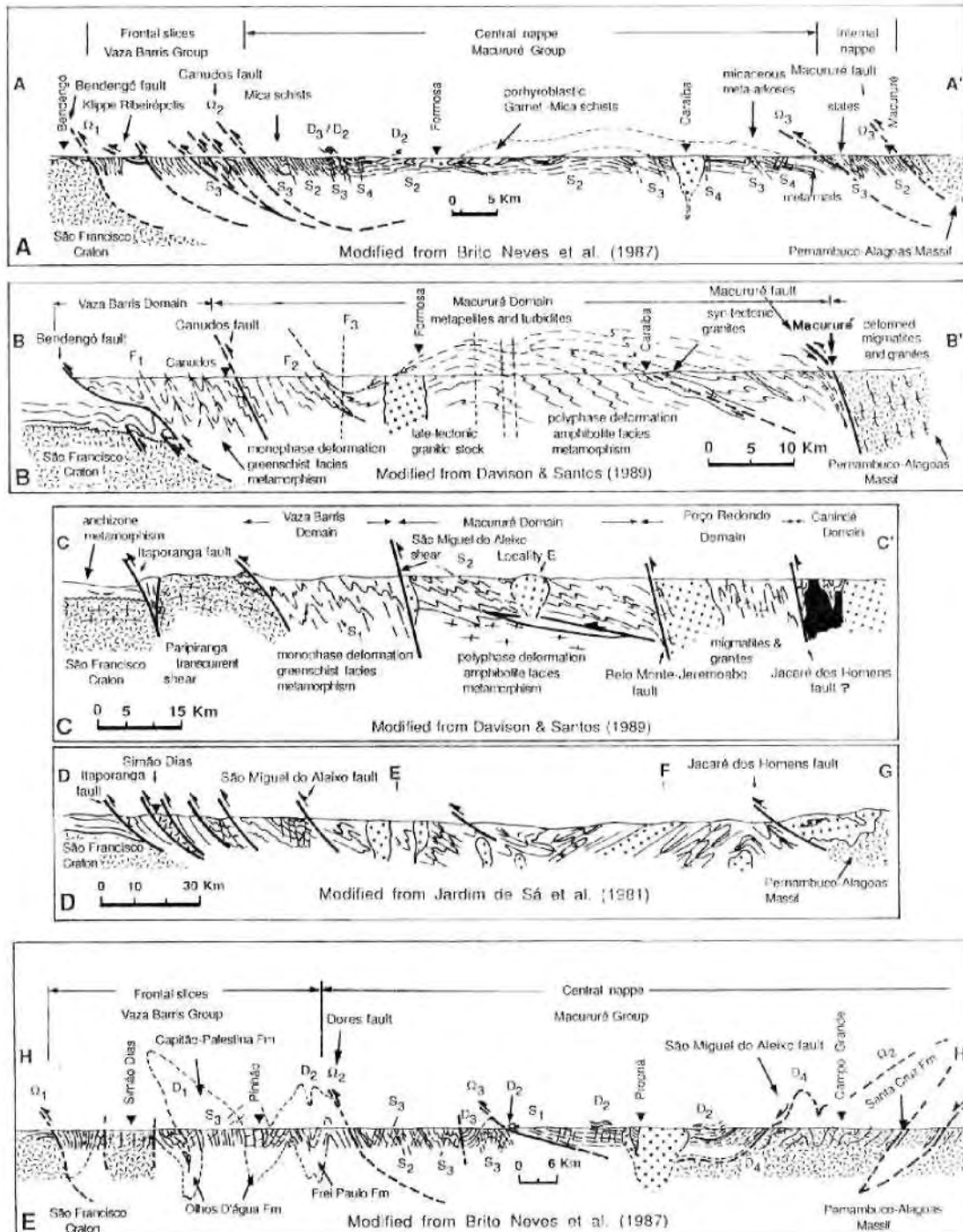


Figure 2.6 - Cross sections of the Sergipano Fold Belt, Section lines AA', BB', CC', DEFG and HH' are shown in Figure 2.3. See text.

pressures, whereas to the far east and northeast of Carira, the S_1 foliation is marked by muscovite and/or biotite, or by sericite/chlorite, reflecting greenschist facies metamorphic conditions (Jardim de Sá et al. 1981; Santos et al. 1988).

At the northeastern end of the Sergipano Fold Belt, M_1 varies from the prehnite-pumpellyite up to the high amphibolite metamorphic facies, and M_2 is somewhat weaker, though the presence of kyanite probably records a slight increasing of pressures (Jardim de Sá et al. 1981).

In this region (Figs. 2.6 D & E), S_0 , S_1 and S_2 are flat lying and sub-parallel, and are co-axially refolded by open to tight, up-right to overturned, northward verging folds and high-angle thrusts involving the Macururé Group and the crystalline basement. The folds, whose axial planar foliation is marked by greenschist facies mineral assemblages, have been interpreted either as F_3 folds (Brito Neves et al. 1987; Campos Neto & Brito Neves 1987) or as back-folds due to back-thrusting developed during progressive D_2 deformation (Jardim de Sá et al. 1986).

2.6 - Geochronology

2.6.1 - Age of sedimentation

Although the exact age of the sedimentation in the Sergipano Fold Belt remains unknown, the sediments are generally considered to be as old as Late to Middle Proterozoic.

Two swarms of basic dikes cut the northern margins of the São Francisco Craton. In the western part of the craton, the dikes are 2000Ma old and are unconformably overlain by the Estância Group (Jardim de Sá et al. 1986). In the southern part of the craton, the dikes are 1300Ma old (Cordani 1973) and have been interpreted as evidence of a phase of extension of the basement that may have been responsible for the development of the basin (Silva Filho et al, 1978 a).

A Late Proterozoic age of sedimentation is the most feasible interpretation for the metasediments in the southern part of the Sergipano Fold Belt, because of the >900Ma age for the Bambuí Group (section 2.2.2). A similar argument has been applied to the Macururé Group, on the basis of syn-sedimentary tectonic processes (Jardim de Sá et al. 1986).

2.6.2 - Age of deformation and metamorphism

It is generally accepted that the Sergipano Fold Belt resulted from tectono-metamorphic events that range from 900 to 600 Ma. The peak of metamorphism is dated between 673-600Ma (Brito Neves & Cordani 1973; Gava et al. 1983) on the basis of several Rb-Sr and K-Ar ages.

Brito Neves et al. (1977 c) presented a 23-point, 501-479 Ma range of Rb-Sr ages (average 490Ma) obtained from clay minerals of the cratonic Lagarto sediments, and interpreted the data as indicative of the anchimetamorphism affecting the Estância Group.

Santos et al. (1988) and Davison & Santos (1989) however presented a 861-805Ma range of Rb-Sr ages (average 838Ma) for late to post-tectonic granites in the vicinities of the town of Coronel João Sá (Fig. 2.3), and argue that the Macururé Group (or the northern part of the belt) may be older than the southern part,

2.7 - Geophysics of the Sergipano Fold Belt

Rand et al. (1980) made the first compilation of the gravity and magnetic data then available for the area of the Sergipano Fold Belt (Fig. 2.7 A) and produced an interpretation that the belt consisted of a continental crust formed by blocks of different densities, with no evidence of any crustal thickening, including a rootless Canindé Complex (Fig. 2.7 B).

Santos et al. (1988) added detailed gravimetric and magnetometric data collected in the area of the Carira Project, and reinterpreted all data along the AA' section line (Fig. 2.7 A). They modelled the upper crust of the northern part of the belt in terms of fault-bounded blocks with an intermediate composition northward of the São Miguel do Aleixo fault and concluded that 1: the main regional faults are probably deep-rooted structures, and 2: the Sergipano Fold Belt thickens from 3 to 13 km, in the northern end of the section (Fig. 2.8).

2.8 - Tectonic evolution

The models for the tectonic evolution of the Sergipano Fold Belt are currently strongly debated in the geological literature of the area.

Silva Filho et al. (1978 a) first introduced plate tectonic concepts for understanding the tectonic evolution of the Sergipano Fold Belt. They postulated a doubly vergent subduction process involving two passive margin-type basins. This model was challenged by Rand et al. (1980) and Jardim de Sá et al. (1981).

Silva Filho & Brito Neves (1979) turned to a model which is an important attempt at describing the evolution of the Sergipano Fold Belt by also considering the sedimentary record. They postulated sedimentation in a single passive margin (Fig. 2.9) closed by the collision of the Pernambuco-Alagoas Massif and the São Francisco Craton.

They described the tectonic evolution in four stages: the onset, the taphrogenic, the geosynclinal, and the orogenic stages. Their model is as follows:

1. The **onset** stage recorded the initial extension of the crust, erosion of the basement highs and deposition of the Itabaiana and Santa Cruz quartzites in grabens (Fig. 2.9).

2. The **taphrogenic** stage involved the continued extension of the crust, the erosion of the rejuvenated relief (the Jacarecica conglomerates and pebbly phyllites). The subsequent thermal relaxation produced subsidence and the first marine incursion (the Jacoca carbonates). The phase of maximum extension is recorded by the Capitão-Palestina diamictites and associated volcanism.

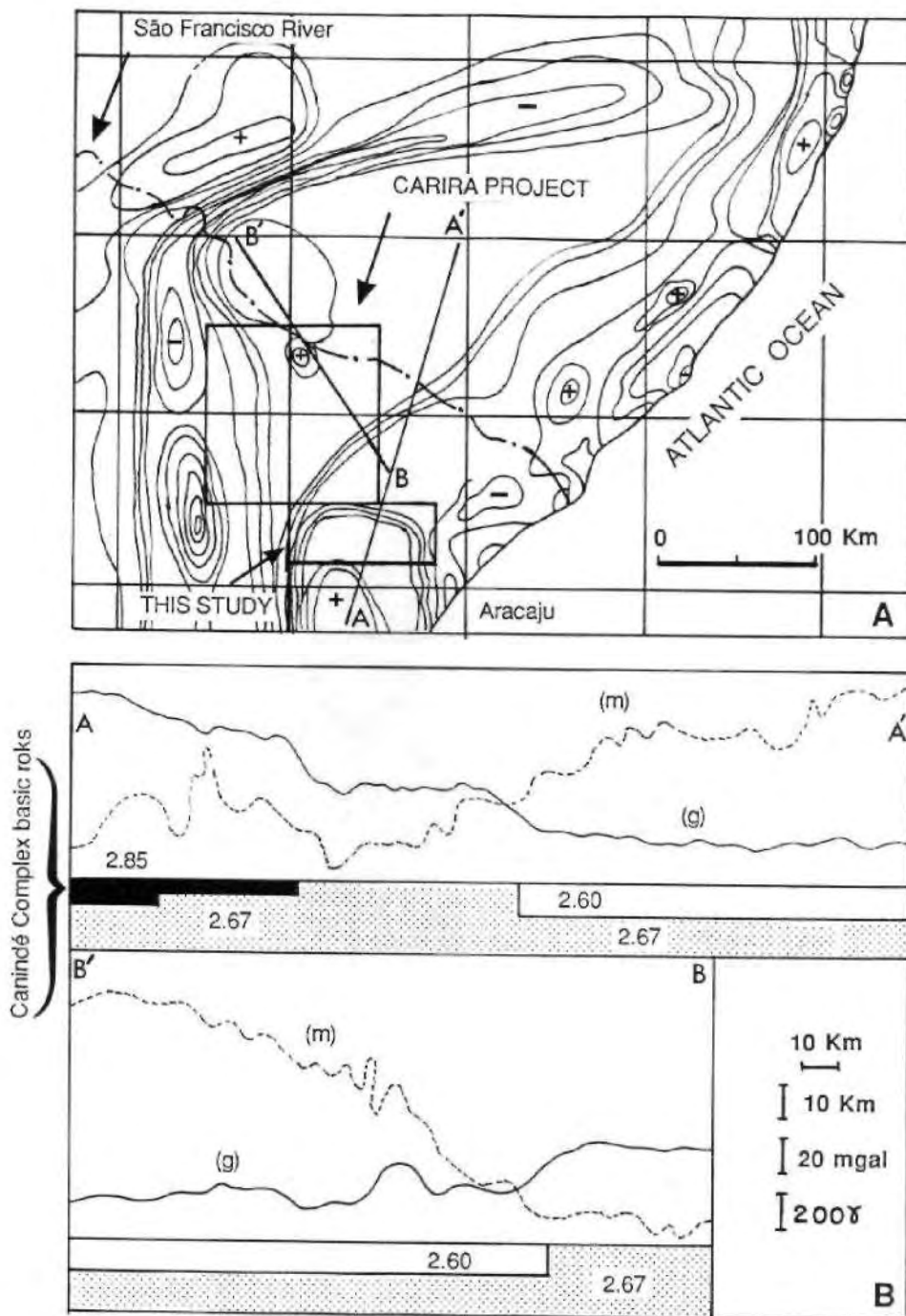


Figure 2.7 - (A): Bouguer anomaly map of the eastern part of the Sergipano Fold Belt, showing the profiles AA' and BB'. Values and contour levels are not available in the original publication. (B): Profiles AA' and BB', showing the observed gravity data (g) and magnetic data (m). (Modified from Rand et al. 1980).

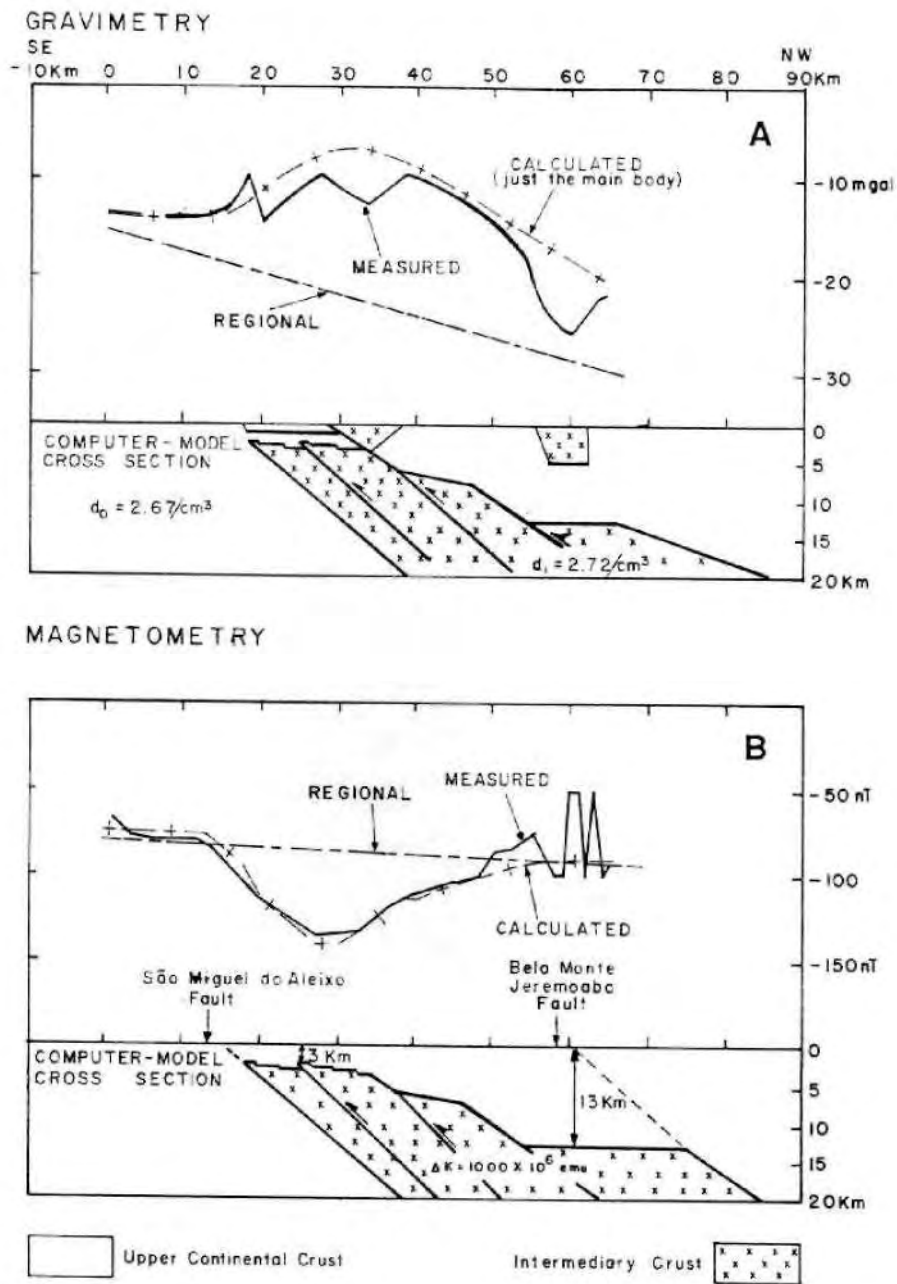


Figure 2.8 - (A) Measured and calculated gravity profiles along a general SW - NE line across the lowest right corner of the area of the Carira Project (Figure 2.7). (B) Measured magnetometer and calculated profiles along the same general direction, as in A (modified from Santos et al. 1988).

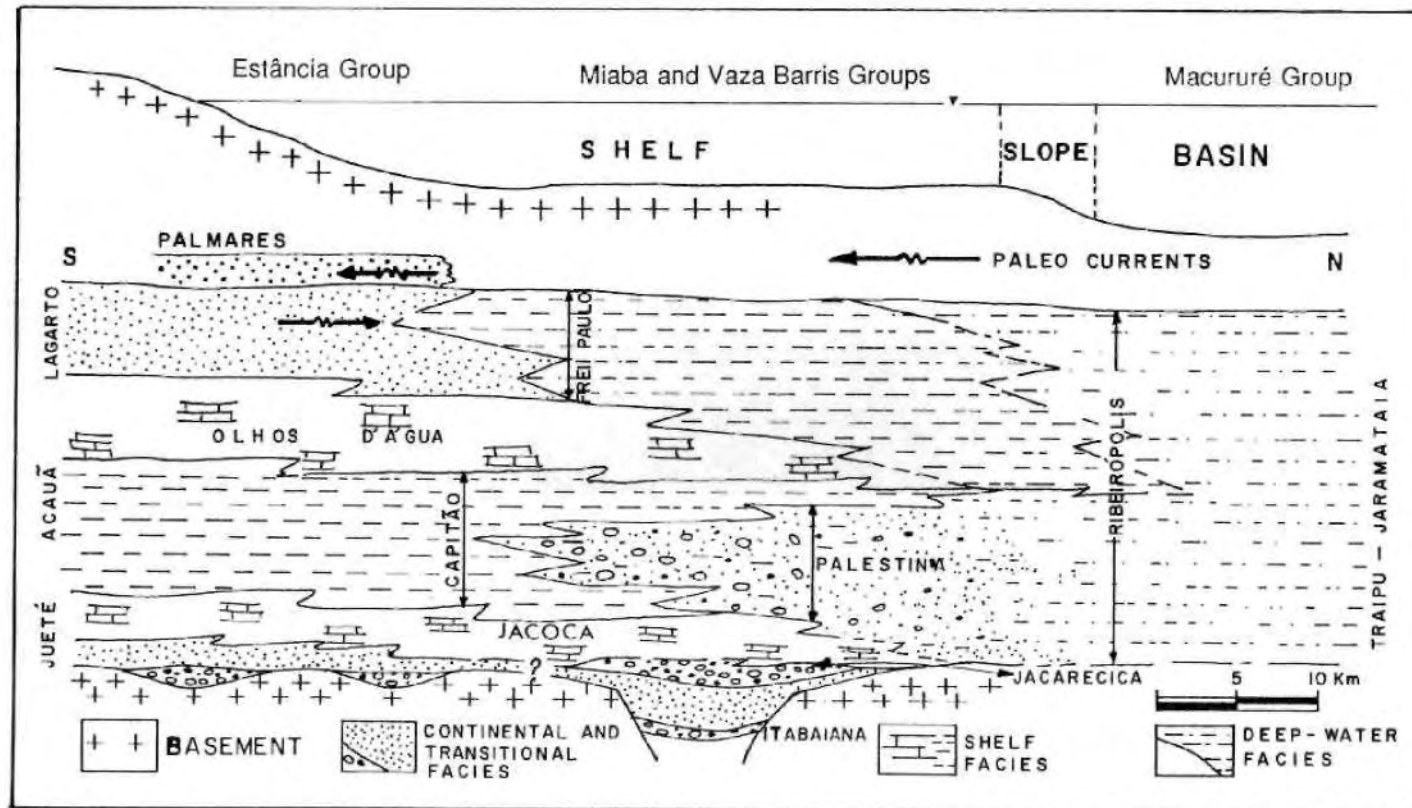


Figure 2.9 - Schematic representation of the undeformed Sergipano Fold Belt (see text). From Silva Filho et al. (1978a) and Silva Filho & Brito Neves (1979).

3. The geosynclinal stage corresponded to the final extension of the basin, thermal relaxation and gradual sinking of the crust, and deposition of the third sedimentary cycle, in different environments: the Estância Group on the platformal or pericratonic area, the Vaza Barris Group and the top of the Macururé Group in the deeper part of the basin (Fig. 2.9).

4. In the **orogenic** stage, the closure of the basin resulted in folding, uplift and erosion of the internal zones and supplied siliciclastics for the deposition of the Palmares and Juá Formations, respectively in foreland and in tramontane basins.

Subsequent to the above model, although different hypotheses have been produced to explain the closure of the basin, the basic stratigraphy of the southern part of the Sergipano Fold Belt and its tectonic implications have not been questioned. In particular, the origin of the Palmares sandstones has not been challenged. In these models the basement domes have been treated as simple tectonic slices.

These conceptual models are illustrated in Figure 2.10. The currently most accepted model involves collision between the São Francisco and the Pernambuco-Alagoas blocks, probably in an intracratonic setting (Fig. 2.10 C-E).

Jardim de Sá et al. (1986) argued for a low-angle simple shear-thrust regime (Fig. 2.10 C) where the thrust stacking would explain the crustal thickening to the north, and back-thrusting would explain the northward vergence in the northern part of the belt. The strike-slip movement along the main faults is the ultimate evidence of the progressive shortening and locking-up of the regional folds.

Brito Neves et al. (1987) and Campos Neto & Brito Neves (1987) described evidence of nappe structures in the whole belt and attempted to relate these structures to deep-rooted crustal faults (Fig. 2.10 D).

In contrast to the above models, Davison & Santos (1989) emphasises the role of possible large-scale sinistral strike-slip movements along the high-angle thrusts (Fig. 2.10 E) to juxtapose entirely different structural domains.

2.9 - Plate Tectonic setting of the Sergipano Fold Belt

The Sergipano Fold Belt is considered part of the Pan-African-Brasiliano fold system, which in Brazil and Africa consists of a frame of cratons and fold belts (Fig. 2.11 A; Brito Neves 1975; Torquato & Cordani 1981; Porada 1989). As it is surrounded by six other cratons and five fold belts (Fig. 2.11 B) the São Francisco Craton appears to play a special role in the evolution of the entire system (Couto 1984).

The regional and wider importance of the Sergipano Fold Belt was first highlighted when Allard (1969), and Allard & Hurst (1969) pointed out the extreme similarity between the Vaza Barris Group and the Nadjolé schists of Gabon, Africa, which are part of the 1300km-long West Congolian fold belt (Coward 1981 a; Schermerhorn 1981). Subsequently, different correlations of the Sergipano Fold Belt have been proposed for its African counterparts (Cordani 1973; Torquato 1974; Torquato & Cordani 1981; Jardim de Sá et al. 1981; Trompette 1982).

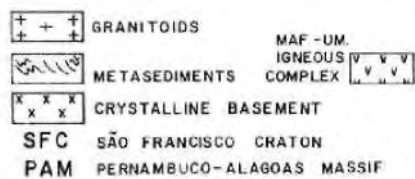
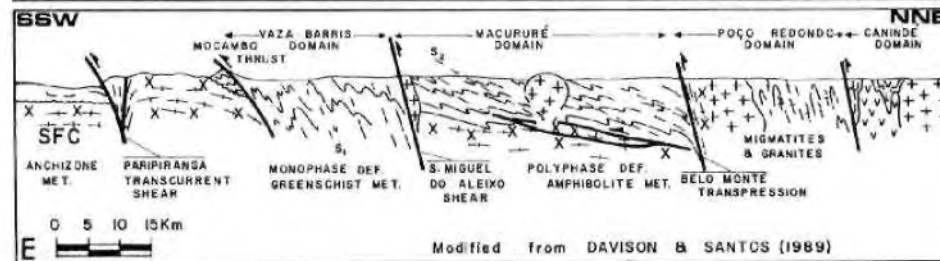
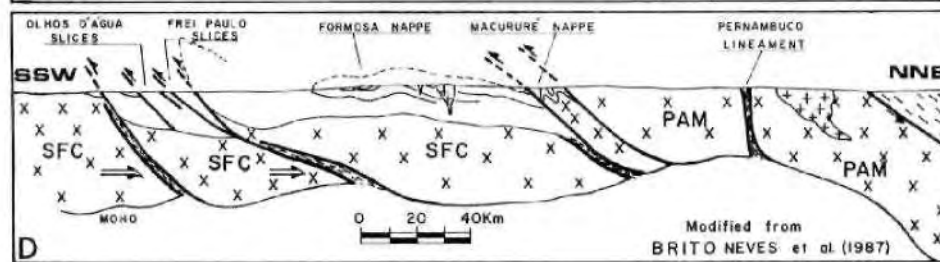
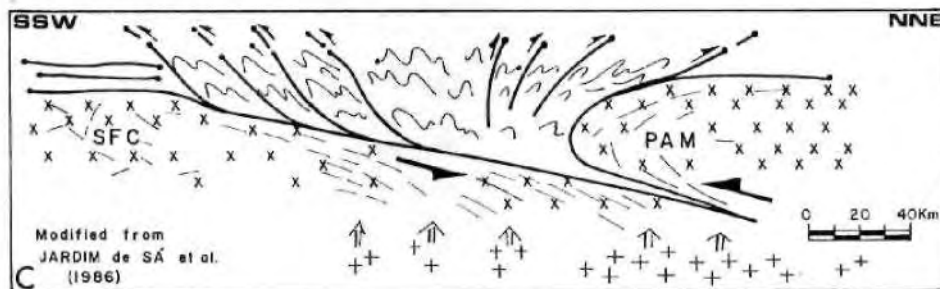
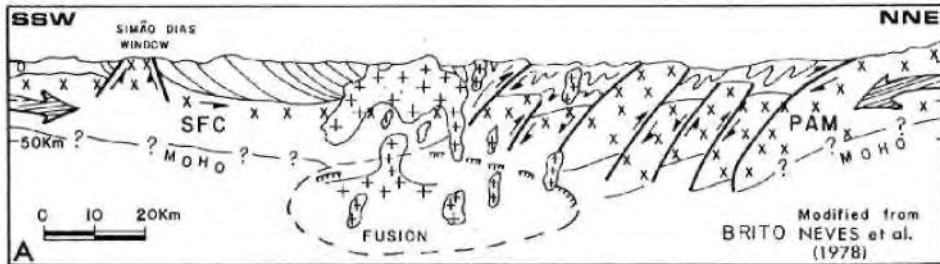
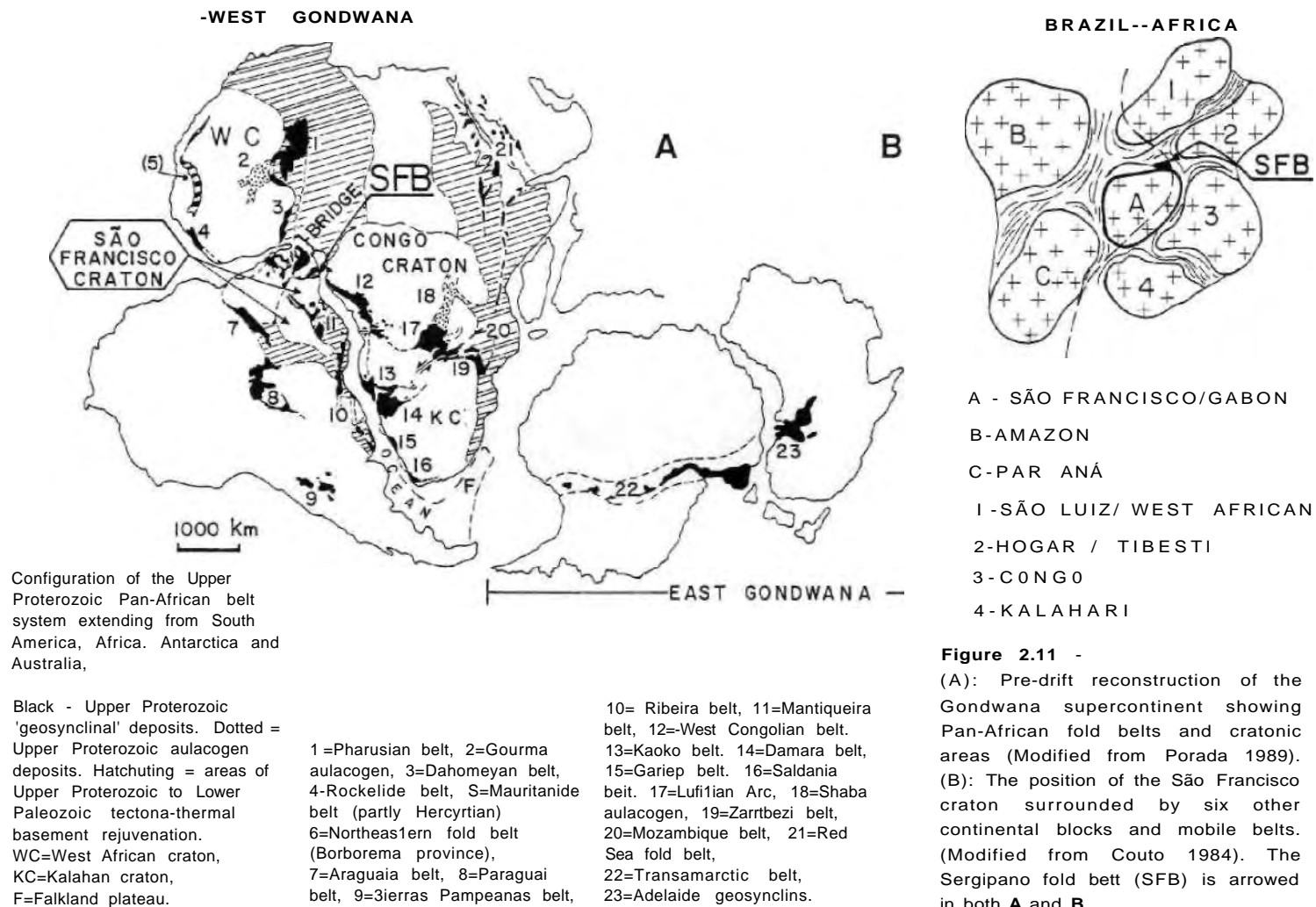


Figure 2.10 - (A to D): General SSW-NNE cross sections to show different models that have been proposed for the closure of the Sergipano basin. (E): A model for the probable tectonic juxtaposition of different basins (see text for details).



Davison & Santos (1989) discussed several possible correlations, and concluded that the Sergipano Fold Belt is probably part of a much longer E-W orogen stretching along the northern border of the São Francisco and West Congo Cratons in their pre South Atlantic configuration (Fig. 2.11 B) and attributed a key role to the Sergipano Fold Belt for the understanding of the Brasiliano orogeny.

2.10 - Discussion

Figure 2.12 is a cartoon to represent the main geological features and the two principal models for the tectonic evolution of the Sergipano Fold Belt. The model in Figure 2.12 A involves a single basin closed by a frontal collision, leading to the evolution of a classic fold-and-thrust belt, whereas the model in Figure 2.12 B argues for an oblique collision between the Pernambuco-Alagoas Massif and the São Francisco Craton, with the juxtaposition of different domains due to large-scale strike-slip movements along the regional faults.

The first model does not consider the existence of the basement domes cored by metasediments near the foreland. The second model, although being increasingly applied in the current literature of fold belts and collision zones (as in Hodsworth & Strachan 1991), does not take into account the difference in the sense of the strike-slip movements along the regional faults on both sides of the Tucano-Jatobá basin.

Apart from the detailed description of the lithofacies in the Estância Group (Saes 1984; Moraes et al. 1987; Conceição Filho & Sales 1988) and from lithofacies analysis in the Vaza Barris Group, in the very southern part of the Carira Project, an area comparatively poor in outcrops and with numerous fault contacts (Santos et al. 1988), no comprehensive and detailed study has been carried out around the Itabaiana and Simão Dias domes since the research of Humphrey & Allard (1967, 1968, 1969).

From their pioneer research, several indications of a possible tectonically controlled sedimentation were given, particularly about the origin of the diamictites and about the uplift of the Itabaiana dome. These indications have been renewed in a general approach by Silva Filho et al. (1978 a & b) and Silva Filho (1982), but have never been looked in detail by other researchers working in the area subsequently.

This overview obviously points to the Itabaiana Dome Area as a key if any reasonable contribution is to be made in the geology of the southern Sergipano Fold Belt, towards a better understanding of the entire belt and towards the understanding of the Late Proterozoic craton-belt system of Brazil and Africa.

In fact, among the belts which surround the São Francisco Craton, the Sergipano Fold Belt uniquely has crystalline basement domes mantled by a relatively preserved low to medium grade metamorphic sequence. The Itabaiana Dome Area, contains sedimentary and structural relationships best preserved than anywhere else in the Sergipano Fold Belt, and is suitable for the detailed study of the basement-cover relationships. These relationships are considered the key in the understanding of the tectonic evolution of Proterozoic fold belts by Naha & Mohanty (1989), who studied the Aravalli Group in India.

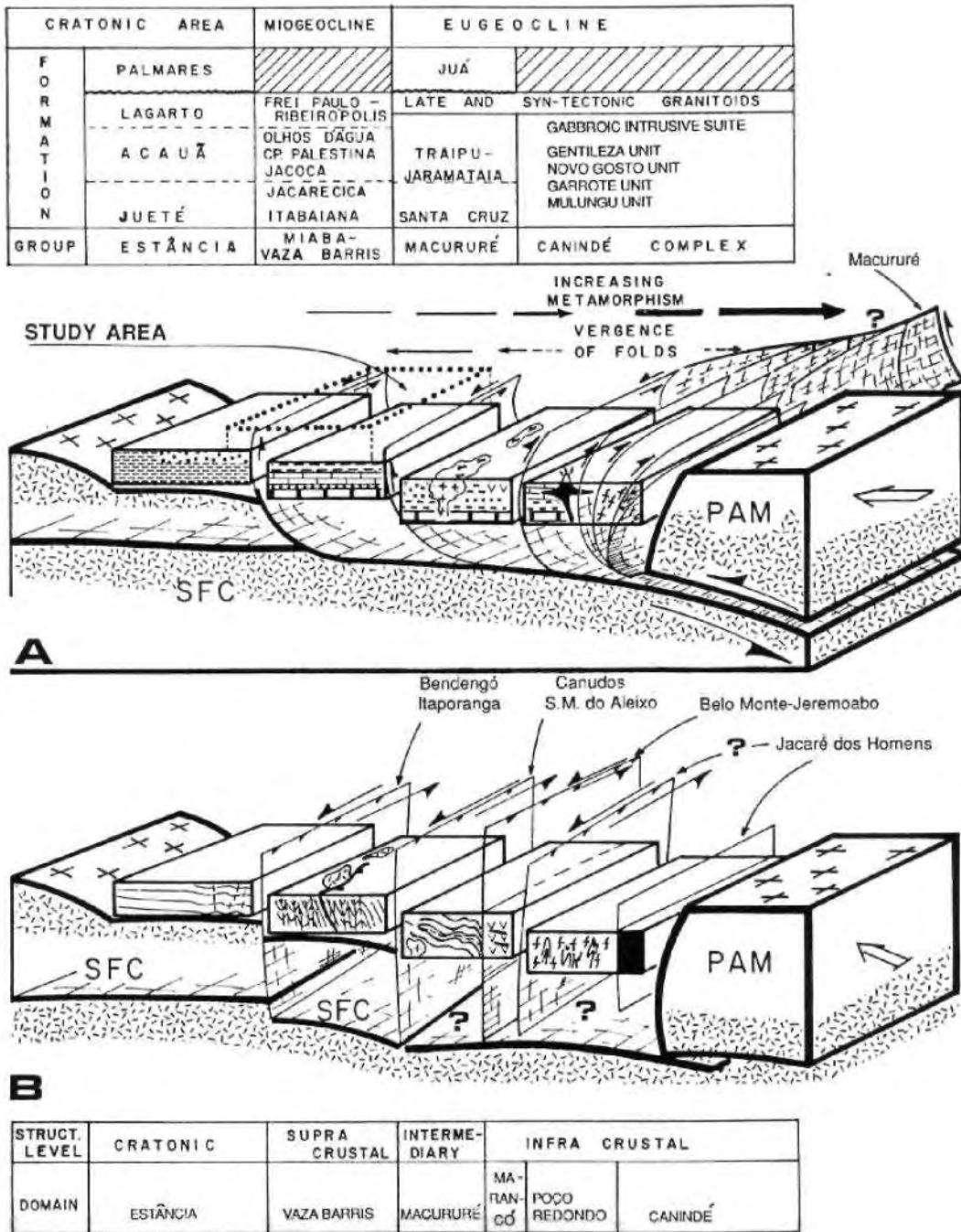


Figure 2.12 - Cartoons to illustrate the two main hypotheses for the tectonic evolution of the Sergipano Fold Belt. (A): A continuous basin with laterally equivalent lithologies now imbricated by major SSW verging thrust faults associated with minor strike-slip movement. (B): Basins with different lithological, tectono-metamorphic and magmatic characteristics, juxtaposed along major strike-slip faults which result from an oblique collision.

2.11 - Conclusions

1 - The Sergipano Fold Belt resulted from the evolution of a Middle-Late Proterozoic possibly intracratonic basin closed during the 900-600Ma Pan-African-Brasiliano orogeny. The geology of the Sergipano Fold Belt can be summarised as in Figure 2,12.

2 - The stratigraphy of the belt (Fig. 2.12 A) is comprised of the cratonic Estância Group, the miogeoclinal Miaba and Vaza Barris Groups, and the eugeoclinal Macururé Group. These are separated by ESE-WNW trending, regional thrust and strike-slip faults. The Archean-Early Proterozoic crystalline basement crops out in the Jirau do Ponciano mantled dome, in the northern part of the belt, and in the Itabaiana and Simão Dias mantled domes, in the southern part of the belt. The first age of sedimentation in the southern part of the belt is more likely to have been around 1000-900Ma.

3 - The structural evolution is generally described in terms of F_1 - F_2 folding phases associated with thrusting and greenschist up to amphibolite facies (650Ma old) metamorphism. The main mappable structures are ESE-WNW trending, moderately inclined to up-right, south-southwestern verging, open to tight and gentle plunging F_2 folds, which co-axially re-fold recumbent F_1 folds and/or an intense S_1 foliation. The F_2 folds developed a pervasive, pressure solution-type axial planar foliation (S_2), and is associated with the ESE-WNW trending regional faults. F_1 - F_2 structures are co-axially refolded by local, kink-style or cylindrical, open to tight, up-right to overturned F_3 folds which have a spaced cleavage axial planar foliation. Other minor structures (transversal, open to tight, upright, kink-style folds, kink bands and crenulations), are likely related to late-stage strike-slip movement along the regional faults.

4 - Many aspects of the geology of the Sergipano Fold Belt demand specific research, particularly the detailed study of the age of the sedimentation, the lithostructural continuity between the southern and northern parts of the belt, and the origin of the Canindé, Marancó and Poço Redondo Domains.

5 - This thesis aims to describe in detail the stratigraphic and structural relationships of the Itabaiana Dome Area, and to describe the tectonic evolution of the southern part of the Sergipano Fold Belt. Further objectives are to apply the data resulting from this research for the understanding of the tectonic evolution of the Sergipano Fold Belt, and to discuss the implications for the evolution of Pan-African - Brasiliano fold belts, in particular, and Proterozoic fold belts in general.

5 - The Itabaiana Dome Area uniquely contains two gneissic domes mantled by a relatively well preserved, low grade metasedimentary sequence and basement-cover relationships. The research area is so far considered the best region for such detailed studies in the Sergipano Fold Belt.

Chapter 3 - Stratigraphy of the southern part of the Sergipano Fold Belt

3.1 - Aims

This chapter aims:

- 1 - To present the stratigraphic analysis of the Itabaiana Dome Area.
- 2 - To present the stratigraphy of the southern part of the Sergipano Fold Belt.
- 3 - To discuss the implications of the data for the tectonic evolution of the Sergipano Fold Belt and adjacent cratonic areas.

This chapter presents first the geology and stratigraphy of the Itabaiana Dome Area with a brief description of the formations, lithofacies and sedimentary structures. This is followed by an analysis of the distribution of the lithofacies and an interpretation of the sedimentary environments for the siliciclastic and the carbonate megasequences in order to highlight the implications for the paleogeography of the basin in the Itabaiana Dome Area. The results of this research are combined with data from the literature, in order to erect the stratigraphy of the southern part of the Sergipano Fold Belt and to discuss the implications for the evolution of the Sergipano Fold Belt.

This chapter contains 22 figures (Figures 3.1-3.22), one table (Table 3.1) and additional documentation, presented in the appendix A1 (Appendices A1.1 -A 1.8). In all the photographs hereafter, the white pen is 12cm long and the hammer 30cm long. Other scales are indicated where appropriate.

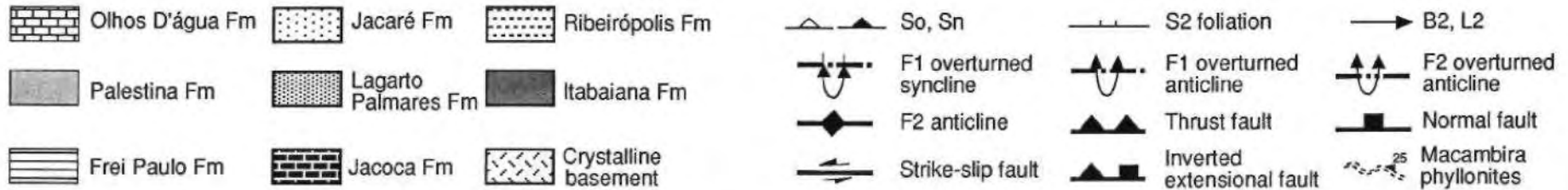
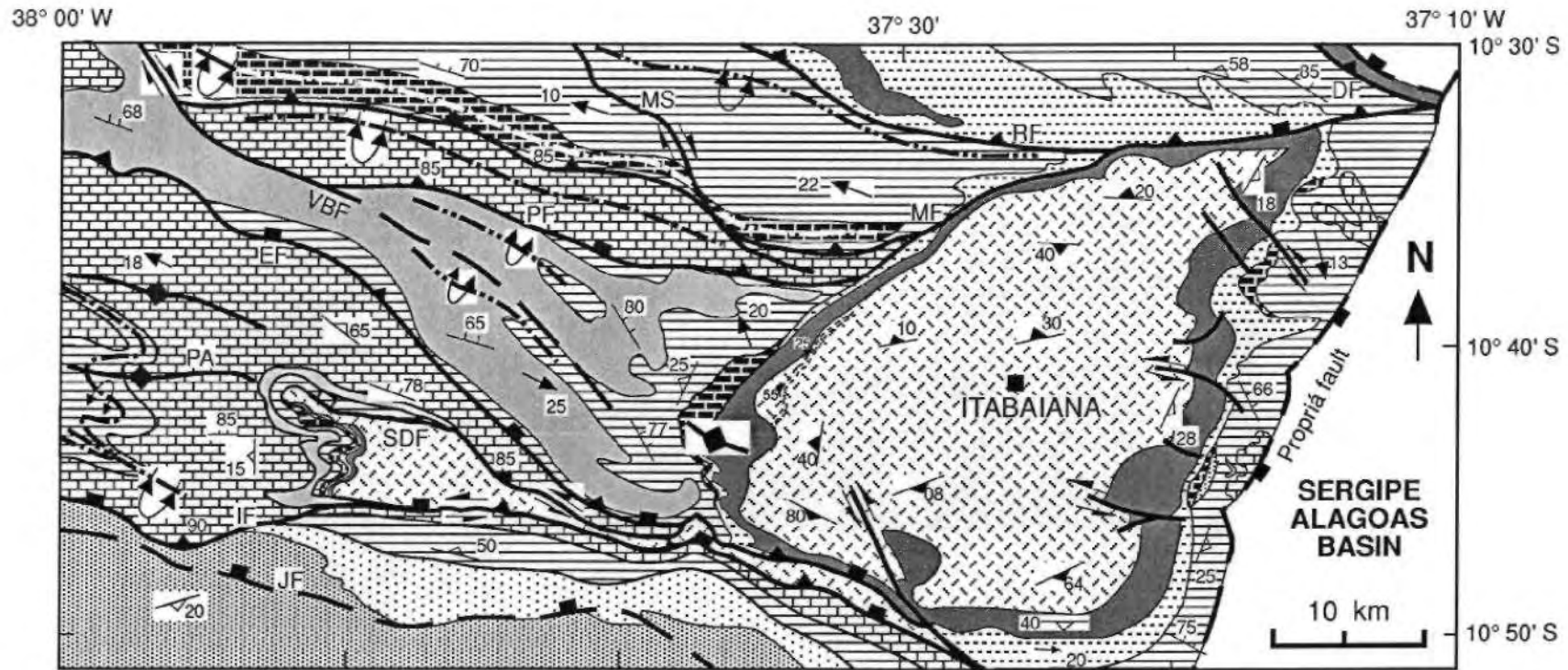
The geological map of Figure 3.1 was originally constructed at 1:50,000 scale but is presented (enclosure) at 1:100,000 scale. It contains the names of all the relevant localities and the outcrops numbered 1-1217. Figure 3.1 is also presented as a summary lithostructural map in the main body of this thesis.

3.2 - Introduction

The Itabaiana Dome Area is comprised of an amphibolite grade gneiss-granitic complex (the crystalline basement) outcropping in the Simão Dias and Itabaiana domes and a highly deformed greenschist grade metasedimentary sequence, mostly made up of quartzites, phyllites, diamictites and metacarbonates, together with generally flat lying sandstones (in the SSW part of the area, Fig. 3.1).

The metasediments occur to the west of the the Propria fault, surround the two basement domes and extend westward in WNW-ESE trending units. Other rocks in the mapped area include the Mesozoic sediments of the Sergipe-Alagoas basin, eastward of the Propria fault, and a local fan of Tertiary-Quaternary debris and paraconglomerates in the southern part of the Itabaiana dome (Gava et al. 1983). These were not examined in detail during this study.

The Itabaiana dome is a 450km² elliptical dome centred around the town of Itabaiana (Fig. 3.1). The dome, the longest axis of which extends for 42km in the SW-NE direction, is surrounded by the Itabaiana quartzites that outcrop in a series of prominent ranges.



PA = Paripiranga anticline, JF = Jacaré fault, IF = Itaporanga fault, SDF = Simão Dias fault, EF = Escarpa fault, PF = Pelada fault, VBF = Vaza Barris fault, MF = Mocambo fault, MS = Mocambo shear, RF = Ribeirópolis fault, DF = Dores fault.

Figure 3.1 - Summary lithostructural map of the Itabaiana Dome Area. Based on the geological map of Figure 3.1 (enclosure).

These ranges are (anticlockwise from south to west, Fig. 3.1): the Montes, Cajueiro, Comprida, Itabaiana, Merem, Canção, Capunga, Machado, Saco, Cagado, Macambira and Miaba ranges. Figure 3.2 shows a panoramic view of the Miaba range. The Simão Dias dome is much smaller than the Itabaiana dome and occurs in the vicinity of the town of Simão Dias and to ESE, in a narrow fault-bounded strip,

The main mappable structures are WNW-ESE or NW-SE trending thrust and strike-slip faults and some major folds (Fig. 3.1). From south to north, the main faults are the Jacaré, Itaporanga, Simão Dias, Escarpa, Pelada, Mocambo, Ribeirópolis and Dores faults (Fig. 3.1). The trace of the main strike-slip faults (the Vaza Barris and the Mocambo shears) lies within the metasediments. The Capunga, Montes and other local shear zones cut across the eastern and southern borders of the Itabaiana dome. The mappable folds generally occur to the north of the Itaporanga fault, and are of a F_2 phase of folding, such as the Paripiranga anticline and the sequence of folds of the Miaba range (Fig. 3.2).

The geological mapping was carried out on outcrops along roads and tracks, and along several streams and rivers (Fig. 3.1): the Vaza Barris and Salgado rivers and Jacoquinha stream (west of the Itabaiana dome); the Cova and Montes streams, and the Lomba, Trairas and Jaarecica rivers (in the Itabaiana dome); the Sergipe and Dangra rivers and the Jacoca, Morcego and Moças streams (east of the dome).

3.3 - Stratigraphy of the Itabaiana Dome Area

The metasedimentary cover is divided into the Miaba, Lagarto and Vaza Barris Groups which, together form a Mid- to Late Proterozoic, ~1000-4000m thick sedimentary wedge unconformably deposited on the Archaean to Early Proterozoic Itabaiana and Simão Dias gneisses (Fig. 3.3).

In the stratigraphic column of Figure 3.3, the pattern of the formations applies to the summary map of Figure 3.1, whereas the formation symbols (P€I, P€Ja, PC P, etc) apply to the full geological map (Fig. 3.1 enclosure).

The Miaba Group comprises the Itabaiana, the Ribeirópolis and the Jacoca Formations. It is conformably covered by the Lagarto Group which comprises the Lagarto-Palmare, the Jacaré and the Frei Paulo Formations. The Vaza Barris Group unconformably overlies the Lagarto Group and comprises the Palestina and the Olhos D'água Formations.

Although the computation of the thicknesses in the area is generally hampered by the polyphase deformation, the relative variations of thickness within each formation can be determined in some parts of the area.

The stratigraphy has been established as the result of the detailed mapping and construction of 12 sections across the basement-cover contact (summarised in Fig. 3.4).

The sections of lines AA' to LL' are plotted on a 1:143,000 scale copy of the geological map of the area (Appendix A 1.1, enclosure). The sections AA', EE', GG", JJ' correspond to Figures 3.5-3.8. The more complete stratigraphic sections are (Figs. 3.5 & 3.8) are AA', in the western side of the Simão Dias dome, and JJ' in the



Figure 3.2 - A panoramic view of the Miaba range as seen from the inner Itabaiana dome, showing the Itabaiana quartzites affected by gentle to open F2 folds. The outcrops of the crystalline basement (the low land in the foreground) is generally covered by colluvium. The S-N distance is about 5km.

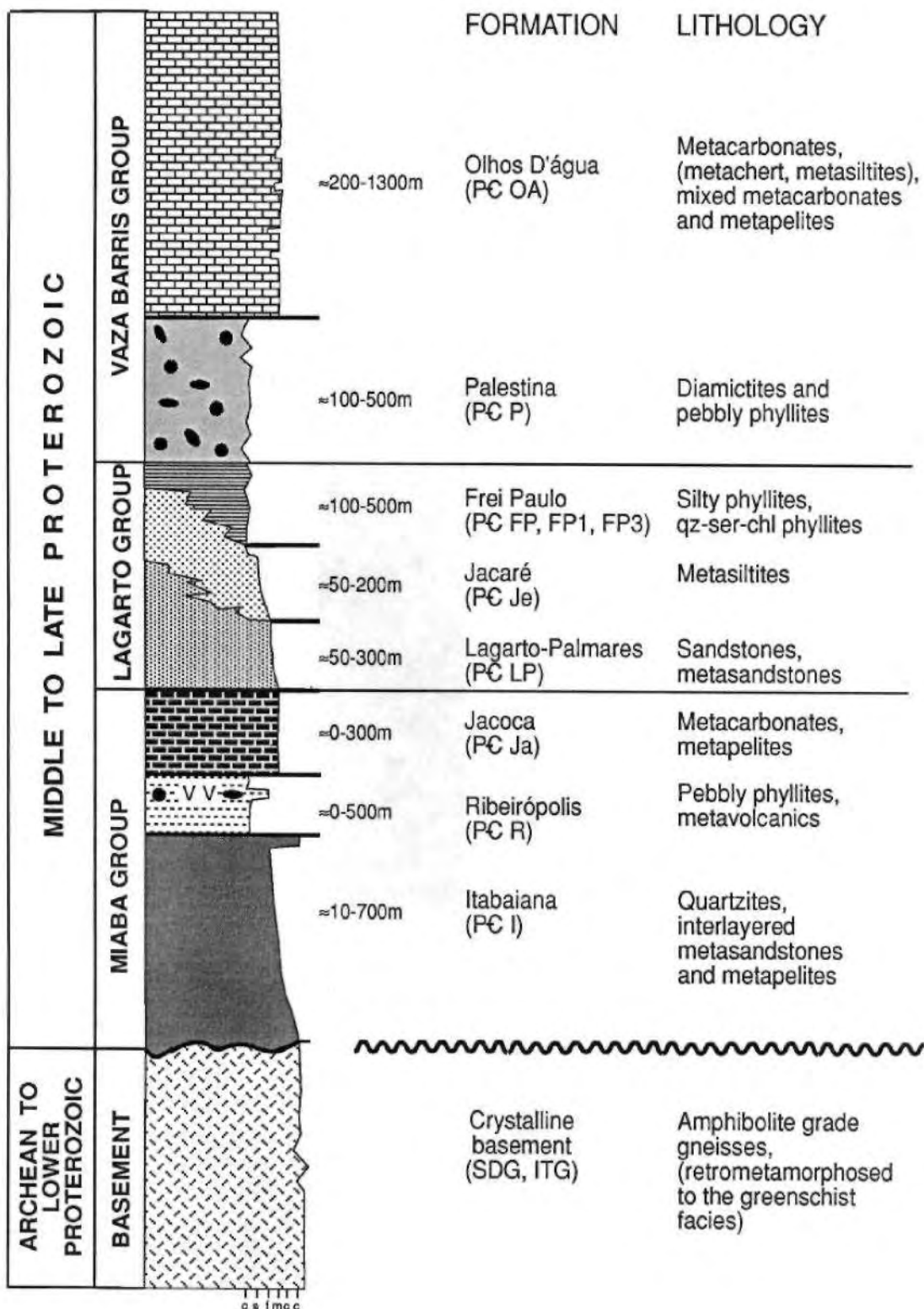


Figure 3.3 - Summary stratigraphy of the Itabaiana Dome Area. The Formation patterns apply to the summary map (Fig. 3.1). The Formation symbols (e.g. PC I) apply to the main geological map of Figure 3.1 (enclosure).

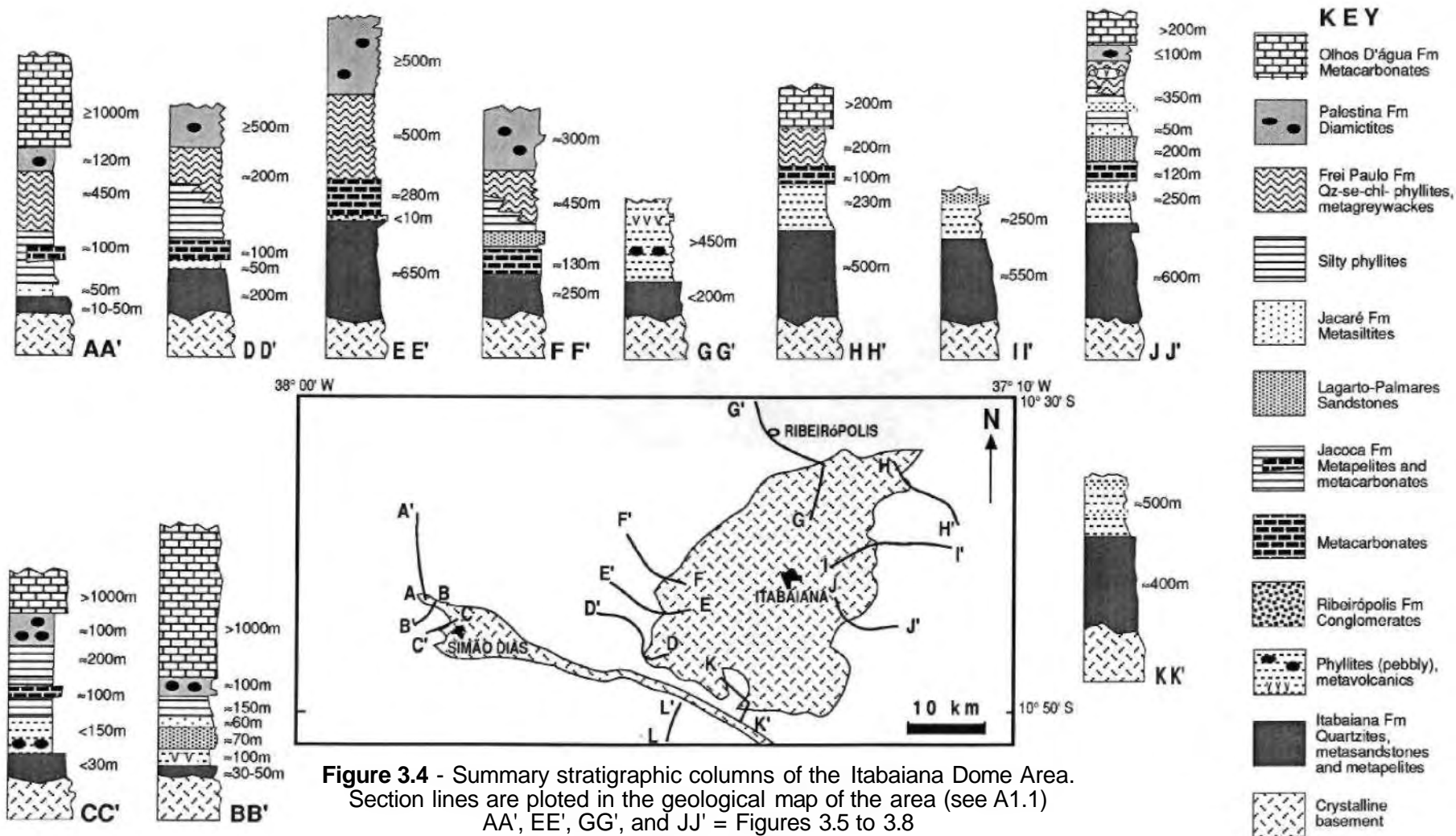


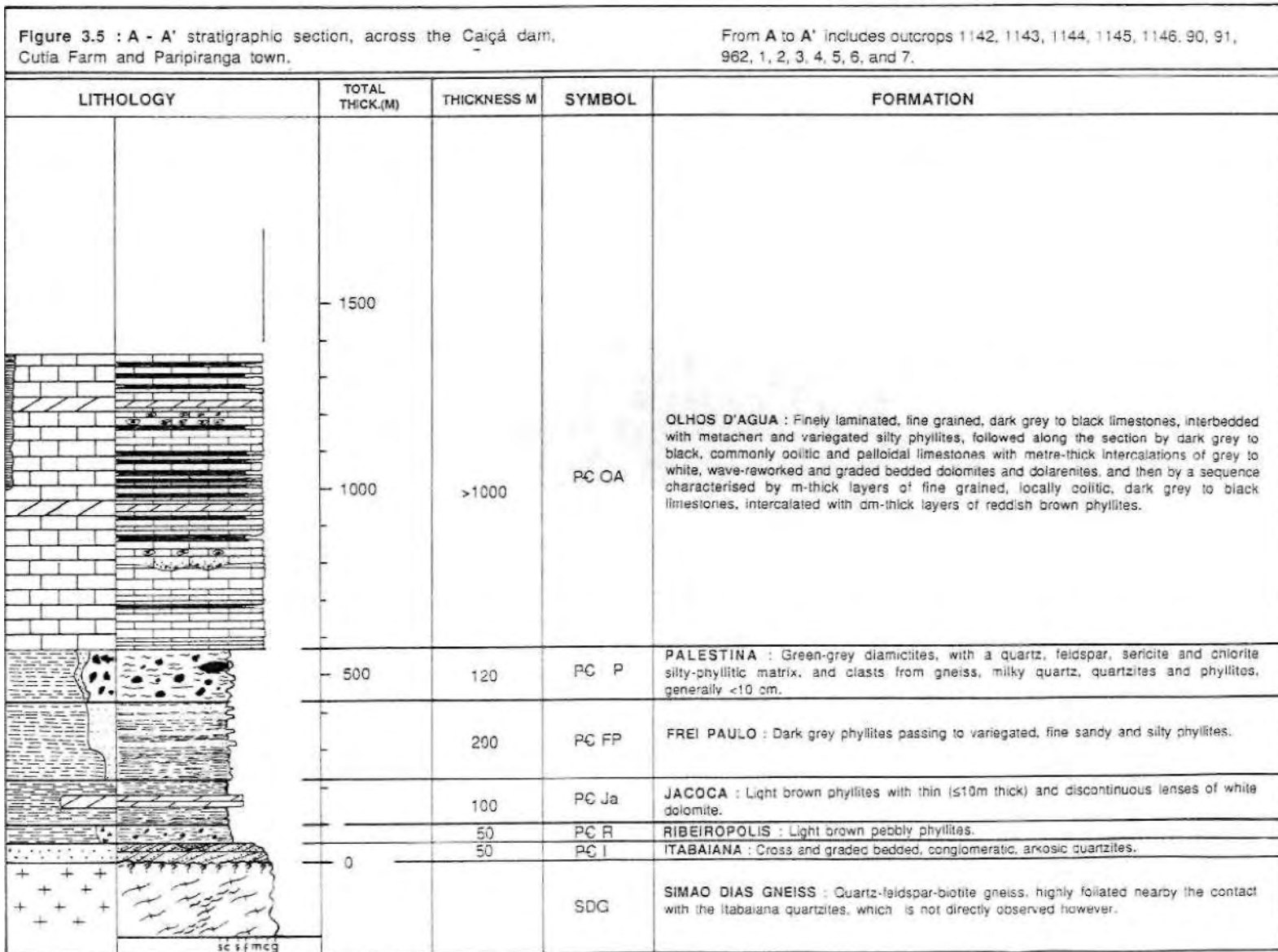
Figure 3.4 - Summary stratigraphic columns of the Itabaiana Dome Area.

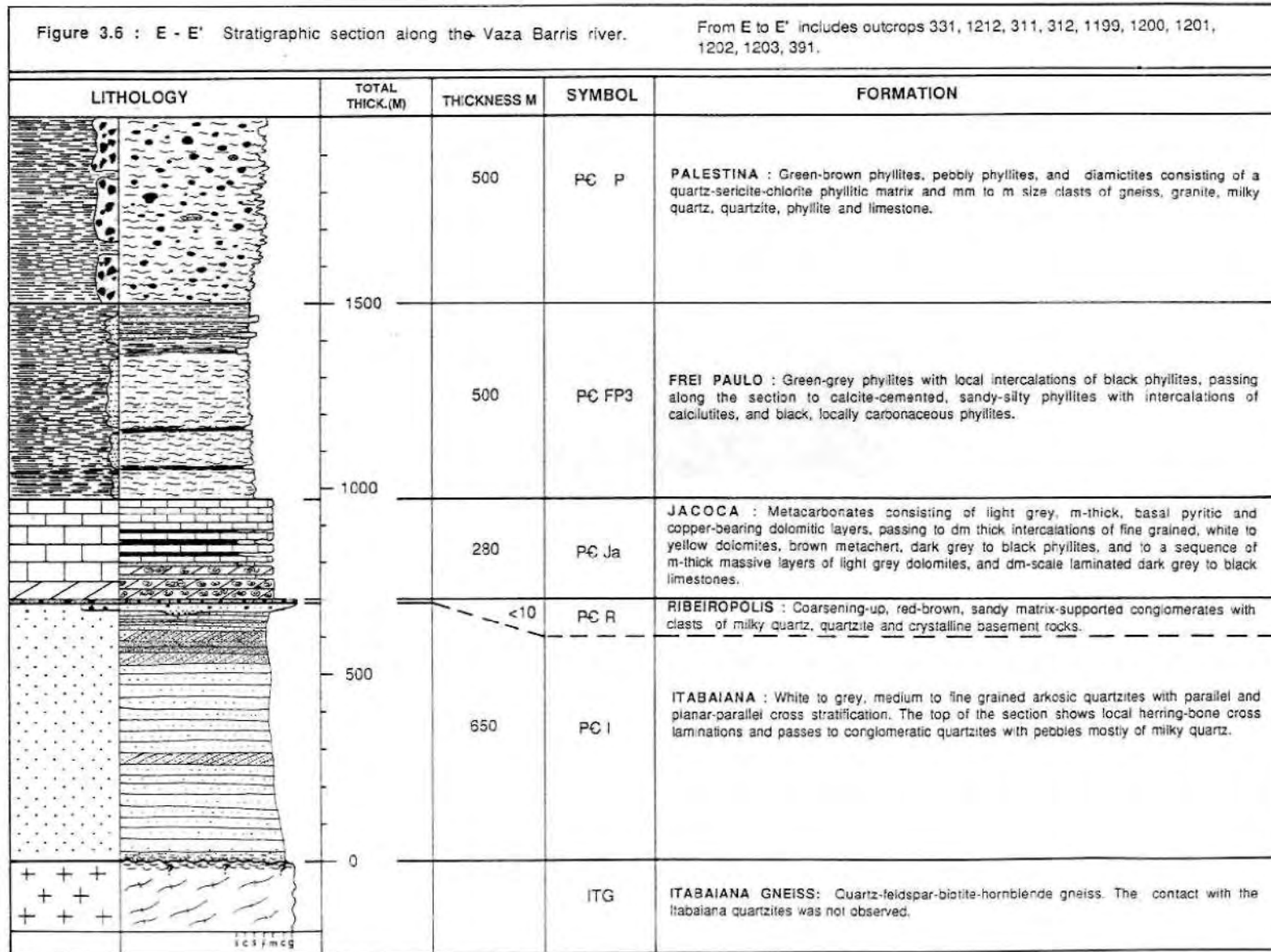
Section lines are plotted in the geological map of the area (see A1.1)

AA', EE', GG', and JJ' = Figures 3.5 to 3.8

LL' = Figure 3.14

BB', CC', DD', FF', HH', II', KK' = A1.2 to A1.8





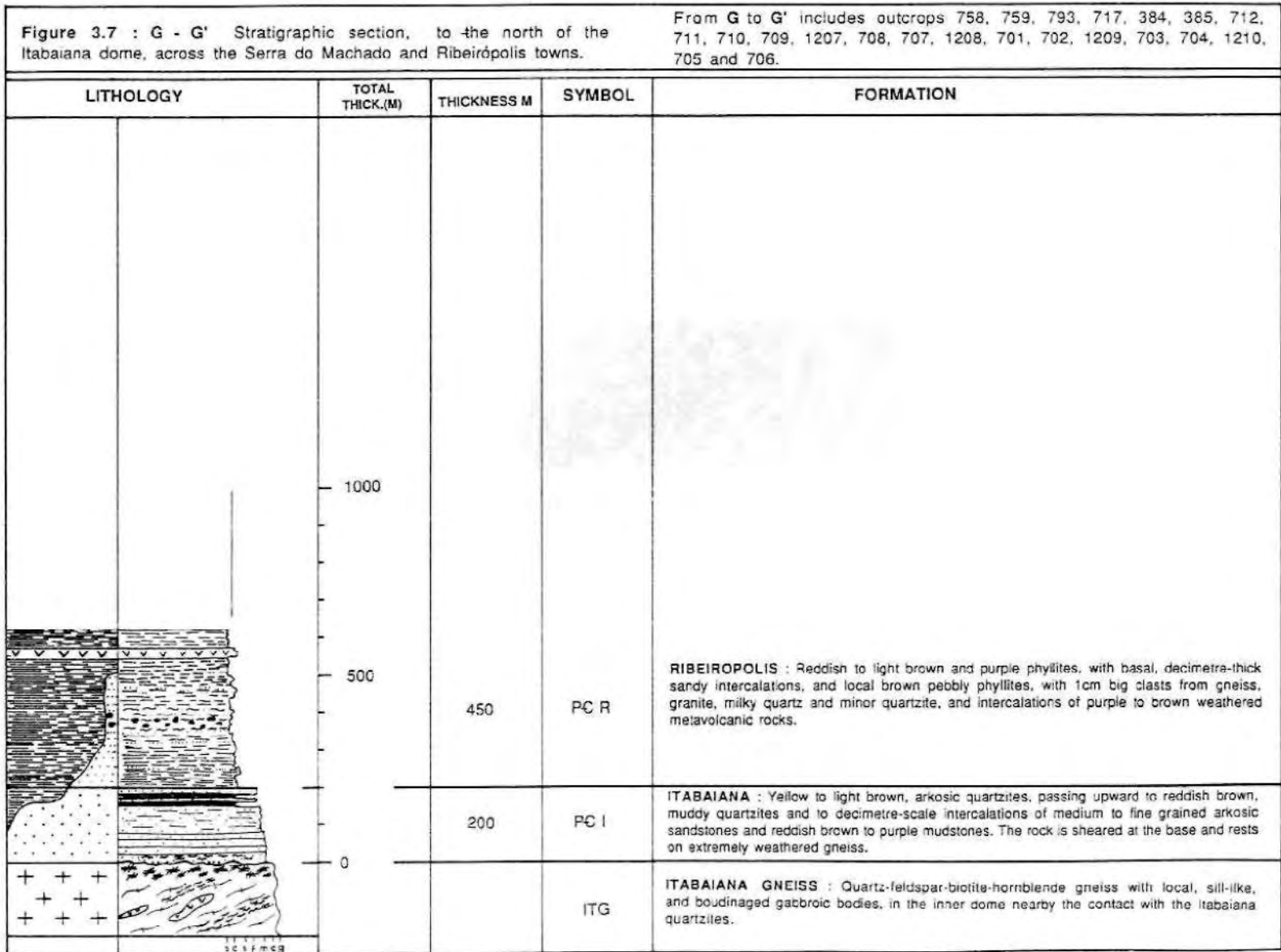
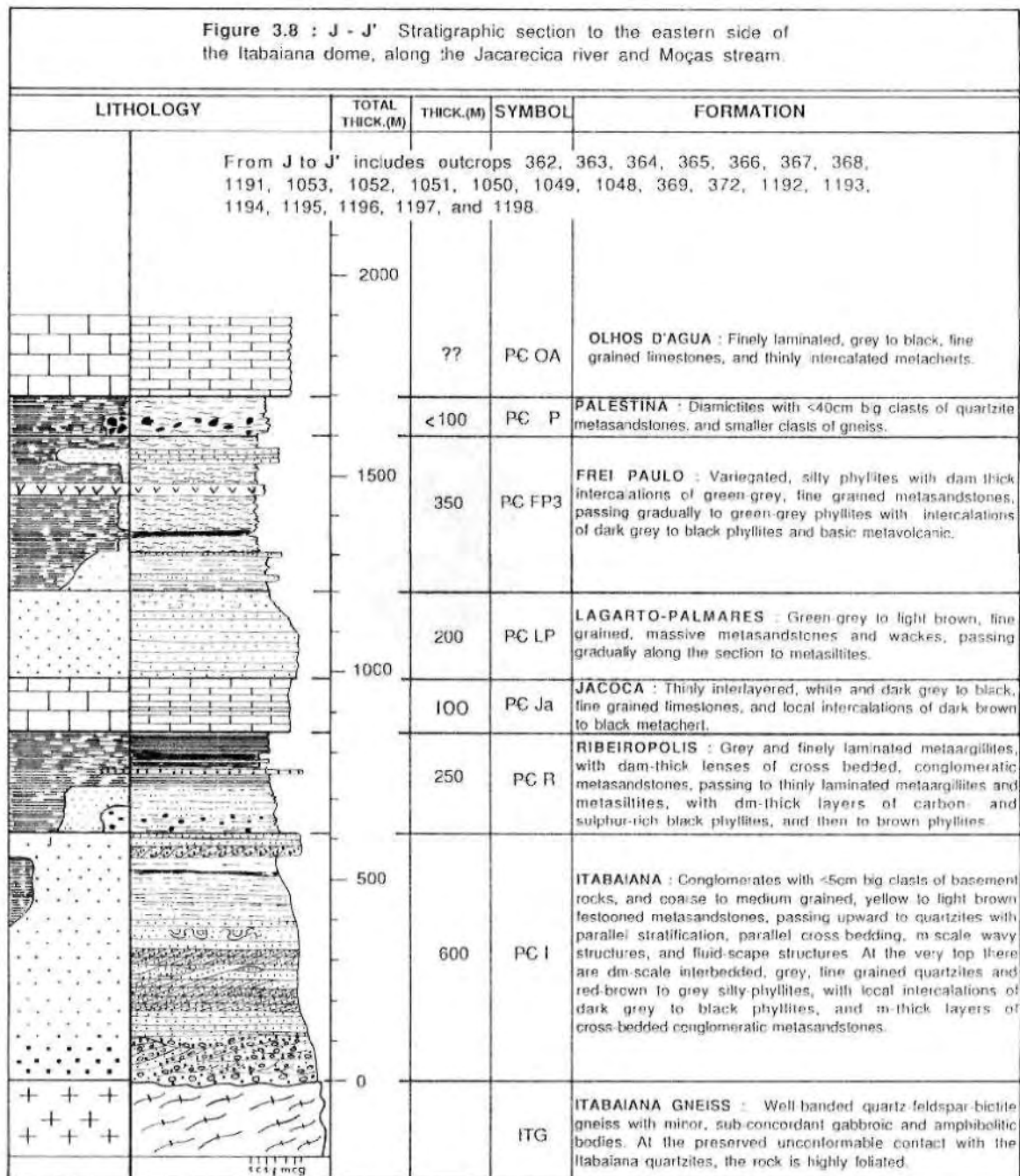


Figure 3.8 : J - J' Stratigraphic section to the eastern side of the Itabaiana dome, along the Jacarecica river and Moças stream.



eastern side of the Itabaiana dome. Sections EE' and GG' contain relevant information for lateral correlation. Section LL' (Fig. 3.14) is specific for the upper part of the Lagarto Group. Sections BB', CC, DD', FF', HH', II' and KK' contain additional information and are presented in the Appendix A1 (A 1.2 to A1.8).

3.3.1 - The crystalline basement

The crystalline basement is a Rb-Sr 2500Ma old gneissic-granitic complex (Hurley 1966). It consists of amphibolite grade, granitic to granodioritic gneisses and orthogneisses with mylonites and phyllonites derived from these lithologies. Small, local, sheet-like granitic bodies, and disrupted bodies of amphibolites, hornblende gabbros and gabbro pyroxenites are also evident. To the south of the Itabaiana Dome Area the basement gives 1800 Ma Rb-Sr ages (Brito Neves & Cordani 1973; Mascarenhas et al. 1984).

The gneisses and orthogneisses are composed of coarse-grained (=0.5cm on average) quartz, plagioclase and K-feldspars, biotite (hornblende), muscovite, sericite, chlorite and epidote. Accessories are apatite, sphene, zircon, and opaque minerals. Garnet occurs locally.

The gneisses and orthogneisses are distinguished by the more or less continuous metamorphic banding. The former have a laterally continuous layering defined by bands of medium- to coarse-grained quartz and feldspars interbanded, on a centimetric scale, with biotite-muscovite-epidote (hornblende) rich bands (Fig. 3.9 A). The orthogneisses commonly show an inhomogeneous and less continuous banding with 1 cm size feldspar porphyroblasts which are more or less rotated and elongated according to the intensity of the local deformation.

In thin section, both lithologies show commonly elongated quartz grains with undulose extinction and saussuritised feldspars. Biotite and muscovite or sericite, and chlorite normally occur as fine flakes disposed along banding-parallel mica-domains. Biotites are transformed to chlorites along the cleavage surfaces which have associated with thin Films of red-brown iron oxide. Where found, hornblende is commonly retrogressed to epidote.

Basement-derived mylonites generally consist of a <1mm fine-grained matrix and mm-size porphyroclasts of K-feldspars, plagioclase and epidote. They commonly show S-C fabric relationships (Lister & Snoke 1984). The matrix consists of recrystallised quartz and feldspars grains with a preferred orientation parallel to the S planes. The C planes are marked by extremely fine grained quartz, epidote, sericite, chlorite and biotite.

3.3.2 - The basement-cover contact

The crystalline basement is overlain by the Itabaiana, Ribeirópolis, Palestina and Olhos D'água Formations (Fig. 3.1). The basement-cover contact is generally low-angle dipping around the Itabaiana dome (dipping away from the centre, in all directions) and in the western Simão Dias dome, but dips at high-angles in the rest of the area.



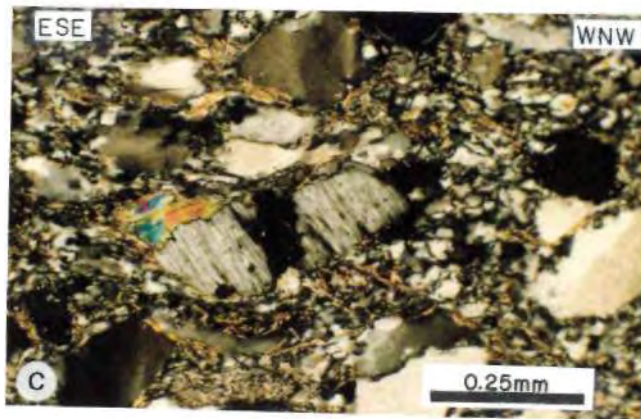
A : Homogeneous banding of the Itabaiana gneiss consisting of quartz-feldspar dm-thick layers and intercalated cm-thick mica layers.
Outcrop 334, NW of São Domingos town.



B : Undeformed unconformable contact between highly foliated gneiss and basal Itabaiana conglomerates.
Outcrop 365, Jacarecica river, eastern Itabaiana dome.



C : Quartz-feldspar-sericite-chlorite phyllonites of the western Itabaiana dome, affected by pervasive shear bands which indicate a top down to WNW movement. Outcrop 323, SW of Macambira.



D : Sheared Itabaiana quartzites overlying the phyllonites in C. A top down to WNW movement is also indicated by the fractured pulled-apart feldspar, and rotated quartz grains. Photograph under crossed polars. Thin section parallel to the elongation lineation and perpendicular to the bedding-parallel foliation. Same locality as C.

Figure 3.9 - The crystalline basement and the contact relationships.

Despite discontinuous outcrops and the weathered appearance of the grasses in some places, it can be seen that the basement and cover are generally sheared or mylonitic along the contact the basement-cover contact is mostly undeformed along the eastern margin of the Itabaiana dome (Fig. 3.9 B). and in parts of the western border, between the town of Macambira and the northern edge of the Miaba range (Fig. 3.1)

In the Macambira area, however, the Itabaiana quartzites occur in some places directly above basement-derived quartz-feldspar-sericite-chlorite phyllonites. Southwest of Macambira, where a secondary road cuts the basal contact and leaves the dome to the west (Fig. 3.1, outcrop 323), the phyllonites dip 20° to NNW and are affected by small-scale, asymmetric, WNW verging folds and by a pervasive and finely spaced set of shear bands which dip 25° to WNW (Fig. 3.9 C).

These structures indicate a top down to WNW extensional movement. In thin section, the basal Itabaiana quartzites from this locality are also mylonitic. They contain elongated, pulled-apart and rotated feldspar grains, and elongated quartz grains, both with pressure shadow zones. The structures shown in the quartzites resemble imperfectly developed shear bands (Fig. 3.9 D) but also indicate a top down to the WNW extensional movement.

The phyllonites can be traced southwards from outcrop 323 to outcrop 1217 in the Cova stream (Fig. 3.1), where the phyllonitic foliation dips 55° to W and the extensional shear bands dip 50° to WNW.

Humphrey & Allard (1969) described that in the northern edge of the Miaba range the phyllonites trend to the SW and pass underneath the locally SE trending basal unconformity, between the Itabaiana quartzites and the gneisses. They also described NW trending meso-scale folds that have deformed the phyllonites, together with the shear bands and the Itabaiana quartzites.

In at least two other western localities the Itabaiana gneisses are also affected by low-angle, WNW dipping local extensional faults (outcrop 554, ENE of Macambira) or extensional shear bands mostly affecting the mica-rich layers (outcrop 1215, Cova stream). A generally low-angle, WNW plunging mineral stretching lineation is also present in these outcrops. All of the kinematic indicators observed in these outcrops indicate top down to WNW extensional movement.

3.3.3 - The Miaba Group

The Miaba Group consists of the Itabaiana quartzites, the Ribeirópolis pebbly phyllites, and the Jacoca carbonates. The thickness of this group varies from 200m. in the western Simão Dias dome, to 1100m on the eastern and western sides of the Itabaiana dome.

The Itabaiana Formation (P€ I)

The Itabaiana Formation is 400-700m thick in the eastern and western borders of the Itabaiana dome, 30-200m in the rest of the area, and is comprised of a sandy and a muddy lithofacies (Fig. 3.10).



A : Medium to fine grained, planar-parallel cross bedded quartzites of the middle section of the Itabaiana Formation. Outcrop 963, Comprida range, eastern Itabaiana dome.



B : Conglomeratic quartzite of the upper Itabaiana Formation. Outcrop 312, Capitão Farm.



C : The muddy lithofacies of the Itabaiana Formation, consisting of m-thick, laterally discontinuous layers of cross-bedded metasandstones and wackes, intercalated with red-brown phyllites. Outcrop 227, western Simão Dias dome.

Figure 3.10 - The Itabaiana Formation (PC I).

The sandy lithofacies surrounds most of the Itabaiana dome, the western part of the Simão Dias dome and is also found in the Volta range (in the NE corner of the area). It consists of white to grey or yellow, fine to medium grained (0.15 - 0.50mm) feldspathic quartzites, orthoquartzites and minor, decimetre to centimetre-thick siltstone beds. Mappable slices of mylonitic Itabaiana quartzites occur within the Simão Dias gneiss (Fig. 3.1).

The muddy lithofacies occurs along the Redonda and Campina ranges to the north of the Itabaiana dome (Fig. 3.1) and also in the western part of Simão Dias dome. It consists of 1 m-thick layers of arkosic sandstones and arkosic quartzites interbedded with 1m-thick layers of reddish brown mudstones and phyllites.

The most typical section (Fig. 3.8) starts with local bodies of 10m-thick matrix-supported conglomerates and conglomeratic sandstones, with basement-derived clasts. These pass gradually into 100's of metres of 10-30cm thick beds of white to grey, fine to medium-grained, small to meso-scale parallel cross-bedded feldspathic quartzites (Fig. 3.10 A).

At the top, this fining upwards sequence consists of grey to reddish brown, fine-grained metasandstones, metasiltites and meta-argillites, but 1-10m-thick lenses of conglomerates (Fig. 3.10 B) or conglomeratic and cross-bedded sandstones may occur instead, particularly to the eastern and western margins of the Itabaiana dome.

The basal feldspathic content (< 20%) diminishes up-section and most of the Itabaiana Formation shows a remarkably homogeneous quartzitic composition (with less than 5% of opaque minerals, zircon and tourmaline as accessories). Herring bone cross-stratification, convolute laminations and wavy laminations are also displayed.

The muddy lithofacies consists of muddy and micaceous quartzites and/or 10-100cm thick layers of parallel cross-bedded, arkosic metasandstones intercalated with red-brown phyllites (Fig. 3.10 C).

The correlation of the quartzites and muddy lithofacies which occur along the Campina, Redonda and Volta ranges (originally mapped as quartzitic lenses of the Frei Paulo-Ribeirópolis Formation, in Gava et al. 1983 and Santos et al. 1988) with the typical Itabaiana quartzites is supported by (a): the gradual passage of the Itabaiana quartzites to the muddy lithofacies in road cuts in the Redonda and Machado ranges; and (b): the Volta thrust, in the northeastern corner of the area, which places muddy, micaceous quartzites and unmappable slices of basement-derived mylonites over the Frei Paulo phyllites.

The Ribeirópolis Formation (P€ R)

The Ribeirópolis Formation is proposed here as a formation to merge the Jacarecica Formation and the Ribeirópolis facies of the Frei Paulo-Ribeirópolis Formation of the old stratigraphy (Figs. 2.3 & 2.5 B).

This proposal is based on field evidence which shows a gradual passage from the quartzites and interbedded arkosic metasandstones and phyllites (Itabaiana Formation in the northern part of this study area) to red-brown silty phyllites in the Machado and Redonda ranges (Fig. 3.1). These phyllites continue up to the northern end of the area,

across the Ribeirópolis town where, together with lenses of pebbly phyllites and intermediary and acid volcanic rocks, form the Ribeirópolis facies of the Frei Paulo-Ribeirópolis Formation (Gava et al. 1983; Santos et al. 1988). This assemblage is very much similar to the assemblage mapped in gradual transition to the Itabaiana quartzites in the western Simão Dias dome (Appendices A 1.2-A 1.3) and which Humphrey & Allard (1967, 1969) mapped in the Jacarecica Formation.

The Ribeirópolis Formation consists of pebbly phyllites and local conglomerates (Figs. 3.11 A & B), white, grey to red-brown silty phyllites (Fig. 3.11 C), metagreywackes, argillites, quartz-sericite phyllites (Appendix A1.8) and generally weathered metavolcanic rocks with acid to intermediary composition. All these rocks were previously in the Jacarecica Formation and in part of the Frei Paulo-Ribeirópolis Formation (Silva Filho et al. 1978 a & b).

The Ribeirópolis Formation occurs in gradational contact with the Itabaiana Formation. In one locality (Flecheira farm, outcrop 471, Fig. 3.1) the contact is sheared along a low-angle, WNW dipping ramp. The formation is 0-300m thick around the basement domes, but may attain 500m along the WNW-ESE trending belts to the north and south of the Itabaiana dome. A small body of pebbly phyllites is mappable between the towns of Frei Paulo and Macambira (Fig. 3.1).

Due to the great variety of lithofacies, this formation lacks a type-section, but generally the pebbly phyllites and conglomerates occupy basal positions and the phyllitic facies occurs towards the top of the unit.

It is noticeable that in part of the western Simão Dias dome the Ribeirópolis Formation consists of highly foliated intermediate metavolcanics and blue to green colour phyllites (A 1.2), and that the conglomeratic lithofacies are more important in the eastern and western Itabaiana dome, where a thin and discontinuous layer of coarse sandy-supported, well-cemented, brown, coarsening-up conglomerate is present (Fig. 3.6).

A composite stratigraphic section through the Ribeirópolis Formation (Fig. 3.8) starts with white to grey, or light brown, silty argillites with parallel stratification, containing 1-10m-thick intercalations of fine- to medium-grained metagreywackes, graded bedded 5mm-grained conglomeratic sandstones, and pebbly phyllites with 10-15cm size clasts of basement rocks, milky quartz and quartzites.

This sequence passes upwards into finely laminated grey meta-argillites and light brown metasiltites which are overlain by light brown, calcareous phyllites with intercalations of carbonaceous phyllites. This succession indicates a gradual passage upward to the overlying Jacoca Formation. The basal third of this type section also occurs in the western Itabaiana dome where basal, white to grey, silty phyllites locally contain 5cm size clasts of quartzites and basement rocks (Appendix A1.4).

On the northern side of the Itabaiana dome (Fig. 3.7) the formation starts with red-brown to purple silty phyllites, and passes northward with intercalations of pebbly phyllites, light brown and purple phyllites, and possible porphyroclastic units (weathered metarhyolites and metadacites have been described as part of this sequence by Santos et al. 1988). At the southern margin of the dome, light brown silty phyllites with thin intercalations of fine metagreywackes are found (Appendix A1.8).



A : Light grey pebbly phyllites with a silty matrix and clasts from basement rocks, quartzite and milky quartz. Outcrop 227, western Simão Dias dome,



B : Coarsening-upward matrix-supported conglomerates with clasts from quartzite, milky quartz, and basement rocks. Note the sharp contact with the Jacoca dolomites. Outcrop 311, Capitão Farm.



C : Red-brown, silty phyllites of the base of the Ribeirópolis Formation in the northern border of the Itabaiana dome. Outcrop 1206, east of Serra do Machado village.

Figure 3.11 - The Ribeirópolis Formation (PC R).

The Jacoca Formation (P€ Ja)

The Jacoca Formation conformably overlies the Ribeirópolis Formation with a gradual or sharp contact. Locally it is in direct contact with the Itabaiana quartzites (outcrop 312, Capitão farm, Fig. 3.1).

The Jacoca Formation is comprised of two lithofacies: metacarbonates and a mixed lithofacies of metasiliciclastics and metacarbonates, or mixtites. The metacarbonates occur as 100-300m thick mappable bodies around the eastern and western parts of the Itabaiana dome (Fig. 3.1). The mixtites are absent or 100m thick in the western part of the Simão Dias dome and in a WNW-ESE trending band mapped to the north of the Mocambo fault (Fig. 3.1).

The best exposures of the metacarbonates are in the steep walls along the Salgado and Vaza Barris rivers, in the Capitão farm (outcrops 311-312, Fig. 3.1) where a vertical succession of sub-lithofacies can be followed in deformed and relatively undeformed areas.

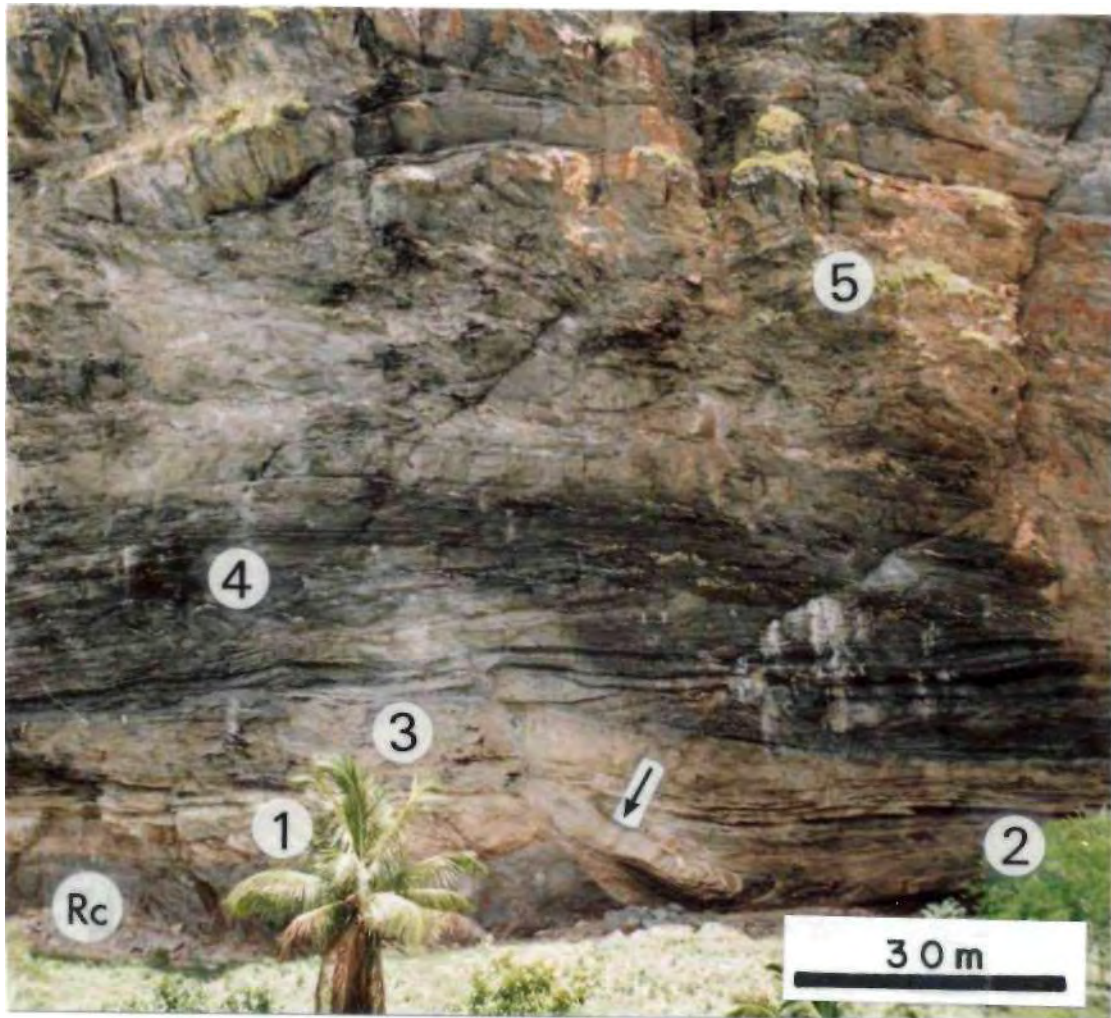
The typical section (Fig. 3.12) starts with a 3m thick layer of laminated white to light grey, 1-3cm thick beds of dolomites containing 1cm thick beds of pyrite and chalcopyrite. These are overlain by a 15m thick layer of thinly laminated dolomites, light brown metachert and calcitic, dark grey to black phyllites and 10m of massive dolomites. In thin section, the finely laminated dolomites display a typical marble texture of equigranular recrystallised calcite grains, interbedded with 1mm-thick micaceous layers composed of sericite, chlorite, biotite, very fine grained quartz and feldspars. These define a layer-parallel foliation.

This unit is overlain by a 40m thick sequence of intercalate, 1-10cm thick layers of grey limestones, calcarenites, and dark grey to black, locally carbonaceous phyllites. These units display parallel laminations and wave truncated current ripples (Fig. 3.13) and pass upwards into a 200m thick sequence of 1m thick layers of light grey metadolomites.

Detailed studies in the lower and upper sections of this formation in the Capitão farm area have also revealed local 1m-scale hummocky cross-stratifications (Castro 1987) and abundant oolites and intraclasts (Guimarães et al. 1991).

In the eastern part of the Itabaiana dome (Fig. 3.8) the Jacoca Formation consists of thinly-laminated, light and dark grey, fine-grained limestones with local, 10cm-thick intercalations of black to dark grey metachert. In the headwaters of the Morcego stream (Appendix A 1.6), the formation consists of interbedded, 1-10cm thick layers of dark grey to black, fine-grained limestones interlayered with light brown metapelites. These pass gradually, along the section, into the green-brown quartz-sericite-chlorite phyllites of the overlying Frei Paulo Formation.

The mixtites consist of discontinuous, 10m thick lenses of light grey dolomites hosted within dominantly light brown phyllites in the western Simão Dias dome (Fig. 3.5 & Appendix A1.3). To the north of the Mocambo fault, they occur as a sequence of 1m thick layers of dark grey to black and fine-grained limestones intercalated with light brown to variegated phyllites.



Wall of the Vaza Barris river, in the Capitão Farm, showing the best expression of the Jacoca Formation, which starts with a basal dolomitic layer (1) deposited on the Fibeirópolis conglomerates (Re), overlain by thinly interbedded dolomites, metachert and dark grey phyllites (2), overlain by m-thick, massive layers of dolomites (3, in the core of the fold) and by intercalated limestones and dark grey to black phyllites (4), covered by more massive limestones and dolomites (5).

Figure 3.12-The Jacoca Formation (PC Ja).



Wave-reworked, parallel laminated dolarenites and dolosiltites of the middle section of the Jacoca Formation. The truncated current ripples indicate a local westward sedimentary flow. Outcrop 312, Capitão Farm.

(1cm = diameter of the coin)

Figure 3.13- Primary sedimentary structures in the Jacoca Formation.

3.3.4 - The Lagarto Group

The Lagarto Group is a name proposed here to identify a new stratigraphic unit in the southern part of the Sergipano Fold Belt. It is a 100-700m thick coarsening-up siliciclastic sequence which conformably overlies the Miaba Group and is mappable in the southern part of the studied area (Fig. 3.14), as well as in the core of the Paripiranga anticline (Appendix A1.2) and to the east of the Itabaiana dome (Fig. 3.8).

The Lagarto Group comprises three interfingering Formations: the Lagarto-Palmares sandstones, the Jacaré metasiltites and the Frei Paulo phyllites.

The Lagarto-Palmares Formation comprises the Lagarto and Palmares Formations described by Silva Filho et al. (1978b) and Silva Filho (1982). It is based on field observations for a gradual transition between these rocks in the Itabaiana Dome Area (Fig. 3.14 and Appendix A 1.2) which confirms the same relationship described in a cratonic area, 100km to the south of Itabaiana (Saes 1984).

The interfingering of the Lagarto-Palmares sandstones with the Frei Paulo phyllites in the southern part of the study area, through a WNW-ESE trending band of metasiltites, has required the definition of the Jacaré Formation.

The Lagarto-Palmares Formation (P€ LP)

The Lagarto-Palmares Formation is a coarsening-upward sequence of mudstones and siltites, fine sandstones and siltites, and medium, massive sandstones (Fig. 3.15). These can be subdivided into a basal, an intermediate and an upper unit.

Although these sediments are flat-lying everywhere in the southern part of the area, the maximum thickness of the formation is actually unknown as the upper unit covers most of the lower units, and the upper surface is erosional. The thickness of 200m adopted here for each of the lower two units is taken from descriptions by (Silva Filho 1978b), based on well data and measured sections outside the area of this study. The preserved thickness of the third unit is estimated at 300m on the basis of topographic relationships.

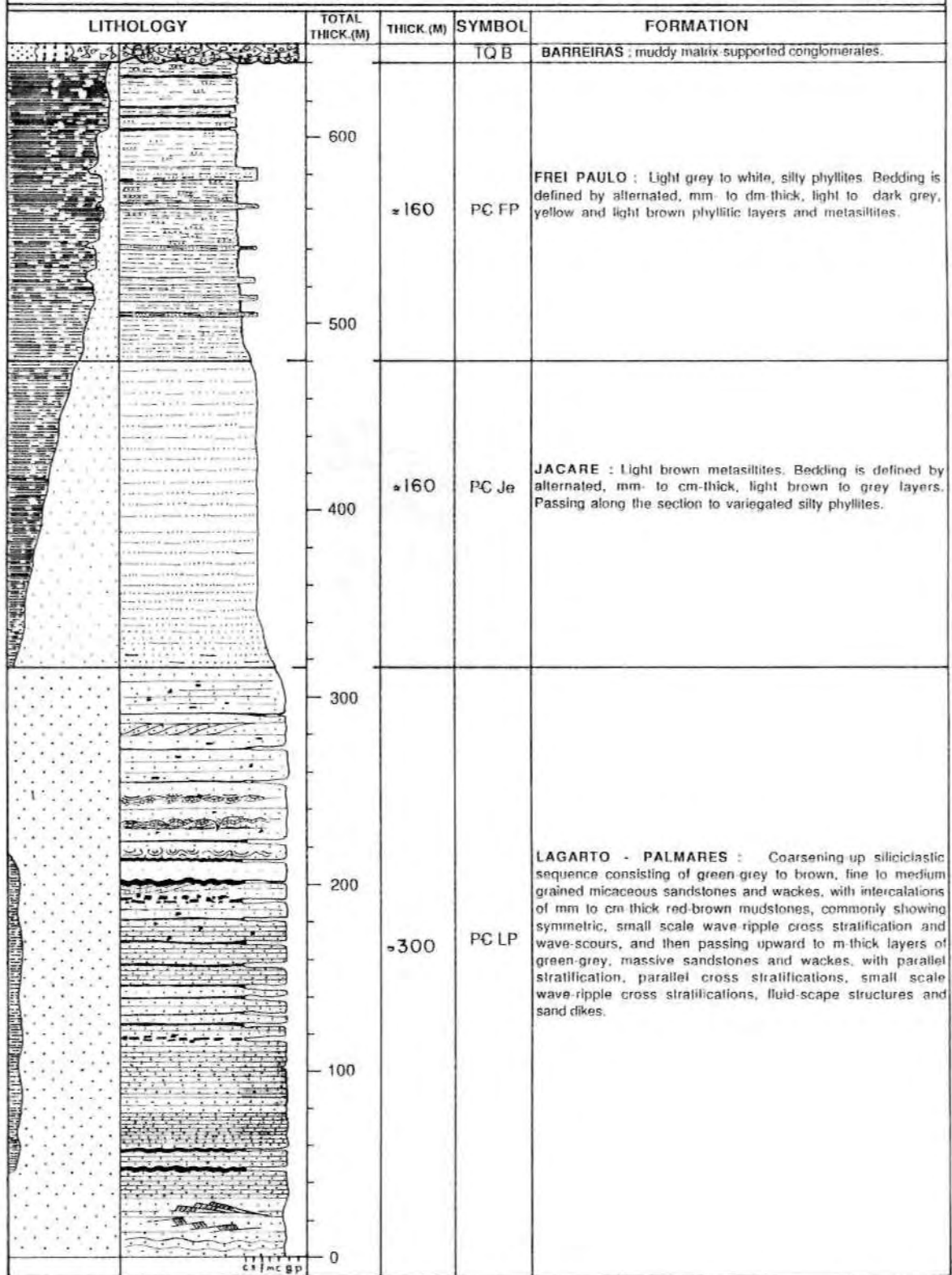
The Lagarto-Palmares Formation conformably overlies the Jacoca Formation but may well be locally in contact with the Itabaiana and Ribeirópolis Formations, as suggested in the western part of the Símão Dias dome, in places where the Jacoca Formation is not directly observed (e.g. outcrops 289 to 285, Fig. 3.1, and Appendix A1.2).

The basal unit consists of mudstones and siltstones intercalated with 10-20cm thick lenses of generally 0.15mm grain size, cross bedded sandstones (Fig. 3.15 A), and is dominant along the southern border of the study area. The sandy layers are marked by repeated cycles of 1 cm parallel lamination capped by generally symmetric and small-scale wave ripples, bounded by sharp truncation surfaces (Fig. 3.15 B).

The intermediate unit consists of fine-grained (< 0.15mm grain size), light brown to grey, 1-10cm thick layers of laterally continuous micaceous sandstones interlayered with 1mm-1cm thick layers of red-brown argillites and siltites. These are the typical Lagarto sandstones, as described by Silva Filho et al. (1978b) and Silva Filho (1982). They commonly display the cyclic sequences of micaceous sandstones and red-brown

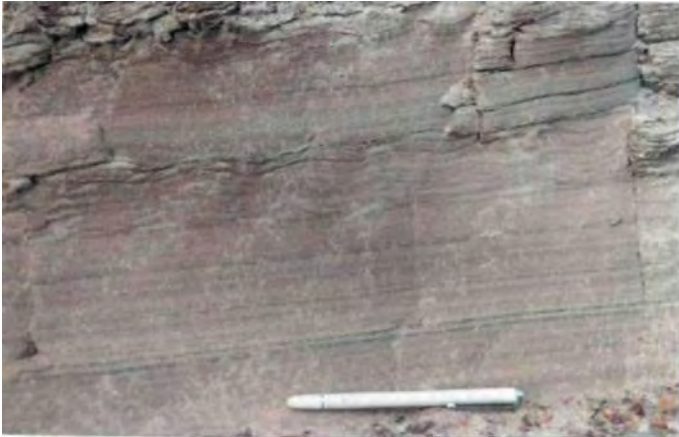
Figure 3.14 : L - L' Stratigraphic section of the upper Lagarto Group.

From L to L' includes outcrops 434, 483, 485, 486, 487, 488, 489, and 490.

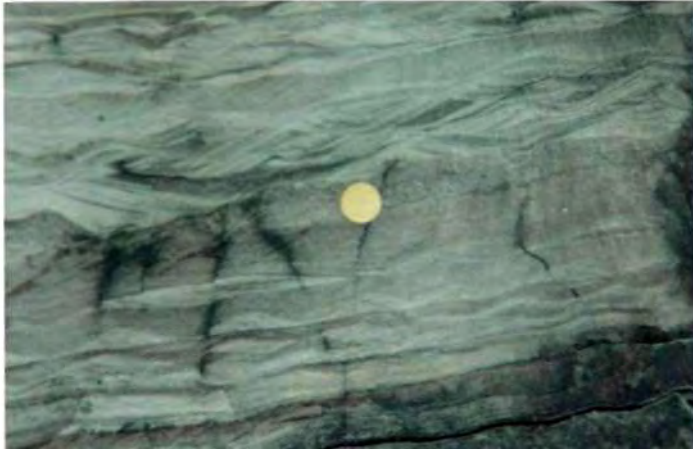




A : The lower unit consisting of interlayered siltstones and mudstones, and fine grained sandy bodies. First outcrop on the right side of the paved road Lagarto to Simão Dias, in the southern border of the area.



B : Detail of the above outcrop, showing the repeated cycles of parallel lamination and symmetric wave-ripples, separated by sharp truncation surfaces.

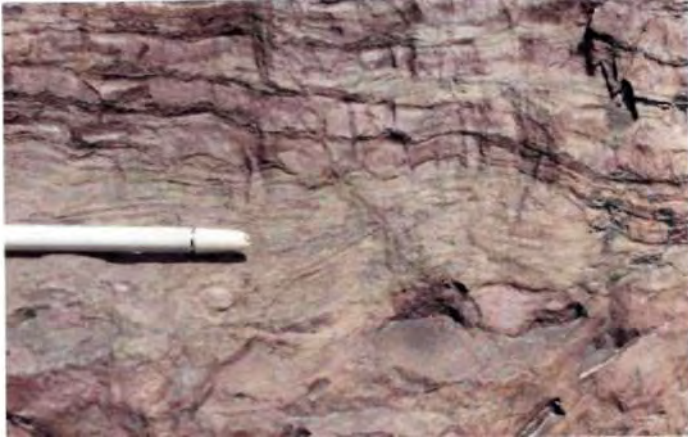


C : Micaceous sandstones with wave-ripple cross stratifications above symmetric wavy structures, at the base of the upper unit. Outcrop 484, Limeira Farm, road Lagarto to Itabaiana. (8mm = diameter of the yellow dot)



D : Metre-thick layers of the Palmares sandstones. Note the parallel lamination and the typical rounded pattern of erosion. Same outcrop as C.

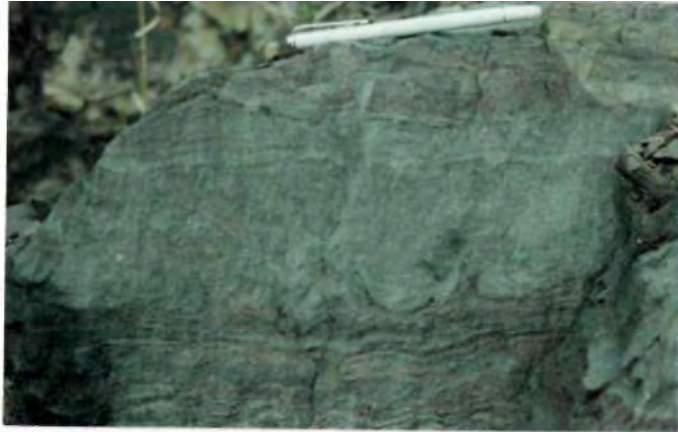
Figure 3.15 - The Lagarto-Palmares Formation (P€ LP)



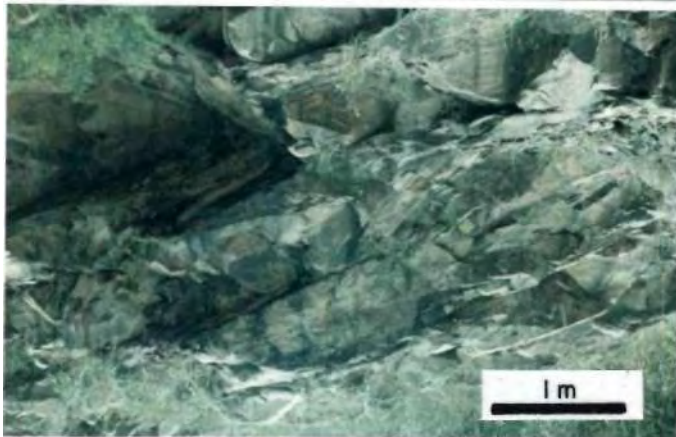
E : Sand-mud couplets deposited on a wave-reworked micaceous sandy layer. Note the truncation surface just above the white pen, and the incipient crenulation cleavage imprinted in the muddy layers.



F : Disrupted muddy layer within massive sandstones.



G : Convoluted lamination in the base of a thicker sandy layer deposited on a thinly layered sequence.



H : Metre-scale, parallel cross stratifications indicating normal way-up and a northward directed flow.

Figure 3.15 (continued) - E to H: Sedimentary structures in the Lagarto-Palmares Formation, outcrop 484, Limeira Farm road Lagarto - Itabaiana.



I: Typical hills sustained by metre-scale rounded boulders of massive sandstones, which dominates the landscape of the southern Itabaiana dome area. Road Lagarto to Itabaiana, just entering the southern part of the mapped area.



J : Small hills supported by the rounded boulders of parallel laminated (see C) metasandstones of the Lagarto-Palmares Formation in the core of the Paripiranga anticline (Anão dam) Outcrop 285, western Simão Dias dome.



K : Detail of the boulders of metasandstones, showing the parallel lamination. Same locality as **B**.

Figure 3.15 - (continued) I to K: The outcrop pattern of the massive Lagarto-Palmares sandstones in the Itabaiana Dome Area.

argillites, as seen in the outcrop 283 (road Simão Dias-Lagarto) and outcrops 156-158 (St. Antônio farm, S of the Simão Dias town, Fig. 3.1). These features are also seen in the outcrops 434, 435 in the Comandante farm, and outcrop 484 in the Limeira farm (S of the Itabaiana dome, Fig. 3.1).

The upper unit of the Lagarto-Palmares Formation starts with cm-thick layers of fine to medium grained, brown to grey, parallel-laminated micaceous sandstones, with abundant symmetric wave ripples and wave-ripple cross stratification (Fig. 3.15 C). This passes, in a continuous road-cut exposure, into a sequence of metre-scale beds of either massive or parallel-laminated, green-grey, calcite-cemented micaceous sandstones and wackes (Fig. 3.15 D). Primary structures, such as sand-mud couplets, disrupted muddy layers, sand dikes, and fluid-escape structures are found (Fig. 3.15 E-G), together with metre-scale parallel cross stratification indicative of a northward sedimentary input into the basin (Fig. 3.15 H).

The massive sandstones correspond to the Palmares Formation, as described by Silva Filho et al. (1978b) and Silva Filho (1982). They contain 1-10mm size discoid fragments of reworked, red-brown mudstones, and a typical bedding-fracture controlled pattern of erosion that produces rounded boulders (Fig. 3.15 D). These boulders dominate the topography of the southern area and are particularly seen along the road Itabaiana-Lagarto, and also in expressive outcrops mapped in the core of the Paripiranga anticline (Fig. 3.15 IK).

Petrographic studies (Table 3.1) have shown that the sandstones of the Lagarto-Palmares Formation are submature sediments, composed by subangular to subrounded, generally 0,15-0,45mm size grains of quartz, k-feldspars, plagioclase, granite, opaque minerals, zircon, and aggregates of micro-crystalline quartz, calcite, epidote and flakes of muscovite. Some grains of micro-crystalline quartz suggest derivation from mylonites, and few clasts of extremely fine-grained material might be derived from phyllonites, phyllites, or even volcanic rocks. Flakes of biotite and chlorite are found kinked, but the chlorite also occurs in zones of diffuse boundaries, possibly formed by low grade metamorphism.

In the cratonic area Saes (1984) described a mineral composition for the Palmares sandstones similar to that in Table 3.1, and interpreted the source areas as granite-gneiss crystalline basement with belts of low grade metamorphic rocks.

The Jacaré Formation (PC Je)

This formation consists essentially of light brown, micaceous, 10-100cm thick layers of metasiltites, or consists of light brown to variegated metasiltites (Fig. 3.16 A) with subordinated, 1-10m thick lensoid bodies of fine- to medium-grained, light brown metasandstones.

The metasiltites are mappable along an E-W trending band in the southern area and in the core of the Paripiranga anticline (Fig. 3.1). The thickness is estimated as =150-200m (Fig. 3.14) but is probably less in the core of the Paripiranga anticline, where the outcrop width is smaller.

MIDDLE-UPPER SECTION OF THE LAGARTO-PALMARES FORMATION

Outcrop	Quariz+chert+ quartzite	Feldspars	Lithic fragments	Micas	Carbonate	Other	Matrix (cement)
DR 155	172	129	72	22	16	88	101
%	28.6	21.5	12	3.6	2.6	14.6	16.8
% Q, F, L	46.1	34.6	19.3	-	-	-	-
DR 159	167	141	88	27	1	65	111
%	27.8	23.5	14.6	4.5	0.1	10.8	18.5
% Q, F, L	42.2	32.6	22.2	-	-	-	.
DR 284	247	59	59	13	-	109	113
%	41.1	9.8	9.8	2.1	.	18.1	18.8
% Q, F, L	67.7	16.1	16.2	-	-	-	-
DR 285	274	80	48	35	-	41	125
%	45.4	13.2	7.9	5.8	-	6.7	20.7
% Q, F, L	68.2	19.9	11.9	-	-	.	-
DR 434	154	138	64	32	34	47	131
%	25.6	23	10.6	5.3	5.6	7,8	21.8
% Q, F, L	43.2	38.7	18.1	-	-	.	-
DR 484	119	102	75	38	13	78	175
%	19.8	17	12.5	6.3	2.1	13	29.1
% Q, F, L	40.2	34.4	25.4	-	-	-	-

FREI PAULO METASANDSTONES OF THE NORTHERN PART OF THE AREA

Outcrop	Quartz+chert+ quartzite	Feldspars	Lithic fragments	Micas	Carbonate	Other	Matrix (cement)
DR 212	181	130	86	38	19	11	136
%	30.1	21.6	14.3	6.3	3.1	1.8	22.6
% Q, F, L	45,6	32.7	21.7	-	-	-	-
DR 1167	106	103	37	60	80	58	156
%	17.6	17.1	6,1	10	13.3	9.6	26
% Q, F, L	43.1	41.8	15	-	.	.	-
DR 1171	230	92	62	46	3	36	131
%	38,3	15.3	10.3	7.6	0.5	6	21.8
% Q, F, L	59.9	24	16.1	-	-	-	-
DR 1173	71	40	12	36	226	39	226
%	11.8	6.6	2	6	37.6	6.5	37.6
% Q, F, L	57.7	32.5	9.8	-	-	-	-

Table 3.1 Petrography of the sandstones of the Lagarto group.

In samples DR-155, 159, 284, 285, 434 and 485, the matrix and the cement include mostly very fine-grained quartz, sericite, carbonate and iron (?) oxide. Grain size is 0,15-0.45mm and the grains are generally subangular to subrounded, with low to high sphericity, in samples DR-212, 1167, 1171 and 1173 (deformed calcareous metasandstonea of the Frei Paulo formation in the northern part of the area), the matrix and cement include mostly carbonate, very fine quartz, sericite and iron {?} oxide.

In all the samples, micas are flakes of muscoviie, biotite and chlorite (some are kinked).

Other minerals include mostly opaque grains, some zircon and epidote.

Lithic fragments are mostly from very fine-grained quartz aggregates (mylonites), gneisses or granites, metachert, and grains entirely consisting of very fine-grained sericite and quartz (possibly from phyllites or metavoicanics).

% Q,F,L, means normalized percentage to Q=quartz+quartzite+chert, F=feldspars+plagioclase, and L=lithic fragments.'

In the vicinity of faults and shear zones, these rocks attain a dark brown to black colour, are silicified and indurated, and show a vitreous texture, as observed in outcrops 437, 438 and 485 within the Comandante and Limeira farms (Fig. 3.1).

The Frei Paulo Formation (P€ FP, FP1, FP3)

The Frei Paulo Formation is widespread (Fig. 3.1): it occurs along a WNW-ESE band in contact with the Jacaré Formation, in the southern part of the study area, and also in a WNW-ESE trending band passing around the Frei Paulo town. It is also mapped around the basement domes, as well as in the Vaza Barris river valley (between the Escarpa and Pelada faults), and to the west of the Paripiranga town. The thickness is estimated between = 100m (in the western part of the Simão Dias dome) and 300m to >500m elsewhere, particularly in the Vaza Barris valley area.

This formation comprises rocks of the original Frei Paulo and Capitão Formations, as defined by Humphrey & Allard (1967,1969), and rocks of the Frei Paulo-Ribeirópolis Formation, as defined by Silva Filho et ai. (1978b). It also incorporates new areas where the typical Frei Paulo phyllites were mapped during the course of this research, such as those narrow bands to the north of the Escarpa and Mocambo faults, and to the south of the Pelada fault (Fig. 3.1).

The Frei Paulo Formation is comprised of three main lithofacies respectively termed PG FP, FP1 and FP3 (Fig. 3.1, enclosure). The lithofacies P€FP consists of 1-10mm thick beds of light grey to brown, silty and variegated phyllites, which are the typical Frei Paulo phyllites (Fig. 3.16 B).

The lithofacies FP1 consists of trappable bodies of arkosic metasandstones and wackes. It also consists of light brown phyllites with -10-100cm thick interbedded layers of fine- to medium-grained metasandstones (e.g. outcrops 846, 848-850, to the west of Paripiranga, Fig. 3.1) or even tens of metres thick bodies of metasandstones and quartzites (e.g. outcrops 353, 354, and 356, to the west of Macambira).

The lithofacies FP3 comprises quartz-sericite-chlorite phyllites and intercalated fine- to medium-grained metagreywackes (Fig. 3.16 C), light brown phyllites associated with thinly interbedded dark grey to black phyllites, metasilites, calcilitites (or metarhytmities, Fig. 3.16 D) and interbedded limestones and metagrey wackes (Fig. 3.17).

The variegated phyllites are a key horizon as they are found overlying the Jacoca carbonates, to the east and west of the Itabaiana dome, and underlying the Palestina diamictites to the west of the Simão Dias dome (Fig. 3.1). Their lateral and vertical juxtaposition with the other lithofacies is observed in the stratigraphic sections across the eastern and western parts of the Itabaiana dome (Fig. 3.6 & Appendices A1.4-A1.6), and also between the Jacarecica river section (Fig. 3.8) and the variegated silty phyllites that occur along the Areia Branca-Saco Torto road (outcrops 371, 372, Fig. 3.1).

Each lithofacies of the Frei Paulo Formation is dominant, but not exclusive, in a particular area geographically related to the regional faults. The variegated silty phyllites are most important to the south of the Escaipa fault, whereas between the Escarpa and Pelada faults, and in the eastern side of the Itabaiana dome, the main lithofacies are the



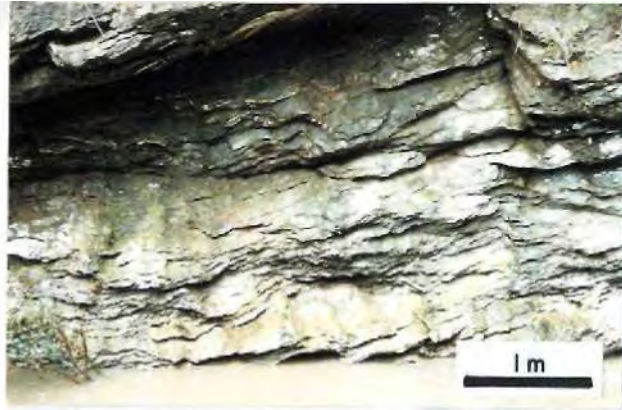
A : Light brown, fine sandy and well laminated Jacaré metasilites. Outcrop 489, road Lagarto to Itabaiana.



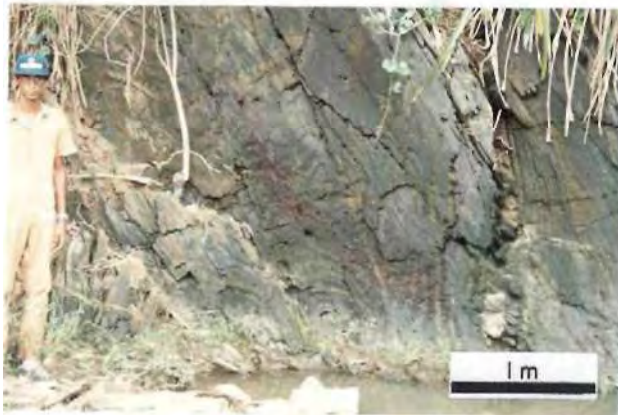
1



B : Typical variegated Frei Paulo phyllites (P€ PF) consisting of intercalated, pale and dark grey phyllitic layers, with subordinated thin silty and sandy layers. Outcrop 490, road Lagarto to Itabaiana. The pen is 15cm long.



C : Quartz-sericite-chlorite phyllites of the Frei Paulo Formation (facies PC FP3). Outcrop 1035, Morcego stream, northeastern part of the Itabaiana dome.



D : Interlayered, dark grey to black phyllites and light brown, thin metasilts of the facies PG FP3. Outcrop 874, Vaza Barris river valley.

Figure 3.16 - The Jacaré (PC Je) and the Frei Paulo (PC FP) Formations.

green-grey, quartz-sericite-chlorite phyllites, metagreywackes, minor lenses of metasandstones, the metarhythmites and interbedded metagreywackes and metalimestones.

Around the town of Frei Paulo (Fig. 3.1), the Frei Paulo Formation consists of light-brown and silty phyllites with common intercalations (some of them mappable) of brown to green-grey, fine- to medium-grained, calcite-cemented, micaceous metasandstones. The petrography of these sandstones is similar to the Lagarto-Palmares sandstones and wackes, but the carbonate content is greater (Table 3.1).

The very narrow band of the Frei Paulo Formation, which lies just to the north of the Mocambo fault (Fig. 3.1), consists of light-grey to brown silty phyllites to the NE of Pinhão (outcrops 275 and 816), to the NNW of Macambira, towards to Frei Paulo (outcrops 541 and 1009) and in the northwestern corner of the area (outcrop 1086). It also consists of brown silty phyllites and fine-grained, calcite-cemented metasandstones with 1-10cm thick lenses of black and very fine-grained limestones (outcrops 1165 and 1166) which occur along the Mocambo fault zone. In this area, the Mocambo fault is hundreds of metres wide and controls the local E-W trend of the Salgado river and a small tributary to the west.

The metasandstones are more weathering-resistant and are brecciated in some scattered places along the fault, but a microscopic study of fresher samples has revealed the same petrography of the fine to medium grained, micaceous, calcite-cemented metasandstones mapped within the Frei Paulo Formation along the track from the Salgado to Riachão and Rosa Amélia farms (outcrops 1167 to 1173, southeast of Mocambo). These sandstones are also observed within the Frei Paulo phyllites, to the west of the Paripiranga town (outcrop 848) and 1m-thick intercalations of metasandstones and metagreywackes occur just to the north of the Comandante farm, where approaching the Escarpa fault and entering into the Vaza Barris river valley (outcrops 441-443, Fig. 3.1).

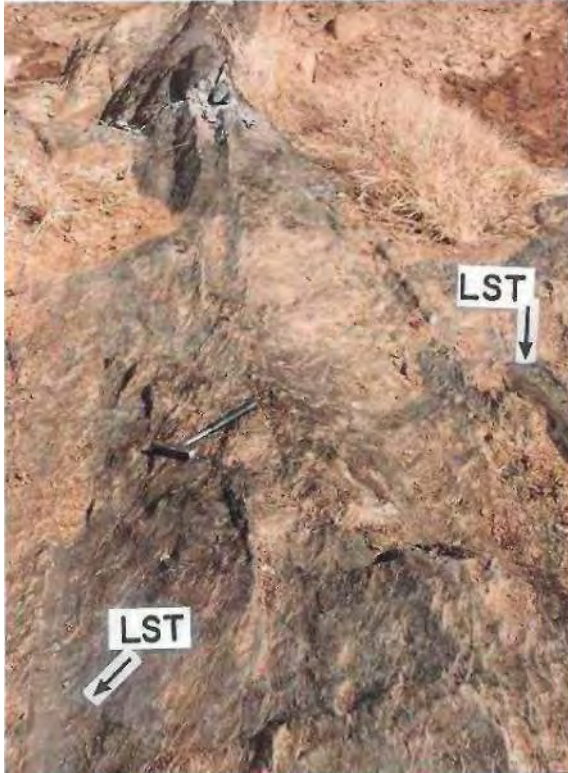
Parallel lamination is the most typical sedimentary structure observed in the Frei Paulo Formation, though small-scale wave-ripples and parallel cross stratification are found locally (outcrop 71, S of Simão Dias).

3.3.5 - The Vaza Barris Group

The Vaza Barris Group is a 2000m-thick sequence unconformably overlying the previous formations and the crystalline basement, and comprising the Palestina diamictites and the Olhos D'água metacarbonates. The group does not include the Capitão Formation of Humphrey & Allard (1967, 1969) and the Frei Paulo-Ribeirópolis Formation defined by Silva Filho et al. (1978 a,b) and redefined by Santos et al. (1988).

The Palestina Formation (P€ P)

This formation consists of diamictites, pebbly phyllites and minor phyllites, and contains local, generally 10m thick lenses of quartzites. It corresponds to the original Palestina Formation as defined by Humphrey & Allard (1967, 1969).



A : Intercalations of dark grey, fine grained limestones (arrowed) in the blue-grey pebbly phyllites (see detail in B). Outcrop 405, Vaza Barris river valley.



B : Detail of A to show the 1 -2cm size clast of basement granitic rock in the pebbly phyllites (near the head of the pen).

Figure 3.17 - Interlayered limestones and metagreywackes of the Frei Paulo Formation {fades PC FP3},

The diamictites and pebbly phyllites consist of generally flattened and elongated granules, pebbles and cobbles of basement rocks with less clasts from quartzites, phyllites, and metacarbonates. They are supported in a green- to blue-grey, extremely fine and foliated sericitic-chloritic matrix (Fig. 3.18).

The variations in thicknesses and lithological characteristics of this formation is evident from the outcrops in the Vaza Barris river valley, those in the Jacarecica river, and those around the Simão Dias dome (Fig. 3.1). A thin body of highly deformed pebbly phyllites occur within mylonitic gneisses in a 100 m-scale outcrop nearby the village of Olhos D'água (outcrop 395, Fig. 3.1).

In the area confined between the Escarpa and Pelada faults, the diamictites are much more significant than elsewhere, and the thickness is roughly estimated to be 500m. Clasts greater than 10cm are common and the matrix is generally more phyllitic than elsewhere (Fig. 3.18 A). Lenses of dark brown to black, medium to coarse-grained quartzites occur locally.

In the Jacarecica river, the diamictites are found only in a narrow body which is folded within the quartz-sericite-chlorite phyllites and metasandstones of the Frei Paulo Formation. They contain irregular boulders and pebbles of Itabaiana quartzites and Lagarto-Palmares metasandstones (Fig. 3.18 B), which have not been found in the rest of the area, nor reported in the literature.

Around the Simão Dias dome the thickness of the Palestina Formation is probably 100m. The matrix is siltier than elsewhere and the clasts are generally smaller than 10cm (Fig. 3.18 C), although an isolated metre-scale block of granitic rock has been found near the trace of the Simão Dias fault (outcrop 90, very close to the SE of Paripiranga, Fig. 3.1).

The Olhos D'água Formation (P€ OA)

The Olhos D'água Formation is 200-1300m thick and consists of metacarbonates that conformably overlie the Palestina diamictites (Fig. 3.1). It can be described in terms of three different lithofacies (Fig. 3.19): laminated carbonate rhythmites, oolitic limestones and dolostones, and mixed carbonate and siliciclastics (mixtites).

The best exposures are along the section from Paripiranga to the north (Fig. 3.5). The section starts with hundreds of metres of laminated metacarbonate rhythmites, which consist of 1-10cm thick and interbedded layers of light and dark grey to black, fine-grained limestones, with local 1-3cm thick intercalations of light brown metasilites (Fig. 3.19 A), brown to purple metapelites and chert. Small to medium-scale cross stratification are found locally.

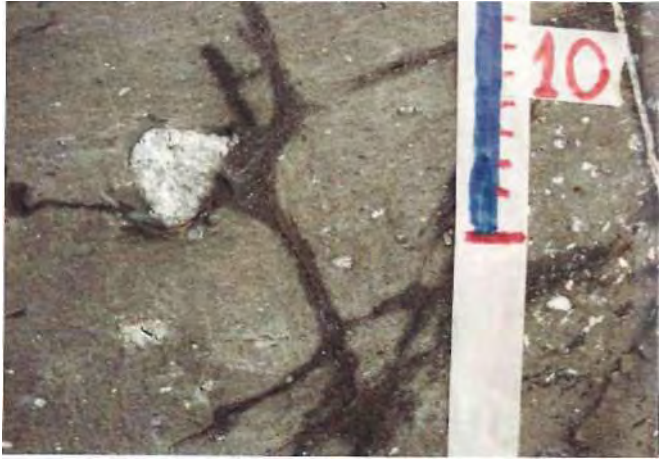
These rocks pass up section into a sequence (probably also 100's of metres thick) metalimestones and metadolostones consisting of interbedded, 1-10cm thick layers of fine-grained, black limestones, in many places oolitic, pelloidal and oncolitic (Fig. 3.19 B). This lithofacies also contains 1-10mm thick intercalations of brown metapelites, and 10-100m thick layers of grey to light-brown dolarenites which display small-scale parallel cross stratification, wave scours, intraclasts and graded bedding (Fig. 3.19 C).



A: Green-grey Palestina diamictite with elongated clasts of granite and gneiss in a phyllitic matrix. Outcrop 405, Vaza Barris river valley, road from the Olho D'água village to the Barracão Farm.



B : Boulders of Itabaiana quartzites and Lagarto-Palmares metasandstones within the Quartz-sericite-chlorite phyllitic matrix of the Palestina diamictites. Outcrop 1197, Jacarecica river.



C : Basement granitoid clasts in the silty matrix of the Palestina diamictites. outcrop 90, road Paripiranga to Simão Dias. The scale is in cm.

Figure 3.18 - The Palestina Formation (PC P).

67



A: Folded example of finely laminated, dark grey limestones with interbedded thin layers of light brown metasiltyites. Outcrop 71, to the south of Simão Dias.



B : Oncoid structures in the Olhos D'água limestones. Outcrop 829, road from Paripiranga to Cicero Dantas, western part of the area.



C : Intercalated dolomites and doloarenites, indicating a wave-reworking process and formation of intraclasts. Note the graded bedding and the intraclasts in the lowest grey layer, and a possible shrinkage fracture (arrowed). Outcrop 131, northeast of Paripiranga. The scale is in cm.



D : Interlayered, dark grey to black, fine-grained limestones and red-brown, finely laminated metapelites. Outcrop 31, road Simão Dias to Pinhão.

Figure 3.19 - The Olhos D'água Formation (PC OA).

At the top of the section, this sequence passes gradually into hundreds of metres of mixtites, which consist of fine-grained, 10-100cm thick beds of black limestones, intercalated with 1-10cm thick layers of brown to red-brown, commonly variegated, pyritic metapelites (Fig. 3.19 D).

These mixtites form the WNW-ESE trending hills that occur along the Escarpa and Pelada faults (Fig. 3.1), and the siliciclastic interbeds become increasingly significant northward. This can be observed along the road Simão Dias to Pinhão and along the Salgado river, to the northwest of Macambira, going from the Jacoquinha farm to the Mocambo fault (Fig. 3.1) where there are several 10-100cm thick intercalations of dark grey to black phyllites (outcrops 1160-1164).

The Olhos D'água Formation also occurs in the Capitão range, in the NW corner of the area, and in two separate bodies cut by the Propria fault, to the east of the Itabaiana dome (Fig. 3.1), where the laminated meiacarbonate rhythmites dominate and appear to show a gradual passage from the green-grey Frei Paulo phyllites (see Appendix A1.6).

3.4 - Lithofacies and depositional environments

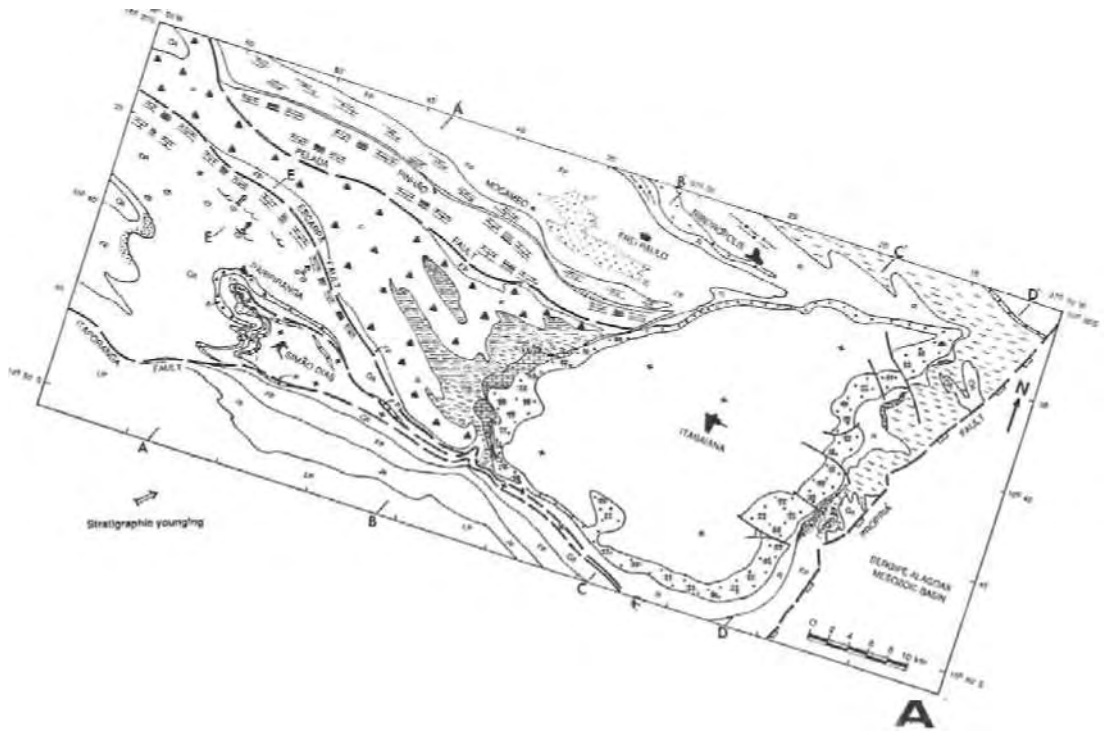
3.4.1 - Lithofacies distribution and paleogeography

Straügraphically, the sedimentary record of the Itabaiana Dome Area can be summarised in terms of two siliciclastic and two carbonate megasequences. The siliciclastics megasequences start respectively with the Itabaiana Formation and the Lagarto Group, the upper part of each being completed with conglomeratic/volcanic facies (the Ribeirópolis and Palestina Formations). The carbonate megasequences comprise respectively the lithofacies of the Jacoca and Olhos D'água Formations.

Figure 3.20 A shows the facies distribution throughout the area. Figure 3.20 B attempts to show a block diagram constructed with interpretative cross sections in the basin (AA' to DD'). It is evident from Figure 3.20 A that the sedimentary record shows a wide distribution of facies (and thickness) associated with the basement domes and the Pelada, Escarpa, Simão Dias and Itaporanga faults (which are projected vertically down into the cross-sections of Fig. 3.20 B).

If such variations are an indicator of sedimentary sources at different distances from the depocenters, as generally found in shallow water environments (Fairchild 1989), some aspects of the evolution of the sedimentation in the Itabaiana Dome Area deserve particular attention. This may be considered in terms of particular times of sedimentation (Fig. 3.20): T1 = Itabaiana time, T2 = Ribeirópolis-Jacoca time, T3 = Lagarto Group time, T4 = Palestina time and T5 = Olhos D'água time.

Overleaf: Legend for Figure 3.20.



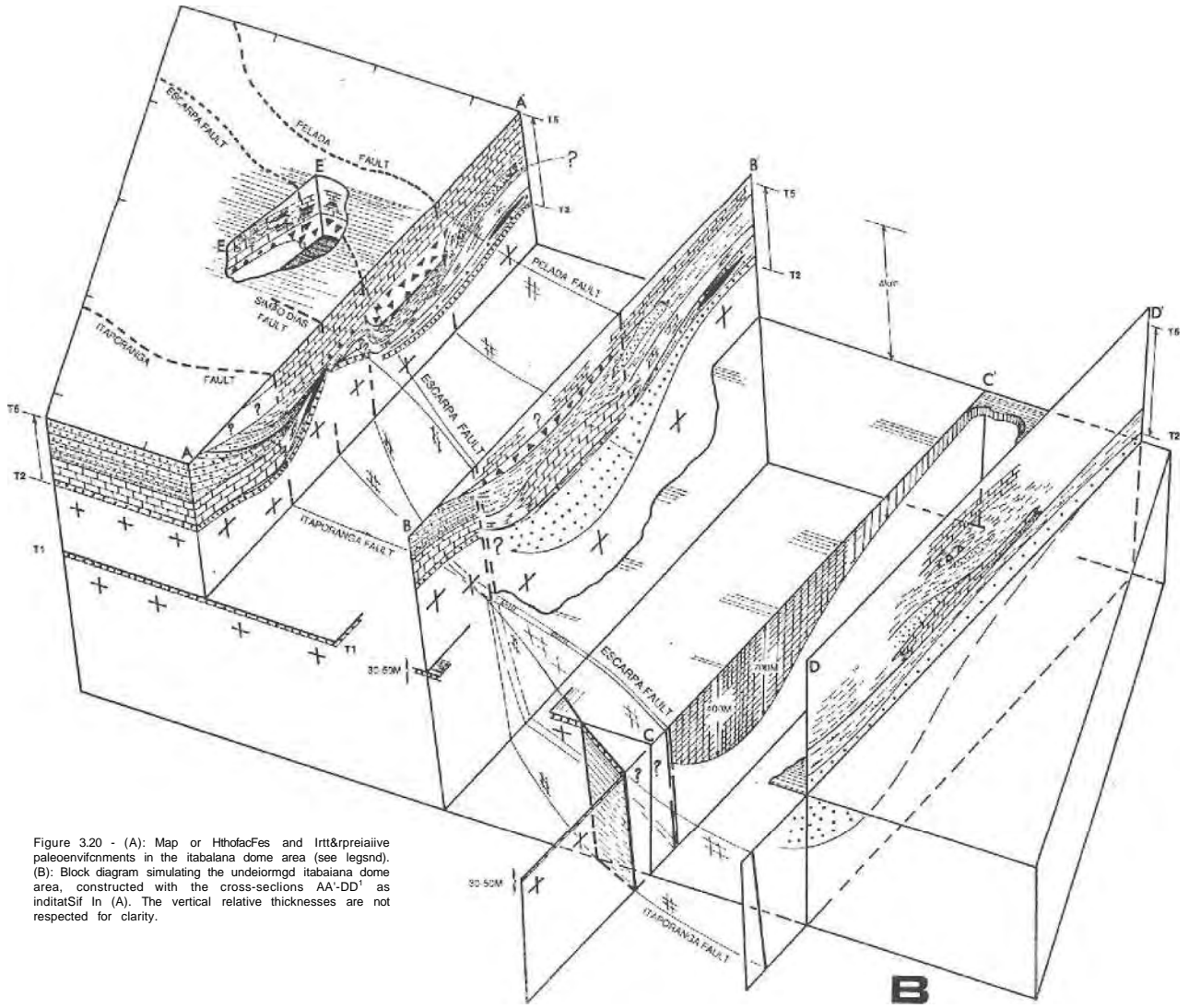
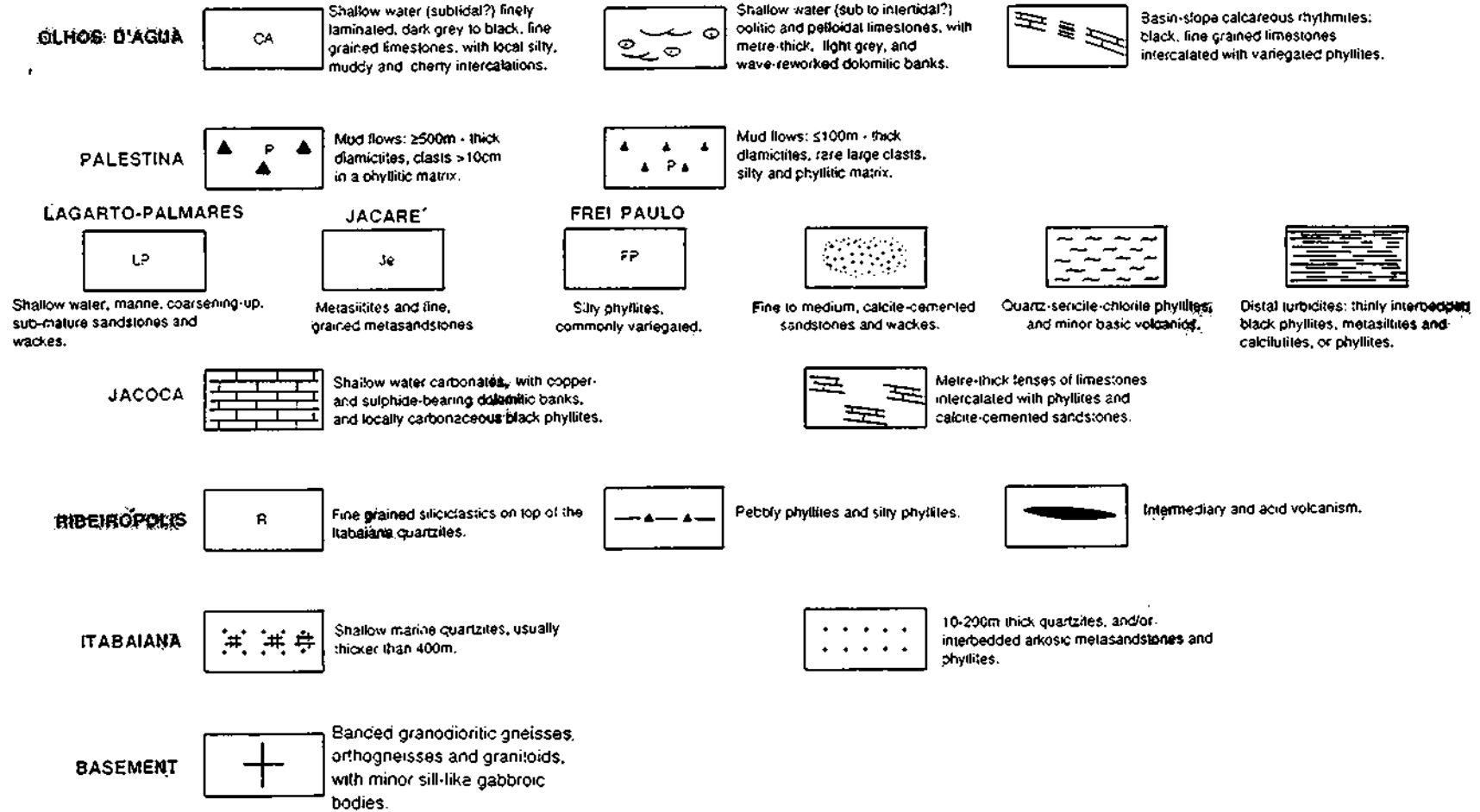


Figure 3.20 - (A): Map of the Itaipava and Itaipava paleoenvironments in the Itaipava dome area (see legend). (B): Block diagram simulating the dome area, constructed with the cross-sections AA'-DD' as indicated in (A). The vertical relative thicknesses are not respected for clarity.

FORMATION

LITHOFACIES



LEGEND FOR FIGURE 3.20

Chapter 4 - Structures and metamorphism of the Itabaiana Dome Area

4.1 - Introduction

This chapter aims to present the structural analysis of the Itabaiana Dome Area and to discuss the implications for the evolution of the southern part of the Sergipano Fold Belt.

The description of the structures in the Itabaiana Dome Area is followed by an interpretation of the structural evolution of the southern part of the Sergipano Fold Belt. The data are also discussed to produce an interpretation of a tectonic regime likely to explain the field and laboratory observations made during this research.

The chapter contains 24 figures (Figs. 4.1-4.24), two tables (Tables 4.1-4.2) and an appendix on strain analysis (Appendices A2.1-A2.3). The geological map of the Itabaiana dome (Fig. 3.1, enclosure) shows the section lines of the main structural cross sections (AB, CD, EF) presented in Figure 4.20 (enclosure). The localities and outcrop numbers are found on the geological map of Figure 3.1.

Hereafter, where mentioned the X, Y and Z axis, and the XZ, XY and YZ planes, the author is referring respectively to the orthogonal axis and planes of the D_2 (second deformational event) finite strain ellipsoid, deduced for each outcrop on the basis of the available macro and microscopic structural relationships.

4.2 - The structures of the Itabaiana Dome Area - Introduction

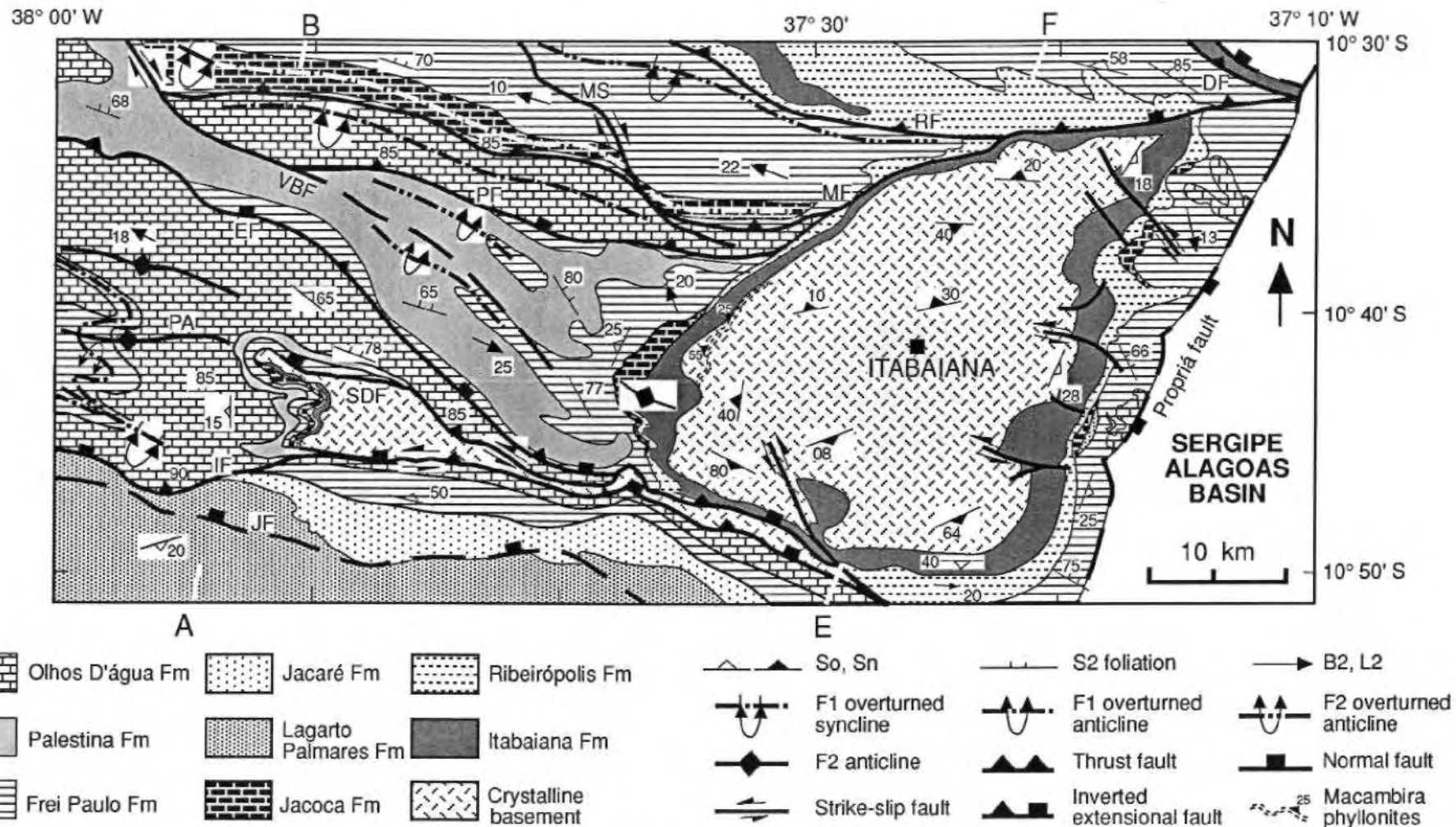
Figure 4.1 is a summary lithostructural map of the Itabaiana Dome Area. The main structures are F_1 and F_2 folds, with their associated foliations and lineations, and a set of WNW-ESE striking high-angle thrust and sinistral strike-slip regional faults.

The F_1 folds are inferred structures which occur to the west and north of the Simão Dias dome, respectively within the Frei Paulo Olhos D'água and Jacoca Formations (Fig. 4.1). The F_2 folds are mostly the Paripiranga anticline (to the west of the Simão Dias dome), some overturned sync lines and anticlines which occur to the north, northwest and west of the Itabaiana dome, and the open folds which affect the Miaba range, in the western side of this dome (Fig. 4.1).

The regional faults are the Itaporanga, Simão Dias, Escarpa, Pelada, Mocambo, Ribeirópolis and Dores faults. The main strike-slip faults are the dextral strike-slip Vaza Barris fault and the Mocambo dextral shear. Other NW-SE trend strike-slip faults cut across the Itabaiana quartzites and also affect the basement, in the eastern and southern margins of the Itabaiana dome.

The Itabaiana Dome Area is comprised of a domain of cratonic, non deformed and non metamorphosed sediments, and a domain of highly deformed, green schist facies metasediments and minor metavolcanics mantling the Itabaiana and Simão Dias gneissic domes.

The cratonic domain lies on the southwestern corner of the area and is separated from the deformed and metamorphosed domain by the Itaporanga fault (Fig. 4.1). The



PA = Paripiranga anticline, JF = Jacaré fault, IF = Itaporanga fault, SDF = Simão Dias fault, EF = Escarpa fault, PF = Pelada fault, VBF = Vaza Barris fault, MF = Mocambo fault, MS = Mocambo shear, RF = Ribeirópolis fault, DF = Dores fault.

Figure 4.1 - Summary lithostructural map of the Itabaiana Dome Area. Sections AB and EF are shown in Figure 4.21 .

deformed metasedimentary wedge occupies the rest of the area, but is separated by the SSW-NNE striking Propriá fault from the Mesozoic Sergipe-Alagoas basin, in the southeastern part of the area.

As will be described along this chapter, the structures of the Itabaiana dome record three ductile to ductile-brittle deformational events (D₁-D₃) characterised by folds, faults and shear zones and accompanied by a sub-greenschist to greenschist metamorphism.

These events affected the bedding of the metasediments (S₀) and the metamorphic banding of crystalline basement (S_n), and developed a varied set of planar features (axial plane foliations and fold axial planes) and linear features (fold axis, intersection and elongation lineations). The folds, planar and linear features belonging to each D₁-D₃ deformational event are respectively termed F₁-F₃, S₁-S₃; and L₁-L₃ and are defined in detail in Table 4.1.

4.2.1 - Basement structures

The basement certainly underwent earlier deformations, as 10-100cm size isoclinal, rootless folds are intrafolial to the metamorphic banding in highly foliated gneisses cut by the undeformed basal unconformity (e.g. Fig. 3.9 B). Nevertheless, the scarcity of such evidence precludes the establishment of the earlier evolution of the crystalline basement, before the deformation events which are the focus of this thesis.

More than that, the basement also shows evidence of being affected by three folding events, which correspond to the structures affecting the metasedimentary cover, as will be demonstrated in this chapter.

For simplicity, terms such as S_{n-1}, F_{n+1}, etc, to describe the structures in the basement will be avoided, and the metamorphic banding of the gneisses and orthogneisses (S_n) is simply considered the planar feature to be affected by the D₁-D₃ deformational evolution (Table 4.1).

4.2.2 - Summary of the deformational events and structural domains

The D₁ deformation affects S₀ and S_n and is represented by recumbent folds (F₁), associated with the axial planar foliation (S₁), and with an intersection lineation (L₁₋₀). The D₂ deformation is characterised by nearly upright folds (F₂), which co-axially refold F₁ folds and S₁. Planar structures associated with F₂ folds are the axial plane (PA₂) and an axial planar foliation (S₂). The linear features, generically termed L₂, are the fold axis (B₂), the intersection lineation (L₁₋₂) and an stretching lineation (L_s). D₂ is also responsible for the high-angle thrust faults observed in the area (Fig. 4.1).

The D₃ deformation is indicated by transversal, commonly upright folds (F₃), which affect S₂ (and the older planar structures). The associated planar elements are the axial plane (PA₃) and the axial plane foliation (S₃), whereas the linear elements are the fold axis (B₃) and an intersection lineation (L₃₋₂).

The relative chronology between the deformational events has been distinguished on the basis of many examples of refolded folds, folded foliations, combined with cross-

Planar elements prior to D₁ deformation

S₀ = bedding in the sediments and metasediments.

S_n = metamorphic banding in gneisses and orthogneisses of the crystalline basement.

First deformational event (D₁)

F₁ = folds affecting S₀ and S_n and being re-folded by folds of the second deformational event.

PA₁ = axial plane of the F₁ folds.

S₁ = axial planar foliation associated with F₁ folds.

B₁ = F₁ fold axis.

L₁₋₀ = intersection lineation defined by the intersection of S₁ with S₀ or S_n.

Second deformational event (D₂)

F₂ = folds co-axially folding F₁ folds or S₁.

PA₂ = axial plane of the F₂ folds.

S₂ = axial planar foliation associated with the F₂ folds or a foliation generally trending WNW-ESE or NNW-SSE, and cross cutting S₁.

B₂ = F₂ fold axis.

L₁₋₂ = intersection lineation defined by the intersection of S₁ and S₂.

L_s = elongation lineation defined in the metasediments, basement rocks and fault-related rocks, by elongated minerals, clasts, porphyroclasts, oolites, pellets, and other strain markers.

L₂ = generic name for the linear features related to this event.

Third deformational event (D₃)

F₃ = NE trending folds and crenulations affecting S₂ (and the older planar features) or folding F₁ and/or F₂ folds.

PA₃ = axial plane of the F₃ folds.

S₃ = axial planar foliation associated with the F₃ folds or a fracture cleavage foliation generally trending NE-SW or NNE-SSW, and cross cutting S₂ (and the older planar features).

B₃ = F₃ fold axis.

L₃₋₂ = intersection lineation defined by the intersection of S₃ and S₂.

L₃ = generic name for the linear features related to this event.

Table 4.1 - Main structural features of the Itabaiana Dome Area.

cutting relationships of foliations. Refolded folds are considered the best evidence amongst other available criteria for regional correlations of structures in polydeformed areas (Williams 1985).

The superposition of D_1 and D_2 deformation events on rocks which have different mechanical behaviours, developed an accentuated structural partitioning and a strong anisotropy with a regional WNW-ESE trend in the study area (Fig. 4.1).

As a consequence, six structural domains have been defined in the Itabaiana Dome Area, on the basis of different styles of the F_2 folds, the relative attitude of S_1 and S_2 , and also using the nature of the S_2 foliation together with variations in the trends of S_2 and L_2 (Fig. 4.2).

The sediments and the crystalline basement are divided into the cratonic, Simão Dias and Itabaiana domains. The deformed metasediments are divided into the regional, west and east domains (Fig. 4.2).

The cratonic domain, comprises mostly the flat-lying Lagarto-Palmares Formation, but also encompasses deformed Jacaré metasilites and Frei Paulo phylites. The Simão Dias domain consists of the Simão Dias gneisses which are affected by tight F_2 folds, and by a WNW-ESE trending S_2 foliation.

The Itabaiana domain comprises the Itabaiana gneisses, which are affected by open-tight F_2 folds associated with a normally S_2 spaced cleavage. This domain shows a varied style of internal deformation according with the position in the Itabaiana dome (which is likely associated with the variable thickness of the Itabaiana quartzites).

The regional domain comprises the metasediments outside of the Itabaiana dome, and is characterised by sub-parallel and steep dipping S_1 and S_2 foliations, by tight F_2 folds, and by a WNW-ESE trend for S_2 and L_2 . The west and east domains are on the western and eastern borders of the Itabaiana quartzites surrounding the Itabaiana dome (Fig. 4.2). Both characteristically present a flat-lying S_1 foliation affected by open to tight F_2 folds associated with NNW-SSE trending S_2 and L_2 .

The stereographic plots of the D_1 - D_2 structures for each structural domain are shown in Figure 4.3 .

4.3 - The D_1 Deformation

The F_1 folds are generally WNW-ESE trending, SSW verging, isoclinal and recumbent folds that affect S_0 and S_n , and develop a strong axial planar foliation (S_1) which cuts across the fold hinges (Figs. 4.4 A & B). These folds are generally rootless and commonly range from 10's of centimetres to 10's of metres, and may have their overturned limbs cut by subhorizontal thrusts (Fig. 4.4 C).

S_1 mostly trends WNW-ESE and commonly dips at high angles (90° - 60° generally to the NNE, but also to the SSW) in the regional and Simão Dias domains, or at 60° to 50° in the Itabaiana domain. S_1 is relatively flat-lying in the west and east domains (Fig. 4.3 A), where the range of attitudes is from $20^\circ/318^\circ$ to $60^\circ/033^\circ$ (west domain) and from $30^\circ/046^\circ$ to $15^\circ/130^\circ$ (east domain).

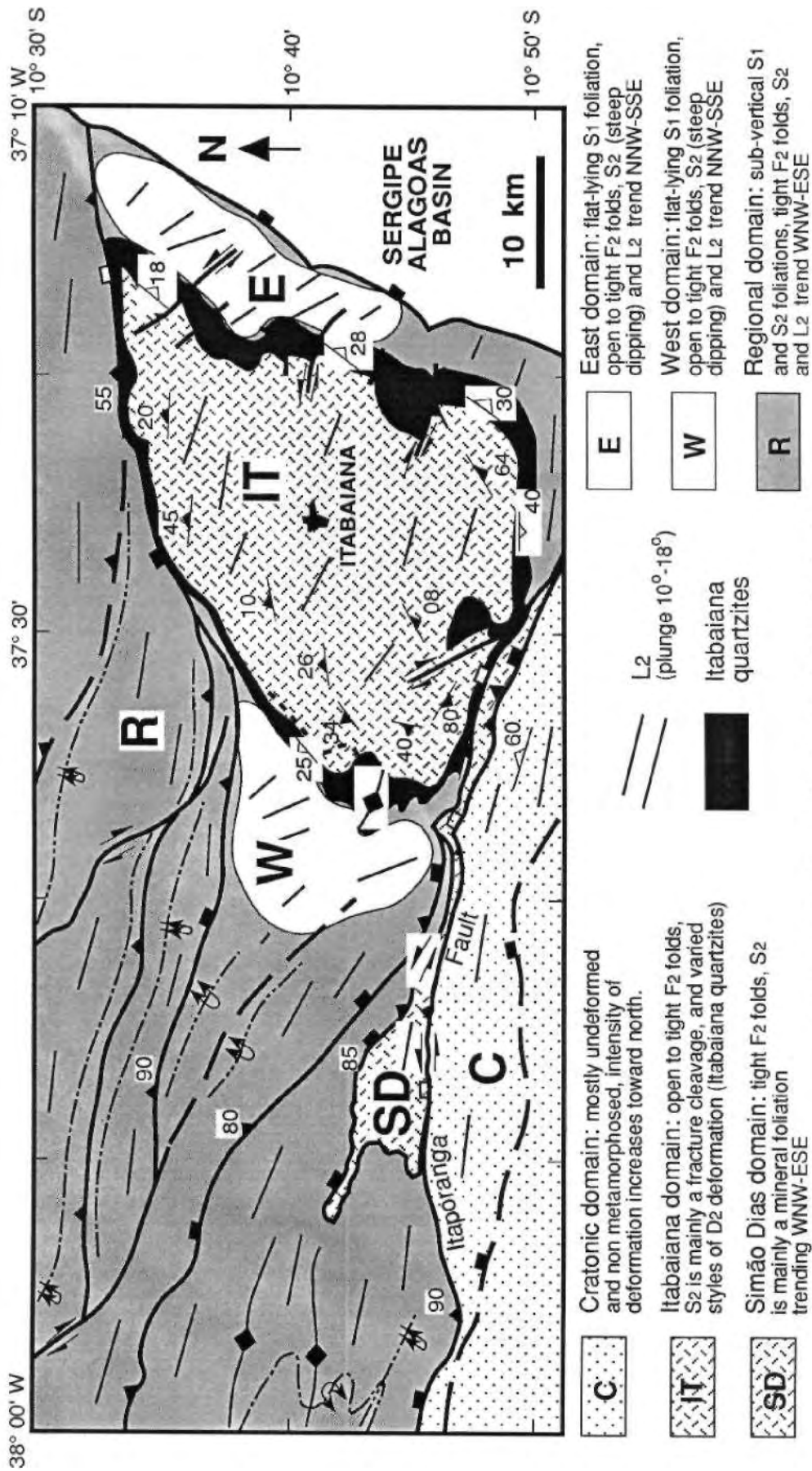


Figure 4.2 - The main structural domains in the Itabaiana dome area (see text).

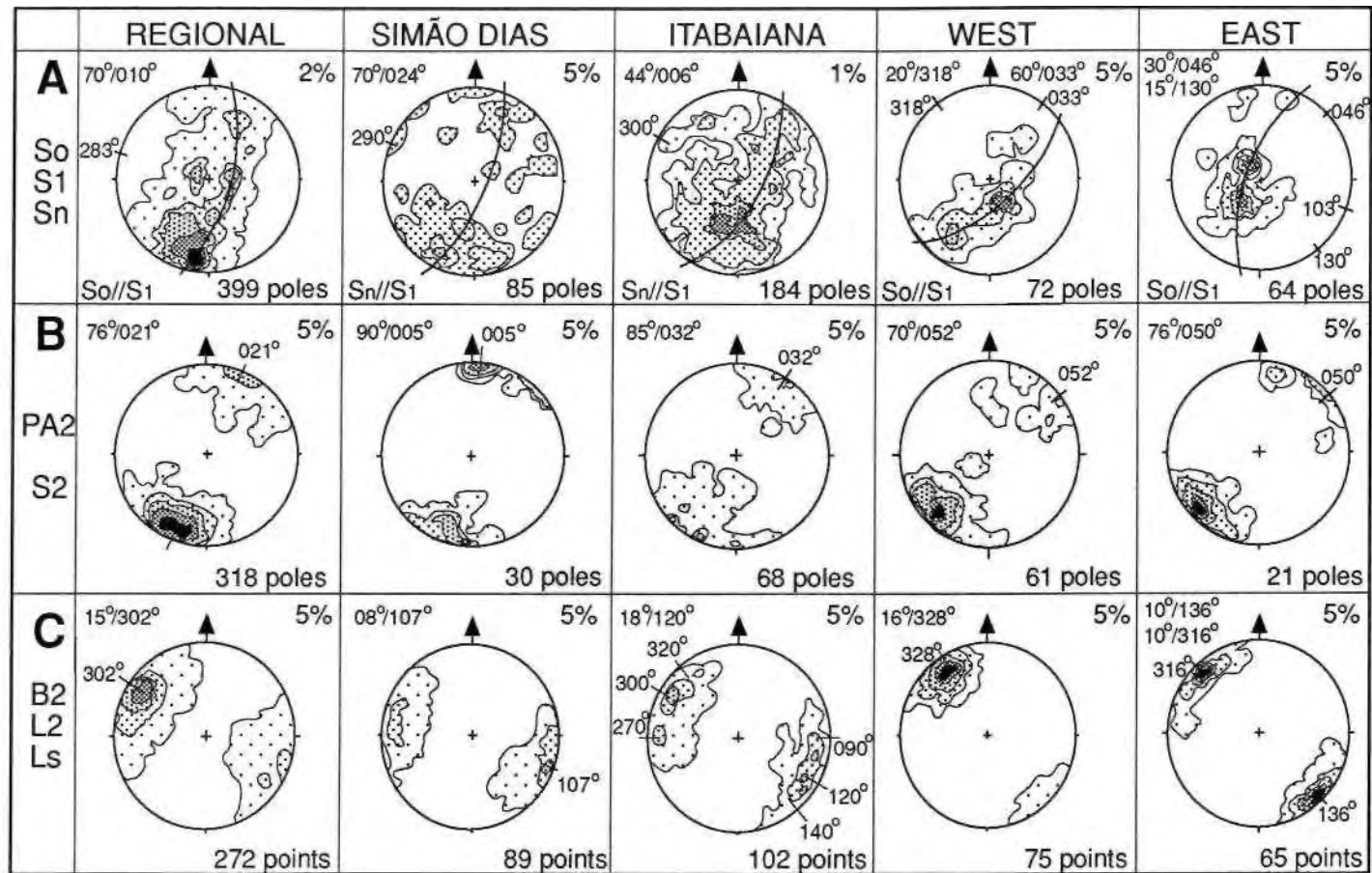
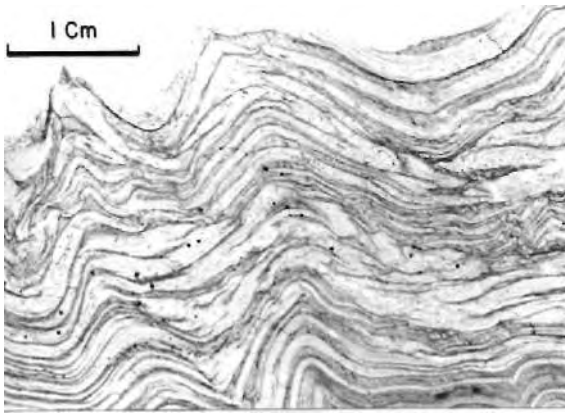


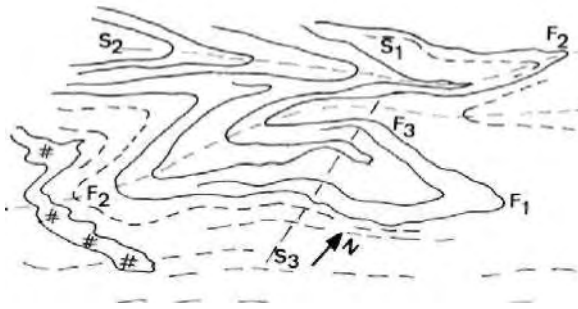
Figure 4.3 - Lower hemisphere stereographic plot of the D₁ and D₂ structural elements for each structural domain in the Itabaiana dome area. Contour intervals are either in steps of 1, 2 or 5% per 1% area. In A and B are the poles to the planes of So, S₁, Sn, PA2 and S2, whose attitude(s) of the maxima is (are) indicated in the upper left corner, for each domain. The attitude(s) of B2, L2 and Ls for each domain is (are) shown in the upper left corner of C.



A- F₁ recumbent folds affecting Frei Paulo phyllites, and co-axially refolded by F₂ folds. Note the layer-parallel foliation and the transposed F₁ fold hinges. Photograph of an entire thin section cut perpendicular to the fold axis. Outcrop 1040, along the Morcego stream.



B - F₂ folds in the Simão Dias gneisses, co-axially refolded by isoclinal F₂ folds (both arrowed) and affected by transversal, gentle F₃ folds (see line drawing below). Note the Si parallel quartz vein in the hinge zone of the F₂ fold to the left. Outcrop 305, north of Simão Dias.



Line drawing from the photograph in B, showing the structural relationship between F1, F2, F3 and S1, S2, S3

Figure 4.4 - D1 structures in the Itabaiana dome area

As a consequence of the recumbent F_1 folding, S_1 is generally nearly parallel to S_0 and S_n . The statistical analysis of the poles to S_0 , S_n and S_1 (Fig. 4.3 A) shows more or less complete Π girdles defining great circles, but the maximum concentration of poles observed in the regional, Simão Dias and Itabaiana domains indicates a 44° - 70° dip to NNE. This attitude is as a consequence of the vergence of the F_2 folding (discussed in section 4.4 below).

S_1 is a foliation defined by a planar-parallel orientation of sericite (or muscovite), chlorite, locally biotite (Fig. 4.4 D) and very fine grained quartz, in phyllites, diamictites and metacarbonates, with addition of feldspars and epidote (transformed from hornblende) and trails of opaque minerals in the basement rocks. In the quartzites it mostly consists of sericite (or muscovite) and elongated quartz grains.

Quartz and carbonate veins are injected sub-parallel to S_1 , and are deformed by F_2 folds. Syn-D₁ quartz veins are common in the basement gneisses and in the phyllitic metasediments, whereas carbonate veins are common in the metacarbonate formations.

The quartz-sericite-chlorite Frei Paulo phyllites, which are the dominant rock type in the west and east domains, have a pervasive layer-parallel fabric defined by sub-millimetre layers of micro-crystalline quartz intercalated with <1mm-thick mica domains (sericite, chlorite and local biotite), and sub-parallel quartz veins, generally affected by the D_2 structures (Fig. 4.4 E).

A strong S_1 foliation consisting of oriented flakes of sericite and opaque minerals is observed sub-parallel to the bedding of Frei Paulo sandy phyllites in the western part of the area (outcrops 848, 849, Fig. 3.1).

L_1 linear features are the fold axes (B_1) and the intersection lineation (L_{1-0}), which may be marked by oriented flakes of micaceous minerals, quartz ribbons, or quartz and feldspars. The amount of field information on D_1 linear structures collected in the area is insignificant for purposes of statistical analysis, but where these elements were observed (e.g. outcrops 31, 305, 311, 720, 1040, 1112, Fig. 3.1) they are nearly parallel to L_2 linear features.

4.4 - The D_2 Deformation

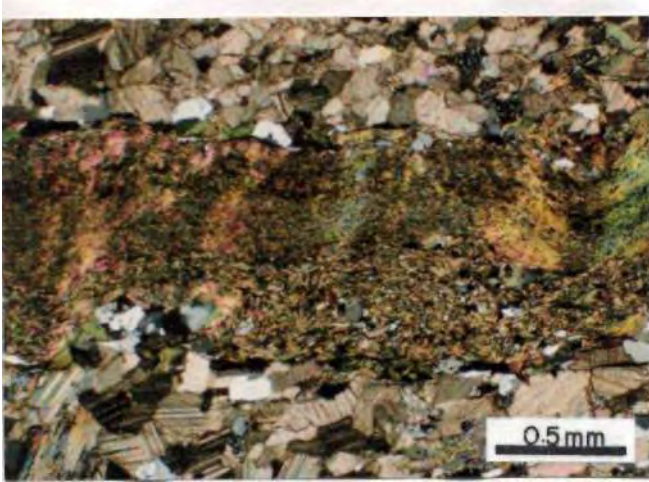
4.4.1- F_3 folds and structural elements

F_2 folds are open to isoclinal, gently inclined to upright, WNW-ESE trending, asymmetric with a SSW vergence. They are gently plunging folds that affect S_1 , S_0 and S_n (Fig- 4.5). They co-axially refold the F_1 folds, and range in size from micro crenulations to km-scale folds (observed in the aerial photographs) and are generally associated with a penetrative axial planar foliation (S_2).

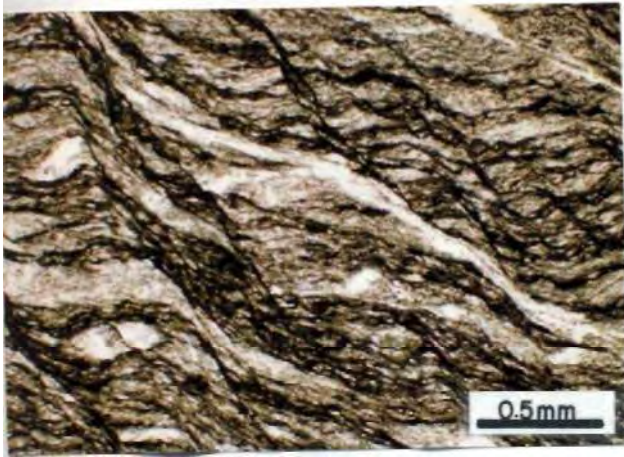
The S_2 foliation is mainly a pressure solution or a mineral foliation, and less commonly a slaty cleavage or a spaced cleavage. It generally dips at 60° - 90° to NNE in the regional, Simão Dias and Itabaiana domains, and to NE in the west and east domains (Fig. 4.2 B).



C - Mesoscopic F1 folds in the basal to middle section of the Jacoca Formation. Note the sub-horizontal axial planar foliation in the hinge zones, and the carbonate vein along the sub-horizontal thrust through the overturned limb of the upper fold. Outcrop 311, Capitão farm.



D - Layer-parallel S_1 foliation defined by <1 mm layer of sericite, chlorite, minor biotite, quartz and feldspar, in a specimen of dolomites of the Jacoca Formation. Note the marble texture defined by the euhedral, equigranular calcite/dolomite grains. Same outcrop as in C. Photographed under crossed polars.



E - S1 foliation defined by quartz veins injected sub-parallel to the layers of quartz- and mica-rich domains in the Frei Paulo quartz-sericite-chlorite phyllites. These features are deformed by F2 crenulations associated with a discrete crenulation cleavage and a pressure solution-type foliation. Outcrop 1195, Jacarecica river. Photographed under planar parallel light.

Figure 4.4 (continued).
90



A - Very tight F2 folds in the Frei Paulo interlayered calcilutites, metasiltites and metapelites (PC PF3). The arrow points to an overthickened hinge zone developed in the less competent layers of metapelites. The intense S2 axial planar foliation cross cut the fold hinges, but is parallel to the limbs. Outcrop 266, road from Mocambo to Carira.



B - Open, slightly asymmetric F2 anticline affecting the well-banded Itabaiana gneiss, and associated with a fracture cleavage axial planar foliation, Outcrop 504, road from Campo do Brito to Itabaiana.

Figure 4.5 - D2 folds in the metasediments (A) and in the gneissic basement (B) of the Itabaiana dome area.

The pressure solution foliation is normally defined by iron and/or manganese oxide seams along sub-parallel surfaces and are best developed in tightly folded metacarbonates (Fig. 4.6 A), and in the phyllitic rocks. In some cases the pressure solution process appears to have evolved progressively from the development of crenulations (as in Fig. 4.4 E), resulting in sharp zones of concentration of iron oxides and very fine micaceous minerals, comparable to the discrete crenulation cleavage of Gray (1977).

The mineral foliation is commonly marked by parallel, fine-grained sericite, chlorite and some biotite, which in the diamictites and gneisses are accompanied by very fine-grained quartz and feldspars. The slaty cleavage is more common in phyllitic rocks and interbedded phyllites and metasilts (Fig. 4.6 B).

L_2 linear features are also penetrative and consist of the fold axis (B_2), the intersection lineation (L_{1-2}) and the elongation lineation (L_s), which are all parallel to each other and plunge, generally at low angles (08° to 16°) either to WNW or ESE, in the regional, Simão Dias and Itabaiana domains, and either to NNW or SSE in the west and east domains (Fig. 4.2 C). The double plunge of L_2 can be observed in the walls of large outcrops (e.g. outcrop 90, to the SE of Paripiranga, Figure 3.1). The shift of the directions of L_2 in the west and east domains, relative to the regional domain, confirms the change of the strike of S_2 (compare Figs. 4.3 B & C).

L_{1-2} is defined by the intersection of finely-spaced, mica-rich S_2 planes with S_1 or S_0 , S_n (Fig. 4.7 A), or by a pencil-like lineation (Fig. 4.8 B). Mullion structures may locally occur in tightly folded metacarbonates. L_s is defined by flattened and elongated oolites and pellets in metacarbonates, by pyrite and fine-grained quartz in phyllites, and by pulled-apart grains of K-feldspar, plagioclase, and clasts of basement rocks in the diamictites and pebbly phyllites. In mylonitic quartzites L_s consists of ribbons of quartz and trains of deformed opaque minerals, and pressure shadow zones developed around K-feldspar and tourmaline clasts (Fig. 4.7 C). In the gneiss and basement derived mylonites, L_s consists of quartz ribbons, trains of elongated feldspars and aligned grains of epidote, or pulled-apart resistant grains such as K-feldspars and hornblende (Fig. 4.7 D).

A mineral lineation defined by hornblende and feldspars is locally observed on the limbs of open to very tight F_2 folds affecting the basement gneisses. The lineation plunges at low to high angles to the north, but the few examples (outcrop 12, N of Simão Dias and outcrop 404, road Campo do Brito-Itabaiana, Fig. 3.1) do not allow to trace it across the area. It might be a relict of older deformations affecting the basement.

Trains of 1-10m scale F_2 folds are a common feature, particularly in proximity to the regional faults, and normally show a sinistral asymmetry on the horizontal surfaces.

4.4.2 - The regional faults

Despite most of the regional faults having a clear signature defined on aerial photographs or maps of aeromagnetic anomalies (see section 5.4) they are not as obvious in the field. A locality with a typical brittle fault plane has not been found, nor described in the literature.



A - Penetrative pressure solution S2 axial planar foliation imprinted in the hinge zone of tightly folded, thinly laminated Olhos D'agua limestones. Outcrop 253, southwestern part of the area.



B - Sub-vertical S2 slaty cleavage developed in the Frei Paulo distal turbidites (lithofacies PC PF3). Bedding is defined by the alternated layers of light brown metasilites and metapelites. Outcrop 266, road Mocambo to Carira.

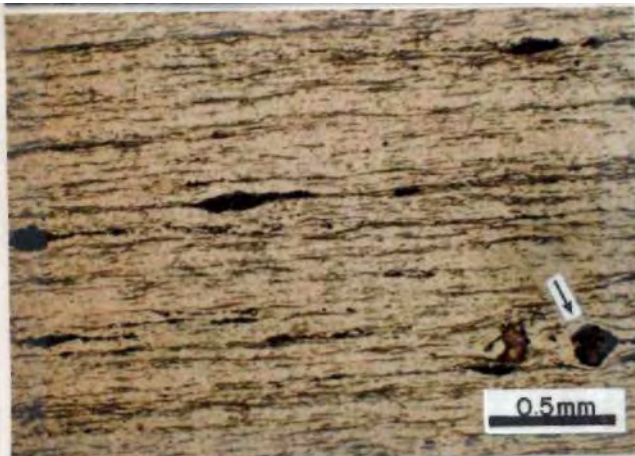
Figure 4.6 - The S2 foliation.



A - L1-2 lineation defined by the intersection of planar parallel oriented flakes of sericite (S2) on a Si surface defined by flattened quartz grains and quartz ribbons, in the Itabaiana quartzites. Note the trains of opaque minerals parallel to the flakes of sericite. Outcrop 886, southern Itabaiana dome.



B - Pencil-like L1-2 lineation defined by the intersection of a penetrative S2 foliation imprinted on basement-derived mylonites. Note the sub-vertical foliation parallel to the hammer (S3), and intersecting L1-2 in order to define the length of the pencil structure. Outcrop 95, road Si mão Dias to Paripiranga.



C - Trails of elongated opaque minerals and pressure shadow zones along tourmaline grains (arrowed), defining the elongation lineation in the Itabaiana quartzites. Photograph under plane-polarized light. Same outcrop as in A.



D - Impressive parallelism between L1-2 and the elongation lineation in tightly folded mylonitic gneisses of the southern part of the Itabaiana dome. Outcrop 889, Lomba river.

Figure 4.7 - The L2 lineation.

Nevertheless, the fault zones normally correspond to mylonitization and intense folding of the country rocks, and the penetrative foliation generally dips at high angles or sub-vertically to the NNE. The best outcrops of these rocks are along the roads cutting across the Simão Dias, Itaporanga and Dores faults (Fig. 3.1).

The F_2 folds outside and the folds inside the fault zones are comparable in all their characteristics. They show compatible mineral assemblages along the axial planar foliations, and similar orientation of the axial planes, axial planar foliations, fold axes, intersection lineations and mylonitic lineations. All these linear elements are nearly parallel and gently plunging (Fig. 4.8 A) to WNW or ESE.

The **Simão Dias fault** is a <2km wide zone of imbricated steep-dipping slices of highly folded quartzite- and basement-derived mylonites and phyllonites, better exposed at the northern border of the Simão Dias dome (outcrops 19-20, 306-307 Fig 3.1).

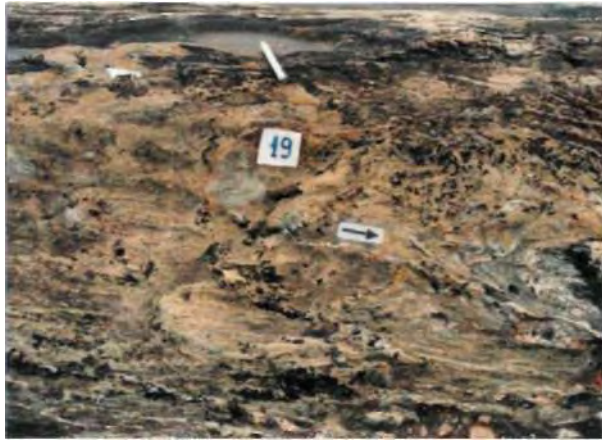
Several kinematic indicators, such as S-C relationships (Berthe et al. 1979; Lister & Snoke 1984; Shimamoto 1989), porphyroblast-tail systems (Passchier & Simpson 1986), and shear bands (Plat & Vissers 1980; Passchier 1984) all indicate top to the south, combined with E-W strike-slip movements (Fig. 4.8 B & D).

At its eastern termination inside the Itabaiana Dome Area, the Simão Dias fault consists of a <1km wide zone of sub-vertically imbricated slices of Itabaiana quartzites, Ribeirópolis phyllites and basement gneisses and derived mylonites. These are tightly to isoclinally folded and exhibit a strong pencil-like intersection lineation parallel to a mineral stretching lineation (as along the Lomba river and Montes stream, and on the Arrasudor farm - outcrops 888, 889, 916, 926 to 930, 933 and 934, Fig. 3.1).

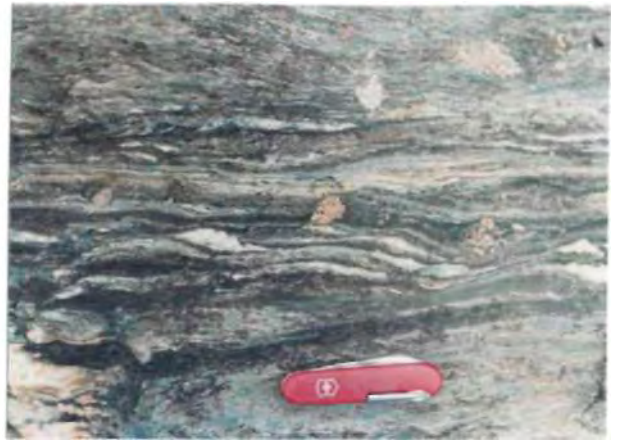
The **Itaporanga fault** is a <500m wide zone of mylonitic gneisses and mylonitic Olhos D'água metacarbonates. Feldspar porphyroblast-tail systems and small-scale sigmoidal porphyroclasts and slices of carbonate rocks observed on horizontal surfaces (nearly parallel to the XZ plane), in the mylonitic gneisses and mylonitic dolomites (outcrop 276, road Simão Dias to Lagarto) all indicate a sinistral movement for this fault. This is confirmed by subvertical, sinistral shear bands affecting polydeformed metacarbonates elsewhere along the fault zone (Fig. 4.8 E).

In the SW corner of the area (outcrop 839, Fig. 3.1), the Itaporanga fault separates sheared and silicified Lagarto-Palmares sandstones which dip 85° to 356° , and contains a striae lineation plunging 24° to 080° , from highly folded Olhos D'água metacarbonates. In a single, flat-lying outcrop at the same locality, a well-cemented and somewhat stratified breccia, containing generally 10cm size angular clasts of deformed Olhos D'água metalimestones is also found.

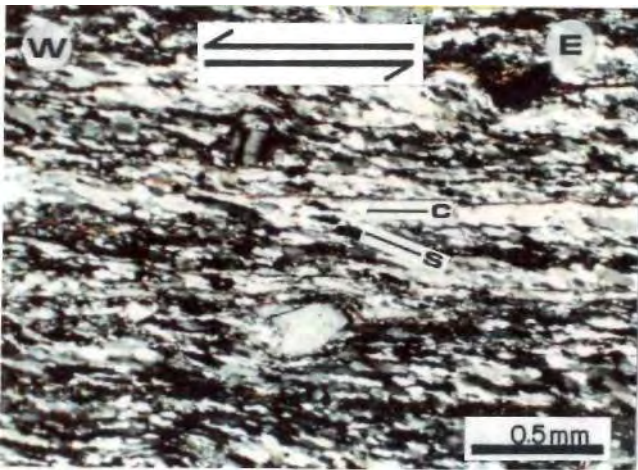
The **Dores fault** zone is exposed in the road to the Volta Village in the NE corner of the area (outcrop 1105, Fig. 3.1). It places subvertical, highly sheared quartzites and basement-derived phyllonites on Frei Paulo phyllites and is also marked by percolation of manganese and iron oxides. Shear bands affecting the quartzites and the phyllonites respectively indicate a top to the south and a E-W sinistral strike-slip movement (the latter is shown in Fig. 4.8 F).



A- Small-scale very tight folds affecting phyllonites derived from gneisses. The arrow indicates the fold axis which is parallel to a strong elongation lineation,



B - Sinistral shear bands displacing elongated ribbons of aggregated fine grain quartz veins emplaced parallel to the mylonitic foliation.



C - S-C relationship in the phyllonite indicating an E-W sinistral shear movement seen in the XZ plane. Photograph under crossed polars.



D - Top to the south movement indicated by the sinistral shear along the S₂ foliation seen in the YZ plane. Note the asymmetric tails of the microcline porphyroclast. Same sample as in C Photographed under planar parallel light

Figure 4.8 - Structural relationships along the regional faults. A-D are from the same outcrop (number 19) in the Simão Dias fault zone, road Simão Dias to Pinhão.



E - E-W sinistral movement indicated by shear bands in highly foliated Olhos D'agua limestones. The handle of the hammer points to the south.



F - WNW-ESE sinistral movement indicated by shear bands in basement-derived phyllonites emplaced in the hanging-wall of the Dores thrust. The white pen points to the north.

Figure 4.8 (continued) - (E) is from the Itaporanga fault, outcrop 147 to the south of Símão Dias, and (F) is from the Dores fault, outcrop 1105 to the southwest of the Volta village.

The Escarpa **fault** places tightly folded Frei Paulo variegated phyllites on tightly folded Olhos D'agua metacarbonates. This is best observed on the road from Simão Dias to Pinhão (outcrops 31-32), and along the secondary road from Olhos D'agua to the Vaza Barris river (outcrop 415, NE of Olhos D'agua, Fig. 3.1).

The trace of the **Pelada fault** corresponds in the field to a zone of intense quartz veining (between Macambira and Pedra Mole), and to a localised zone of shearing in the Palestina diamictites (outcrop 113, in the western part of the area, Fig. 3.1).

The **Mocambo fault**, as seen in the outcrops 1065 and 1066 of the Salgado river (Fig. 3.1, enclosure), consists of a <km wide zone of intensely foliated and brecciated Frei Paulo metasandstones). The outcrops do not allow any determination of the sense of movement, but in this area the Mocambo fault controls the local E-W trend of the Salgado river and a secondary drainage (as observed on aerial photographs).

The Vaza **Barris, Mocambo and Montes strike-slip faults**, and the faults displacing the eastern-southern border of the Itabaiana dome, are also observed on the aerial photographs, and some can also be seen in the field. For example, sheared diamictites with clear indication of dextral movement are observed in the Vaza Barris fault zone (outcrop 1078, northwestern part of the area, Fig. 3.1).

It is noteworthy to mention that in the aerial photographs the dextral displacement along the Vaza Barris fault and Mocambo shear dies along their traces and vanishes parallel to the regional foliation towards the Itabaiana dome. The southeastern end of the Vaza Barris fault coincides with a broad area of intense quartz veining (Fig. 3.1).

The **Jacaré fault** is the most prominent of several NW-SE to WNW-ESE trending lineaments observed in aerial photographs and topographic maps within and outside the southern mapped area. The fault trace roughly corresponds to a topographic break between 600m high hills to the south from 400m high hills to the north of it, as observed in the 1:100,000 topographic maps used as basis for the geological mapping.

These hills are formed by the Lagarto-Palmareis sandstones, which are intensely fractured, silicified and indurated (outcrops 78 and 957, southwestern part of the area, Fig. 3.1). The Jacaré fault is interpreted as a normal fault with uncertain age relative to the other regional faults.

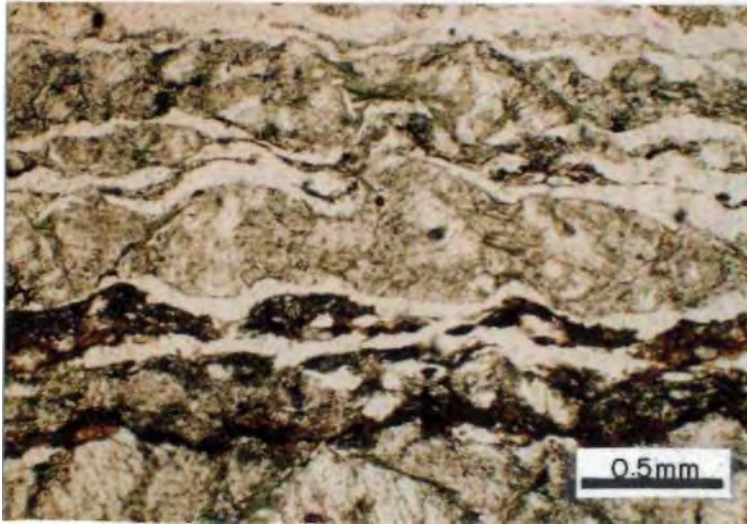
4.4.3 - D₂ deformation fabrics

Commonly in rocks that contain elements with different competences, e.g. diamictites with coarse-grained clasts in a fine-grained matrix, or even in mylonitic gneisses (Fig. 4.9), the competent grains, clasts, or porphyroclasts are typically fractured, pulled-apart and rotated, in order to accommodate the more ductile deformation of the matrix. Pressure shadows and tails are also commonly developed around rigid elements in a more ductile matrix.

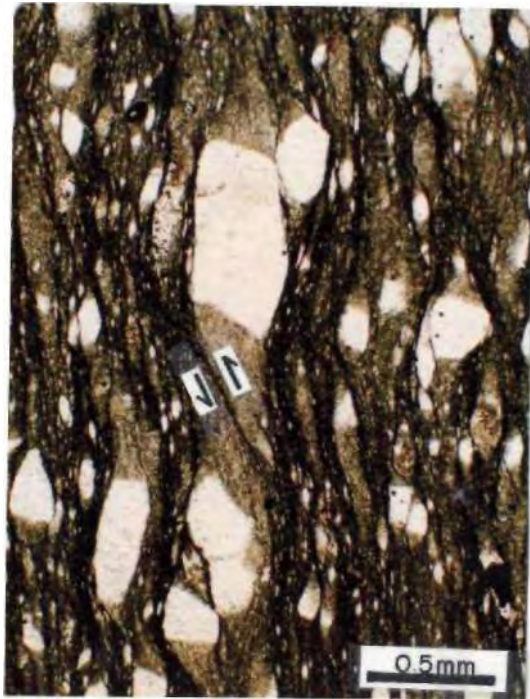
The fractures in the grains are filled by veins of fibrous quartz or calcite, or fibrous overgrowth of chlorite and sericite (Figs. 4.9 A & B). The low pressure tails developed around the coarse-grained rigid particles normally consist of dynamically recrystallised quartz and feldspar, and very fine sericite, chlorite and minor biotite (Fig. 4.9 C).



A - Low pressure tails and voids developed in a fractured and pulled-apart feldspar clast of the Palestina diamictites, and infilled with quartz, chlorite and sericite. Outcrop 90, road Paripiranga to Simão Dias. Photographed under planar parallel light.



B - Train of fractured and pulled-apart feldspars in a mylonitic gneiss of the southern Itabaiana dome. Chlorite and quartz infill the low pressure tails and voids. Outcrop 583, west of São Domingos. Photographed under planar parallel light.



C - Shear bands cutting the tails of fine grained quartz, sericite and chlorite developed on both ends of the clasts in Palestina diamictites, and indicating a top to the south movement in a thin section parallel to the YZ plane. Photographed under planar parallel light. Outcrop 193, south of Pedra Mole.

Figure 4.9 - D2 deformation fabrics.

The micaceous minerals in the tails and voids are coarser than those along the foliation planes. In thin section from one locality within the Simão Dias gneiss (outcrop 101, WSW of Simão Dias, Fig. 3.1) needles of actinolite infill the fractures in pulled-apart fragments of hornblende.

4.4.4 - Strain analyses

The deformed clasts and respective tails in the Palestina diamictites and pebbly phyllites generally form ellipses which are observable in many subhorizontal and subvertical surfaces nearly parallel to the XZ, XY and YZ planes in the outcrops (Fig. 4.10) and in the oriented thin sections (Fig. 4.11).

A qualitative observation of hundreds of such ellipses in the field and in thin sections (Figs. 4.10 A-B & 4.11) is sufficient to reveal that the X-parallel axis, which lies parallel to F_2 fold axis and L_{1-2} , is generally much longer than the Y-parallel axis.

However, particularly in the core of the Paripiranga anticline, or in the hinge zones of larger F_2 folds (outcrops 90, 239 and 299, Fig. 3.1), and in outcrops located closer to the western margin of the Itabaiana dome (e.g. outcrop 987) the clasts are generally undeformed, or even rounded without any tail in the YZ plane (Figs. 4.10 C & D), even though they are very elongated in the X direction.

An extensive quantification of the strain recorded by the clasts in the Palestina Formation was carried out throughout the area, by measuring the axis of the clasts in outcrops or in oriented thin sections. These data (Appendices A2.1-A2.3) were treated according to different methods of strain quantification (Flinn 1962, 1965; Hsu 1966; Lisle 1979; Borradaile 1981). The measurements were carried out on clasts of milky quartz, granite, gneiss, and grains of feldspar, which are the majority in outcrops and thin sections. This is an attempt to avoid extreme contrast of ductility if clasts of metasediments were also studied.

Clasts were measured directly on surfaces nearly parallel to the XY and YZ planes, in the outcrops 36, 90, 107 and 108 (Appendix A2.1). These data allowed direct calculation of the X/Y and Y/Z axial ratios. The strain ellipsoids calculated using the maximum and minimum ratios for each surface are plotted on Flinn's and Hsu's diagrams (Figs. 4.12 A & B). In both the diagrams, all the finite strain ellipsoids lie in the field of constriction or apparent constriction.

As displayed in Figures 4.12 A & B, the strain ellipsoid calculated for outcrop 90 has the most prolate of the four ellipsoids. Outcrop 90 lies in the protected core of a = 1km scale and open F_2 fold and shows no intense S_2 foliation (Fig. 3.18 C) compared to the other outcrops, which are characterised by tight folding and a pervasive S_2 foliation.

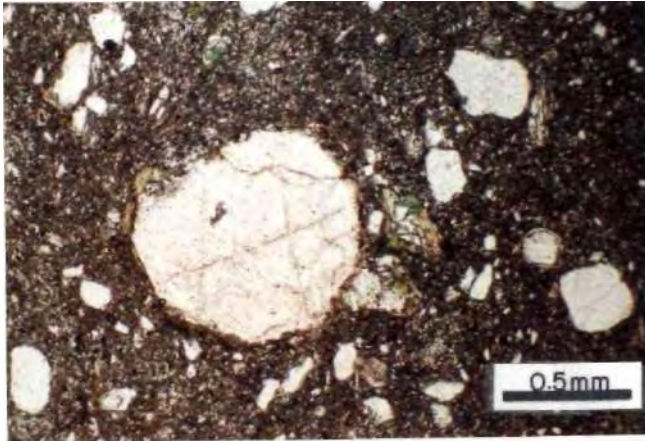
In the outcrops 44, 107, 108 and 405 (Appendix A2.2) it was possible to measure also the parameters S and D of Borradaile (1981), respectively for the matrix and the clasts, in surfaces nearly parallel to the XZ and YZ planes. As defined by Borradaile (1981), the ratio (S-D)/D can be considered as the minimum amount of ductile deformation of the matrix relative to the clast, which is considered as a rigid panicle.



A - Boulder of granite fractured and pulled-apart along the WNW-ESE structural grain of the Palestina diamictites. Note that the fractures are healed by fibrous quartz (fibres // X in the XZ plane) and also cut through the phyllitic matrix (arrowed). Outcrop 1073, Vaza Barris river valley, northwestern area.



B - Elongated, fractured and pulled-apart clasts of the Palestina diamictites, defining an elongation lineation // X and to the L1-2 lineation in the XY plane. Outcrop 107, Vaza Barris river valley, north of Paripiranga.



C - Photograph taken under planar parallel light of a thin section cut parallel to the YZ plane, showing undeformed clasts surrounded by flakes of chlorite. Outcrop 90, in the hinge zone of a large-scale F2 fold, road Paripiranga to Simão Dias.



D - Rounded and elongated clasts in a surface // to the YZ plane in Palestina diamictites. Note that the smaller clasts away from the larger clasts (voids) are elongated // Y and shortened // Z (roughly parallel to the hammer). Outcrop 193, Vaza Barris river valley, south of Pedra Mole.

Figure 4.10 - Elongation of clasts in the XZ, XY and YZ planes.

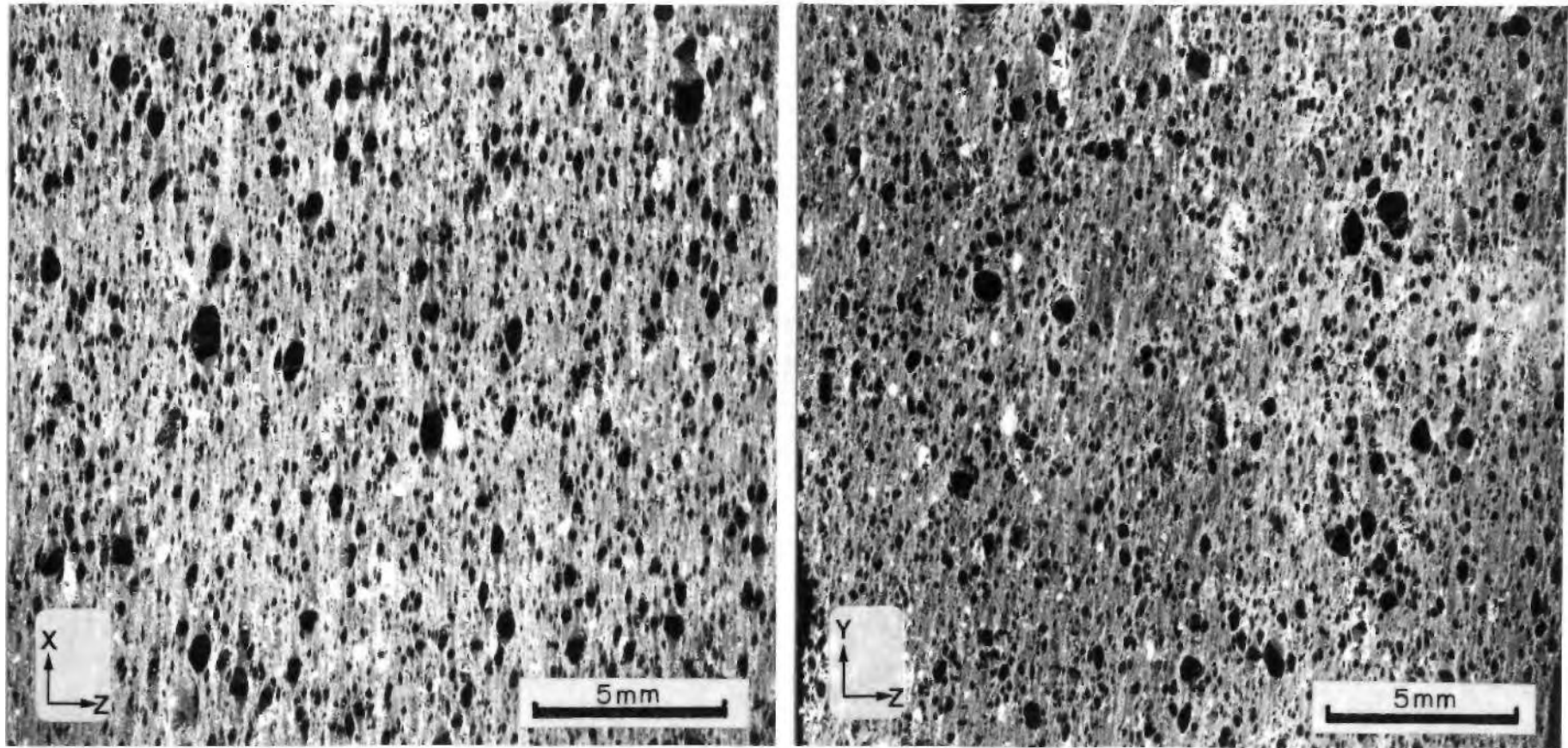


Figure 4.11 - Photograph of thin sections parallel to XZ (left) and YZ (right) in a Palestina pebbly phyllite, outcrop 186, half way between Olhos D'agua and Pedra Mole (Figure 3.1 in the folder). Note that the clasts are much flatter in XZ than in YZ, and that the X-parallel tails are better developed and longer than the Y-parallel tails. The ellipses defined by the clast-tail systems have a greater axial ratio in the thin section containing the stretching lineation (parallel to X in the XZ plane) than the ratio observed in the thin section perpendicular to it (YZ).

Parameter	Outcrop 36	Outcrop 90	Outcrop 107	Outcrop 108
$a = X/Y$	2.44	3.98	2.57	1.82
$b = Y/Z$	1.64	1.58	1.70	1.59
$k = (a-1)/(b-1)$	2.25	5.13	2.24	1.39

Parameter	Outcrop 36	Outcrop 90	Outcrop107	Outcrop108
$-\bar{\epsilon}_3$	0.49	0.46	0.53	0.46
ν	-0.12	-0.43	-0.28	-0.13

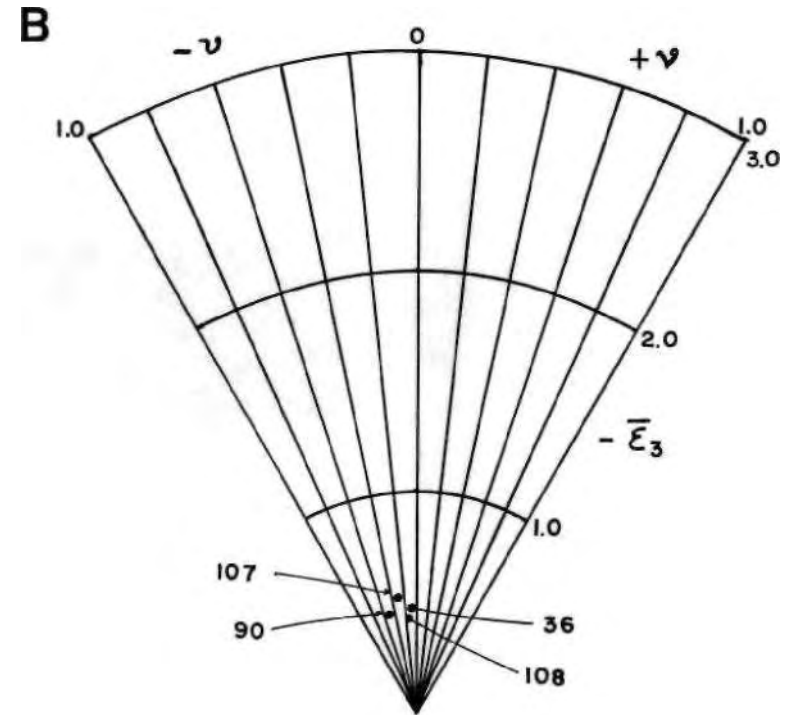
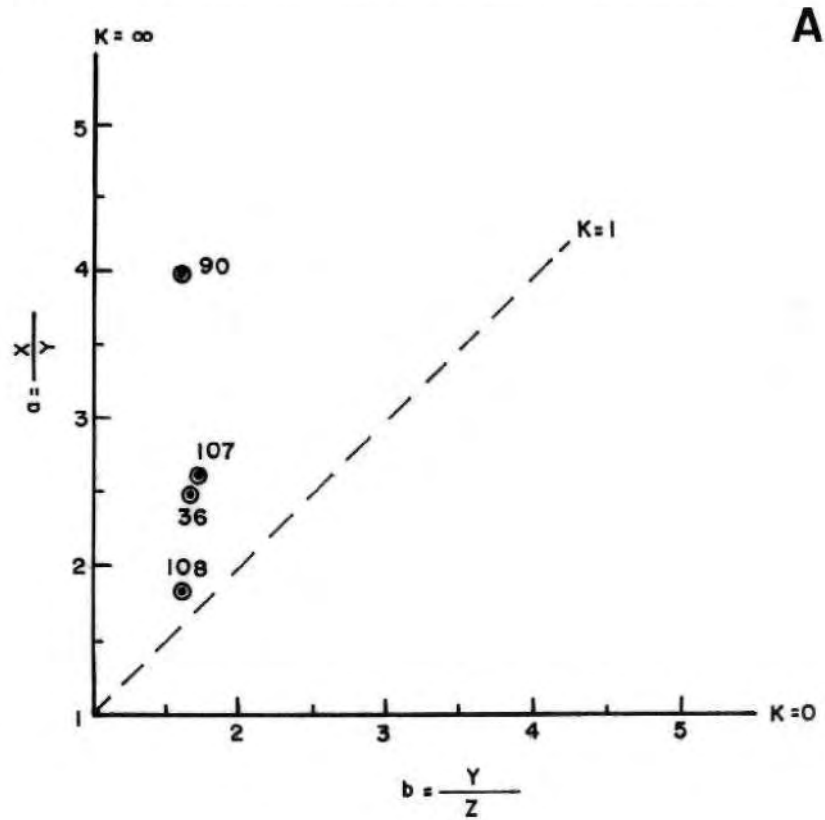


Figure 4.12 (A-D) - Plot of the strain ellipses calculated for the clasts of the Palestina diamictites, using the axial ratios in **bold** in Appendix A2.1. All the ellipses lie in the constrictional field on both the Flinn (1962) diagram (A), and in the Hsu (1966) diagram, (B). Note that the most excentric strain ellipse is from outcrop 90, in both diagrams. See text.

Ellipses defined by clasts and clasts+tails were also measured in thin sections cut parallel to the XZ and YZ planes of the Palestina pebbly phyllites in the outcrops 33,36, 42, 84, 90, 111, 140, 142, 186, 188, 192, 193, 239, 246, 249, 341, 405 and 997 (Appendix A2.3).

The harmonic mean of the X/Z and Y/Z axial ratios were calculated for the data in Appendices A2.2 and A2.3 and are summarised in Table 4.2 . These means were also used for the computation of the parameters a, b and K of the strain ellipsoid (Flinn 1962, 1965) of each outcrop (Table 4.2), whose plot in the Flinn's diagrams of Figures 4.12 C & D indicates both constrictional and flattening deformation.

The graphic method of Fry (1979) was applied upon enlarged photographs of thin sections parallel to XZ and YZ planes in outcrops 186 and 188, which are characterised by development of intense S_2 pressure foliation (Fig. 6.11). The ellipses defined by this method were parallel to the X or Y directions, and the computation of the a, b and K parameters from their axial ratios (Table 4.2) indicates strain dominated by flattening ($K < 0$) in areas of tight folding. These results are compatible with those from the analysis of the data for the same outcrops in the Appendix A2.3 (apart from the large discrepancy of values of K for outcrop 186).

Thus, an average shape of cigar shaped ellipsoid with circular or slightly elliptical sections perpendicular to the long axis describes the clasts in the less D_2 -strained areas (a prolate geometry with $X \gg Y > Z$). In areas of more intense D_2 deformation a cigar shape geometry whose circular basal section underwent flattening in the YZ plane ($X \approx Y > Z$) probably matches the average shape of the clasts of the Palestina Formation.

Lisle (1979) discussed the difficulties of quantifying strain in polymict conglomeratic rocks with a marked competency contrast, and where there is practically no fluctuation (such is the case with the Palestina rocks). He proposed that in many cases the harmonic mean of the axial ratio of the clasts on each surface is a better approximation of the shape of the strain ellipse.

These conclusions are valid for the clasts in the Itabaiana quartzites and Ribeirópolis pebbly phyllites on the western border of the Itabaiana dome (for example in outcrops 312, 470 and 471, Fig. 3.1), and also in the Olhos D'água Formation (outcrops 5, 7, 829 and 1061, all around Paripiranga).

4.4.5 - Syn- D_2 vein systems

In thin section, highly foliated phyllites, pebbly phyllites and metacarbonates show that quartz and calcite veins commonly cross-cut S_2 , and are also dissolved/shortened by the S_2 pressure solution seams (Fig. 4.13 A). From samples of different localities (for example outcrops 84, 140, and 249, Fig. 3.1) it has been observed that the transversal veins are also affected by micro-scale F_2 folds, or are disrupted, displaced and progressively rotated to positions sub-parallel to S_2 .

The rotation of the vein segments, as well as the mineral grains or fragments, mostly occurs along, subvertical sinistral shear bands and shear fractures which trend at low angles to the S_2 foliation (Fig. 4.13 B), and less commonly along subvertical dextral shear bands and shear fractures trending at high angles to the foliation.

Data measured at the outcrops below (see A2.2)

OUTCROP	CLAST					CLAST + TAIL				
	X/Z	Y/Z	a=X/Y	b=Y/Z	K=a-1/b-1	Xt/Z	Yt/Z	a	b	K
44	1.57	1.56	1.00	1.56	0.0	2.99	2.30	1.30	2.30	0.2
107	1.73	1.49	1.16	1.49	0.3	2.99	1.97	1.51	1.97	0.5
108	1.61	1.22	1.31	1.22	1.4	6.07	2.83	2.14	2.83	0.6
405	2.71	1.63	1.66	1.63	1.0	8.39	4.07	2.06	4.06	0.4

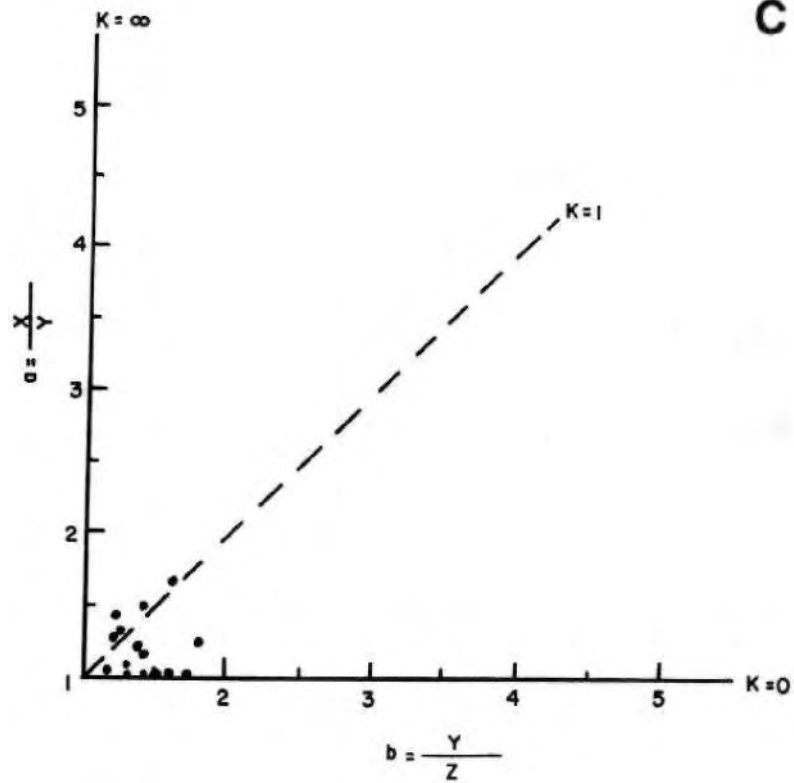
Data from oriented thin sections from the outcrops below (see A2.3)

OUTCROP	CLAST					CLAST + TAIL				
	X/Z	Y/Z	a=X/Y	b=Y/Z	K=a-1/b-1	Xt/Z	Yt/Z	a	b	K
33	2.30	1.80	1.27	1.8	0.3	4.40	2.70	1.63	2.70	0.4
36	1.40	1.50	0.93	1.5	<0	3.80	1.70	2.23	1.70	1.8
42	2.10	1.40	1.5	1.4	1.3	4.40	2.50	1.76	2.50	0.5
84	1.10	1.50	0.73	1.5	<0	4.50	2.10	2.14	2.10	1
90	1.60	1.20	1.33	1.22	1.5	3.70	1.20	3.08	1.20	10
107	1.70	1.20	1.41	1.2	2.1	4.20	1.20	3.50	1.20	13
111	1.50	1.30	1.15	1.3	0.5	3.40	2.00	1.70	2.00	0.7
140	1.40	1.30	1.07	1.3	0.2	3.40	1.60	2.10	1.60	1.8
142	1.50	1.30	1.15	1.3	0.5	4.20	1.60	2.62	1.60	2.7
186	1.70	1.50	1.13	1.15	0.9	5.20	2.60	2.00	2.60	0.6
188	1.80	1.70	1.05	1.7	0.1	4.60	3.70	1.24	3.70	0.1
192	1.40	1.60	0.87	1.6	<0	3.70	2.30	1.61	2.30	0.5
193	1.60	1.50	1.07	1.5	0.1	4.80	2.70	1.78	2.70	0.5
239	1.50	1.50	1	1.5	0.0	4.10	2.30	1.78	2.30	0.6
246	1.40	1.40	1	1.4	0.0	3.50	2.50	1.40	2.50	0.3
249	1.50	1.50	1	1.5	0.0	5.10	2.00	2.50	2.00	1.5
341	1.70	0.90	1.88	0.9	<0	4.20	2.00	2.10	2.00	1.1
405	1.70	1.40	1.2	1.4	0.5	4.80	2.20	2.40	2.00	1.4
997	1.60	1.20	1.33	1.2	1.7	4.60	1.50	3.07	1.50	4.1

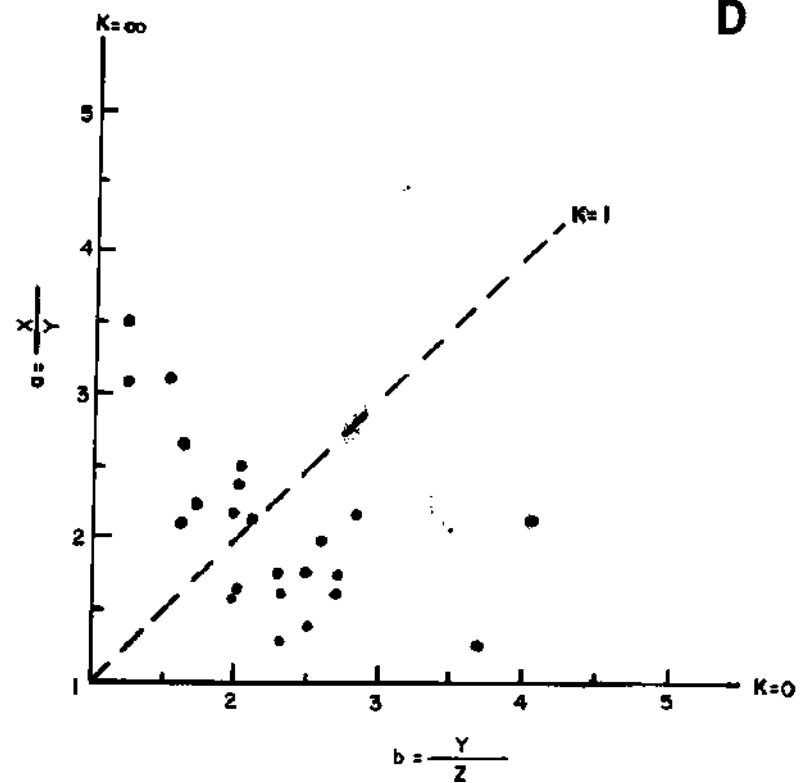
Fry (1979) method applied to thin sections from the outcrops below

OUTCROP	CLAST					CLAST + TAIL				
	X/Z	Y/Z	a=X/Y	b=Y/Z	K=a-1/b-1	Xt/Z	Yt/Z	a	b	K
186	3.86	3.20	1.20	3.20	0.1					
188	4.00	2.70	1.50	3.70	0.3					

Table 4.2 - Summary of the harmonic means of the X/Z and Y/Z axial ratios of clasts and clasts+tail, together with the a, b, and k parameters of the finite strain ellipsoids plotted in the Flinn diagrams of Figure 4.12 C and D. Compare the k parameter obtained for outcrops 186 and 188, by direct measurement of clasts in thin sections and by application of the Fry (1979) method to the same thin sections.



C

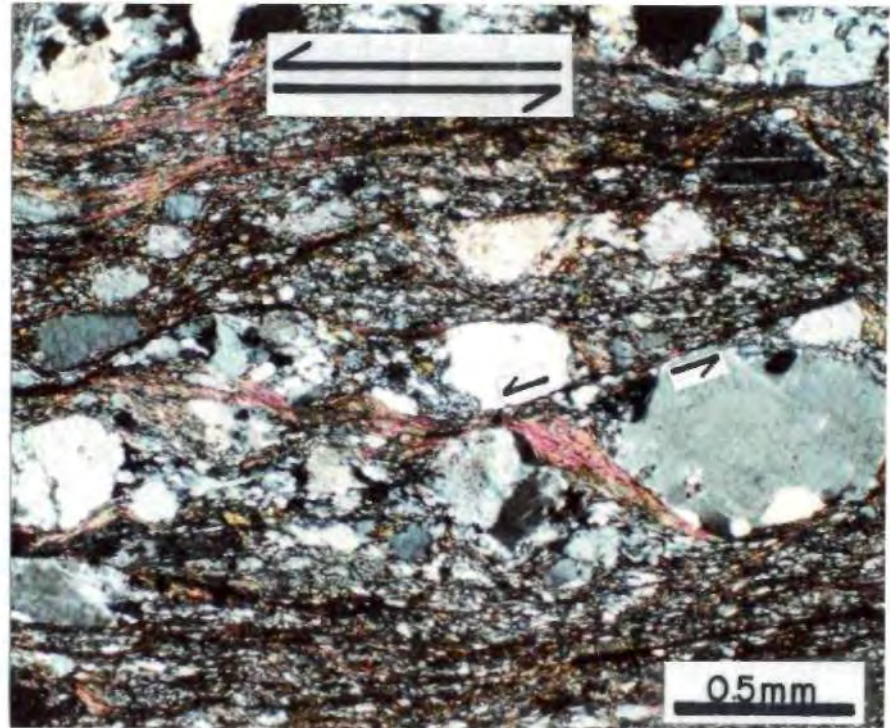


D

Figure 4.12 (continued) - Plot of the finite strain ellipsoids calculated for the clasts of the Palestina diamictites, using the harmonic means in Table 4.2. In C are plotted the ellipsoids calculated for the clasts. In D are plotted the ellipsoids calculated for clasts+tail. The a, b and K parameters are in Table 4.2 .



A - Quartz vein emplaced perpendicular to, and also affected and shortened by the S2 pressure solution-type foliation in the Palestina diamictites. Thin section // XZ plane, photograph under planar parallel light. Outcrop 90, southeast of Paripiranga.



B - Sinistral, synthetic shear bands and shear fractures displacing K-feldspar and plagioclase porphyroclasts, and also the mylonitic foliation in mylonites of the Simão Dias dome. Photograph under crossed polars, thin section parallel to the XZ plane. Outcrop 28, north of Simão Dias.

Figure 4.13 - Syn-D2 Veins and sinistral shear bands.

This situation probably reflects a progressive sequence of D_2 deformational events, which is also supported by other observations in the area, such as shear bands and shear fractures displacing tails and the material infilling the inter-grain low pressure voids (for example, in thin section of outcrop 140),

4.4.6 - Inter-foliation slip away from the fault zones

As well as being found along the regional faults, the S-N directed shortening associated with the D_2 deformation was coupled with a component of inter-foliation slip along the WNW-ESE trending regional foliation, in the rocks at distance from the fault zones.

This is documented by transverse fractures and asymmetric tails in the clasts of the diarnictites and pebbly phyllites, which systematically indicates a component of a top to the south, and another of a E-W sinistral movement along the steep dipping S_2 foliation (Fig. 4.14).

Evidence of horizontal dextral movements along the foliation planes of the rocks away from the fault zones are much more localised, although they are found both in thin sections and in outcrops. The examples occur on the Comandante farm, and mainly in the Simão Dias gneisses (Fig. 3.1, enclosure), particularly along the borders of the Itaporanga and Simão Dias faults.

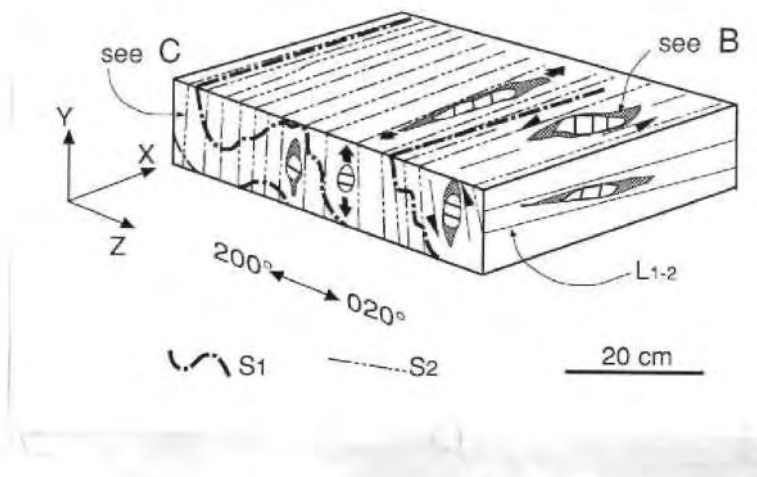
On the Comandante farm, a series of NW-SE trending, generally subvertical shear zones defined by silicification, induration, and quartz veining of the the Jacaré metasilites and fine sandstones, together with drag-folding of a steep dipping bedding sub-parallel penetrative foliation. In the Simão Dias gneiss (and less commonly in the Itabaiana gneisses), the dextral movements are indicated by 10-100cm wide, subvertical ductile and brittle-ductile shear bands and shear zones affecting gneisses, mylonites and phyllonites (Fig. 4.15).

4.5 - The D_3 Deformation

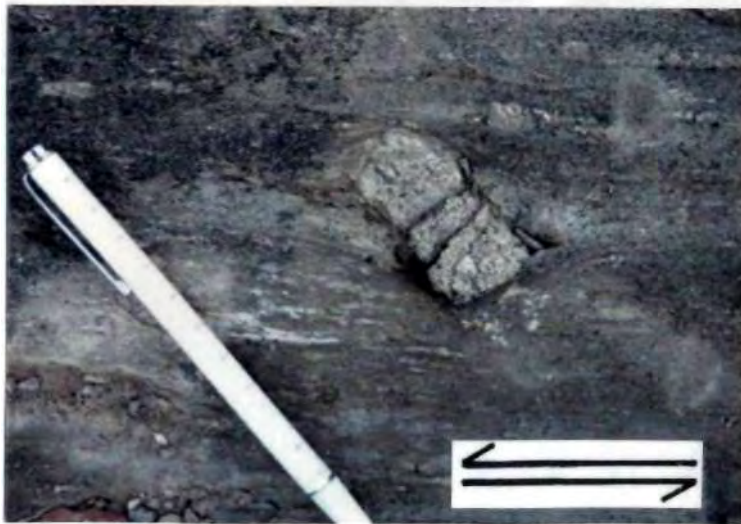
This is a non-penetrative event indicated by 10cm- to 10m-scale, NE-SW trending, generally open and upright, kink-style F_3 folds, 1mm-10cm size crenulations and kink bands affecting the S_2 foliation and the older planar elements (Fig. 4.16).

The mesoscopic F_3 folds are normally associated with a spaced cleavage axial planar foliation (S_3). The average trend of the axial plane of the F_3 folds (PA_3) and the S_3 foliation is NE-SW in all the structural domains, and the dip normally ranges between 60° and 90° , to the NW or to the SE (Fig. 4.17 A).

Even in the areas where the F_3 folds are absent, S_3 is marked set of closely spaced, SW-NE trending, steep dipping to subvertical partition planes (Fig. 4.17 A) which may be marked by pressure solution seams (e.g. outcrops 880-890, along the Lomba river, Fig. 3.1). This set cross-cuts the S_2/S_1 foliations and defines the pencil-like L_{1-2} intersection lineation (e.g. Fig. 4.7 B). Finely spaced, subvertical and undeformed, and generally 1cm thick quartz or carbonate veins are commonly found emplaced along these planes, particularly in phyllites, phyllonites and metacarbonates.



A - Idealised block diagram showing the top to the south and the WNW-ESE shear movement along the planes of the S2 foliation in the Palestina diamictites. Based on observations from many outcrops.

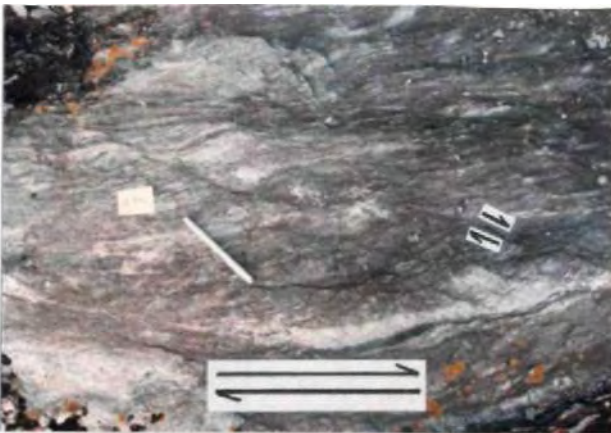


B - Clast of granite seen in a surface nearly parallel to the XZ plane, showing transversal fractures and asymmetric pressure shadow tails indicative of an anticlockwise rotation parallel to the WNW-ESE grain of the belt. The pen points to the north. Outcrop 405, south of Pedra Mole.



C - Same relationship as in B, but in a vertical surface nearly parallel to the YZ plane, and indicating a top to the south movement along the planes of the steep-dipping S₂ foliation, which cross cuts the folded S₁ foliation. Outcrop 36, road Simão Dias to Pinhão.

Figure 4.14 - Inter-foliation slip in the metasediments.



A - Sub-vertical, dextral shear bands affecting the mylonitic foliation of gneisses. Outcrop 296, north east of Simão Dias.



B - Sub-vertical dextral movement along the WNW-ESE structural grain of the gneisses. The dextral shear fractures affect at high angle the quartz-feldspar layers, and at low angle the chlorite-hch layers arrowed). Outcrop 1144, south of Paripiranga.



C - Sub-vertical, dextral shear bands affecting sub-vertical phyllonites. Outcrop 495, road Campo do Brito to Itabaiana.

Figure 4.15 - Sub-vertical dextral shear bands in the basement rocks. (A) and (B) are from inside the Simão Dias dome, (C) is inside the Itabaiana dome. In all photographs the 12cm-long white pen indicates the north.



A - Open F3 folds refolding thinly laminated Olhos D'agua limestones. The arrow points to tight F2 fold hinges. Note the subvertical detachment surface within layers of different competence.



B - Detail of the arrowed area in A, to show the folded F2 folds and the sub-vertical S2 foliation. Note the kink style of F3 folds. Outcrop 147, to the south of Simão Dias.



C - Small-scale, steeply plunging crenulations of the S2 foliation imprinted on phyllitic layers of the Olhos D'agua mixtites. Outcrop 31, road Simão Dias to Pinhão.



D - Conjugate kink bands affecting the sub-vertical strong fabric of mylonitic gneisses. Outcrop 873, Lomba river, southern part of the Itabaiana dome.

Figure 4.16 - The D3 structures in the Itabaiana Dome Area.

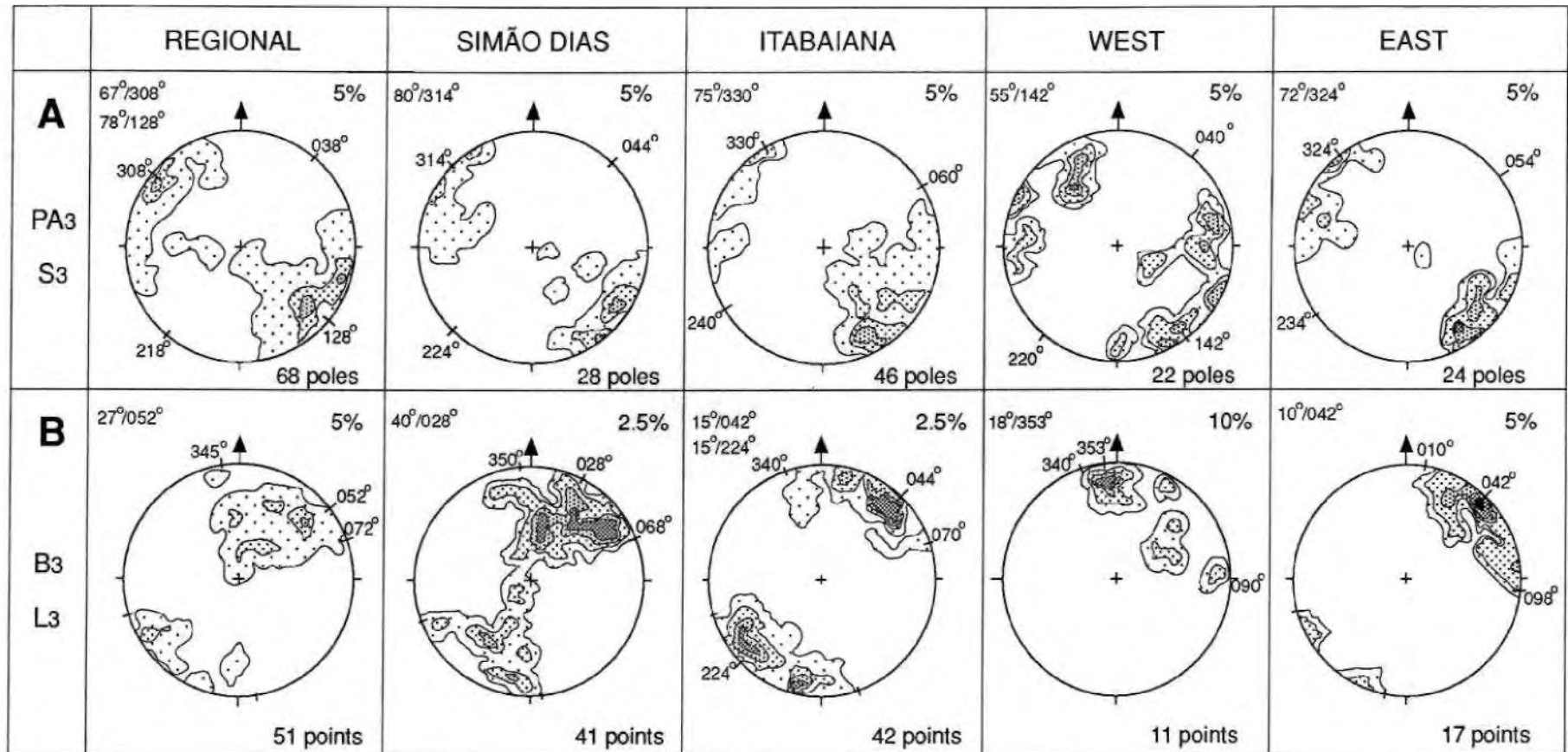
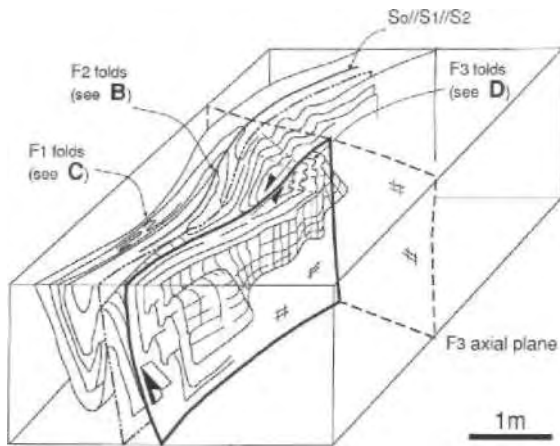


Figure 4.17 - Lower hemisphere stereographic plot of the D3 structural elements in the Itabaiana dome area. Contour intervals are either 2.5, 5 or 10% per 1% area. In A are the poles to the planes of PA3 and S3, whose attitude(s) of the maxima is (are) shown in the upper left corner for each domain. In B are indicated the range of orientations and the mean orientation of B3 and L3, whose attitude(s) of the maxima is (are) shown in the upper left corner.



A - Diagram to show intrafolial, isoclinal F_1 folds, co-axially folded by mesoscopic, very tight F_2 folds, refolded by transversal F_3 folds. The horizontal surface of the diagram is based on a field sketch of the outcrop made by Prof. K.R. McClay. The structural relationships in the vertical surfaces are interpretative.



B - Two F_2 hinges refolded by transversal, open and kink-style F_3 folds. The arrowed area is shown in D.

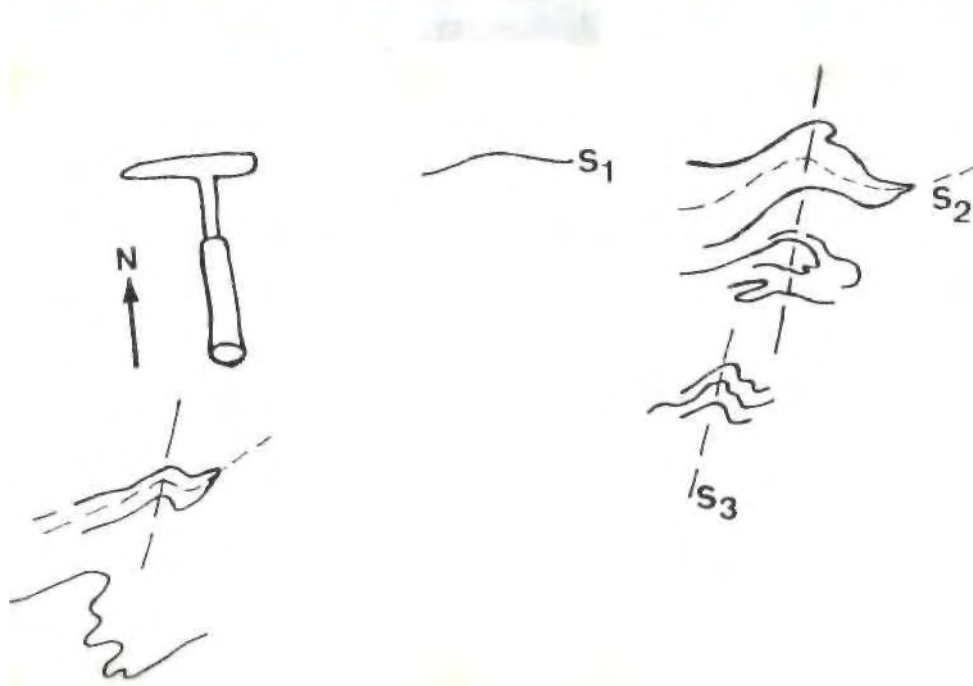


C - Intrafolial, isoclinal, possible F_1 folds (arrows) in the limb of the mesoscopic F_2 folds in B. Note the disrupted fold hinges.



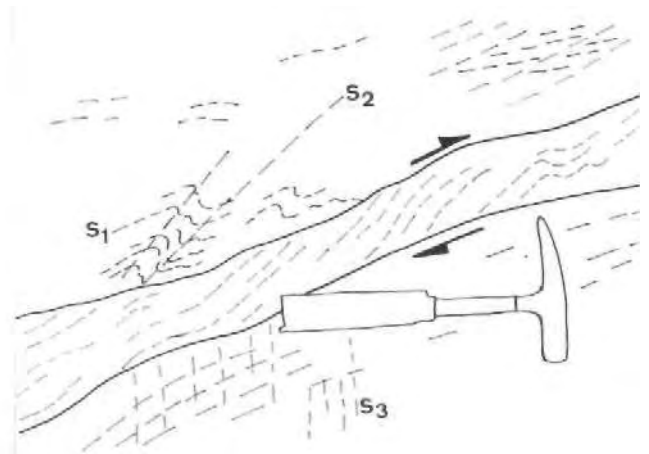
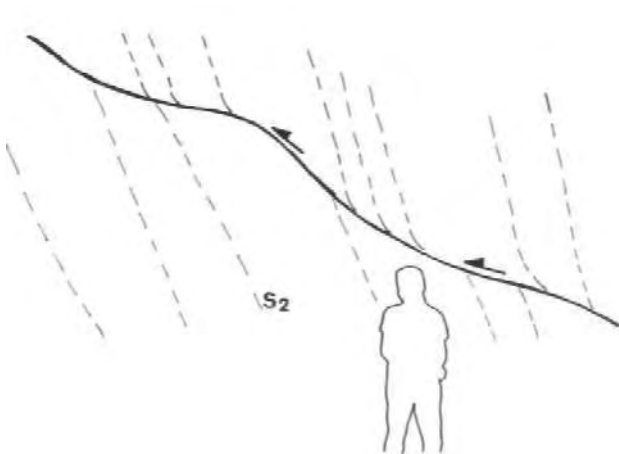
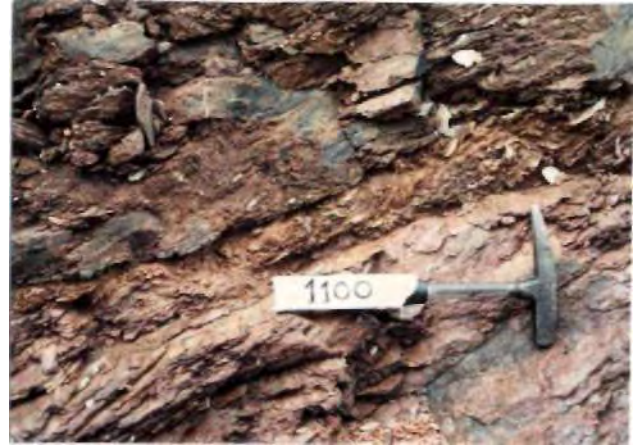
D - Detail of B to show the train of F_a folds associated with a sub-vertical fault plane with a metre-scale sinistral displacement.

Figure 4.18 - The $F_1 \times F_2 \times F_3$ interference pattern illustrated in the Olhos D'água limestones (outcrop 147, Itaporanga fault zone, south of Simão Dias).



Isoclinal, E-W trending, upright and gentle plunging F2 folds affecting orthogneisses refolded by transversal, upright and sub-vertical F3 folds, whose axis is controlled by the dip of S1/S1//S2 (see line drawing).

Figure 4.18 (continued) - E - F2 X F3 interference pattern in the basement rocks (outcrop 305, north of Simão Dias).



A - Ramp-flat geometry of a top to the south thrust in polydeformed Palestina phyllites. In the outcrop it can be observed a layer-parallel (S₁) foliation folded by F2 folds associated with a strong S₂ foliation. Outcrop 45, road Simão Dias to Pinhão.

B - Low-angle, top to SSW shear zone cutting D1-D3 polydeformed Frei Paulo phyllites. The F2 folds are decapitated by the shear zone. The shear foliation is also folded (see line drawing). Outcrop 1100, along the road Serra do Machado to Volta.

Figure 4.19 - Late-stage, post D3 deformation in the Itabaiana dome area.

Detailed analysis of the aerial photographs has also revealed a regional set of fractures spaced at a km-scale and trending SW-NE, parallel with the S_3 orientation. These fractures cross-cut the WNW-ESE trending structural grain of the area, and partially control the drainage pattern in both the metasediments and crystalline basement,

L_3 linear features are the F_3 fold axis (B_3) and the intersection lineation ($L_3^{\wedge 2}$) which plunge gently to sub-vertically generally to the NE or to the SW (Fig. 4.17 B). The dispersion of L_3 linear features reflects the scattering of the contour of maximum concentration of points from NNW to E.

The F_3 folds and kinks are better developed in highly anisotropic lithologies, such as phyllitic matrix metasediments, thin horizons of metapelites within metacarbonates, and basement-derived mylonites and phyllonites.

The best examples are found in those areas where $S_2 \gg S_0$ (or S_n) and S_j are all subvertical, probably because of the F_j and F_2 structural repetition of layers of contrasting competence with sub-parallel foliation planes certainly provided many slippery surfaces parallel to the regional anisotropy. In such areas, the transverse F_3 folds deform the co-axial interference pattern developed by the F_j and F_2 folds (type 3 of Ramsay 1967), as shown in Figures 4.4 B & 4.18.

Isolated, very broad to open style F_3 folds refold the $F_1 F_2$ co-axial pattern, in areas where probably a relatively small amount of inter-foliation slip nucleated along the subvertical S_2/S_T surfaces (as is likely the case in Fig. 4.4 B). In areas where comparatively larger amounts of inter-foliation slip developed, trains of tighter F_3 folds may occur associated with local strike-slip faults (Fig. 4.18 D).

Late-stage shearing and thrusting

In some localities, the subvertical S_2 and S_3 foliations are affected by low-angle, NNE dipping, discrete thrust-fault planes or local shear zones (Fig. 4.19) which may be accompanied by sets of sigmoidal tension fractures and rotated quartz veins. A top to SSW movement is indicated on these structures.

4.6 - The structural domains

Despite the polyphase deformation, the vertical cross-sections (AB, CD and EF of Fig. 4.20, enclosure) show a structural pattern dominated by south vergent F_2 folds and high-angle thrust faults. The structural facing defined by small-scale F_2 folds and the S_2/S_1 relationships suggest that large-scale and overturned F_2 folds occur in the area.

In the Itabaiana Dome Area cross-section balancing techniques, as used in the frontal parts of foreland fold and thrust belts (Dahlstrom 1969; Hossack 1979; Woodward et al. 1985) are difficult to apply, because of the penetrative ductile deformation that the area has undergone, together with the lack of an undeformed stratigraphic column with which to construct an undeformed template for the restored section.

Non-balanced cross sections and more artistic interpretations are valid in these areas, particularly if they also show orogen-parallel tectonic transport (Woodward et al.

1985) and pervasive ductile deformation (Cooper & Trayner 1986) as is the case in the Itabaiana Dome Area.

However, although no attempts of line or area balancing have been done, the structural cross-sections AB, CD and EF show a correspondence between the depth of metasediments and the basement which is in accordance with the interpretations of the gravimetric and aeromagnetic data (see section 5.5).

The variations in the style of the F_2 folds and in the intensity of the D_2 deformation, together with the variable attitude of the D_1 - D_2 structural elements across the area, are the basis for the characterisation of the different structural domains (sections 4.3 & 4.4).

4.6.1 - The cratonic domain

The sediments in the southernmost part of the largely unmetamorphosed cratonic domain, and are only affected by broad NW to WNW trending folds, which are observed in aerial photographs and revealed by the changing dips of the relatively flat lying Lagarto-Palmares sandstones.

A gradual increase in the intensity of the S_2 foliation is observed in many parts of the southern area: the foliation starts in the south as locally observed micro crenulations imprinted on mudstones of the Lagarto-Palmares Formation and passes into well defined cleavage planes in the Jacaré metasilites and into a micaceous foliation in Frei Paulo phyllites, towards the trace of the Itaporanga fault.

4.6.2 - The regional and Simão Dias domains

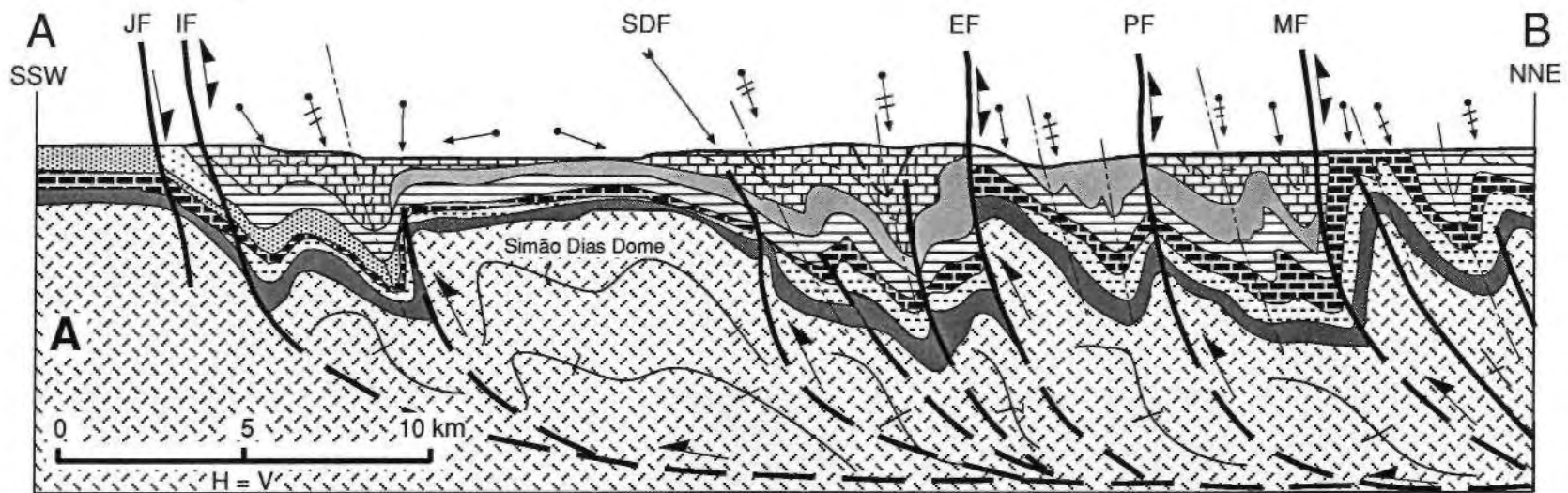
Apart from the open style of the Paripiranga anticline (Fig. 4.19 A), these domains are characterised by generally very tight to isoclinal F_2 folds with axial planes generally dipping 60° to NNE.

The high amplitude/wavelength ratios generally observed in the F_2 folds, which commonly display overthickened hinges transposed by S_2 (Fig. 4.6 A) indicates a significant amount of flattening in these folds. The intense shortening results in a nearly subvertical layered sequence formed by planes of S_0 , S_n , S_1 , and S_2 planes. Thus, it is generally not easy to distinguish S_1 from S_2 in the field.

However, various examples of 1-10cm-scale, co-axially refolded F_1 folds are found (Fig. 4.4 A), and there is also evidence of S_1 folded in the hinge zones of mesoscopic F_2 folds (e.g. outcrop 45, road Simão Dias to Pinhão, Fig. 3.1). In addition, a strong bed-parallel sericitic foliation (S_1) is well documented in the flat-lying Frei Paulo sandy phyllites folded by the Paripiranga anticline to the WSW of Paripiranga (outcrop 848, Fig. 3.1).

With the above characteristics, it does not seem to be a coincidence that in the regional domain the clasts of the Palestina diamictites are more flattened in the YZ plane than they are elsewhere. Also this domain is the lonely with evidence of the late-stage, subhorizontal thrusts and shears described in the previous section.

Finally it is noteworthy to mention that the frequency of S_r and S_2 - parallel quartz veins increases toward the northern border of the area, as observed in the



JF=Jacaré fault, IF=Itaporanga fault, SDF=Simão Dias fault, EF=Escarpa fault, PF=Pelada fault, MF=Mocambo fault

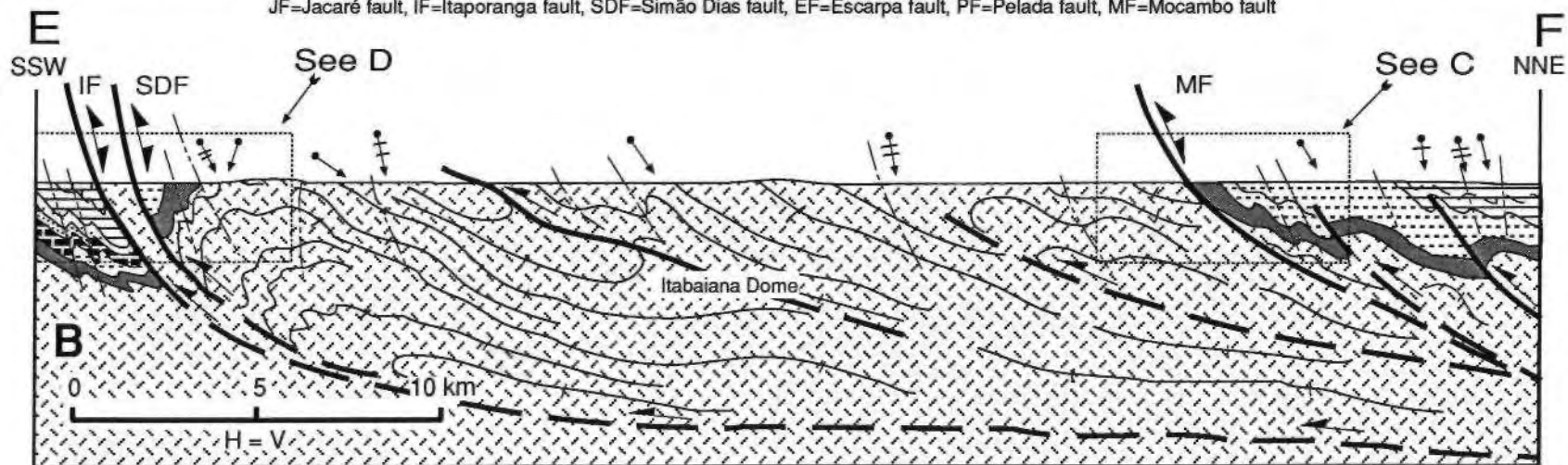


Figure 4.21 (A-E) - Summary vertical cross sections AB and EF, respectively shown in A and B. The legend and the two areas in the rectangles of B are shown in C and D (continued).

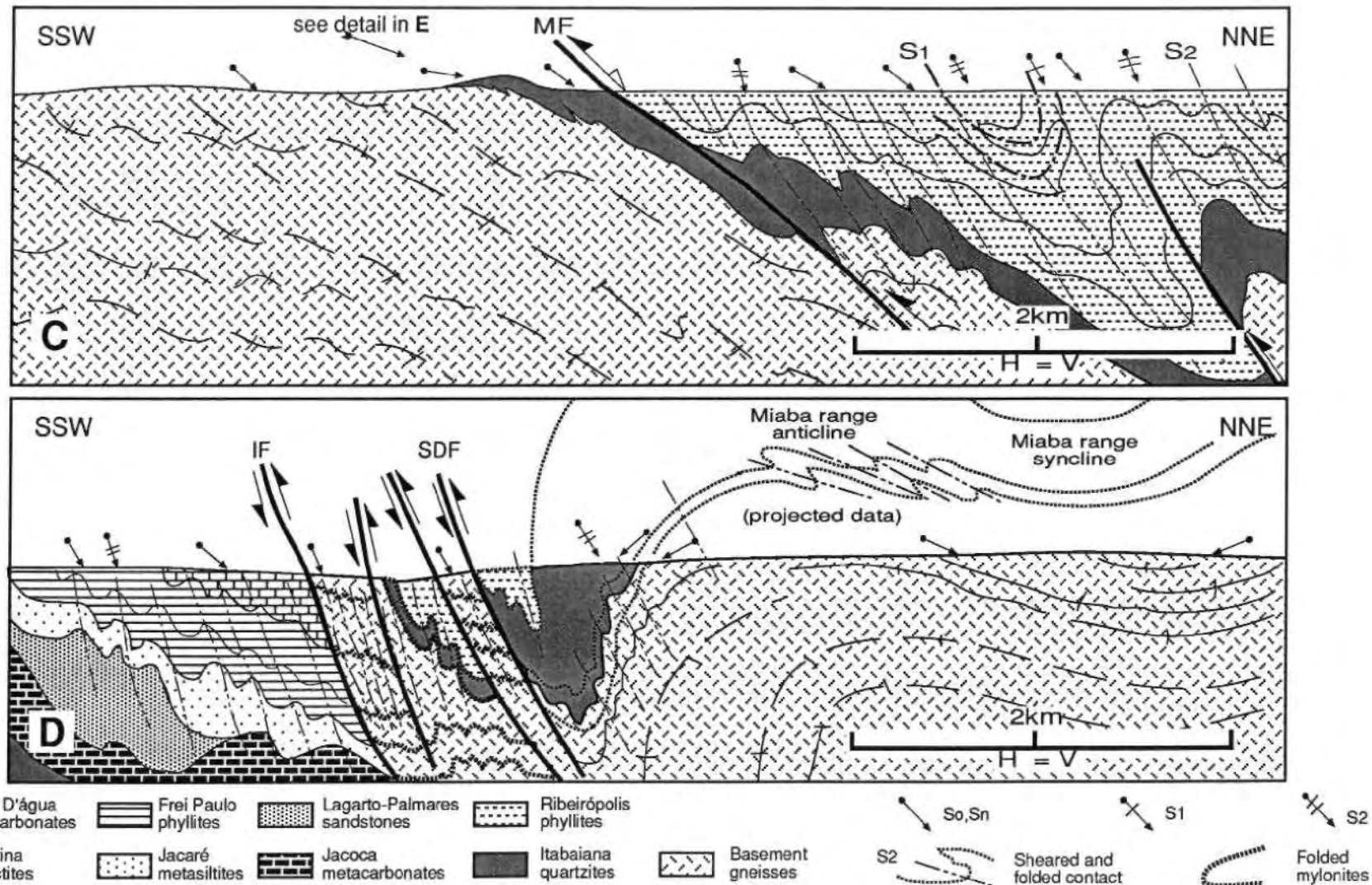


Figure 4.21 (continued) - Structural details in the northern (C) and southern (D) borders of the Itabaiana dome. Detailed structural relationships in the northern margin of the dome are shown in Figure 4.21 E.

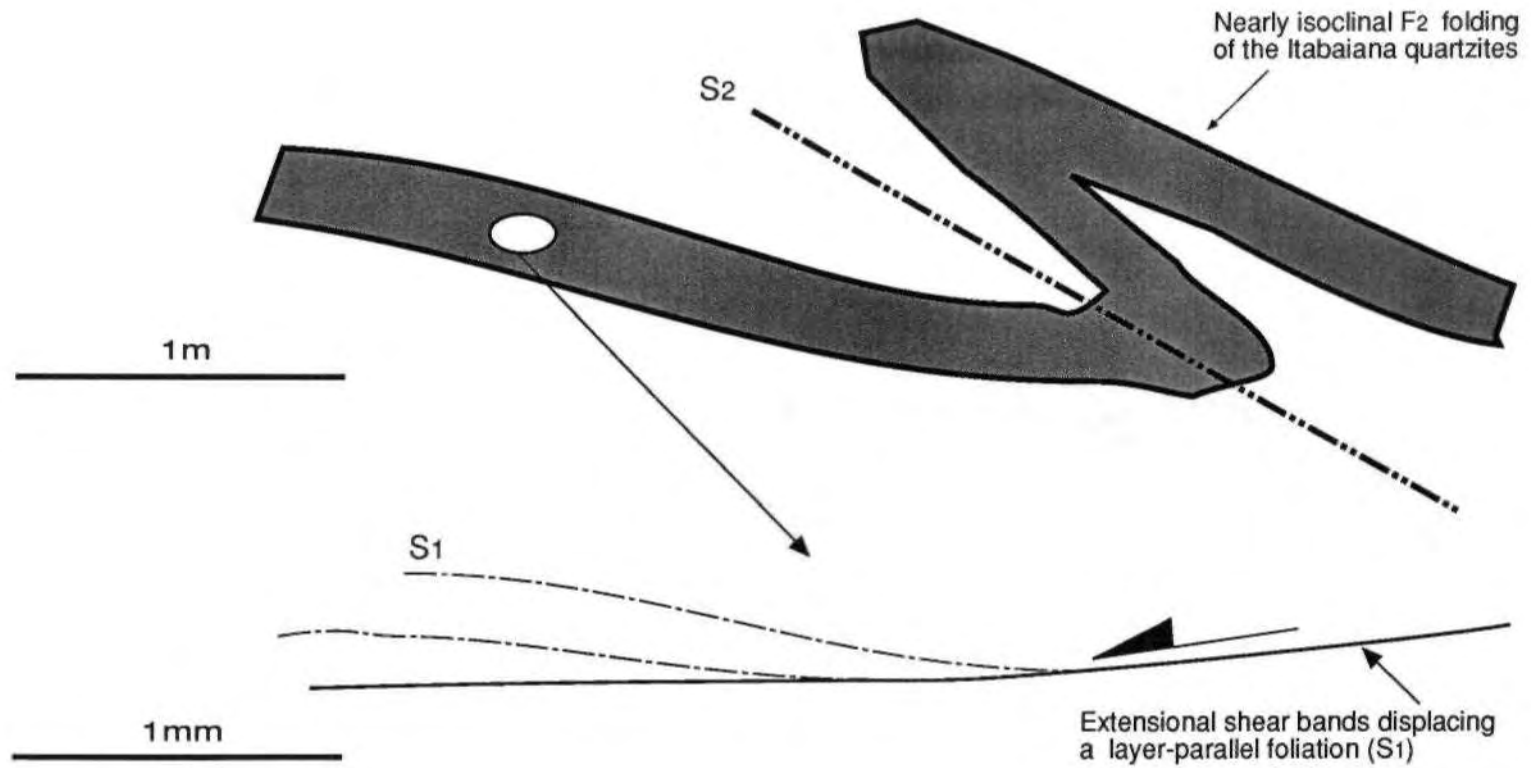


Figure 4.21 E - Detailed structural relationships in the northern margin of the Itabaiana dome (data from outcrop 384, WSW of the town of Serra do Machado)

Palestina diamictites in all sections across the Vaza Barris river valley, and also within the Ribeirópolis and Frei Paulo phyllites of the northern part of the area, which matrix is coarse-grained in places than the phyllitic rocks to the west, east and south of the Itabaiana dome (e.g. outcrops 528, 700, 701, and 1101, Fig. 3.1).

4.6.3 - The Itabaiana domain

The F_2 folds within the Itabaiana gneisses are generally more open than those in the regional and Simão Dias domains, and as a consequence S_2 normally cuts S_n/S_1 , at higher angles (confirmed by the statistical analysis, Fig. 4.3 B). Rootless and generally recumbent F_1 folds are found in some places, mostly on the limb of the F_2 folds. The S_n/S_1 surfaces are also affected by gentle to open, 100-1000m-scale F_3 folds observed in road cuts, dams and quarries.

The superposition of open F_2 and F_3 folds with orthogonal axes and vertical axial planes explains the scatter plot of S_n/S_1 with a maximum concentration near the centre of the diagram (Figs. 4.3 A & B). This also explains the relative dispersion of L_2/B_2 between 270° - 320° and 090° - 140° (Fig. 4.3 C).

A detailed study of the structures across the Itabaiana domain (Fig. 4.21 B), has revealed important differences in the structural styles and deformational patterns in the gneisses and in the Itabaiana quartzites on each part of the Itabaiana dome, as summarised in Figures 4.21 C-E & 4.22.

At the northern border of the dome the Itabaiana quartzites are affected by m-scale, overturned, isoclinal, and SSW verging F_2 folds (Fig. 4.21 C), and contain a layer-parallel mylonitic foliation with evidence of subhorizontal shear bands indicating a top to the south movement (Fig. 4.21 E). These folds are also observed within mylonitic quartzites and gneisses approaching the southern border (Figs. 4.22 A & B). In this area, Humphrey & Allard (1969) described imbricated slices of quartzites and crystalline basement (to the NNW of Macambira).

The southern limb of the Itabaiana dome comprises mylonitic gneisses and quartzites folded by Z asymmetry small-scale F_2 folds in cross sections (Fig. 4.21 D) and this relationship is confirmed by the shallower dip of the S_2 foliation cutting the steep-dipping to subvertical mylonitic foliation (Figs. 4.22 C & D).

It can be concluded that the Itabaiana dome very probably lies in the core of a large-scale, southward verging F_2 anticline, whose overturned steep-dipping southern limb is cut by high-angle thrusts in the area between the Itaporanga and Simão Dias faults (Fig. 4.21 C). These faults are likely responsible for the imbrication of subvertical slices of mylonitic Itabaiana quartzites, Ribeirópolis phyllites and basement-derived mylonites of the Lomba river, Montes stream and Arrastador farm (Fig. 3.1, enclosure).

The 700m-thick Itabaiana quartzites are only slightly deformed in the eastern and western parts of the dome, where different styles of deformation are observed. In the eastern part of the dome, the gneisses and the quartzites are mainly cross-cut by the subvertical and localised strike-slip faults (Fig. 4.1) whereas in the western pan of the dome, the quartzites are folded by the large-scale F_2 anticlines and synclines in the Miaba range (Fig. 4.1).



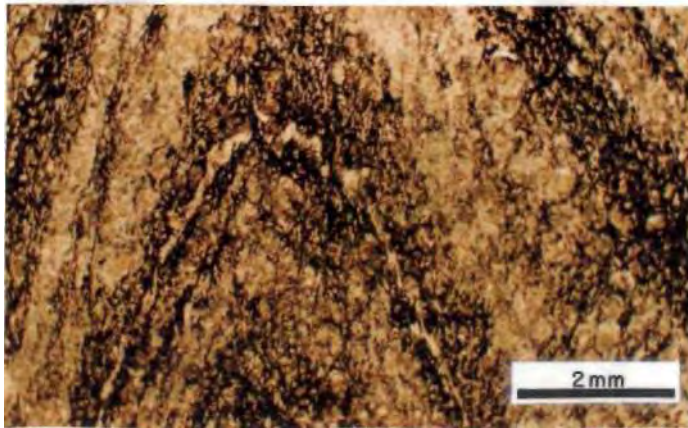
A - Isoclinal, SSW verging F2 folds affecting highly sheared Itabaiana quartzites and the crystalline basement (see B). Outcrop 334, northwest of São Domingos.



B - Highly sheared Itabaiana gneisses affected by F2 folds and small-scale top to SSW thrust faults propagated in the overturned limb. At the base of the outcrop in A.



C - Northward verging, asymmetric and small-scale F2 folds affecting basement derived mylonites (see D). Note the shallower dip of the strong S2 foliation. The strong intersection lineation is parallel to the elongation lineation in the mylonites. The knife is 8cm-long. Outcrop 492, north of São Domingos.



D - Hinge zone of F2 folds in the mylonitic gneiss of C. The S2 foliation is defined by iron oxide and some biotite. Photograph taken under plane-parallel light of a thin section cut perpendicular to the fold axis.

Figure 4.22 - Structural relationships in the southern part of the Itabaiana dome.

The structural relationships in the northern and southern borders of the Itabaiana dome support the interpretation of an overturned F_2 anticline for the Simão Dias dome (Fig. 4.21 A). In fact, as in the northern margin of the Itabaiana dome, the northern border of the Simão Dias dome comprises imbricated slices of tightly folded quartzite- and gneiss-derived mylonites (e.g. of outcrops 26, 306, 307, 1106, 1108, 1109, Fig. 3.1), with vergence towards the south.

4.6.4 - The west and east domains

These domains are mainly characterised by the differential intensity of the D_2 deformation in the succession of the metasediments, and by a nearly 25° clockwise rotation of the directions of D_2 structural elements (compare the plot of these structures with the other domains, Figs. 4.3 B & C).

All the formations above the thick quartzites show a pervasive and flat-lying S_1 foliation, which dips respectively to NW and SE in the west and east domains (Fig. 4.2 A). However, the F_2 folding is rather important in the Frei Paulo and Palestina Formations, whereas the Jacoca Formation commonly show D_1 structures relatively unaffected by D_2 . Within the west domain, this pattern of deformation is better observed nearer the thick Itabaiana quartzites of the Miaba range, in the Capitão farm outcrop (see section 4.7).

The west and east domains are also relatively free of evidence for the D_3 deformation, but some structures compatible with this event in the west domain deserve special attention, in two localities of the Itabaiana-Ribeirópolis interface.

In one place (outcrop 338, WNW of Macambira, Fig. 3.1), the Ribeirópolis phyllites are affected by NNE trending, asymmetric, ESE verging, 1m-scale folds. The location is very close to the probable contact with the Itabaiana Formation. The fold axis plunges 05° to directions between 200° - 237° and there is also a subtle lineation (18° to 317°) defined by elongated <1mm size grains of opaque minerals.

In the Miaba range (outcrop 471, Flecheira farm, Fig. 3.1), the Ribeirópolis pebbly phyllites rest on Itabaiana conglomeratic quartzites with an intense layer-parallel foliation (Fig. 4.23 A) parallel to the sheared contact. This contains fragments of quartzite and dips at 20° to 260° (Fig. 4.23 B).

The Itabaiana quartzites are affected by two sets of spaced cleavage (respectively dipping 75° to 121° , and 85° to 035°), and the pebbly phyllites are cut by a foliation dipping 40° to 250° . The drag of this foliation approaching the shear zone, and the fractured and pulled-apart, sigmoidal-shaped clasts of milky quartz trapped within the shear zone (Fig. 4.23 C), all indicate a top to ESE sense of movement. The clasts within both Formations have a prolate shape defining an elongation lineation which plunges 15° to 310° .



A- White Ribeirópolis pebbly phyllites resting on top of Itabaiana quartzites with a strong, layer-parallel foliation.



B - Detail of A above, showing the sheared contact. Note the low-angle shear zone cutting highly foliated phyllites above, and the clasts of quartzites trapped just above the contact with the quartzites (marked by the hammer).



C - Detail of asymmetric tails in a fractured and pulled apart clast of milky quartz showing the top to the SSE shear movement.

Figure 4.23 - The sheared contact between the Itabaiana and Ribeirópolis formations in the west domain. Outcrop 471, western slope of the Miaba range.

4.7 - The Capitão farm outcrop

This outcrop (Fig. 4.24) is the largest and most important in the research area and lies in the west domain, in the junction between the Salgado and Vaza Barris rivers (outcrop 311, Fig. 3.1).

The outcrop is characterised by a series of mesoscopic recumbent folds associated with subhorizontal thrusts and possible local duplexes that affect the Jacoca carbonates just above the basal Ribeirópolis conglomerates, and by a series of small-scale structural relationships (Figs. 4.24 A-F & details 1-8). Figures 4.24 A & B are respectively based on photo line drawing and on a 1:100 scale geological map of the bottom of the outcrop. The sketched details 1-4 are documented by the photographs of Figures 4.24 C-F.

In this outcrop, a layer-parallel foliation (S_1) is associated with small-scale, recumbent folds that affect metachert horizons inside dolomitic layers intercalated with dark grey phyllites (details 1-2). The S_1 foliation cuts the phyllitic layers at higher angle than in the dolomitic layers (Figs. 4.24 C & D), and it is also affected within those layers by generally open folds which locally evolve to kink-style, tight and asymmetric folds, with a horizontal axial planar foliation (details 2-3 and Fig. 4.24 E). Many carbonate veins emplaced within the phyllites, and parallel to S_1 (detail 4 & Fig. 4.24 F), occur boudinaged, disrupted, pulled-apart or folded elsewhere along the same phyllitic layers (detail 5).

Together, these structures suggest a progressive event of layer-parallel shearing (D_1), responsible for the simultaneous development of extensional and compressional features which were subsequently rotated and deformed, as sketched in detail 6.

Some small-scale back-folds, box folds, and low-high angle back-thrusts locally observed in that outcrop also fit in such a progressive layer-parallel shearing, but with a component of backward displacement, probably due to impossibilities for the thrust sheets to move further to the south. These structures also occur in the flat-lying Jacoca carbonates of the east domain, which equally show strong evidence of inter-layer shearing superimposed on a layer-parallel S_1 foliation, and back folding associated with subhorizontal thrusting in small-scale (e.g outcrop 1051, Moças stream, Fig. 3.1).

In the Capitão farm outcrop, the basal formations are also affected by isoclinal and overturned folds developed in the hanging wall of steep dipping normal faults (Figs. 4.24 A & B) which appear to merge along a subhorizontal detachment (the competent layers are boudinaged along the locally sheared Ribeirópolis-Jacoca contact), resembling a listric extensional geometry.

Davison & Santos (1989) interpreted the subhorizontal thrusts as a post-extensional feature, attributing the lack of inversion along the normal faults to the difficulty of the thrusts to overcome their steep dip. It is interpreted here that the D_1 extension is post- D_1 subhorizontal thrusting. This interpretation is supported by: (a) megaboudins of the Jacoca dolomites occur several meters one from each other, along the basal contact, indicating no recovering of the extension even along the low-angle detachment, not only along the steeply dipping ramps; (b) one of the boudins is internally folded, which is better explained if the folding happened before the extension.

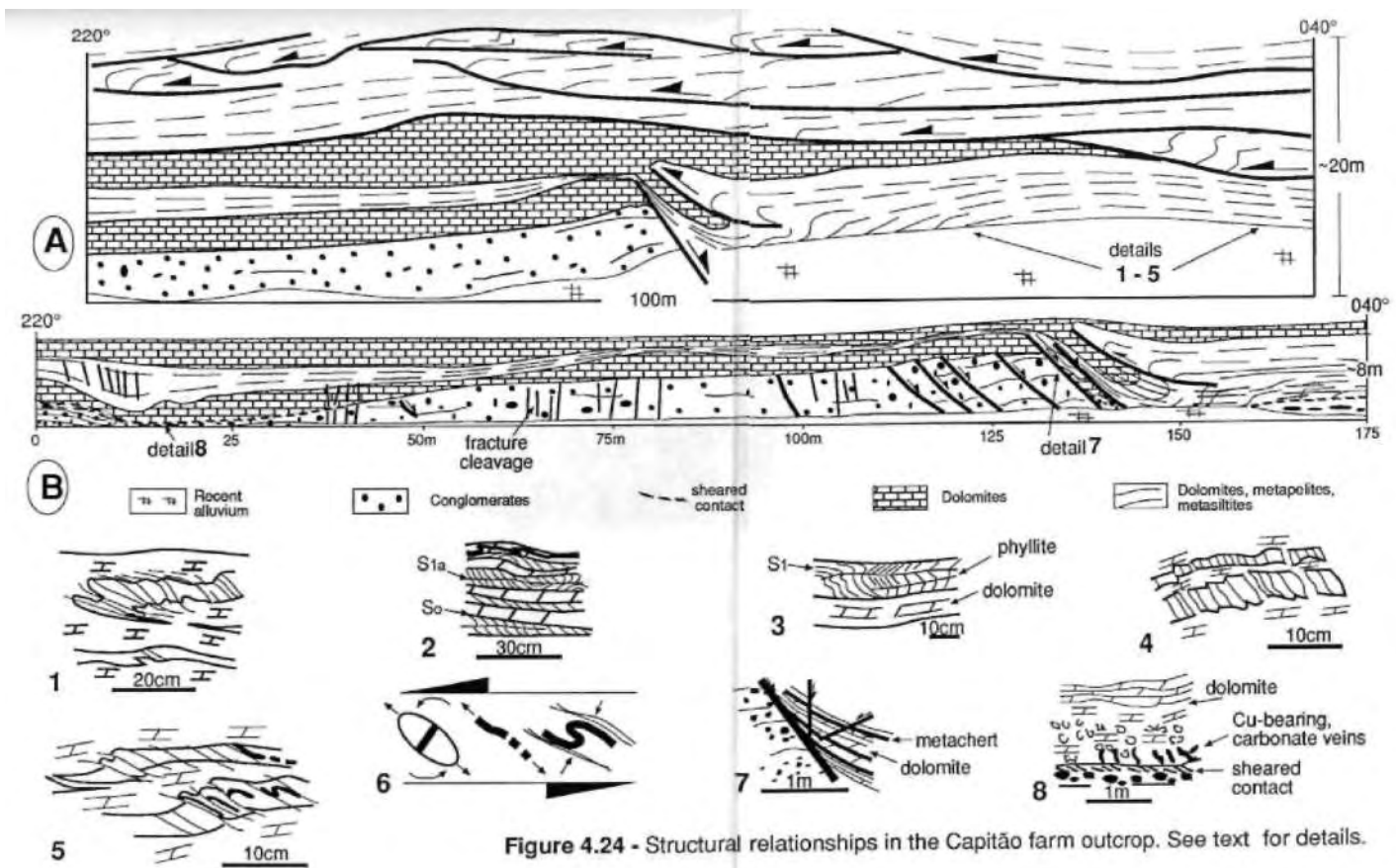


Figure 4.24 - Structural relationships in the Capitão farm outcrop. See text for details.



C- Intrafolial, recumbent F1 folds in the metachert layers within marble. Note the strong layer-parallel S1 foliation. The knife is 8cm-long.



D - Recumbent F1 folds in the intercalated black phyllites. Note the S1 foliation changing angle of dip from the dolomitic marble to the phyllites.



E - The S_1 foliation affected by asymmetric folds internal to the phyllitic layers. Note the new sub-horizontal foliation developed (S_{1a}). 8mm = diameter of the yellow dot.



F - Carbonate veins parallel to the S_1 foliation in the black phyllites, and showing partial to complete process of boudinage. Folded and rotated vein fragments are found few metres beside of that place, in the same layers.

Figure 4.24 (continued) - Small-scale structures in the Capitão farm outcrop.

The folds in the hanging wall of the normal faults have overthickened hinges, have overturned limbs associated with reverse faults, have a curved axial planar foliation which mimics the listric plane of the normal fault, (Fig. 4.24 B) and the fold limb nearest the fault is extremely thinned and locally faulted in more brittle conditions (detail 7). They are here interpreted as the accommodation required to solve the space-problem caused by the downward movement of the hanging wall in listric extensional systems (Wernick & Burchfiel 1982; Gibbs 1984).

Contractional structures commonly found in the hanging wall of extensional fault systems have been attributed to local stress fields due to the rotation of blocks above the crest of a ramp-flat basal detachment (Brumbaugh 1984; McClay & Ellis 1987), or even attributed solely to a velocity discontinuity between extending blocks (Brumbaugh 1984).

However, as the outcrop shows no evidence of several, rotated blocks separated by high-angle faults, it is proposed here that the accommodation took place by a combination of folding and reverse faulting under ductile and ductile-brittle conditions, associated with the extreme difference of thicknesses and competence of layers. To accommodate the down throw of the matter along the steep dipping normal fault developed in the competent Ribeirópolis conglomerates, the thinly interlayered dolomites, metachert and phyllites probably acted more ductilely than two layers of more massive dolomites of the basal Jacoca Formation.

The basal dolomitic layer was boudinaged along the sheared contact with the conglomerates (detail 8), whereas the thinly interlayered dolomites above the steep dipping normal fault were ductilely deformed in a roll-over syncline-anticline pair, so that the matter migrated from the limbs to the hinge of the folds, in a way similar to the convergent bed-parallel shearing described by Higgs et al. (1991) for such situations.

The overlying massive dolomites initially accommodated the folding of the thinly interlayered sequence. With the continued extension, the progressive thinning of the limb of the fold nearer to the fault was brittlely faulted (detail 7) and the progressive tightening and overturning of the syncline-anticline pair led to more thickening of the hinge. The reverse fault started to propagate in the overturned limb of the fold pair within the massive dolomites, probably because the more competent duplicated layer could not accommodate the final stage of tightening of the fold.

The set of closely spaced and steep-dipping fractures which cuts the laminated rocks and the layer-parallel S_1 foliation, just in the area above the horizontal extension of the dolomites and conglomerates (left side, Fig. 4.24 B)_f is interpreted as a local accommodation to the extension, even though the fractures show orientations compatible with S_2 in other parts of the area.

4.8 - Metamorphism in the Itabaiana Dome Area

Metamorphic conditions in the Itabaiana Dome Area are indicated by seriate, chlorite, biotite found normally along with the S_1 , and S_2 regional foliations, together with quartz and feldspars (Fig. 4.4 D). Epidote occurs as a transformation of hornblende in the basement rocks and derived mylonites (section 3.3.1).

Sericite, Chlorite and biotite (and locally actinolite, section 4.4.3) are also found as fibrous overgrowths along the pressure shadow tails and voids associated with the deformed clasts and porphyroclasts observed in metasediments and in basement rocks and derived mylonites (Figs. 4.9 A & C).

The data may even suggest a direct timing relationship between metamorphism and D_1 and D_2 deformational events. However, as porphyroblast-matrix relationships are absent in the Itabaiana Dome Area, nor they have been described elsewhere in the southern part of the Sergipano Fold Belt, it can only be suggested, on the basis of the mineral assemblages and textural relationships above, that the metamorphism generally ranges from sub- to greenschist conditions, and that the basement underwent metamorphism at higher temperatures than the metasediments.

In fact, Essene (1989) states that if the temperatures of the greenschist facies normally range within 300°-450°C, the presence of hornblende-epidote paragenesis implies the extension of the upper limit of this facies to 450°-550°C.

Actually, the similar deformational processes observed in the resistant grains of the diamictites, pebbly phyllites and mylonites (section 4.4.3), which are attributed in the general literature to processes like fracturing and cataclasis, frictional sliding, diffusive mass transfer and crystal plasticity (McClay 1977; Knipe 1989), together with the ductile deformation of the highly strained quartz grains, have all been interpreted as compatible with greenschist, up to low amphibolite metamorphism in other deformed areas (Simpson 1985; Carl et al. 1991).

The higher frequency of syn- D_2 and syn- D_3 quartz veins, and the increased grain size of the micaceous minerals, observed toward the northern part of the area (section 4.6.2) suggest that probably there was also a slightly positive gradient of temperatures of the metamorphism, northward from the cratonic domain.

4.9 - Discussion and conclusions

The results of the structural analysis in the Itabaiana Dome Area indicate that the southern part of Sergipano Fold Belt underwent a polyphase, ductile to ductile-brittle progressive deformation (D_1 - D_3) responsible for the SSW directed tectonic transport of the rocks toward the São Francisco Craton.

Basement and cover were involved in the F_2 folding and thrusting and also in the D_3 deformation. On the basis of the strong coincidence of styles and similar orientation of each of the F_1 , F_2 and F_3 folding events, on the similar orientation of D_1 , D_2 and D_3 structural elements, and similar ductile D_1 deformation under greenschist facies, it is interpreted that the basement was also reworked during D_1 .

The D_1 deformation can be interpreted as a progressive event of layer-parallel shearing and shortening which developed the pervasive S_1 foliation, shearing of the basement-cover, rootless intra-folial F_1 folds, and low-angle thrust faulting. The best expression of these structures are found in the Capitão farm outcrop (Fig. 4.24), but there is other evidence outside the Itabaiana Dome Area.

For example, Santos et al. (1988) described recumbent folds coaxially folded by F_2 folds, in a large outcrop just beyond the northwestern corner of this thesis area, and Jardim de Sá et al. (1986) described F_1 recumbent folds and subhorizontal thrusting, 25 km inside the craton, in the Patamute area (west of the Tucano basin, Fig. 2.3).

D_2 deformation records a progressive shortening by nearly upright folding and high-angle, southward vergent thrusting, with a component of orogen-parallel strike-slip movement, probably under a sinistral transpressive regime. The regional faults are interpreted to be the zones of strain concentration in the D_2 progressive shortening and wrenching. The displacement along most of these faults combines a top to the south with a E-W sinistral strike-slip movement, D_3 is interpreted as a non penetrative event of transversal shortening and extension.

These interpretations are supported by several features which match with descriptions of other deformed belts which show a combination of shortening and wrenching strains, such as the parallelism of fold axes and stretching lineations, both perpendicular or at high-angle with the direction of tectonic transport (Lagarde & Michard 1986; Ridley 1986; Ellis & Watkinson 1987), together with the interfoliation slip along strike and dip of the axial plane foliation of the regional folds (Ghosh 1982).

The deformation patterns, as revealed by the abundant strain markers, indicate these movements along the regional faults and also within metasediments away from the fault zones, comparing well with deformation predominantly by simple shear (e.g. Vauchez et al. 1987).

The mutual cross-cutting relationships between S_2 and the quartz and carbonate veins, which are folded, disrupted and rotated by extensional shear bands nearly parallel to S_2 , are commonly found in polydeformed areas, and are normally interpreted as the result of strain hardening after the development of a highly anisotropic sequence, indicative of a progressive deformation (Piatt & Vissers 1980). In such cases, the veins probably represent events of orogen-parallel extension and orogen-parallel slip, a typical feature of strike-slip regimes (Jamison 1991). They are emplaced in the final stages of the ductile deformation, before the deformation enters into the brittle field (Paschier 1984).

Because D_2 shortening and the top to the south shearing probably occurred at various intensities along strike, most of the F_2 folds should have curved hinges at a regional scale (non-cylindrical folds of Williams & Chapman 1979). This may account for the double plunge of L_2 described both in the Itabaiana Dome Area (Fig. 4.3) and to the west of the Tucano basin (e.g. Jardim de Sá et al. 1986; Moraes et al. 1987). A degree of differential slip along the strike of S_2 , S_v , S_0 and S_n , may also account for the fan of directions indicated by the plunge of L_3 throughout the area (Fig. 4.17).

The overall prolate geometry of the deformed strain markers in the Itabaiana Dome area suggests a constrictional strain parallel to the orogen, superimposed by a component of flattening during D_2 . However, as part of the finite strain is most probably due to D_1 , not all the elongation parallel to the orogen can be taken as evidence of D_2 -related strike-slip displacement.

The micro structures and the deformational processes observed in the diamictites, pebbly phyllites and basement-derived mylonites are very similar in the Itabaiana Dome

Area, suggesting equivalent mechanical behaviour during the deformation. Nevertheless, the precise determination of the bulk or the average strain in the research area is made difficult by factors inherent to the Palestina rocks. For example the very fine matrix contrasts with the size of the clasts, which in turn are composed derived from varied lithologies (Ramsay 1967; Hossack 1968; Lisle 1979; Ramsay & Huber 1987). Ramsay (1967) showed that the final shape of a deformed clast is largely dependent of its original orientation relative to the finite strain ellipsoid (the Rf/ϕ method), but Lisle (1979) does not recommend the application of the Rf/ϕ technique in cases where the angle of fluctuation is small or even absent, as is the case in the Itabaiana Dome Area.

Despite the above uncertainties, Borradaile (1981) predicted that for rocks with a large ductility contrast, the clasts probably become parallel to the direction of maximum extension, at only small values of the finite strain. The differences between the K values of the finite strain ellipsoid for the same outcrop (compare outcrops 90 and 107, Fig. 4.12 A & Table 4.2) may be attributed to angular errors in assuming that the measurement plane is the XZ plane of the finite strain ellipsoid, as well as to the orders of magnitude difference in sizes between clasts in outcrops and clasts in thin section.

In the Itabaiana Dome Area some strain has been absorbed by the ductile elongation of clasts, but also the harmonic means of $(S-D)/D$ (Appendix A2.3) indicate superimposition of approximately 65% of shortening of the matrix around the clasts. This highlights the importance of flattening during the D_2 deformation in the Itabaiana Dome Area, particularly where the F_2 folds are tight to isoclinal.

This conclusion is confirmed by the larger values of K calculated for the finite strain ellipsoids of clasts+tail as compared with the K values for clasts alone (Table 4.2; Figs. 4.12 C & D). The increase in the X and Y axes of the ellipsoids reflects the importance of pressure solution processes associated with the S_2 foliation. As a result of flattening of the matrix together with the elongation of the clasts, the D_2 deformation developed an intense L to L-S tectonite fabric in the Itabaiana Dome Area.

As a result of the heterogeneous distribution of lithologies together with the styles and intensity of deformation and metamorphism, six structural domains have been recognised in the Itabaiana Dome Area. These are - the cratonic, regional, west and east domains - all formed by sediments and their deformed and metamorphosed counterparts, and the Simão Dias and Itabaiana domains, which comprise the ductilely reworked gneissic basement.

A sub- to greenschist metamorphism is recorded from the cratonic to the regional domains, but the gneissic domains probably underwent higher temperature deformation at the same facies, as recorded by the hornblende-epidote paragenesis along the metamorphic banding (S_n) and along the S_1 foliation.

The results of this detailed structural analysis of the Itabaiana Dome Area place constraints on the tectonic evolution of the southern part of the Sergipano Fold Belt in that explanations are required for -

- 1 - The coincidence between the stretching lineation in the mylonites and the L_2 linear elements throughout the area.

- 2 - The characteristics of the structural domains, in particular those of the

Itabaiana dome, e.g - The contact and the deformation relationships in different sides of the Itabaiana dome; - The shift of the trend of the D1-D2 structural elements around the dome; and the role of the dome itself and the thick Itabaiana quartzites in the deformation of the area.

These aspects are addressed in the discussion in Chapter 6.

Chapter 5 - Geophysics of the Itabaiana Dome Area

5.1 - Introduction

This chapter presents new gravity and magnetic data collected specifically for this thesis, and is the first analysis of the nature of the crust in the southern part of the Sergipano Fold Belt. Previously published aeromagnetic and radiometric data are also used in combination with the new data.

All the data were processed and analysed in the laboratories of the CPRM (Companhia de Pesquisas de Recursos Minerais, Salvador, Brazil), by Dr. A.C. Motta. The results, which form the basis of this chapter, have been presented in an unpublished report by Motta (1990) but the correlations between the geology and geophysics are responsibility of the author.

This chapter contains 8 figures (Figs. 5.1-5.8), one table (Table 5.1), and an appendix with the data used for the construction of the geophysical cross section (Appendices A3.1-A3.4).

5.2 - Summary of the geophysical and density data of the Itabaiana Dome Area

5.2.1 - Geophysical data

In order to analyse the nature of the upper crust of the southern part of the Sergipano Fold Belt, gravity and magnetic data were collected in the Itabaiana Dome Area, along three section lines, labelled XX', YY' and ZZ' in Figure 5.1.

Sections XX' and YY' were chosen since they cut across the basement domes, in the same position of the cross sections AB and EF (Fig. 4.20, enclosure). Section ZZ' was chosen since it is a southern continuation of the NW-SE trending geophysical section carried out in the area of the Carira Project (Santos et al. 1988). This is designated Z'Z" in Figure 5.2, and the interpretation has already been shown in the Figure 2.8.

Gravity and magnetic data were collected in the field using a Lacoste-Romberg gravimeter (accuracy of 0.01 mGal), and a Geometries magnetometer (Canada), model G-816 (year 1979; accuracy of 1 nT).

The gravity survey was calibrated with a value of 978167.41mGals corresponding to the absolute value of the gravity field at the town of Itabaiana, in the Brazilian national gravity grid (Observatório Nacional, IBGE, according with Motta 1990). The observed and calculated gravity data are shown in Appendices A3.1-A3.3 .

The altitude of each field station was obtained by closed levelling traverses, and the geographic coordinates of each point were derived directly from the planialtimetric maps at 1:100,000 scale (the same as in the geological map, Fig. 3.1, enclosure).

This chapter has also utilised aeromagnetic and radiometric data available for the southern part of the Sergipano Fold Belt (Encal 1978). These are shown in the

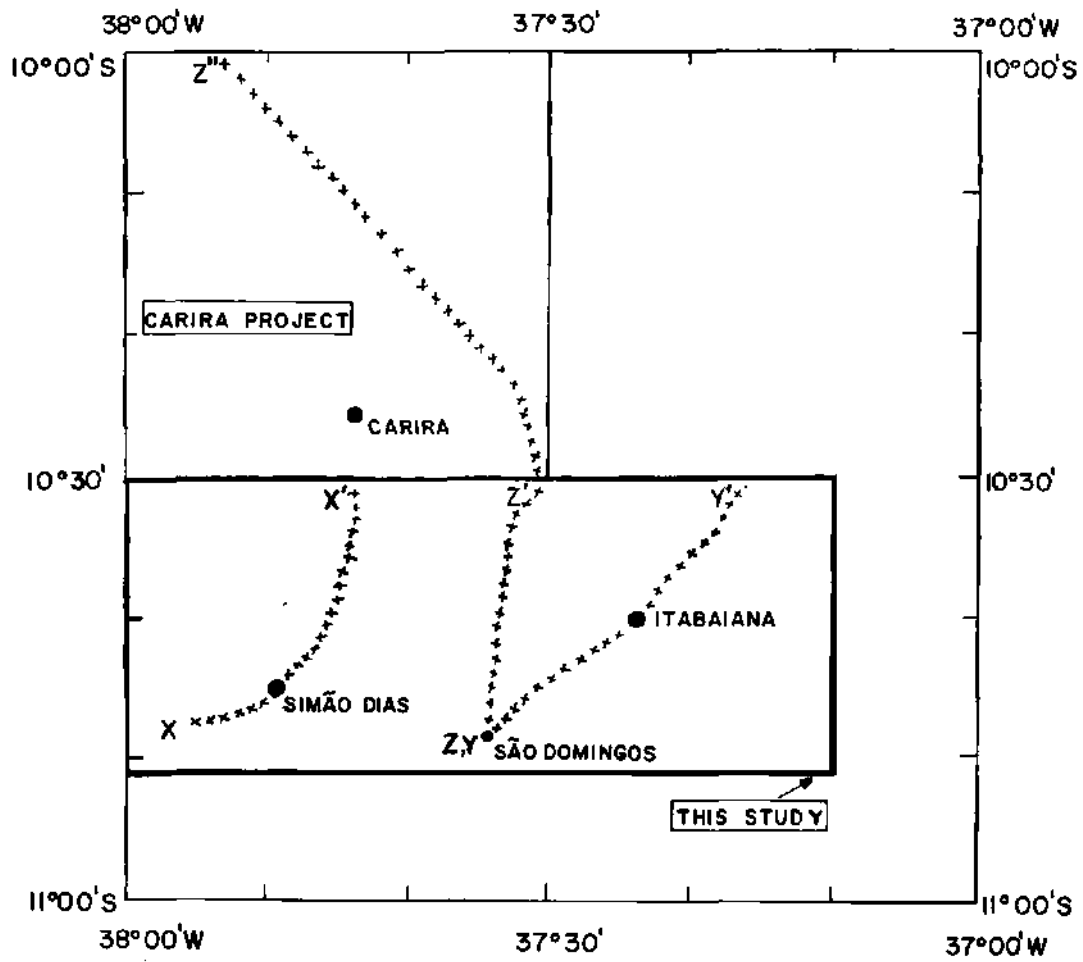


Figure 5.2 - Grid of geographic coordinates with the location of the geophysical section lines in the area of this study (XX', YY' and ZZ') and the continuation of the ZZ' section line in the southeastern part of the area of the Carira Project (Z'Z'').

1:100,000 scale contour map of total intensity of the earth's magnetic field (Fig. 5.3) and in the 1:100,000 scale contour map of total radiometric values (Fig. 5.4).

Because the aeromagnetic data of Figure 5.3 are already filtered and free of the influence of very shallow magnetic sources, unlike the magnetic data collected directly in the field (which show a wide variation over small distances), the ground magnetic data have not been utilised in the interpretation presented in this chapter.

Motta (1990) chose to interpret the magnetic profiles along sections XX' and YY' by using the aeromagnetic data presented by Encal (1978). The observed and calculated anomaly data used for the aeromagnetic interpretation of sections XX', YY' and ZZ' are given in Appendices A3.1-A3.3 .

Computer modelling of the geophysical data was carried out using programmes Geosoft Magpoly (2.1), and Geosoft Gravpoly (2.1), both by Patterson, Grant and Watson Ltd. 1984, (Canada). This software is officially used by the CPRM-Brazil for geophysical interpretations (Motta 1990).

5.2.2 - Density data

In order to permit quantitative interpretation of the gravity data, 85 samples of various rock types in the Itabaiana Dome Area were collected for density determinations.

The results of the density determinations are presented in Appendix A3.4 and summarised in Table 5.1. The average density of 80 samples of all rock types is 2.62 g/cm³. The average density of 52 samples of metasediment is 2.61 g/cm³, and the average density of 28 samples of crystalline basement rock is 2.64 g/cm³.

The average density for different types of non-basement rock is also shown in Table 5.1: phyllites = 2.56 g/cm³; metasandstones = 2.61 g/cm³; diamictites and pebbly phyllites = 2.62 g/cm³; limestones = 2.68 g/cm³; and quartzites = 2.53 g/cm³.

In order to use maximum density contrast for the computer modelling, Motta (1990) adopted 2.64 g/cm³ as the average density for the upper crust in the southeastern part of the Sergipano Fold Belt, and 2.57 g/cm³ for the metasediments. Thus the maximum density contrast between basement and cover in the southern part of the Sergipano Fold Belt was taken as 2.64 - 2.57 = 0.07 g/cm³.

The upper crust was then modelled in terms of blocks of basement and metasediment, each with a density contrast relative to the average density of the crust (2.64), by considering the nature of the rocks on each part of the geological cross sections. Block boundaries and shapes were constrained by surface geology interpreted from the author's geological map and cross sections (Figs. 3.1 & 4.20).

5.3 - Geophysical domains

A detailed analysis of the aeromagnetic anomalies of Figure 5.3 has permitted identification of six geophysical domains (named A- F), each with a characteristic pattern of isolines and range of values (Motta 1990).

Rock	-	Mean density
Basement complex	-	2.64
Phyllites	-	2.56
Metasandstones	-	2.61
Diamictites	-	2.62
Limestones	-	2.68
Quartzites	-	2.53

Table 5.1 - Summary of the average densities of rocks of the Itabaiana dome area.

Comparing the geophysical domains of Figure 5.3, with the geological map of Figure 3.1 (enclosure), it can be seen that each geophysical domain corresponds to rock types with distinct magnetic properties.

5.3.1 - Domain A

This domain occupies a roughly circular-shaped area with the town of Itabaiana in the centre (Fig. 5.3). It comprises aeromagnetic anomalies generally ranging from -100 nT to -300 nT (dominantly between -100 nT and -200 nT) which form ellipsoids whose 2-4km long axis is generally oriented east-west. The shape of these anomalies is most likely a function of the line spacing (2km; Fig. 5.3)

These elliptical anomalies also occur along a relatively narrow zone which extends to the east of Moita Bonita, as far as the Sergipe river (Fig. 5.3). Comparing this figure with the geological map of Figure 3.1, domain A corresponds to outcrops of the Itabaiana gneiss. The continuity of these anomalies towards the northeastern corner of the area of this study (Fig. 5.3) probably corresponds to shallowly buried basement, brought near to the surface by the Dores thrust (section 4.4.2).

5.3.2 - Domain B

Domain B consists of aeromagnetic anomalies which have the same elliptical shape of those in domain A, but the length of the ellipses is generally smaller, and the values generally range between -50 nT and -100 nT. These anomalies occur in two sub-areas adjacent to the western side of domain A (Fig. 5.3).

One sub-area of domain B occurs as an E-W trending narrow strip that passes around Simão Dias and spreads to the east and west of that town. Another sub-area surrounds the junction of the Salgado and Vaza Barris rivers. Comparison with the geological map of Figure 3.1 (enclosure) shows that the anomalies within the E-W narrow strip of domain B correspond to most of the outcrop area of the Simão Dias gneisses.

The continuation of the same pattern of aeromagnetic anomalies to the western border of the study area also indicates that the Simão Dias gneiss most probably continues westward of the Simão Dias dome, and are probably buried at shallow levels below the metasediments. A similar interpretation applies to the sub-area surrounding the junction of the Salgado and Vaza Barris rivers, where surface outcrops generally consist of rocks of the Miaba Group.

The aeromagnetic map of the southern part of the Sergipano Fold Belt at 1:250,000 scale (Encal 1978) has shown that domain B can be traced continuously westwards from around Simão Dias as far as the eastern border of the Tucano basin, outside the area of this study (Motta 1990).

5.3.3 - Domain C

Domain C has a magnetic signature of typically straight isolines whose values range widely in a small distance across their strike. They occur to the north, south and west of domain A (Fig. 5.3).

The straight contours to the north of domain A are continuous toward the northwestern corner of the study area. A similar pattern of anomalies is observed along the northern border of the Simão Dias gneiss (domain B) just to the west of the Itabaiana dome.

The anomalies of domain C correspond major fault zones within the southern part of the Sergipano Fold Belt (Motta 1990). These features are further discussed in section 5.4 .

5.3.4 - Domain D

This domain comprises a narrow WNW-ESE trending zone along the Vaza Barris river valley, in the southeastern corner of the Itabaiana Dome Area (Fig. 5.3).

The anomalies of domain D are similar to those in domains A and B, and correspond to a continuation of outcrops of the Simão Dias gneisses to the southeastern part of the study area, where they probably correspond to exposed slices of basement rocks described by Davison & Santos (1989) at the eastern end of the Itaporanga fault. In that area, the trace of the Itaporanga fault follows the Vaza Barris river valley, and passes through the town of Itaporanga D'Ajuda (Fig. 2.3).

Thus, the 45 km long strip of outcrops of the Simão Dias gneisses mapped in the Itabaiana Dome Area (this study), represents the exposed portion of a E-W trending subvertical slice of the crystalline basement which is at least 100 km long. This slice was tectonically emplaced parallel to the structural grain of the southern part of the Sergipano Fold Belt, very close to its boundary with the adjacent craton.

5.3.5 - Domain E

Domain E shows a pattern of concentric anomalies whose values range from +100 nT to -275 nT and which are much more circular and broader than the anomalies of domains A and B (Fig. 5.3).

These anomalies occur in wide areas to the north and south of domain B, and correspond in the field to outcrops of the sediments and metasediments of the Miaba, Lagarto and Vaza Barris Groups (see the geological map of Fig. 3.1). They also occur in a wide area to the east of domain A. where they correspond to the sediments of the Sergipe-Alagoas basin.

5.3.6 - Domain F

Domain F has the same characteristics as domain E, but the aeromagnetic anomalies are even broader, and the values generally range between -25 nT and -75 nT (Fig. 5.3). These anomalies occur in the northern part of the study area, where the Frei Paulo and Ribeirópolis Formations are dominant. Another two similar areas are situated to the south of the study area.

It can be seen from the geological map (Fig. 3.1) that these anomalies correspond to outcrops of sediments of the Sergipe-Alagoas basin (around Itaporanga DAjuda in Fig. 5.3) and sediments of the Lagarto-Palmares Formation (in the southwestern corner of the study area).

In conclusion, the aeromagnetic anomalies associated with the exposed or shallowly buried crystalline basement (domains A, B and D) show a greater variation than those elsewhere (domains E and F). The pattern can be interpreted as due to a generally greater content of magnetic minerals in the basement than elsewhere (and to the heterogeneous distribution of basic rocks within the gneisses, as is discussed in the next section). This has been confirmed during the collection of the field measurements, by the very low magnetic susceptibilities of the sediments and metasediments (Motta 1990).

5.3.7 - The basement domains and radiometric data

From a detailed analysis of the radiometric anomalies shown in the map of Figure 5.4 (where the geological boundaries of the Itabaiana and Simão Dias gneisses have also been drawn), it can be seen that the crystalline basement has a distinct radiometric signature compared with that of the rest of the area. The areas occupied by the Itabaiana dome and by the broadest part of the Simão Dias dome are characterised by circular to elliptical anomalies with values of radioactivity normally less than 100 cps (scintillations per second), whereas these values range between 200 cps and 300 cps in most of the rest of the area (Fig. 5.4).

However, inside the Itabaiana dome there are values between 100 cps and 200 cps, particularly between Itabaiana and Moita Bonita, and also to the southeast of Itabaiana (Fig. 5.4). The lower values can be attributed to basement of more basic composition, and the higher values to basement of more acid composition, possibly reflecting the heterogeneous nature of the older crust (Motta 1990).

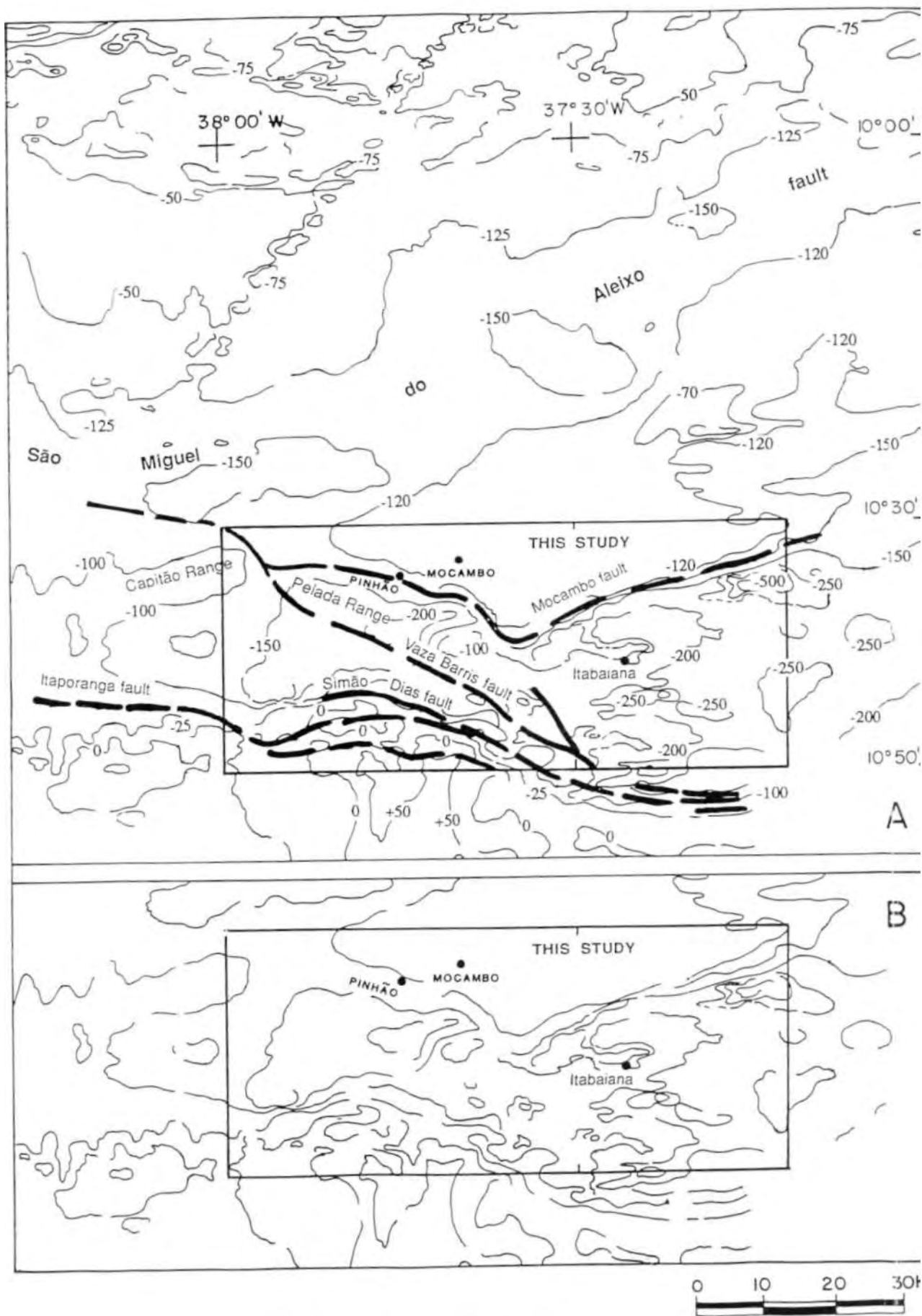
Geological mapping shows (Fig. 3.1) that the basic rocks are more predominant in the south, west and northwestern parts of the Itabaiana dome. Although the field work was not carried out with the principal aim of separating basic and acid rocks in the basement (nor it would be accurately possible because of the discontinuous nature of the basement outcrops), it is clear that the basement is heterogeneous, particularly in the Itabaiana Dome Area.

The above supports the interpretation by Motta (1990) that the basement can be sub-divided into blocks with subtle density contrasts.

5.4 - Aeromagnetic signature of the regional faults in the Itabaiana Dome Area

Figure 5.5 A-B displays part of the 1:250,000 scale map with the aeromagnetic anomalies of the southeastern part of the Sergipano Fold Belt (Encal 1978). This highlights the correlation between the linear aeromagnetic anomalies (typical of domain C) and regional faults, particularly in the Itabaiana Dome Area, as originally interpreted by Motta (1990).

The fault zones corresponding to the São Miguel do Aleixo fault (Santos et al. 1988; Davison & Santos 1989) and to the Itaporanga, Simão Dias, Vaza Barris and Mocambo faults (this study) are indicated in Figure 5.5 A. The aeromagnetic anomalies for the Itabaiana Dome Area are separated in Figure 5.5 B, but without the fault lines.



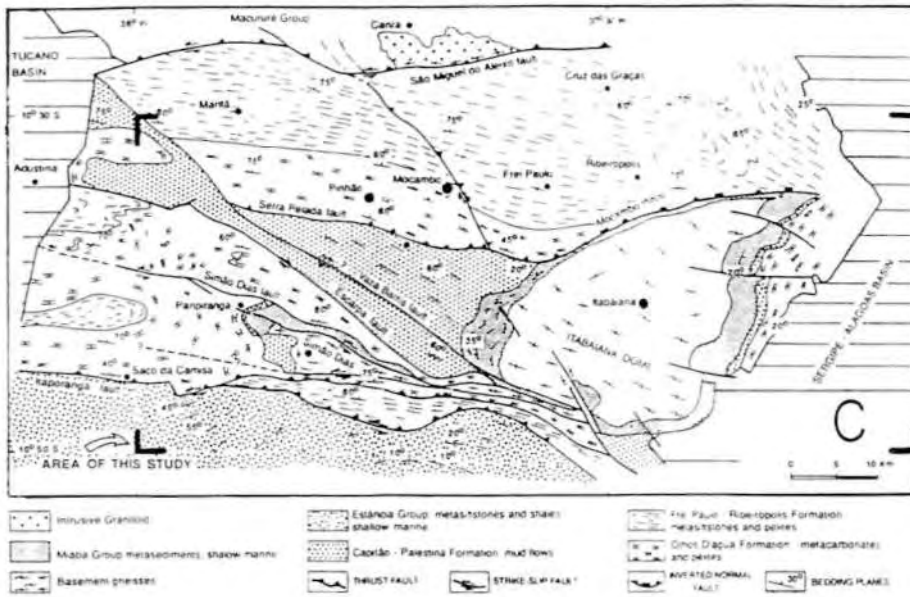


Figure 5-5- The aeromagnetic signature of the main regional faults.

(A): Map showing the aeromagnetic linear anomalies coincident with some of the regional faults within the eastern part of the Sergipano Fold Belt. The numbers in the isolines are values in μT (Modified from Motta 1990).

(B): Reproduction of the same aeromagnetic data for the area of this study, without the trace of the regional faults.

(C): Simplified copy of the geological map of Figure 2.4, highlighting the Serra Pelada and Mocambo faults.

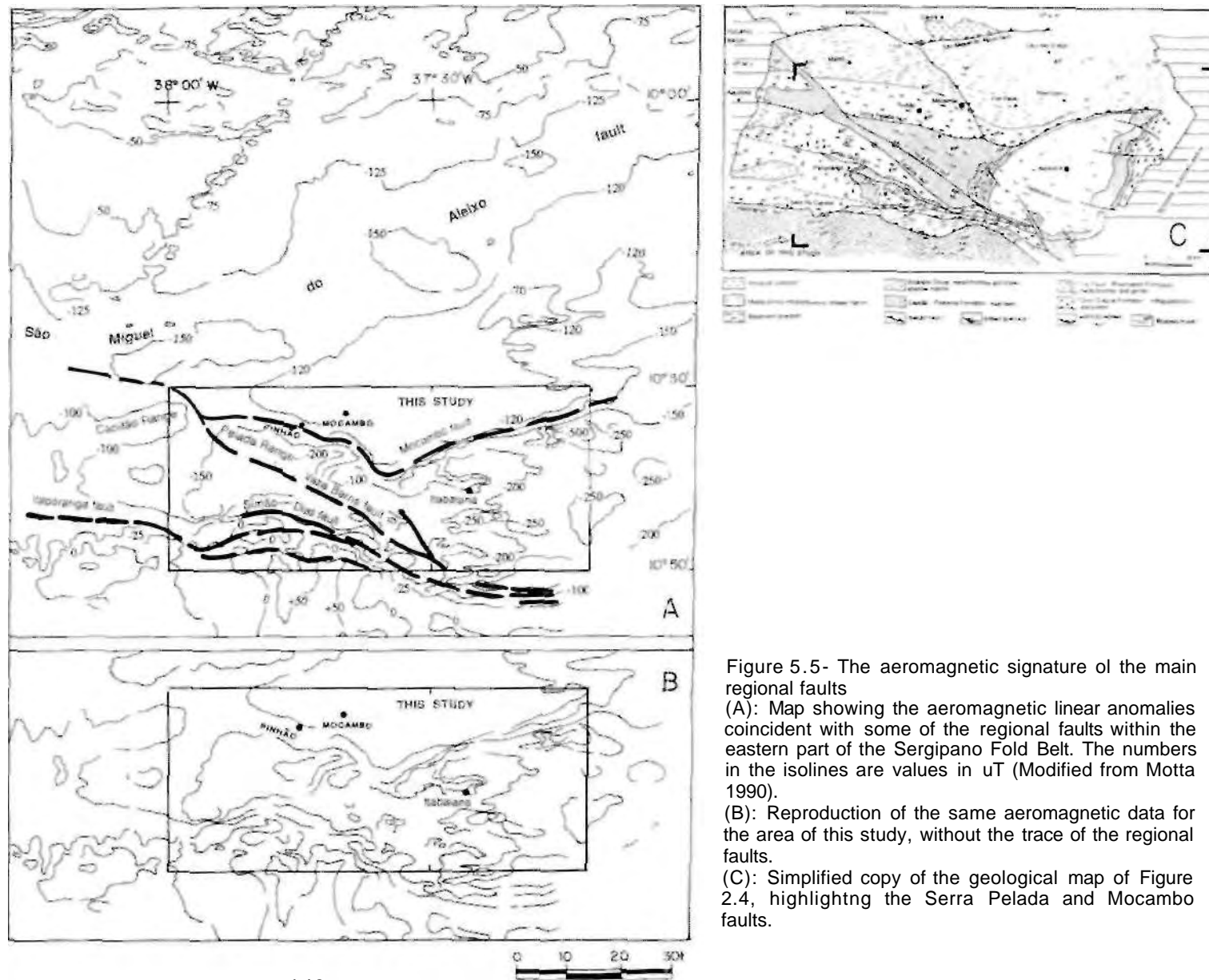


Figure 5.5- The aeromagnetic signature of the main regional faults

(A): Map showing the aeromagnetic linear anomalies coincident with some of the regional faults within the eastern part of the Sergipano Fold Belt. The numbers in the isolines are values in uT (Modified from Motta 1990).

(B): Reproduction of the same aeromagnetic data for the area of this study, without the trace of the regional faults.

(C): Simplified copy of the geological map of Figure 2.4, highlighting the Serra Pelada and Mocambo faults.

Figure 5.5 C is a reduced copy of the geological map (Fig. 2.4), highlighting the array of regional faults previously identified in the geological maps of the Itabaiana Dome Area. By comparing Figures 5.5 A-C, it is possible to see that the aeromagnetic signature of the Mocambo fault (Figs. 5.5 A & B) only partially corresponds to the trace adopted for the same fault in previous geological maps of the area (Fig. 5.5 C).

In contrast, the trace of the Mocambo fault, as shown in Figure 5.5 A, seems to be much more realistic than that adopted in Figure 5.5 C, and additionally does not exclude the Pelada fault. As such, the Mocambo fault as now identified, fits with the entire aeromagnetic signature, and also fits with field observations described in sections 3.3.4 and 4.4.2.

5.5 - Geophysical sections in the Itabaiana Dome Area

Figures 5.6 A, 5.7 A and 5.8 A (all in the enclosure) show profiles of the observed and calculated gravity and aeromagnetic data along the XX', YY', and ZZ' section lines. The gravity interpretative sections are shown respectively in Figures 5.6 B, 5.7 B and 5.8 B, and the aeromagnetic interpretative sections are shown in Figures 5.6 C, 5.7 C and 5.8 C. The interpretations have also taken into consideration the radiometric data (section 5.3).

The crystalline basement was tentatively divided into blocks bounded by several convex upward surfaces, resembling the geometry of listric thrust faults which dip at high angles at the surface and become gradually subhorizontal with depth. Both the basement and the metasediments were tentatively divided into blocks with a contrast of densities, as generally indicated by the profiles (after the original report by Motta 1990).

Comparing the gravity and aeromagnetic profiles of Figures 5.6 and 5.7, it can be seen that the gravity and magnetic interpretative profiles of the upper crust are generally in good agreement, with only local discrepancies.

Also comparing these profiles with the geological cross sections across the basement domes (AB and EF, Fig. 4.20, enclosure) it can be seen that, despite the small amount of geophysical data, the geophysical interpretations support the depth of the basement and metasediments adopted in the geological cross sections.

5.5.1 - The geophysical section XX'

The observed and calculated Bouguer profiles of Figure 5.6 A show increasing values from south to north, although there is a depression between 26 km and 35 km. The concave upward part of the curve corresponds to the Simão Dias dome and to buried blocks of the basement close to the surface, immediately to the north of it, because their average density (2.64) is higher than the density of the metasediments (Motta 1990).

The saddle in the 26-35 km interval may be explained by the greater thickness of the less dense metasediments in the Vaza Barris trough, between the Pelada and Escarpa faults, an area where the basement occurs at depths as great as 4 km (Fig. 5.6 B).

Motta (1990) points out two minor differences between the aeromagnetic and the gravity interpretation. One difference is related to a marked break of the aeromagnetic

values between 10 and 15 km, in the southern part of the Simão Dias dome, and the other concerns the depth of the basement to the north of the Pelada and Mocambo faults (Fig. 5.6 A-C).

At the southern border of the Simão Dias dome, the aeromagnetic interpretation has placed the blocks numbered 8 and 9 inside the Simão Dias dome (block 1) with different magnetic susceptibilities, whereas the gravity profile could be modelled as a single block of uniform density (Fig. 5.6 B).

In the area to the north of the Pelada fault, the aeromagnetic data (Fig. 5.6 C) indicate that the basement occurs at a depth less than 2 km, and continues at this depth immediately to the north of the Mocambo fault.

The gravity profile (Fig. 5.6 B) also suggests that the basement occurs at depths less than 2 km between the Pelada and Mocambo faults, but is deeper toward the Mocambo fault and across it, along a steeper gradient than in Figure 5.6 C.

5.5.2 - The geophysical section YY'

The observed and calculated Bouguer curves in this profile (Fig. 5.7 A) decrease continuously from SSW (Y) to 40 km NNE (Y'), where they reach a minimum and start to increase slightly towards the end of the profile.

In detail, the plot of the observed and calculated Bouguer data across the Itabaiana dome (Fig. 5.7 A) shows open and sinusoidal variations along the profile, which Motta (1990) interpreted to be the result of several blocks with subtle density contrasts (Fig. 5.7 B). Most of the anomaly corresponds to the Itabaiana dome, which is bounded to the north by the Mocambo fault (Fig. 5.7 B). The relative depth of the basement just to the north of this fault is 4 km, and becomes gradually shallower towards the end of the profile.

The aeromagnetic profile shows a pronounced low corresponding to the Mocambo fault (Fig. 5.7 A). The aeromagnetic interpretation of Figure 5.7 C is in good agreement with the gravity interpretation, except for the area to the north of the Mocambo fault, where it has not been possible to distinguish between basement and cover (Motta 1990).

5.5.3 - The geophysical section ZZ'Z''

Figure 5.8 A shows the gravity and aeromagnetic data along the composite ZZ'Z'' profile. Figure 5.8 B displays the gravity interpretation across the northern border of the study area, and also across the boundary between the southern and northern parts of the Sergipano Fold Belt, which is marked by the São Miguel do Aleixo fault, according to Santos et al. (1988) and Davison & Santos (1989).

The Bouguer curves show positive values in the 0-94 km interval, and correspond to two gravity highs (named I and II in Fig. 5.8 A), which are separated by a gravity low (named III).

The first high (I) corresponds to the outcrops of Itabaiana gneiss on the western side of the Itabaiana dome, and to the buried crystalline basement between the Mocambo and São Miguel do Aleixo faults. The second high (II) occurs in the northern part of the

profile, and corresponds to that part of the Sergipano Fold Belt between the São Miguel do Aleixo and Belo Monte-Jeremoabo faults (Fig. 5.8 B).

The interpretation of the Bouguer profile for the northern part of the Sergipano Fold Belt agrees with the geophysical interpretation shown in Figure 2.8. Northward of 94km the negative Bouguer values in the profile reflect the greatest thickness of metasediments in the Sergipano Fold Belt, which can be 13km (Santos et al. 1988).

The gravity low (III) corresponds to outcrops of metasediment between the two gravity highs, which extend to an average depth of 3.5km.

It is also noteworthy that in this gravity profile, the depth of the basement decreases from 2km, just to the north of the Mocambo fault, to 5km at the edge of the study area (Fig. 5.8 B). The depth of 2km, and the smoother gradient of the depth of the basement shown in this profile, are in accordance with the depth and gradient of depths of the basement in the aeromagnetic interpretation of Figure 5.6 C, rather than with the stronger gradient for the depth to the basement in the gravity interpretation (Fig. 5.6 B).

Figure 5.8 B also shows several bodies of rocks with average density of 2.57 or 2.55 (see blocks 6, 7, 9 and 10). Blocks 6, 9 and 10 correspond to outcrops of granite in the northern part of the Sergipano Fold Belt (Motta 1990). Block 7, which lies between the edge of the study area and the São Miguel do Aleixo fault, corresponds to the outcrops of Itabaiana quartzite (see the Campina and Redonda Ranges, Fig. 3.1), and outcrops of phyllites, pebbly phyllites and metavolcanics of the Ribeirópolis Formation (this study).

However, the above interpretation does not eliminate the possibility of buried granitic bodies within or in the vicinity of block 7, just in the footwall of the São Miguel do Aleixo fault.

The aeromagnetic profiles of Figure 5.8 A show two accentuated lows. The low at around 14km corresponds to the Mocambo fault (Fig. 5.8 B), whereas the low between 5 and 8km does not have a straightforward explanation from the surface geology.

It may correspond to faults or subvertical mylonitic zones within the Itabaiana dome, an area generally covered by the colluvium of the Miaba range (Fig. 3.2). Alternatively, it could correspond to blocks with different magnetic susceptibilities within the crystalline basement, in the same way as has been interpreted for the Simão Dias dome (blocks 8 and 9, Fig. 5.6 C). This possibility fits well with the wide variety of lithologies observed within the western part of the Itabaiana dome.

5.6 - Conclusions

Because of the small amount of data, and the lack of seismic sections, geophysical knowledge of the Itabaiana Dome Area is relatively poor. However, computer modelling of the gravity and aeromagnetic field data, and analysis of the aeromagnetic and radiometric anomaly maps available in the literature (Motta 1990), permit the following conclusions to be drawn:

1 - The geophysical cross sections generally support the relative depth of the basement and metasediments used in the structural cross sections presented in Figures 4.20 and 4.21.

2 - The aeromagnetic and radiometric data allow a clear identification of the exposed areas of crystalline basement and the areas of sedimentary cover.

3 - The aeromagnetic data provide good indications of the traces of the regional faults and of shallowly buried slices of crystalline basement. They indicate the continuity of the Simão Dias gneiss to the east and west of the field area, and the slices of Itabaiana gneiss in the hangingwall of the Dores thrust in the northeastern corner of the field area.

4 - The Simão Dias gneisses are most probably the outcropping expression, in the area of study, of an E-W trending tectonic slice which stretches for more than 100km. This slice was emplaced sub-vertically into highly deformed metasediments, along and very close to the northeastern border of the São Francisco Craton.

5 - The crystalline basement is heterogeneous and may be sub-divided into blocks of different density and magnetic susceptibility, which probably reflect variable proportions of basic and acid compositions.

6 - The upper crust in the southern part of the Sergipano Fold Belt may be interpreted in terms of wedge-shaped blocks of metasediment and crystalline basement, which resemble tectonic slices separated by listric-like fault planes merging downwards in a subhorizontal detachment at a depth of 10 km.

Chapter 6 - Geological evolution of the southern part of the Sergipano Fold Belt

6.1 - Introduction

This chapter has four main objectives -

1. To present an interpretation of the geological evolution of the Itabaiana Dome Area.
2. To discuss the implications of the results of this research for the geological evolution of the whole of the Sergipano Fold Belt.
3. To develop a model for the tectonic evolution of the Sergipano Fold Belt.
4. To discuss the implications of this research in the analysis of the tectonic evolution of other Proterozoic fold belts, particularly those of the Pan-African and Brasiliano orogenic system.

The geological evolution of the Itabaiana Dome Area is summarised and discussed in section 6.2 and models for the basin development, sedimentation, and for the structural and metamorphic evolution are proposed. The evolution of the basement domes is discussed.

Section 6.3 discusses the significance of this research with respect to the evolution of the southern Sergipano Fold Belt and for the Sergipano Fold Belt as a whole. A tectonic model is proposed.

Section 6.4 compares the geology of the Sergipano Fold Belt with that of other fold belts in the Pan-African-Brasiliano orogenic system, and the implications for Proterozoic crustal evolution are also discussed.

6.2 - Geological evolution of the Itabaiana Dome Area

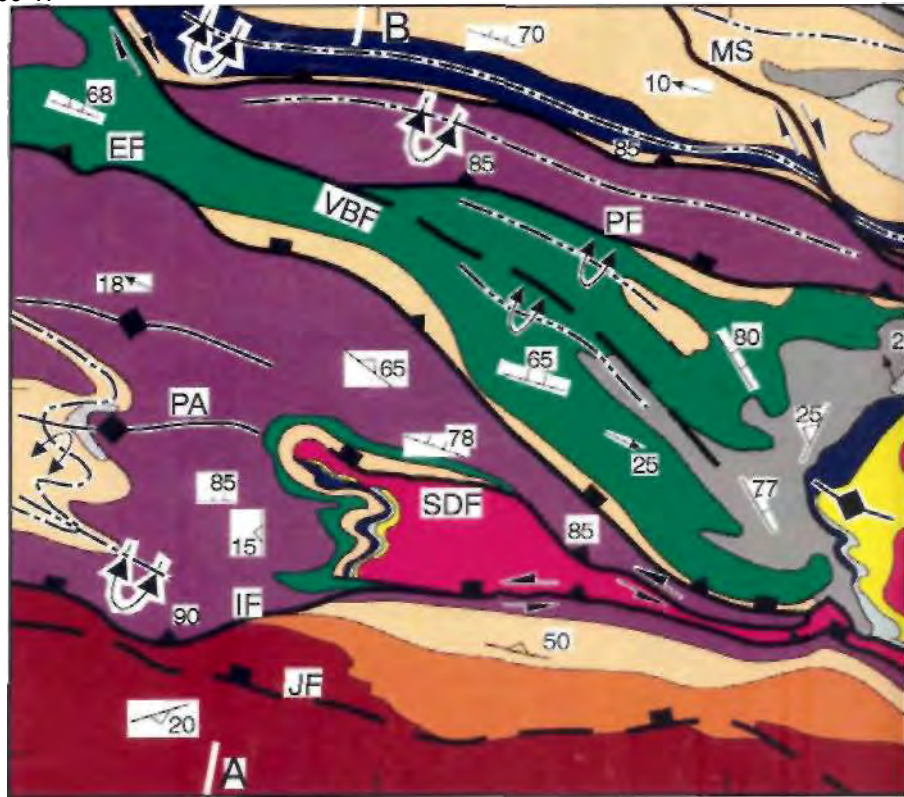
6.2.1 - Introduction

Figure 6.1 is a lithostructural summary map of the Itabaiana Dome Area. Figure 6.2 is a simple domain map depicting the main lithotectonic regions of the Itabaiana Dome Area. The cratonic domain in the south consists of little to non deformed and non metamorphosed sediments (including the Lagarto Group).

The WNW-ESE striking Itaporanga fault separates this domain in the south from the highly deformed, greenschist facies siliciclastic and carbonate metasediments (with minor metavolcanics) and the Itabaiana and Simão Dias gneiss dome complexes of the fold-thrust domain (Fig. 6.2). The SSW-NNE striking Propria fault separates the Proterozoic sequences from the Mesozoic Sergipe-Alagoas basin (Fig. 6.2).

The Itabaiana Dome Area has undergone polyphase contractional deformation, ascribed to the Brasiliano Orogeny, with a peak of metamorphism at 673-600 Ma (Brito Neves & Cordani 1973; Gava et al. 1983). The dominant structures are large, southwest vergent recumbent F_1 folds, SW vergent F_2 folds and associated high angle thrust faults together with two basement gneiss domes mantled by metasediments (Fig. 6.1).

38° 00' W



Olhos D'agua Fm:
metacarbonates,
(metacarbonates
and metapelites)

Palestina Fm:
diamictites and
pebbly phyllites

Frei Paulo Fm:

D variegated and silty
phyllites

D FP1 - calcite-cement
metasandstones, phyllites,
minor metacarbonates

FP3 - quartz-senecite phyllites,
interbedded black phyllites
and shales, metasilites,
calcilutites and greywackes

Jacaré Fm:
metasilites

Lagarto-Palmares Fm:
fine to medium grained
sandstones and wackes

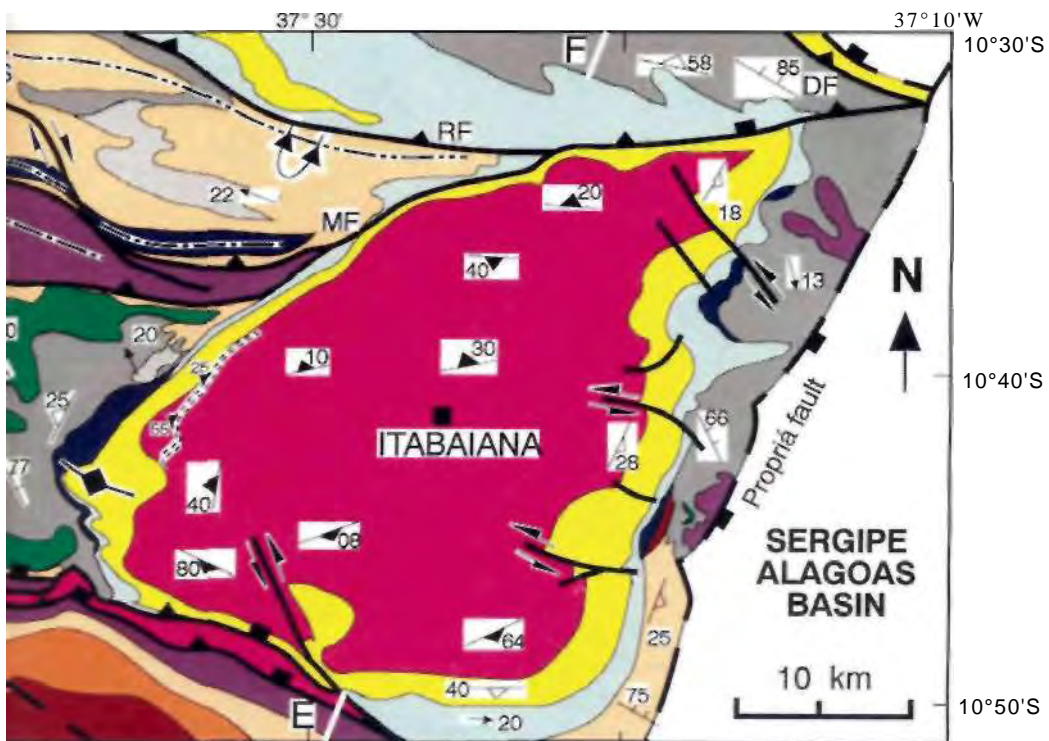
Jacoca Fm :
metarbonates,
(metacarbonates
and metapelites)

Ribeirópolis Fm:
phyllites, pebbly
phyllites, metavolcanics

U Itabaiana Fm:
quartzites (conglomerate
metasandstones and phy

Crystalline basemer
gneiss-granitic complex

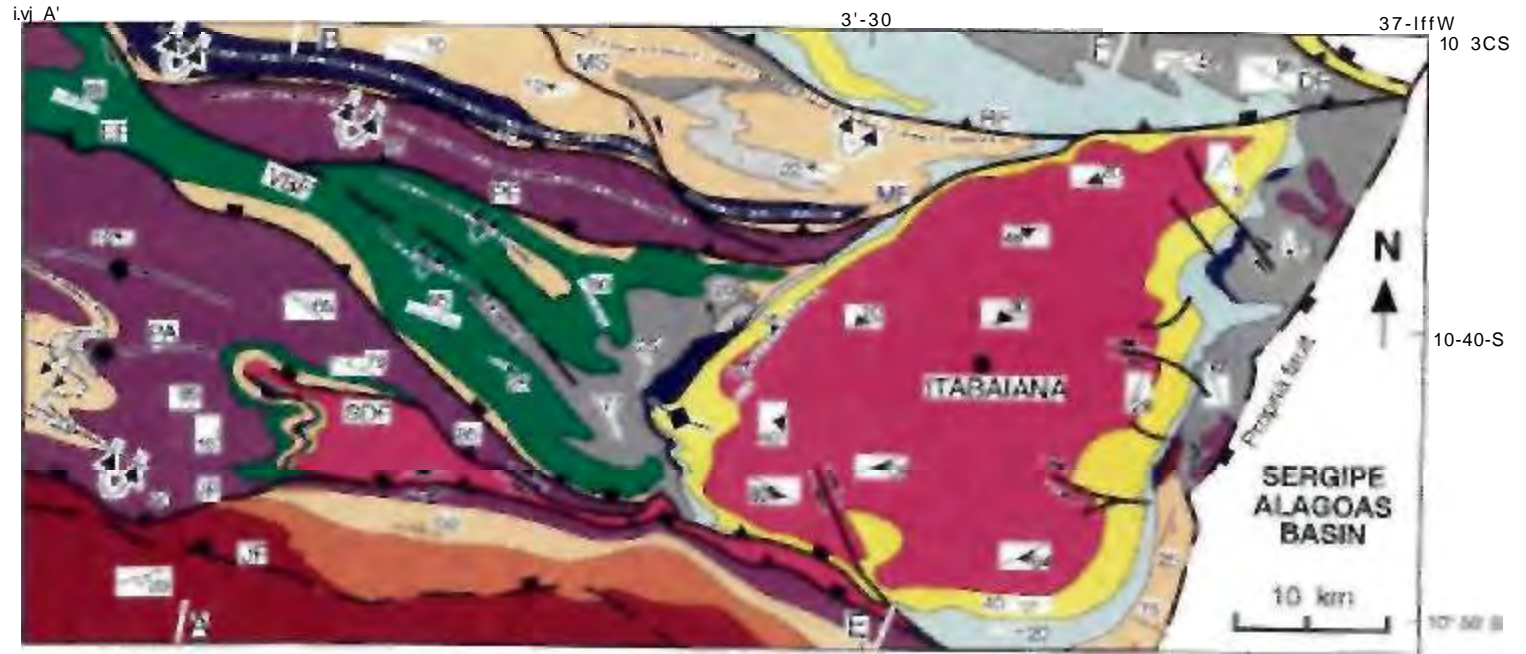
PA = Paripiranga anticline, JF = Jacaré fault, IF = Itaporanga fault, SDF = Simão Dias fault, EF = Es
PF = Pelada fault, VBF = Vaza Barris fault, MF = Mocambo fault, MS = Mocambo shear, RF = Ribe
DF = Dores fault.



-m :
 «es,
 onates
 •elites)
 olis Fm:
 •ebby
 netavolcanics
 aFm:
 (conglomerates),
 stones and phyllites
 ne basement:
 nitic complex
 i fault, EF = Escarpa fault,
 iar, RF = Ribeirópolis fault,

So, Sn	S2 foliation	->- B2, L2
F1 overturned syncline	F1 overturned anticline	F2 overturned anticline
F2 anticline	Thrust fault	Normal fault
Strike-slip fault	Inverted extensional fault	25 Macambira phyllonites

Figure 6.1 - Summary lithostructural map of the Itabaiana dome area. Sections AB and EF are shown in Figure 4.21.



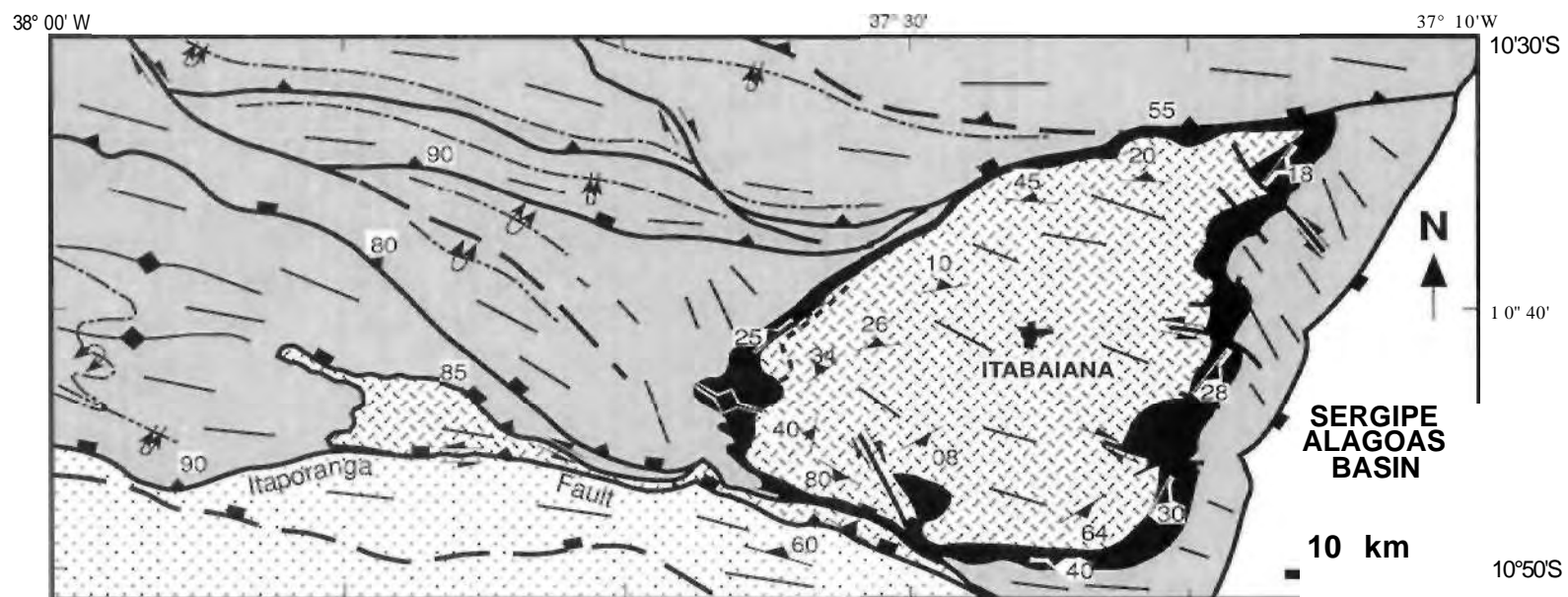
i :llq,-l: *,,-.- .
 •(mMfeanmmi I flll» MV«TOMÉH •
 « minim
 RetPsu« ^m
Df«g**amiir|
 I Lagafio-Paimew? in

 pt>gm.i
 itatniofl* Fm
 □ I (v.....)» v. a
 lit- ludvmeui
 f w i w f i »

So.Sn •32 'oli at, or 32. Li
 - 4 - 4 - - Flowtim M - 4 4 - - FI Otforufned -*M i'LC It
 Fíamoing . Ttirusilv. • Naníí faull
 ^ _ _ _ snw.- slip faun syrens 'n.* .i i! -' ^s Macame4fa
 phylloni'.E

••*•r*t» i—urdiu r...ln.i'i,iiT mnivgaMtaBf ••BwtaBtofli V>

Figure 6.1 - Summary lithostratigraphic natural map of the Itabaiana dome area. Sections AB and EF are shown in Figure 4.21.



Cratonic domain: mostly undeformed and non metamorphosed, intensity of deformation increases towards north

Polydeformed Itabaiana quartzites

Trend of S2 and L2

Polydeformed metasediments

Polydeformed gneisses

* \llcorner .. Macambira phyllonites
i*

Figure 6.2 - The main lithotectonic domains in the Itabaiana Dome Area. See text.

Oblique sinistral strike-slip motion along some of the major high angle thrust faults is also found. Major strike-slip faults are the Vaza Barris fault and the Mocambo shear (Figs. 6.1 & 6.2).

The basement gneiss domes are fault-bounded on their northern and southern margins. The basement gneiss metasediment cover contact is generally sheared and subvertical. The basal unconformity is found undeformed at the eastern margin of the Itabaiana dome (Fig. 6.1). The western margin of the Itabaiana dome has a basement-derived phyllonitic zone parallel to and also along part of the basal unconformity (Fig. 6.1). Extensional shear bands in this zone consistently indicate a top down to the WNW movement (section 3.3.2).

6.2.2 - Stratigraphy of the Itabaiana Dome Area

The Itabaiana Dome Area mapped during the course of this research includes both the cratonic domain (undeformed or little deformed sediments) and the south vergent fold/thrust terrane (Fig. 6.2). A new stratigraphy has been established for the area (Chapter 3) based upon detailed mapping, structural analysis and the application of sequence stratigraphic principles (e.g. Hubbard et al. 1985 a; Wagoner et al. 1987).

This new stratigraphy (summarised in Fig. 6.3) shows that strata deposited essentially on the craton consist of the Estância and Lagarto Groups whereas strata deposited within the basin (probably best described here as a miogeocline) consist of the Miaba, Lagarto and Vaza Barris Groups (Fig. 6.3). Thicknesses on the craton total approximately 1 km whereas in the basin thicknesses total approximately 4 km.

The age of sedimentation is generally inferred to be Mid to Late Proterozoic (1000-900 Ma) based upon lithostratigraphic correlations with the Bambuí Group (Cloud & Dardenne 1973; Misi 1976). Detailed stratigraphic relationships and the sedimentology of the units are described in Chapter 3. These data, combined with stratigraphic and sedimentological descriptions in other research in the southern part of the Sergipano Fold Belt, has allowed new stratigraphic interpretations to be made (Fig. 6.3).

1. The Juetê Formation correlates with the Itabaiana Formation: both unconformably overlie the crystalline basement and are overlain by carbonates. Moreover the meta-arkosic sandstones and red-brown phyllites of the Itabaiana Formation may be correlated with similar lithologies in the Juetê Formation of Suva Filho et al. (1978 a & b) and Saes (1984).

2. The Acauã Formation may be correlated with the Jacoca Formation - both are carbonates and both are overlain by the Lagarto Group.

3. The Lagarto Group includes the Lagarto-Palmares, Jacaré and Frei Pajlo Formations, which are overlain by the Palestina Diamictites - a distinct unit in the basin.

Despite the intense polyphase deformation that has obscured thickness changes and also perhaps original unconformity surfaces, the structural and stratigraphic analysis of this research has enabled to recognise four megasequences (Hubbard et al. 1985 a & b) that divide the sedimentary evolution of the southern part of the Sergipano Fold Belt in two distinct cycles, each one characterised by a lower siliciclastic megasequence and an upper carbonate megasequence (Fig. 6.3).

		CRATON		BASIN
CYCLE	MEGASEQUENCE	GROUP	FORMATION	GROUP
1	UPPER CARBONATE		>v OLHOS D'AGUA	VA2A BARRIS
	UPPER SILICICLASTIC		\ PALESTINA	
		LAGARTO	LAGARTO PALMARES " - V J J X O A K T JACARÉ " ~ ~ ~ < r > FREI PAULO	LAGARTO
II	LOWER CARBONATE	ESTÂNCIA	ACAUÃ - r - - _ . JACOCA	MIABA
	LOWER SILICICLASTIC		JUETÉ ' " > \ - RIBEIRÓPOLIS	
São Francisco craton			X^ ITABAIANA	

Figure 6.3 - Stratigraphy of the Itabaiana Dome Area and southern part of the Sergipano Fold Belt.

Cycle I has a lower siliciclastic megasequence consisting of the Juetê-Itabaiana and Ribeirópolis Formations, and an upper carbonate megasequence consisting of the Acauã-Jacoca Formations. Cycle II has a lower siliciclastic megasequence consisting of the Lagarto and Palestina sequences overlain by the Olhos D'agua upper carbonate megasequence (Fig. 6.3).

It is important to note that each carbonate megasequence exhibits shallowing upwards facies (Section 3.4) and overlies different siliciclastic units and, in places, the basement. The Acauã carbonates are either in sharp contact with the Juetê siliciclastics or with the crystalline basement in the cratonic domain (Silva Filho et al. 1978 a & b; Saes 1984). In the Itabaiana Dome Area, the Jacoca carbonates are in sharp contact with the Ribeirópolis conglomerates and with Itabaiana quartzites, in the Capitão farm area (e.g. Fig. 3.11 B & outcrop 312).

6.2.3 - Depositional environments, facies and thickness distributions

Siliciclastic sedimentation

Cycle I The basal cross-bedded Itabaiana quartzites that unconformably overlie the basement may be interpreted to have been deposited in a shallow marine environment (cf. interpretations by Walker 1985a) whereas the interbedded arkosic metasandstones and reddish brown phyllites of the Itabaiana Formation may be interpreted to indicate rejuvenation and uplift of hinterland areas of the crystalline basement (cf. Dickinson & Suczek 1979). The overlying Ribeirópolis Formation pebbly phyllites probably indicate erosion of tectonically uplifted hinterland areas and deposition by mass flows (section 3.4.4). The lower siliciclastic megasequence indicate a continental to shallow marine sedimentary environment with the clastic source area to the south, together with the development of a miogeocline to the north. Active extensional tectonics during deposition were probably responsible for the mass flow deposits.

Cycle II The lower siliciclastic sequence is characterised by the northward progradation and upward coarsening of the shallow marine sandstones, siltstones and mudstones of the Lagarto Group. Outboard miogeoclinal equivalents of the Lagarto-Palmares sandstones are the Jacaré metasilites and the Frei Paulo phyllites (Fig. 6.1). This may be interpreted to indicate rejuvenation of the hinterland on the craton to the south either by a sea level fall or by tectonism (as compared to the relatively quiescent period during which the shallowing upwards sequence of the underlying carbonates was deposited). The petrography of the Lagarto-Palmares sandstones indicates that they were derived from crystalline basement with additional detrital input from low grade metasediments and metavolcanics (Table 3.1). The sandstone bodies in the Frei Paulo Formation to the north of the Vaza Barris trough suggests erosion of uplifted basement blocks to the north of the trough (section 3.7).

Carbonate sedimentation

From the detailed descriptions and map distribution of the lithofacies in the Itabaiana Dome Area (section 3.4) it is apparent that both the Jacoca and Olhos D'agua Formations strongly suggest that the Itabaiana and Simão Dias domes were paleohighs during the evolution of the miogeocline. Facies interpretations (section 3.4.5) indicate that both are shallowing upward carbonate sequences. A period of relative quiescence may be inferred during the deposition of the Jacoca and Olhos D'agua sequences, because of the lack of slumping, debris flows and turbidites, as found on carbonate platforms that underwent syndepositional tectonism (e.g. Herrington & Fairchild 1989; Bechstadt & Boni 1989).

Cycle I Jacoca carbonates. The Jacoca carbonates die out from the Itabaiana dome into the area between the Pelada and Escarpa faults, and also to the north of the Mocambo fault (Fig. 6.1). The base of the formation starts with what may be interpreted as offshore shelf facies (parallel-laminated and thinly intercalated carbonate and fine siliciclastics, - distal turbidites), and passes upwards into subtidal-intertidal facies, with oolites, intraclasts and wave-reworked structures indicating an agitated, near shore environment

Cycle II Olhos D'agua carbonates. The thick Olhos D'Agua carbonates around the Simão Dias dome pass upwards into subtidal-intertidal facies, with oolites, intraclasts and wave-reworked structures also indicating a near shore environment, and pass into siliciclastic-rich carbonate facies, across the Escarpa fault and Vaza Barris trough, up to the north of the Mocambo fault (Fig. 6.1).

Thickness variations

Despite the limitations imposed by the intense deformation, the estimates of stratigraphic thicknesses indicate that, apart from the Itabaiana quartzites (which are generally =10-50m thick and locally up to =700m in the vicinity of the Itabaiana dome), the siliciclastics are significantly thinner (0-100m) near the basement domes than elsewhere in the map area. The greatest accumulations of siliciclastics (=500m) occur between the Escarpa and Pelada faults, in the so called Vaza Barris trough, as well as to the north of the Mocambo fault (Fig. 6.1).

The Vaza Barris trough, which is also the depocentre for the Palestina diamictites, also contains the most of the volcanics (and probable volcanoclastics) of the Frei Paulo Formation, whereas to the north of the Mocambo fault most of the Ribeirópolis volcanism is found (Fig. 6.1).

Consideration of the stratigraphic, sedimentological and thickness relationships outlined above (and given in detail in Chapter 3) permits an interpretation that Cycle 1 began with a shallow marine deposition onto the basement (Itabaiana sandstones) followed by deepening of the basin and possible active tectonism (Ribeirópolis Formation), to progressive shallowing of the basin and the development of the Jacoca

carbonates (particularly flanking the paleohighs of the Itabaiana and the Simão Dias domes). Cycle II indicates regeneration of the hinterland (probably through tectonism), deposition of the Lagarto Group and the Palestina Formation probably in fault bounded basins (e.g. the Vaza Barris trough) followed by a second shallowing upward carbonate sequence (the upper carbonate megasequence - Fig. 6.3) that infills the basin to the north of the Ituporanga fault.

The wide variety of lithofacies and their overall distribution and thickness variations indicates deposition in an open platformal environment containing relatively deep water environments in extensional fault bounded basins on the craton margin - i.e. a miogeocline with the craton to the south. The fact that now most of these thickness and facies variations are found across major thrust faults supports an interpretation that the thrust faults are inverted extensional faults.

These conclusions are supported by other researchers (Humphrey & Allard 1962, 1967, 1969; Silva Filho et al. 1978 a & b) who interpreted a shallow marine environment and a miogeocline sedimentation in the southern part of the Sergipano Fold Belt. In addition basins with well documented thickness variations together with lateral and vertical superposition of shallow water and relatively deep-water facies and geographically related to regional extensional faults, have been interpreted as examples of syn-extensional sedimentation (e.g. Mitchell & Owens 1990; Trexler & Nitchman 1990; Collier 1991).

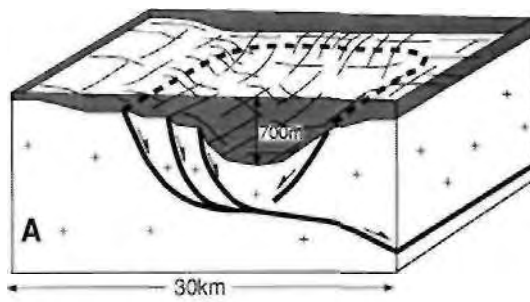
6.2.4 - Basin evolution: a model for the Itabaiana Dome Area

In order to erect a model for the development of a sedimentary basin it is, in ideal cases, necessary to take into account the geometry of the basin, the stratal thicknesses throughout the basin, age relationships, subsidence and thermal histories, compaction effects (Barr 1991), as well, as the nature of the faulting controlling basin development (i.e. mode of extensional faulting - simple shear versus pure shear).

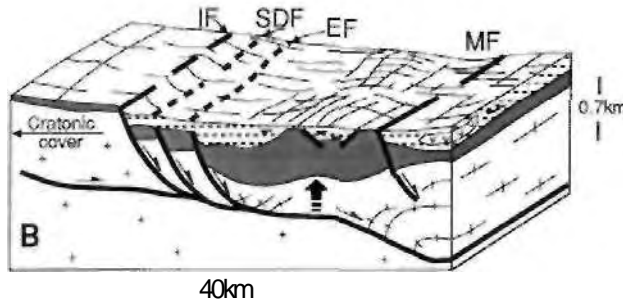
The model of basin evolution for the Itabaiana Dome Area (Figs. 6.4 & 6.5) has been based on the evidence (5:1 to 20:1 thickness variations; facies variations) for a tectonically controlled sedimentation up to the deposition of the third megasequence.

The model assumes a simple shear style, linked listric detachment architecture (cf. Wernicke & Burchfiel 1982; Wernicke 1985; Gibbs 1984, 1987) in which the southern part of the Sergipano Basin is interpreted as a half graben developed upon a listric basal detachment, with a ramp-flat geometry, together with a system of synthetic and antithetic, planar and listric normal faults that accommodate the cumulative strain of the extending hangingwall. The Vaza Barris trough is interpreted as a major, long lived, ramp syncline or crestal collapse graben. Two major periods of extension are postulated corresponding to the development of the two siliciclastic megasequences, followed by periods of relative tectonic quiescence and deposition of the carbonate megasequences.

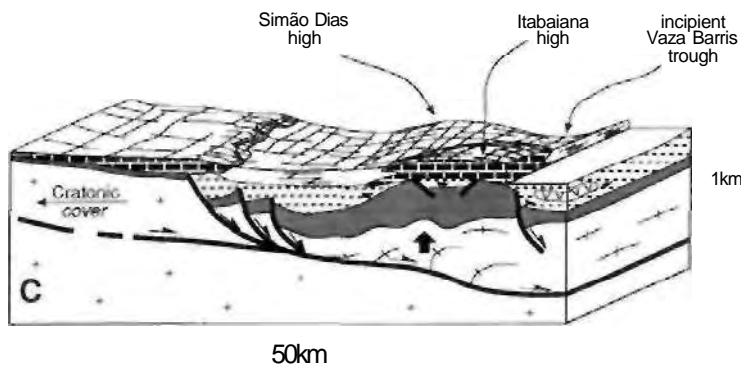
Despite the increasing debate concerning extensional systems of listric versus planar faults (Kusznir et al. 1991), recent seismic investigations across the Rhine graben, between Germany and France (Brun et al. 1991), has resulted for example in a half graben interpretation similar to that proposed here.



Itabaiana quartzites in their deepest depocenter, the site of the future Itabaiana dome



Deposition of the Ribeirópolis coarse siliciclastics and emplacement of the volcanics



Deposition of the Jacoca carbonates

Estância - Miaba Group

Formation Lithofacies

Acauã-Jacoca

limestones,
dolomites

F3 interbedded limestones, siltites,
fine sandstones and pelites

Ribeirópolis

pelites, pebbly pelites
and volcanics

Jueté-Itabaiana

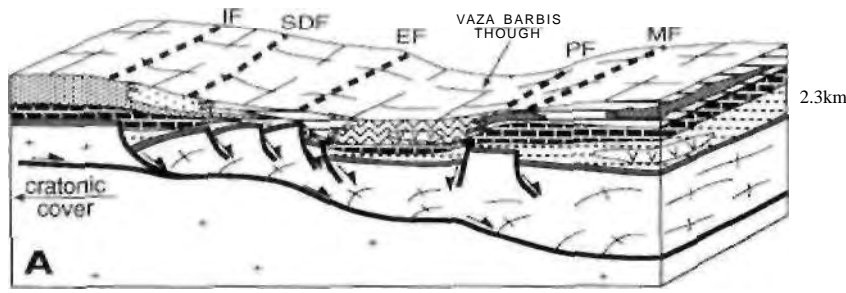
feldspathic arenites,
and interbedded
arkosic sandstones
and mudstones

Crystalline
basement

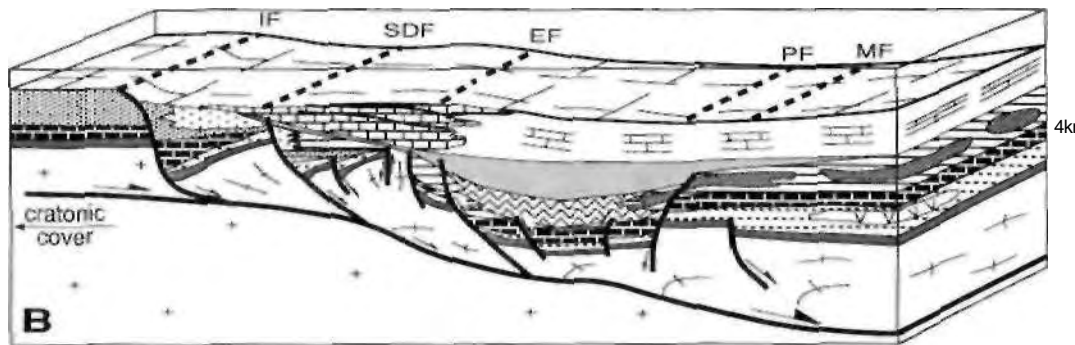
1 amphibolite facies
gneisses and
orthogneisses

S | brittle reworked basement
during extension

Figure 6.4 - Evolution of the basin and its sedimentary infill. A-C shows the deposition of the Estância-Miaba group (Cycle I). The maximum estimated thickness of sediments deposited on each stage is indicated. The depth of the basal detachment is not at scale.



60km
Deposition of the Lagarto Group



80km
Deposition of the Vaza Barris Group

IF = Itaporanga fault SDF = Simão Dias fault,
 EF = Escarpa fault, PF = Pelada fault, MF = Mocambo fault
 LSMS = lower siliciclastic megasequence, LCMS = lower carbonate megasequence
 USMS = upper siliciclastic megasequence, UCMS = upper carbonate megasequence

Group	Formation	Lithofacies
C D C	Olhos / D'agua \ i	interbedded limestones and peiites
		limestones UCM!
C D C	Palestina	diamictites
		FP3 - peiites, silts. minor calcilules fine sandstones, volcanics
C D C	Frei Paulo —	FP1 - sandstones, wackes and peiites
		variegated peiites, minor siltites and fine grained sandstones
C D C	Jacaré	sillites
	Lagarto- PaTmares	mudstones, siltstones, sandstones, wackes USM3
C D C	Acauã-/ Jacoca >	U^-, I '—'—' interbedded limestones, peiites siltites and fine sandstones
		limestones, dolomites LCMS
C D C	Ribeirópolis	<i>m</i> peiites, pebbly peiites and volcanics
	Juetê- Itabaiana	feldspathic arenites, and interbedded arkosic sandstones, mudstones LSMS
C D C	Crystalline / basement v	**1 bridely reworked basement during extension
		amphibolite laces gneisses and oilhogneisses

Figure 6.5 - Evolution of the basin and sedimentary infill. A and B show respectively the deposition of the Lagarto and Vaza Barris Groups (Cycle II). The megasequence boundaries of Figure 6.3 are indicated in the legend.

A linked listric detachment (simple shear model) is favoured because:

1. The thicknesses of most of the sequences increases to the north away from the era ton.
2. The Palestina diamictites are deposited in a long lived trough - Vaza Barris trough.
3. Extensional fault activity is indicated by the presence of large polyolithic clasts of both basement and cover sediments in the succession (cf. Ribcirópolis pebbly phyllites and also Palestina Formation diamictites adjacent to the Simão Dias and Mocambo faults). These indicate uplift and erosion of footwall blocks (and possibly hangingwall blocks) at two periods during the evolution of the basin.
4. The lack of multiple wedge shaped sedimentary sequences within the succession. These would be produced if extension on the basin margin dominantly occurred by an array of domino style faults.

Although other fault styles have been proposed for extensional sedimentary basins (e.g. domino-style faults Barr 1987; Davison 1989; and flexural cantilever models - Kuszniir et al. 1991; Roberts & Yielding 1991) a listric detachment style similar to that proposed for extending continental margins (e.g. Lister et al. 1986) or for the Rhine Graben (Brun et al. 1991) appear to be the most appropriate to explain the original architecture of the southern part of the Sergipano Basin (keeping in mind the difficulties in determining thickness variations obscured by the strong tectonic overprint).

The Model

The model for the evolution of the Itabaiana Dome Area is depicted in Figures 6.4 for the first cycle and Figure 6.5 for the second major depositional cycle.

Cycle 1 Evolution of the lower siliciclastic megasequence.

Deposition of the lower siliciclastic megasequence was synchronous with the development of extensional faulting on a listric detachment that dipped northwards at the craton margin (Fig. 6.4 A), Shallow marine arkosic sandstones with intercalated mudstones of the Itabaiana Formation were deposited at this time. Active extensional faulting is evidenced by local conglomerates and diamictites together with thickness variations of 20:1 across the Itaporanga and Simão Dias faults. The sequence fines upwards into the Ribcirópolis Formation, with continued extension indicated by the Ribcirópolis diamictites.

The Itabaiana dome and also probably the Simão Dias dome evolved as paleohighs (Fig. 6.4 B) at this time with the development of shallow water environments that ultimately lead to the deposition of the Jacoca carbonates (first carbonate megasequence). This extension probably caused progressive uplift of the Itabaiana dome, as part of a rollover anticline. The Mocambo fault is interpreted to have been active at this stage (Fig. 6.3 B).

The model accounts for the local conglomeratic fades within the upper Itabaiana quartzites and in the lower Ribeirópolis Formation (western and eastern sides of the

Itabaiana dome - 150m of Jacarecica diamictites (here in the Ribeirópolis Formation) with 1.2m size clasts of basement, in the north-northeastern border of the Itabaiana dome (Humphrey & Allard 1969), and accounts for the thinning of the Ribeirópolis Formation towards the dome, together with the voluminous Ribeirópolis phyllites to the north of the Mocambo fault, an area that also contain a significant amount of pebbly phyllites, diamictites and volcanics.

Cycle I Lower carbonate megasequence.

This phase of extension was probably followed by a period of thermally driven subsidence, leading to the development of the the Acauã and Jacoca Formations around the Itabaiana dome (Fig. 6.4 C).

Cycle II Evolution of the upper siliciclastic megasequence.

The second major sedimentary cycle records the onset of a second -phase of rifting that begins with the deposition of the Lagarto Group and records the greatest activity during deposition of the Palestina diamictites (Fig. 6.5 A). The Vaza Barris trough probably developed as a ramp syncline during this period and was the major depocentre in the area. The Lagarto Group likely reflects the development of a progradational delta system from the craton, to the south, onto the craton margins (section 3.7).

Cycle II Upper carbonate megasequence.

A second phase of thermal subsidence is postulated to account for the development of the widespread carbonate platform of the Olhos D'agua sequence (Fig. 6.5 B). This may be interpreted as a post-rift sequence that infills the basin and onlaps onto the craton margins.

The basin model outlined above shows many similarities to those proposed for other Proterozoic basins developed on craton margins elsewhere in the world. The Mid- to Late Proterozoic of the Purcell and Windermere Supergroups, in the western Cordillera of North America, shows similar cycles of extensional fault controlled sedimentation passing upwards into shallowing upwards carbonate sequences (Pope 1989). The Adelaidian of South Australia also shows a similar stratigraphic record (Preiss 1987).

6.2.5 - Structural and metamorphic evolution of the Itabaiana Dome Area

Structural evolution

Detailed mapping and structural analysis has shown that the metasediments of the Itabaiana Dome Area underwent three phases of ductile to ductile-brittle deformation (Chapter 4) during the Brasiliano orogeny. The dominant structures are southwest vergent recumbent F₁ folds (probably nappes) and southwest vergent more upright F₂

folds and high angle thrust faults with oblique slip (Fig. 6.1). D_j structures are crenulation and kink folds which are associated with sinistral movement along the major fault structures such as the Simão Dias and Itaporanga faults (Fig. 6.1).

The basement gneiss domes had undergone a history of high grade amphibolite facies deformation and tmetamorphism (section 4.2.1) prior to the D_1 to D_3 Brasiliano deformations which are the focus of this study. D_1 , D_2 and D_3 deformations affected both the gneissic basement domes and their cover of metasediments (section 4.9).

D_j to D_3 deformations are interpreted as a progressive polyphase deformation as the Sergipano Basin underwent contraction with tectonic transport onto the São Francisco Craton, from NNE to SSW. A summary of the structural elements is given in Figure 6.6 and a detailed structural synopsis is given in Chapter 4.

D₁ Deformation

D_1 is interpreted as a progressive event of SSW directed layer-parallel shearing and shortening, responsible for the pervasive subhorizontal S_1 foliation, shearing of the basement-cover contact, and development of rootless intrafolial F_1 folds, and for the outcrop scale low-angle thrusting (Fig. 6.6). The best exposure of D_j structures is in the Capitão farm outcrop (Fig. 4.24) - additional evidence comes from outside the Itabaiana Dome Area (e.g. Santos et al. 1988; Jardim de Sá et al. 1986). Map-scale stratigraphic repetitions are interpreted as F_1 recumbent folds, probably nappes (Fig. 6.1).

D₂ Deformation

D_2 deformation records a progressive NNE to SSW shortening by nearly upright folding and high-angle south vergent thrusting. Penetrative S_2 foliations are developed together with an L_2 lineation and stretching fabric parallel to the strike of the orogen (section 4.9). The regional faults appear to be zones of high strain concentration. Deformed clasts within the Palestina Formation indicate a prolate finite strain ellipsoid (section 4.4.4), which together with syn- D_2 deformed veins (section 4.4.5) are indicative of orogen parallel extension - a common feature observed in many contractional/collisional orogens and probably indicative of a transpressive tectonic regime with a component of orogen-parallel strike-slip movement (e.g. Ellis & Watkinson 1987).

Because D_2 probably occurred under various degrees of shortening with top to the south shearing along strike, the F_2 folds may be expected to have curved hinges on a regional scale and thus may account for the double plunge of L_2 in the Itabaiana Dome Area (section 4.4.1). The Itaporanga fault is interpreted to be the sole thrust or basal detachment for this phase of deformation (Figs. 4.22 A & B).

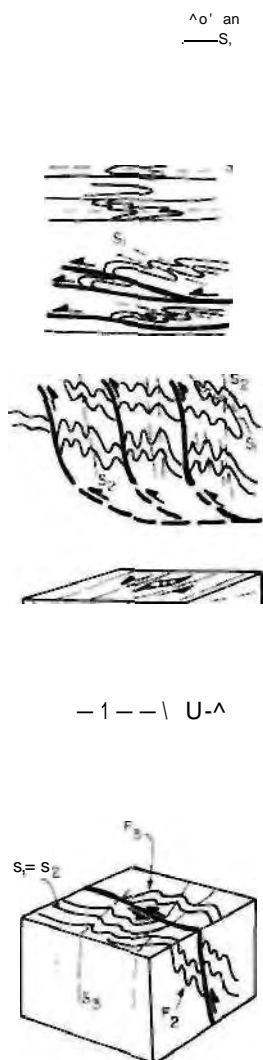
D₃ Deformation

D_3 is a non penetrative kinking, crenulation folding and strike-slip event that is interpreted to be a consequence of the strike-slip movement along the major faults (section 4.9). A differential degree of slip along the pre-existing S surfaces (e.g. S_2 , S_1 , S_Q and S_n) during D_j may account for the fan of L_3 directions throughout the map area (section 4.5 & Fig. 4.17).

EVENT

STRUCTURES

SUMMARY DESCRIPTION OF THE MOST RELEVANT STRUCTURAL FEATURES



S₁ - Penetrative, layer-parallel foliation defined by the preferred orientation of sericite (muscovite), chlorite, biotite, lenticular and discoidal quartz and feldspars. Particularly in the crystalline basement rocks, hornblende may be found along S₁, and is normally transformed to epidote.

F₁ - Intrafolial, generally rootless, cm- to m-scale recumbent folds, associated with a penetrative S₁ foliation and a L_{1,0} intersection lineation.

F₂ - m- to km-scale recumbent folds associated with a penetrative S₁ foliation and with sub-horizontal thrusts propagated through the overturned and thinned limbs.

F₃ - Up to km-scale, open to tight, steeply inclined to upright folds that coaxially fold F₁ and S₁. They are associated with a penetrative S₂ foliation (slaty, pressure solution and crenulation cleavage) and with high-angle thrust faults which show a top to the south and a E-W, sinistral, strike-slip movement.

L1.2 - Penetrative S₁/S₂ intersection lineation parallel to the fold axis and to an elongation lineation (L_s) defined by elongated strain markers such as clasts, porphyroclasts, resistant minerals, oolites and pellets. In the Palestina diamictites the strain markers indicate a top to the south and a E-W and horizontal inter-foliation slip.

F₃ - mm- to m-scale, transversal, open to tight and upright folds, crenulations and kinks which affect S₂ (and older planar features) and are associated with a strong cleavage (S₃). F₃ are sub-horizontal to sub-vertical folds, depending upon the original attitude of the affected planar features, particularly S₁ or S₂. The sub-vertical folds may be associated with local strike-slip faults parallel to the sub-vertical S₂WS.

Figure 6.6 - Summary of the structural and metamorphism data in the Itabaiana Dome Area.

METAMORPHISM	STRAIN SIGNIFICANCE AND TECTONIC REGIME
<p>Sericite, chlorite, biotite, quartz, and feldspar along S₁, (in the basement also some hornblende transformed to epidote). Upper to medium greenschist facies.</p>	<p>Layer-parallel shearing and shortening responsible for SSW directed recumbent folding and sub-horizontal thrusting, developed during a progressive, ductile regime. Implied in the duplication of the stratigraphy and crustal thickening.</p>
<p>Sericite, chlorite, biotite, quartz, and feldspar along S₂. Medium to low- and sub-greenschist facies.</p>	<p>Orogen-perpendicular shortening, by folding and thrusting, and also an orogen-parallel elongation by inter-foliation slip and sinistral strike-slip fault movements. Responsible for crustal shortening and thickening under a ductile transpressive regime.</p>
<p>Local pressure solution along S₃. No associated metamorphism.</p>	<p>Orogen-parallel event of compression and extension, developed at no-metamorphic conditions and interpreted as associated with the late-stage D₂ inter-foliation slip, developed in a progressive deformation, under ductile to brittle-ductile conditions.</p>

EXTRAMORPHIC AND
TELEPHONIC

v-mn

fita

EXTRAMORPHIC AND
TELEPHONIC

i&BSm

EXTRAMORPHIC AND
TELEPHONIC

EXTRAMORPHIC AND
TELEPHONIC

£51

S li»
•III! f

12 III!
li ti
i! s
s?
if li & i

S
tf I If
ij il



r.

O

Evolution of the basement gneiss domes

The presence of basement gneiss domes in the southern part of the Sergipano Fold Belt has important tectonic implications. The origins of basement gneiss domes within orogenic belts have been the subject of considerable debate (Hanks & Wallace 1990). Models for their evolution include - domes produced by fold interference (e.g. Ramsay 1967), diapirism (e.g. Ramberg 1981; Coward 1981b; Brun 1983; Windley 1984), basement cored fold nappes (e.g. Holdsworth 1989; Davis et al. 1991; Brown et al. 1991) or as basement cored anticlines (Murphy 1990). In some instances the presence of extensional shear zones along the margins of the gneiss complexes has led to their interpretation as metamorphic core complexes produced by extensional exhumation and thinning of the contractional orogen (e.g. Coney & Harms 1984; Davis & Lister 1988; Lister & Davis 1989; Malavieille & Taboada 1991).

In the Itabaiana Dome Area the metamorphic grade and the presence of both D₁ and D₂ structural elements in the gneisses (Chapter 4) implies that they are involved in the thrusting and that the basal detachment for the contractional deformation was therefore within the gneisses. The distribution of sediments together with facies and thickness changes around the gneiss domes (see section 6.2.3 above) indicates that they evolved as paleohighs during sedimentation. The extensional fault model proposed for basin formation (Figs. 6.4 & 6.5) can therefore also account for the structural position of the gneiss domes in the fold belt as the result of contractional reactivation of extensional faults bounding basement fault slices.

The contact relationships between the gneiss domes and their metasedimentary cover, however, warrant further discussion. As described in section 3.3.2, the gneiss domes exhibit both unconformity and sheared contacts with the metasedimentary cover. In particular the western flank of the Itabaiana dome contains the prominent Macambira phyllonites which indicate a top down to the west extensional event (section 3.3.2).

Humphrey & Allard (1969) interpreted the phyllonites as an older deformation of the crystalline basement, and that the extensional fabrics were possibly related to the Brasiliano age evolution of the dome. Although their conclusion was based upon the apparently discordant trends of the phyllonites with respect to the basal unconformity, and upon folds and extensional fabrics affecting both the phyllonites and Itabaiana quartzites (section 3.3.2), they did not present conclusive evidence that the Macambira phyllonites are older than the basal unconformity (this was confirmed in a written communication with Professor Gilles Allard in 1992).

The phyllonites are considered here a syn-D₂ extensional structure (to date no phyllonite clasts have not been described in the cover metasediments) and have been affected by F₂ folds together with the extensional fabrics and Itabaiana quartzites, as result of a progressive deformation.

Figure 6.7 summarises in a diagrammatic way the evolution of the Itabaiana dome. A combination of differential uplift of the dome, folding and thrusting during D₂ deformation and a syn-D₂ transpression E-W trending squeezing out of the ductile basement, offers a feasible explanation for the progressive development of a ductile shear zone sub-parallel to the basal unconformity in the western side of the dome (the

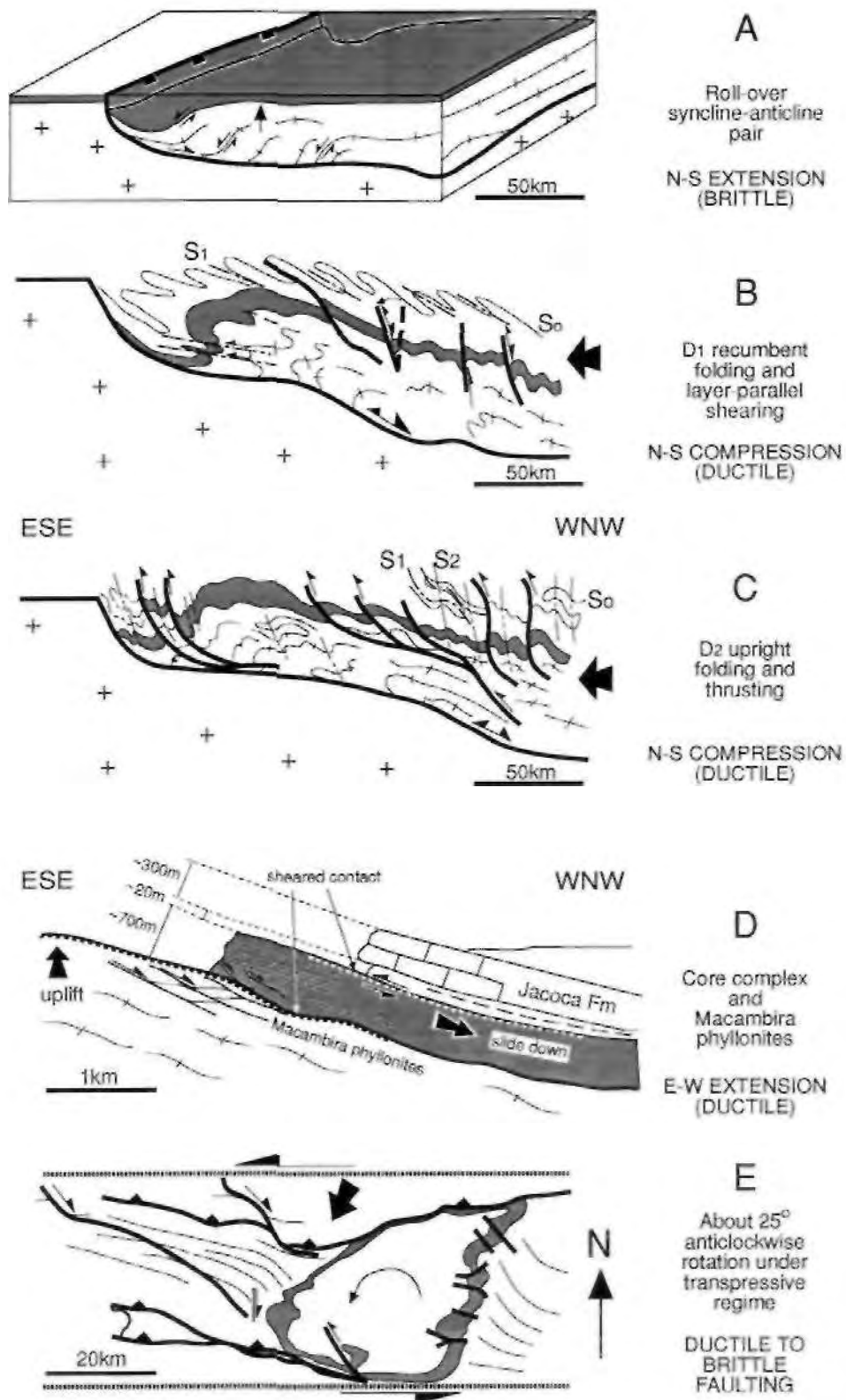


Figure 6.7 - (A-E) Evolution of the Itabaiana dome. The Itabaiana quartzites are shown in dark grey. All the scales are approximate.

Macambira phyllonites), and for the progressive top down to the west movement responsible for the extensional shear bands affecting the phyllonites. During late D₂ deformation the dome probably underwent bulk rotation bounded by the major fault zones (Fig. 6.7 E). The rotation accounts for the particular NNW-SSE orientation of S₂ and L₂ in the eastern and western structural domains (section 4.6.4 & Fig. 4.2) which is not satisfactorily explained by simple stress refraction around a relatively rigid gneiss dome.

The Simão Dias dome probably evolved as a series of basement slices bounded by listric extensional faults (Figs. 6.5 D & E), which were subsequently folded and uplifted during the positive inversion.

Metamorphic evolution

The mineral assemblages and textural relationships (section 4.8) in the Itabaiana Dome Area indicate that the Brasiliano deformation and metamorphism occurred under greenschist facies conditions. The basement gneisses appear to have been retrogressed from amphibolite facies and now display amphibole-epidote-chlorite assemblages. The metasediments generally display greenschist facies assemblages with the development of chlorite in suitable lithologies.

The carbonates and siliciclastics of the Itabaiana Dome Area do not lend themselves to detailed PTt studies (of. England & Thompson 1984; Thompson & England 1984) at greenschist facies and in particular because of the lack of age determinations in this area. In addition there is a distinct lack of porphyroblast development necessary for such studies in polydeformed terranes (Vernon 1989).

Metamorphic conditions appear to range from sub-greenschist facies in the cratonic domain to greenschist facies in the metasediments and greenschist facies retrogression in the basement gneisses (section 4.8 & Fig. 6.6). Textural relationships indicate that the greenschist facies conditions persisted for deformation phases D₁ and D₂ whereas D₃ appears to be post peak of metamorphism.

6.3 - Tectonic evolution of the southern part of the Sergipano Fold Belt and of the whole Sergipano Fold Belt

6.3.1 - Introduction

In this section are discussed the implications of this research on the Itabaiana Dome Area for the southern part of Sergipano Fold Belt and for the fold belt as a whole. Particular emphasis is placed on the significance of the new stratigraphic interpretations and the structural interpretations. The first part of the discussion is focused upon stratigraphic and structural correlations between the Itabaiana Dome Area and the Carira area to the north.

Figure 6.8 is a geological map of the Itabaiana-Carira area, east of the 38 °W meridian and between the southern and northern parts of the Sergipano Fold Belt. The two parts of the belt are separated by the São Miguel do Aleixo and Dores faults. The

L E G E N D

Vaza Barris Group

Olhos D'água Fm
metacarbonates, and mixed
metacarbonates and
metapelites

Palestina Fm
diamictites and
pebbly phyllites

Lagarto Group

Frei Paulo Fm
variegated and silty
phyllites

FP1 - calcite-cement
metasandstones, phyllites,
and minor metacarbonates

FP3 - quartz-sericite phyllites,
thinly interbedded black shales,
black phyllites, metasilites,
calcilutites and pebbly phyllites

Jacaré Fm
metasilites

Lagarto-Paimares Fm
fine- to medium-grained
sandstones and wackes

Miaba Group

Jacoca Fm
metacarbonates, and mixed
metacarbonates and
metapelites

Ribeirão Fm
silty phyllites, pebbly
phyllites, greywackes,
and metavolcanics

Itabaiana Fm
quartzites (conglomerates)
and interbedded quartzites,
metasandstones and phyllites

Crystalline basement
amphibolite facies gneisses and
orthogneisses (retrometamorphosed
to the greenschist facies)

Macururé Group

Granites

Macururé metasediments
biotite-garnet schists, quartzites (mylonitic)
marbles, phyllites, slates, intercalated phyllites
and metasilites, melagreywackes,
chlorite-quartz schists (mylonitic),
metavolcanics, and staurolite-garnet schists

PA = Paripiranga anticline, JF = Jacaré fault, IF = Itaporanga fault, VBF = Vaza Barris fault, MF = Mocambo fault, MS = Mocambo shear, SDF = Simão Dias fault, EF = Escarpa fault, PF = Pelada fault, and RF = Ribeirão fault

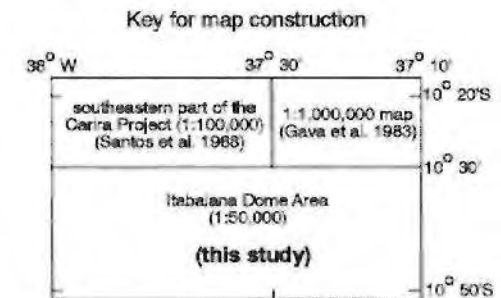
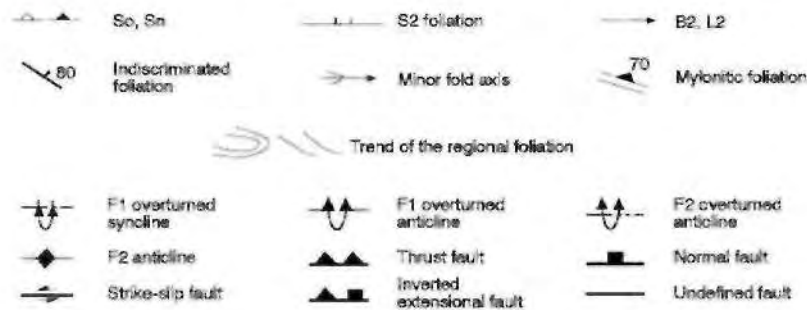
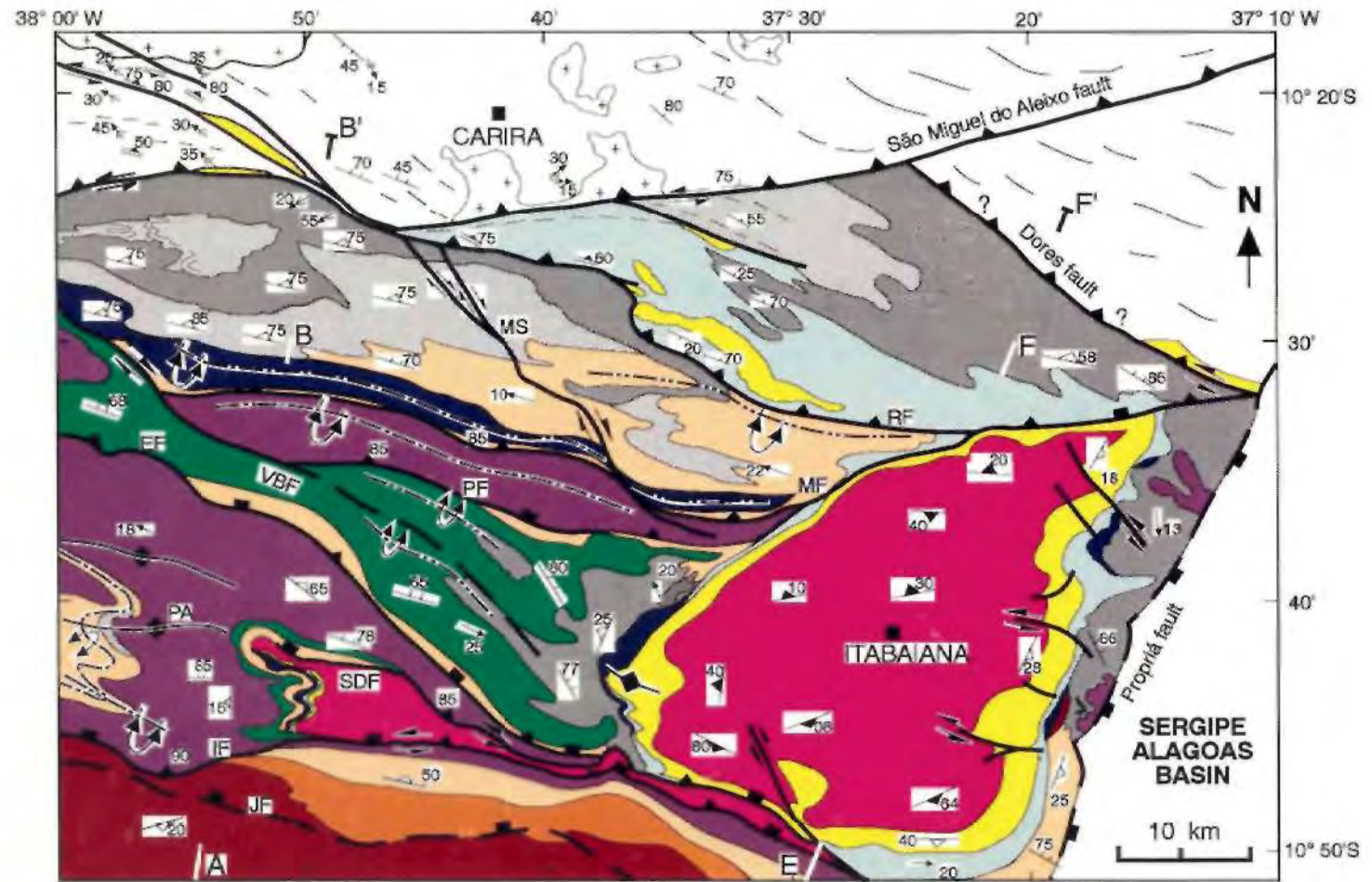


Figure 6.8 (next page) - Geological map of the southern part of the Sergipano Fold Belt, to the east of the 38°W meridian, not considering the Tertiary and Quaternary covers.



Closer to this dome, the carbonate layers of the Jacoca Formation to the north of the Mocambo fault are normally 10-100cm thick, and the siliciclastic fraction consists of meta-argillites, variegated phyllites and dark grey to black phyllites, with subordinate layers of metasiltites and fine grained metasediments (section 3.3.3). Far from the Itabaiana Dome Area, Santos et al. (1988) described the continuation of the Jacoca carbonates (their P₂ lithofacies) as interbedded metasiltites, fine-grained sandstones, together with <10cm-thick layers of metacarbonates and marls. They also described parallel stratifications and small-scale wavy-reworked structures, and interpreted this lithofacies as proximal rhythmites.

This feature can be associated with sandy input from the north-northwest of the Vaza Barris trough, since before the deposition of the Frei Paulo Formation (it is accepted that carbonate sedimentation dies with increasing siliciclastic supply - Sellwood 1986; Hanselman et al. 1974; Grotzinger 1989).

3. The Ribcioropolis Formation mapped to the north of the Itabaiana dome (section 3.3.4) now encompasses the pebbly phyllites, phyllites, metagreywackes, diamictites and metavolcanics which were mapped by Santos et al. (1988) to the south of the São Miguel do Aleixo fault (Fig. 6.8), and interpreted as part of the Capitão-Palestina Formation. Their position relative to the structure is also in agreement with this revised correlation.

4. The lenses of quartzite mapped as the Capitão-Palestina Formation by Santos et al. (1988) are here interpreted to be part of the Itabaiana Formation (Fig. 6.8) as these units are laterally continuous with the Itabaiana Formation mapped in the Redonda and Campina ranges (Fig. 3.1). In the hangingwall of the Dores fault lenses of Itabaiana quartzites have been emplaced riding on slices of basement derived phyllonites thus lending additional weight to this correlation.

6.3.3 - Structure of the southern part of the Sergipano Fold Belt

The structural cross-sections across the southern part of the Sergipano Fold Belt (Fig. 6.9) were constructed using the same style as that for the sections through the Itabaiana Dome Area (Figs. 4.20 & 4.21). The fold pattern of large-scale F₁ folds co-axially refolded by F₂ folds form a classical type 3 interference pattern (Ramsay 1967), disrupted and uplifted by high-angle thrust faults.

The three recumbent F₁ folds in the Itabaiana Dome Area (Figs. 6.8 & 6.9 A) account for the stratigraphic repetition of the Frei Paulo Formation to the west of the Simão Dias dome (section 3.3.3). These folds have 30km of amplitude and may be nappes associated with subhorizontal thrusts - as those described elsewhere in the southern part of the Sergipano Fold Belt (Jardim de Sá et al. 1986; Brito Neves et al. 1987; Campos Neto & Brito Neves 1987).

6.3.4 - Structural and lithostratigraphic interpretations

The structural interpretation above is consistent with the small scale structures observed in the Capitão farm outcrop (Fig. 4.24) and the F₁ fold which repeats the stratigraphy to the west of the Simão Dias dome agrees with the strong layer-parallel S₁

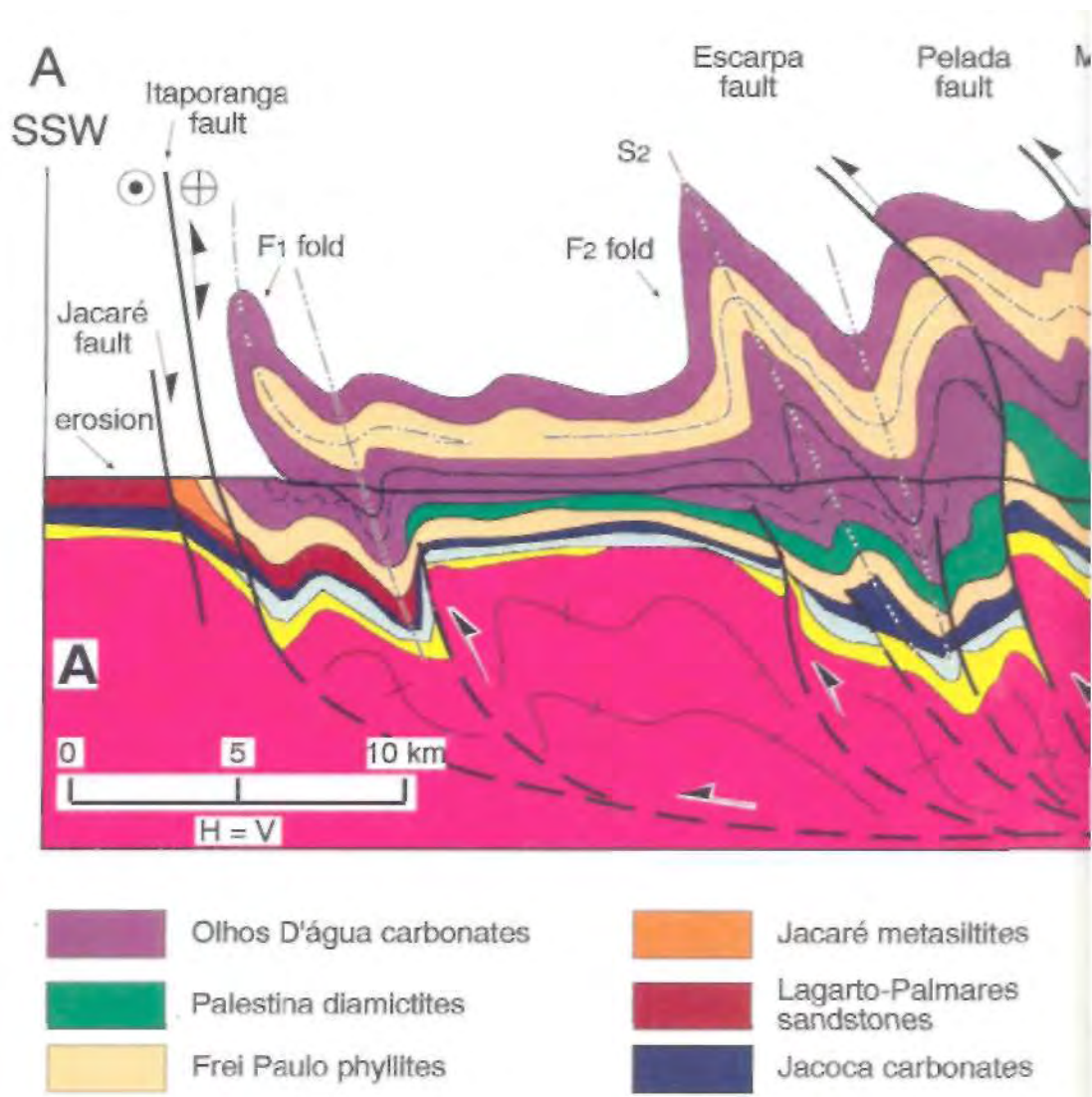
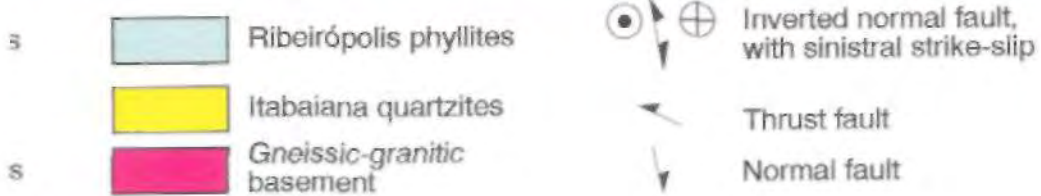
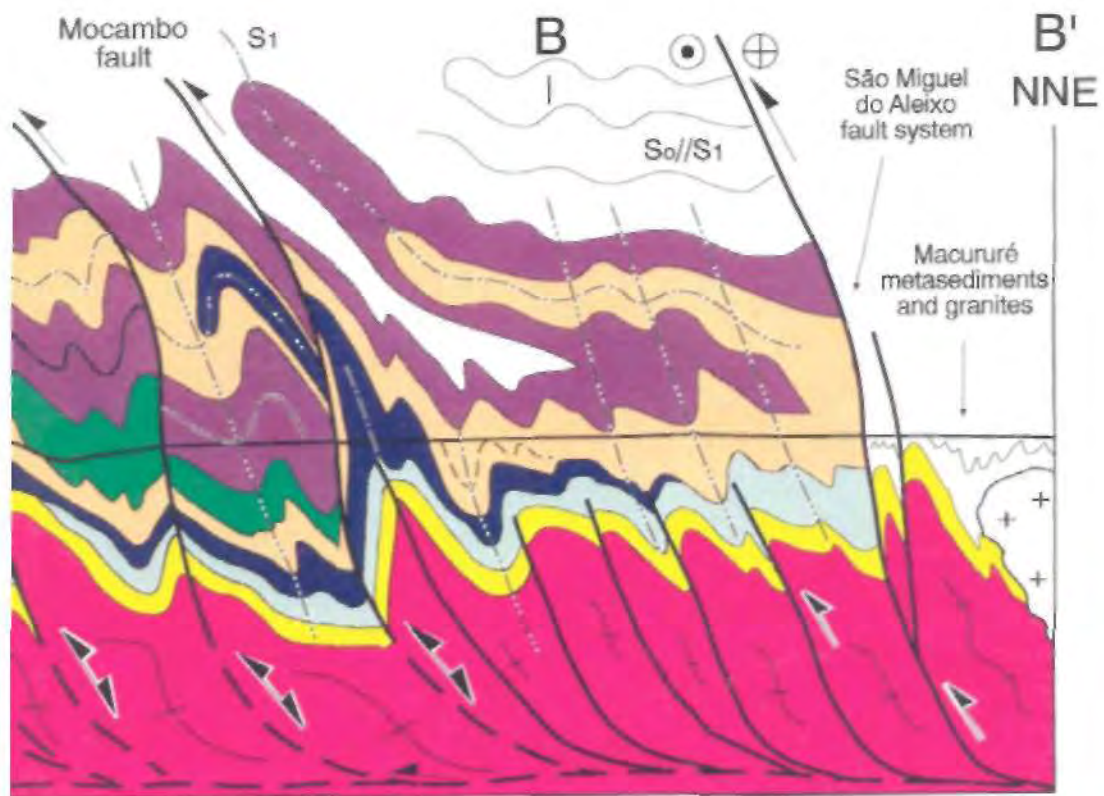


Figure 6.9 - (A-B) Schematic structural cross sections across domains. **A** - cross section along the ABB' section line of Fimiguel do Aleixo fault are projected from nearby data



s across the boundary between the southern and northern of Figure 6.8. The quartzites in the hangingwall of the São data on the geological map of Figure 6.8 (continued).

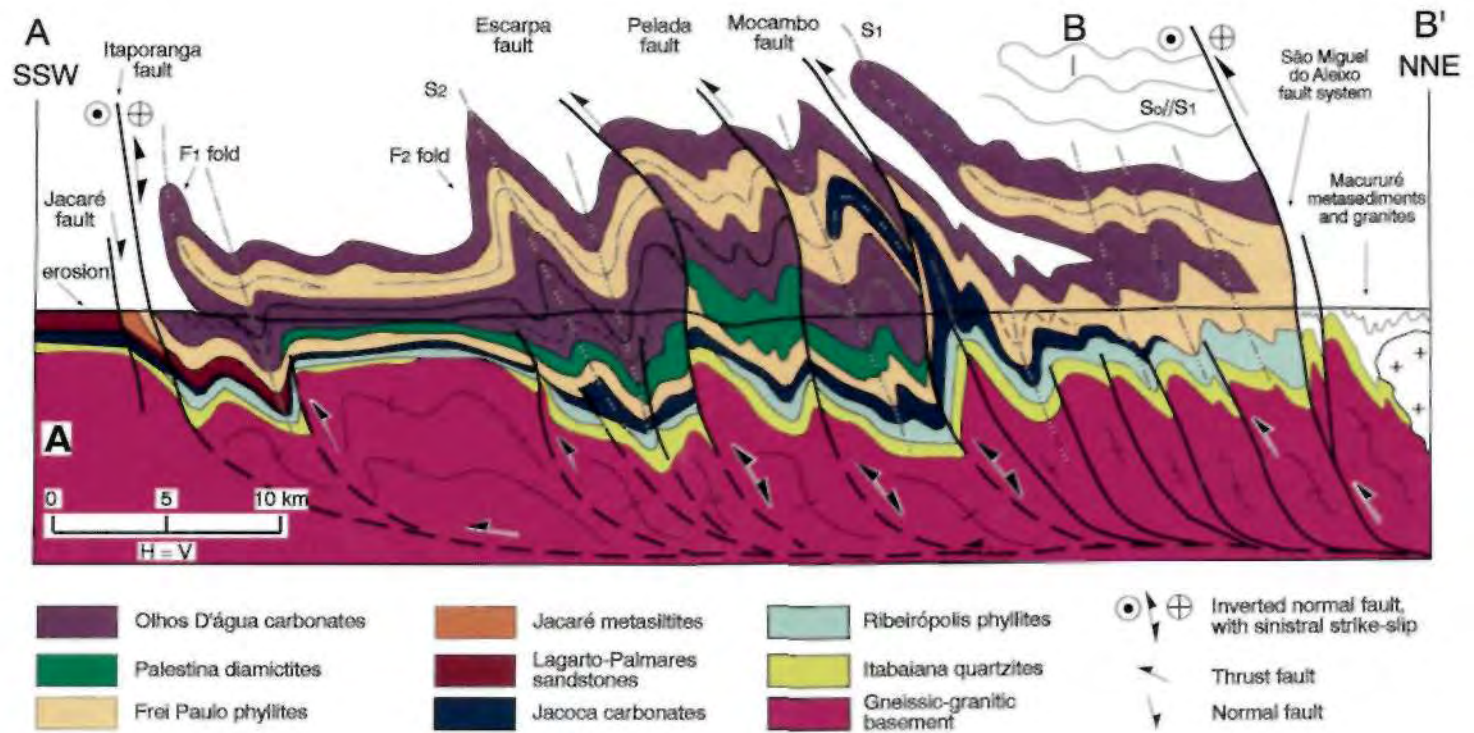


Figure 6.9 - (A-B) Schematic structural cross sections across the boundary between the southern and northern domains. A - cross section along the ABB' section line of Figure 6.8. The quartzites in the hangingwall of the São Miguel do Aleixo fault are projected from nearby data on the geological map of Figure 6.8 (continued).

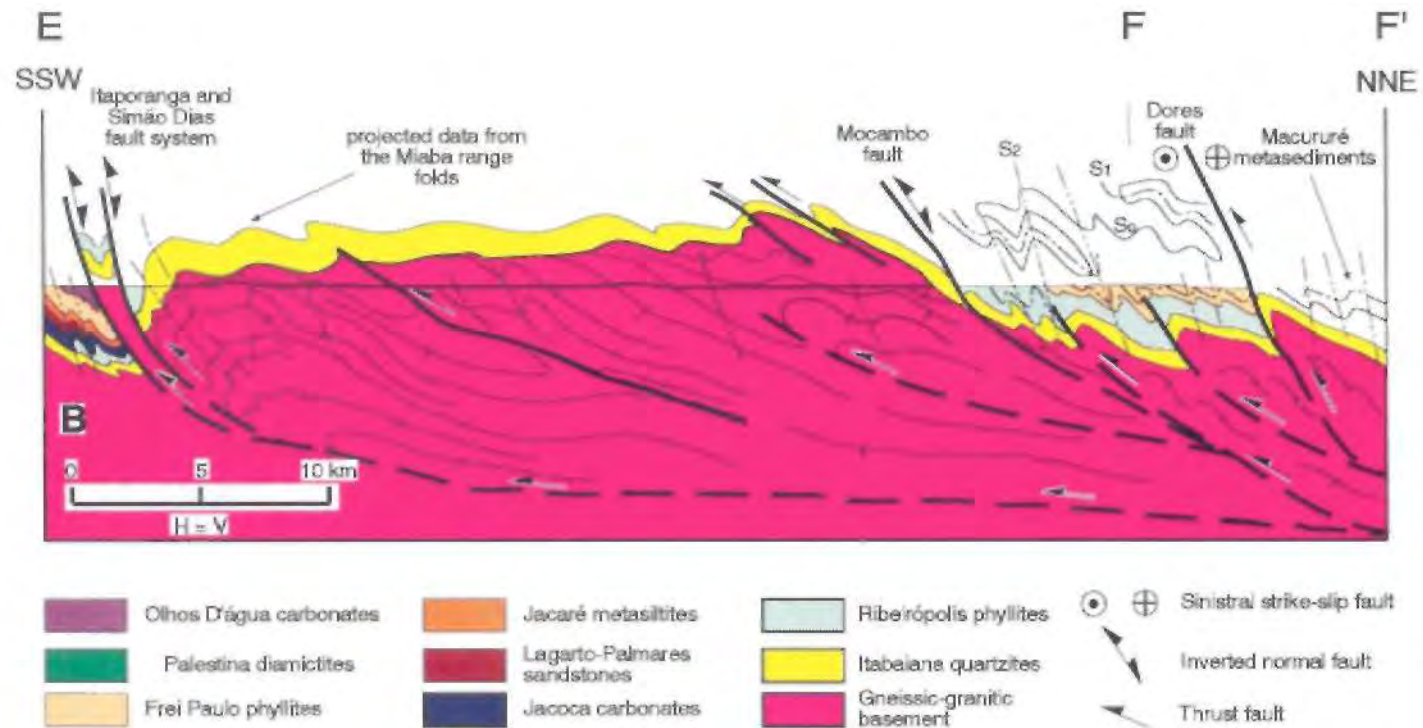


Figure 6.9 - B - Schematic vertical cross section along the EFF' section line of Figure 6.6. The quartzites and the crystalline basement closer to the surface, in the hangingwall of the Dorés fault are projected from data observed in the northeastern corner of the Itabaiana dome area.

fabric described in the Frei Paulo sandy phyllites of that area (section 4.3). Although no structural field evidence has been found as yet for the two F_1 folds to the north of the Pelada fault (Fig. 6.8) such an interpretation combines the stratigraphic repetition to the west of the Simão Dias dome with the lithostratigraphic interpretations to the north of the Mocambo fault, as illustrated in Figure 6.10.

The concept is that the F_1 recumbent folds (possibly associated with low-angle thrusts, as they appear in the Capitão farm outcrop, Fig. 4.24) nucleated in the northern part of the area, near the future Mocambo thrust (Figs. 6.10 A & B). The thick Olhos D'água carbonates may have acted as a barrier to the southward tectonic transport during D_1 , and were folded along all of the northern border of the Vaza Barris trough, which was possibly an important structural discontinuity during basin inversion.

As a consequence of this recumbent folding and/or thrusting, the Frei Paulo sandy phyllites of the northern part of the Vaza Barris trough were thinned and disrupted, being displaced from their northern position toward the western side of the Simão Dias dome.

During the D_2 deformation (Fig. 6.10 C), the subhorizontal F_1 overthickened hinges in the Jacoca and Olhos D'água Formations to the north of the trough, possibly also acted as barriers to the deformation, and were progressively rotated to subvertical positions. With the progressive shortening, the already thinned Frei Paulo phyllites were compressed within the two carbonate hinges, and probably acted as the detachment level for the Mocambo thrust.

6.3.5 - Lithostructural continuity in the Sergipano Fold Belt

This research presents strong evidence for lithological and subdural correlation between the southern and northern pans of the Sergipano Fold Belt, across the Dores and São Miguel do Aleixo faults (Fig. 6.8).

The lithological evidence is provided by the Itabaiana quartzites and slices of basement in the hangingwall of the Dores thrust fault (Fig. 6.8) and by their geophysical continuity with the Itabaiana gneisses (domain A, Fig. 5.3). In fact, as the Macururé Group consists of quartzites (and mantled gneissic domes), mylonitic quartzites, metacarbonates, phyllites, metasillites, metagreywackes, biotite- and staurolite-gamet schists, chlorite-quartz schists, and intermediary metavolcanics (Silva Filho et al. 1978 a & b; Santos et al. 1988), it compares well with the Miaba and part of the Lagarto Group (if the latter were metamorphosed at higher grade and intruded by granites).

This is supported by the fact that the interpretations in the structural cross sections of the southern part of the belt (AB and EF, Figs. 6.8 & 6.9) can be extended across the São Miguel do Aleixo and Dores faults (ABB' and EFF'). The depth of the basement in the hangingwall of the São Miguel do Aleixo fault (Fig. 6.9 A) is supported by geophysical data (section ZZ'Z", Fig. 5.8). The depth of the crystalline basement in the hangingwall of the Dores fault (Fig. 6.9 B) is supported by field and geophysical data (sections 4.4.4 & 5.3).

If the F_1 recumbent folds interpreted for the Itabaiana Dome Area (Figs. 6.9 A & B) are in continuity with the F_1 nappe structures described elsewhere in the Macururé

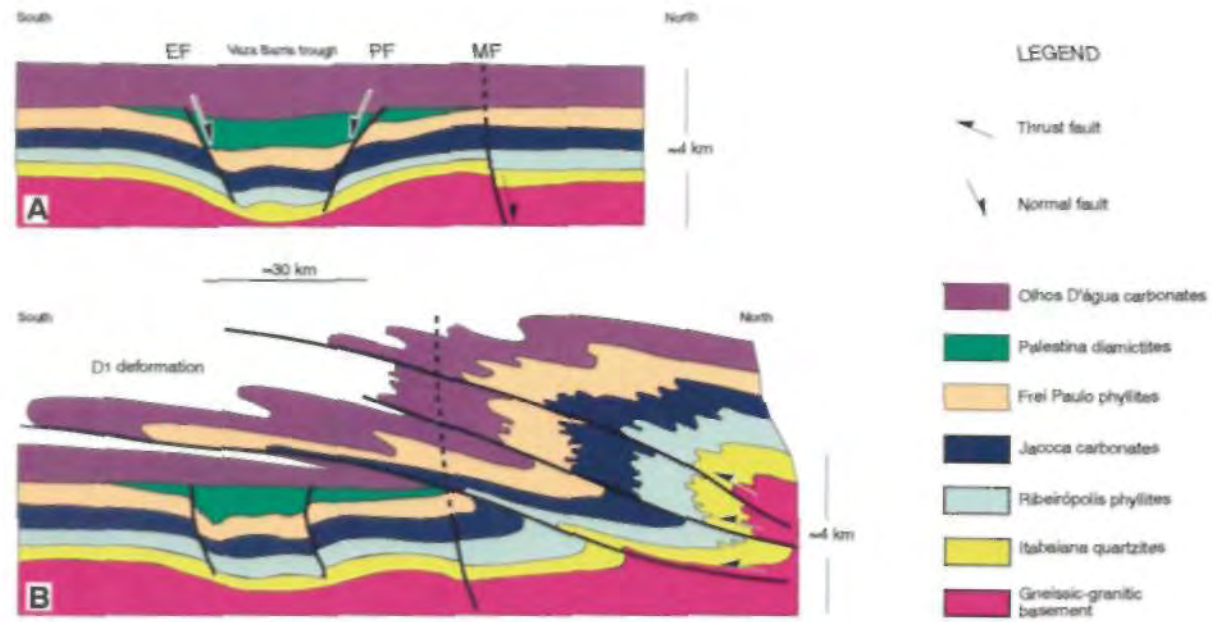


Figure 6.10 (A-C) - Structural and stratigraphic interpretations. A is a diagrammatic representation of the formations in the vicinity of the Vaza Barris trough, between the Escarpa (EF), Pelada (PF) and Mocambo (MF) faults. B is a diagrammatic representation of the F1 folds and low-angle thrusts emplaced above the trough (continued).

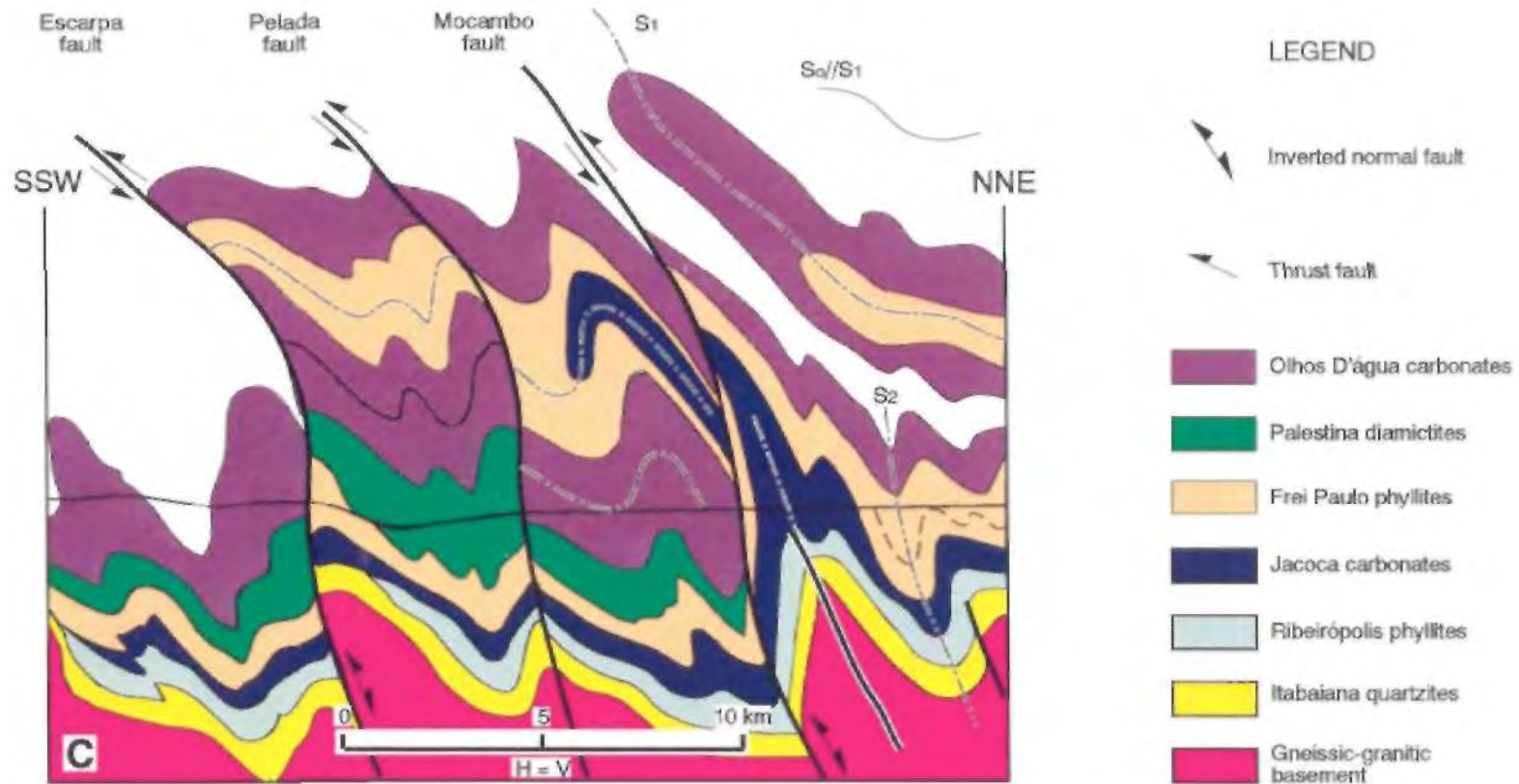


Figure 6.10 - C - Detail of the structural cross section ABB' of Figure 6.8 A, to show the relationships between the Mocambo fault and the interpreted hinge zones of the F1 folds.

Domain (Figs. 2.6 A, B, D & E), the core of the F₁ folds currently outcropping in the Macururé Domain must consist of Miaba- and Lagarto Group-equivalent metasediments, lending support to the lithological continuity discussed above. Thus, the F₁ structures across the domain boundary would form a 10km-thick pile of folded and thrust metasediments above the granites of the Macururé Domain (Fig. 6.9 A), which is in accordance with the interpreted depth of granite intrusion (Giuliani & Santos 1988).

6.3.6 - Tectonic evolution of the Sergipano Fold Belt

The results of this research combined with data from the literature permit the development of a model for the tectonic evolution of the Sergipano Fold Belt. Such a model must account for the basin development (e.g. section 6.2.4 above), the structural development of the fold belt and to relate this to the regional tectonics of the São Francisco Craton.

Tectonic Domains

Three tectonic domains have been recognised in the Sergipano Fold Belt (Fig. 6.11). From south to north these are - the Estância Domain (cratonic), the Miaba/Vaza Barris Domain (southern part of the Sergipano Fold Belt - miogeocline), and the Macururé Domain (northern part of the Sergipano Fold Belt - the eugeocline and the hinterland of the orogen). The occurrence of mantled basement gneiss domes and basement derived migmatites in these domains (Fig. 6.11) indicates that the original sediments were deposited upon extended continental basement of the São Francisco Craton, which is also supported by geophysical data (Santos et al. 1988; Motta 1990), and is accepted in most of the literature of the area (Davison & Santos 1989).

However, the fault-bounded Canindé, Poço Redondo and Marancó Domains (Santos et al. 1988; Davison & Santos 1989) located to the north of the Macururé Domain (Fig. 6.11), can be associated with the evolution of a small oceanic basin, as will be discussed in section 6.4, therefore a collisional suture between the São Francisco Craton and the Pernambuco-Alagoas Massif is inferred to the south of the Canindé complex (Fig. 6.11).

The mafic and ultramafic Canindé complex (Silva Filho 1976) is a 8km thick sequence consisting of metabasites, meta-arkoses, quartzites, marbles and graphite phyllites, overlain by a major gabbroic-pyroxenitic unit. The complex is divided in four units having mostly a geochemistry of island arc-type volcanism (Blais et al. 1989, Bezerra et al. 1989,1990), but one particular unit has characteristics of intraplate basaltic magmatism (Oliveira & Tarney 1991).

The Marancó Domain comprises highly sheared, greenschist to amphibolite facies, metarhyolites and metadacites (80% of the surface), with minor meta-andesites, amphibolites, metapelites, volcanic-derived conglomerates and arkosic/lithic quartzites, metacarbonates, chloritites, and two concordant intrusive bodies of serpentinites. The Poço Redondo Domain consists of orthogneisses and paragneisses migmatized and injected by syn- and post-tectonic granites and granodiorites, and may represent reworked basement (Santos et al 1988; Davison & Santos 1989).

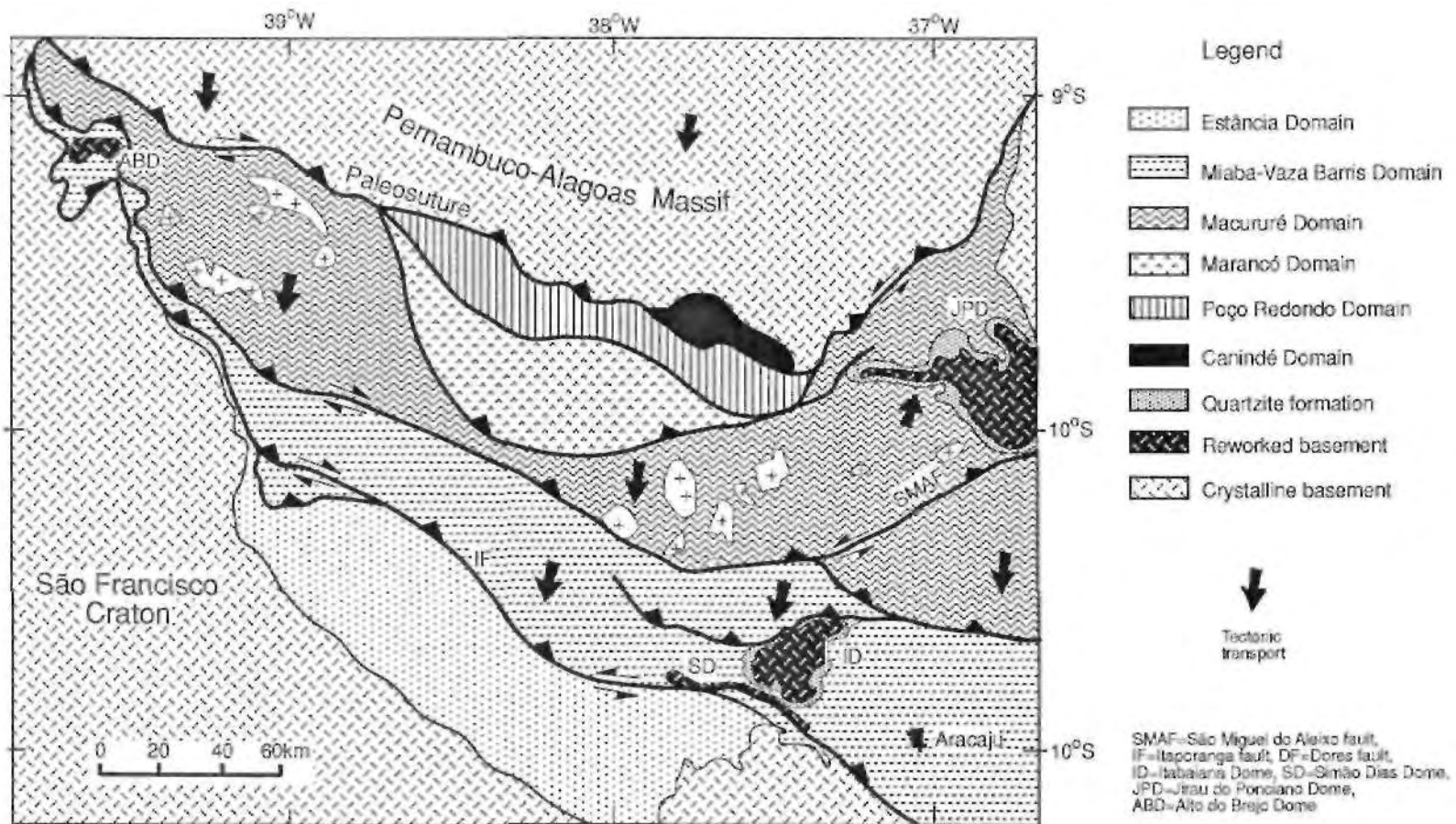


Figure 6.11 - Precambrian tectonic domains in the Sergipano Fold Belt. Just some granites of the Macururé Domain are shown.

Thrust belt and foreland basin models

The results of this research do not support the model of thrust belts and associated foreland basins (Beaumont 1981) which have been proposed for the mobile belt / fold belts around the São Francisco Craton (e.g. Pimentel et al. 1992). Such a model had been proposed and accepted for the origin of the Palmares sandstones (section 2.8 & Fig. 2.9).

The principal argument against this model is that the sediments on the craton are 900 Ma in age (Misi 1976) and are laterally continuous with the sediments that now form the Sergipano Fold Belt (Fig. 6.3). These strata are therefore clearly older than the Brasiliano deformation, hence cannot have been deposited in a foreland basin setting as deformation developed.

Moreover, the sedimentary characteristics of the Lagarto-Palmares sandstones (section 3.3.4 & Saes 1984) do not compare either with continental sedimentation described elsewhere ahead of thrust sheets (e.g. Gustavson 1974; Hirst & Nichols 1986; Nichols 1987) or ahead fault uplifted terranes (e.g. Wescott 1990, Wescott & Ethridge 1990). Similarly, the stratigraphic succession formed by the Lagarto and Vaza Barris Groups (Fig. 6.3) does not compare with the marine sedimentation developed in foreland basins due to accretion of terranes into a passive margin, as interpreted for example in the evolution of the Appalachians and Cordilleran basins of North America (Tankard 1986).

Tectonic model

A tectonic model for the southern part of Sergipano Fold Belt is depicted in Figure 6.10. Figure 6.10 A shows the inferred architecture prior to D₁ deformation whereby the Vaza Barris trough was the locus of deposition of the Palestina diamictites in a basin bounded by the Escarpa and Pelada faults. D₁ deformation was characterised by southward directed tectonic transport with the development of large recumbent fold nappes and possibly thrust out lower limbs (Fig. 6.10 B). The penetrative, flat-lying S₁ foliation in the metasediments was developed at this time. The recumbent folds (and thrusts?) probably evolved from the hinterland of the orogen, to the north of the Mocambo fault.

D₂ deformation (Fig. 6.10 C) is interpreted to have been part of the same south vergent progressive deformation, resulting in bulk shortening of the section, penetrative S₂ foliations and inversion of the original extensional faults, so that these thrusts link to the lower detachment (e.g. Fig. 6.9). The model indicates that the shortening and inversion along the Mocambo fault in the region of the Vaza Barris trough was greater than that in the vicinity of the Itabaiana dome (cf. sections in Fig. 6.9).

This interpretation is supported by the geophysical data (Figs. 5.6-5.8) which indicate that the crystalline basement increases in depth from west to east. Possibly because of the Itabaiana dome, the D₂ shortening was more intense across the Vaza Barris trough (note the narrowing of the outcropping area of the Palestina Formation between the Pelada and Escarpa faults. Fig. 6.8) and in consequence, the diamictites were possibly pushed out of the Vaza Barris trough (Fig. 6.10 A). Such situation, which

is expected in inverted crestal collapse grabens (McClay & Buchanan 1991), matches with the greater amount of inversion of the Mocambo fault in this area.

Strain measurements together with textural and fabric studies indicate that D_2 deformation was characterised by a sinistral strike-slip, transpressive regime (section 4.8). This oblique contractional deformation is interpreted to have been responsible for the rotation of the Itabaiana dome (Fig. 6.6) at this stage, with the basement dome acting as a resistant rigid object that deflected strain trajectories around it

The syn- D_2 transpressive regime in the Itabaiana Dome Area reinforces the interpretation that the Sergipano Fold Belt probably resulted from the accretion of terranes during an oblique collision (Davison 1987; Santos et al. 1988; Davison & Santos 1989). Actually, oblique collision and the resultant transpressive tectonic regimes are a common feature during the accretion of allochthonous terranes to cratonic margins (Howell 1989).

The lack of foreland basin sediments on the craton or within the frontal part of the Sergipano Fold Belt (i.e. clastic sediments derived from the fold belt rocks or in part from the craton (from the peripheral bulge) and undeformed by the Brasiliano orogeny) may be either a function of the present day erosion level, or a foreland basin may not have been developed at all.

A tectonic model that does not necessitate the development of a significant foreland basin (Fig. 6.12) involves an accretionary wedge developed whereby the D_1 - D_2 deformations built up a 10km-thick sequence on the attenuated cratonic margin (Fig. 6.12 A) and the loading in the inner parts of the belt was accompanied by downwarping of the attenuated crust (Figs 6.12 B & C), so that the accretionary wedge did not develop significant relief above sea level and the thrusts did not encroach onto the craton.

A similar argument was proposed by Tankard (1986) who cited COCORP geophysical data as evidence that a 14km-thick wedge when emplaced onto a 4-5km deep attenuated continental margin, did not create relief above sea-level, and hence the crust beneath the wedge must have been deflected downwards for approximately 10km. Fold belts with low topographic elevation and little denudation can also be generated at plate boundaries where the rate of subduction exceeds the rate of overall convergence (Royden & Burchfiel 1989), with the result that the pull-down compensates the uplift by thrusting, folding and magmatism.

In the model of Figures 6.12 B and C the border of the São Francisco Craton probably underwent post- D_1 or post- D_2 extension (cf. similar processes proposed by Houseknecht 1986 and Bradley & Kidd 1991). This may account for the Jacaré extensional fault in the cratonic area to the south of the Itaporanga fault (Fig. 6.1) and for the post- D_1 extension in the Capitão farm outcrop (section 4.7).

Thus, a complex interplay between compressive and extensive stresses may have occurred simultaneously along some of the regional thrusts. Whereas post-contraction extension is a common feature in many orogens (Carl et al. 1991), extension contemporaneous to compression is being an increasingly recognised paradox in the literature of deformation belts (Waters 1991).

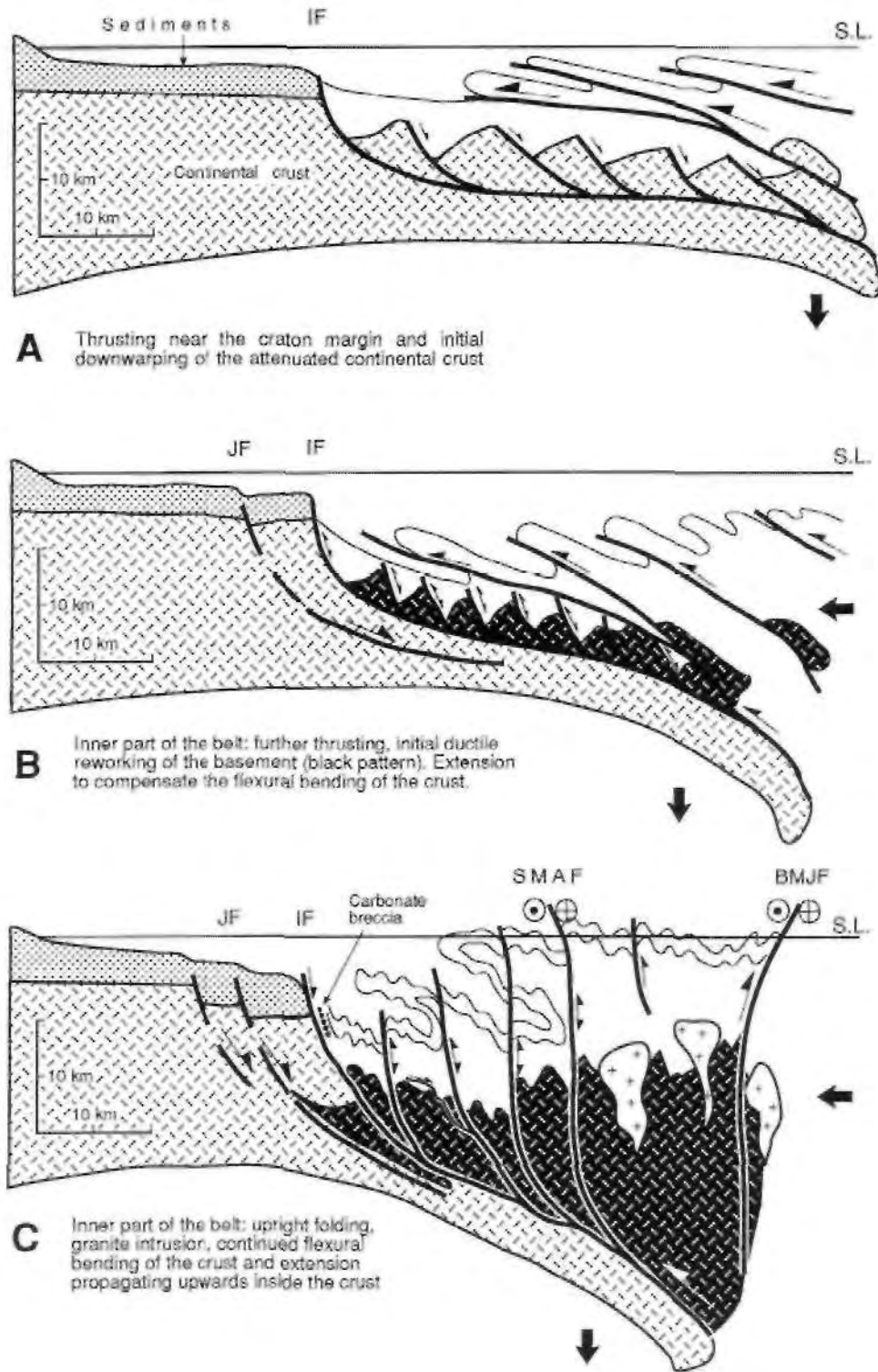


Figure 6.12 - Cartoons to illustrate the progressive tectonic loading, the probable flexural downwarping of the crust, and the lack of thrusting on the São Francisco craton. JF = Jacaré fault, IF = Itaporanga fault, SMAF = São Miguel do Aleixo fault, BMJF = Belo Monte-Jeremoabo fault.

This can account for descriptions of normal and thrust character in different places along the trace of the Itaporanga fault (Brito Neves et al. 1977 a) and can explain the isolated carbonate breccia in the southwestern corner of the study area (section 4.4.2). The carbonate breccia may be the product of an extensional reactivation of the Itaporanga fault between highly folded Olhos D'água carbonates and relatively undeformed Lagarto sandstones (Fig. 6.12 C).

If the model of Figure 6.12 is applicable, the lack of significant syn-tectonic erosion probably implies conservation of a thickened crustal pile (Fig. 6.12 C) probably for longer time than that predicted in PTt studies in other metamorphic belts (e.g. England & Richardson 1977; England & Thompson 1984; Thompson & England 1984; Thompson & Ridley 1987). This may cause differential rates of isotopic rehomogenization of Sr at different parts of the belt, therefore the onset of the deformation may be older than the metamorphic ages suggested by Rb-Sr systems.

The São Francisco Craton and the Sergipano Fold Belt

In order to fully understand the tectonic evolution of the Sergipano Fold Belt its relationship to the São Francisco Craton must be examined. Figure 6.13 shows the São Francisco Craton with the surrounding fold belts, the Borborema Province and the Pernambuco-Alagoas Massif.

To the west of the Sergipano Fold Belt (Fig. 6.13) the Riacho do Pontal Fold Belt evolved in the 2100-1800Ma Transamazonic cycle (Jardim de Sá 1988; Jardim de Sá et al. 1988), and was reactivated in the Brasiliano cycle by the dextral Pernambuco Shear Zone (Gomes 1990). Further west, the 700-500Ma old Rio Preto Fold Belt keeps characteristics of an entirely intracratonic belt, and its crystalline basement was mostly formed during the Transamazonic cycle (Egidio da Silva et al. 1989, 1990).

These data strongly suggest that the southwestern part of the Borborema Province and the São Francisco Craton were a single block since the Early Proterozoic. Porada (1989) proposed a continental bridge across the northern part of the São Francisco and Congo Cratons around 1100-1000Ma (Fig. 2.11 A). This feature may have extended further to the north between Brazil and Africa, and may have been formed as long ago as 2000 Ma, on the basis of structural, lithological and radiometric continuity between the two continents (Hurley et al. 1967; Torquato & Cordani 1981).

Such a single land mass, grouping part of the Borborema Province, the São Francisco Craton and western Africa, is also in agreement with the long-lived Proterozoic supercontinent proposed by Piper (1976, 1987) on the basis of paleomagnetic data. Moreover an Early Proterozoic connection is also suggested by the possible continuity of the granulitic rocks of the São Francisco Craton, the Pernambuco-Alagoas Massif and the Chailu massif of the Congo Craton (Brito Neves et al. 1977 a).

Additional support is given by the unique geochemical similarities of the Early Proterozoic Caraiba and Serrote da Laje copper sulphide deposits (Lindenmayer 1980; D'el-Rey SUva 1985; D'el-Rey Silva et al. 1988; Horbach & Marimon 1988) - hosted by pyroxenites emplaced within high grade gneisses in the São Francisco Craton and in the Pernambuco-Alagoas Massif respectively (Horbach & Marimon 1988).

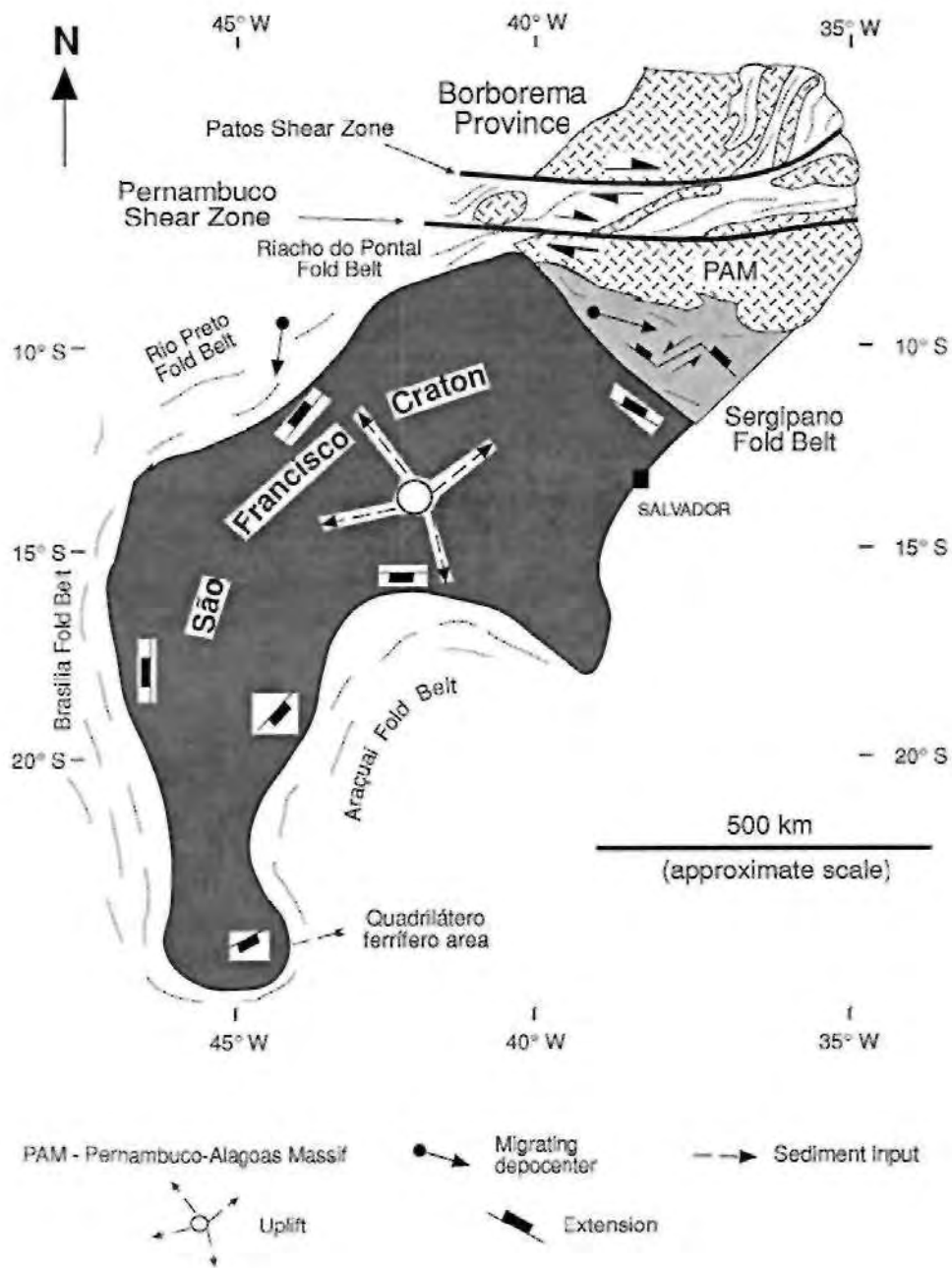


Figure 6.13 - Sketch map showing the São Francisco Craton and regional structural elements of the Brasiliano tectonic cycle used to interpret the evolution of the southern part of the Sergipano Basin.

Pre-Brasiliano extension of the margins of the São Francisco Craton have been described by Aikmin et al. (1990) in the Araçuaí Fold Belt, in the Quadrilátero Ferrífero area and in the west and southern part of the Brasília Fold Belt (Fig. 6.13). Thus, it can be concluded that syn-extensional depositional processes, similar to those proposed in this thesis for the Itabaiana Dome Area, have affected the margins of the São Francisco Craton during the Middle to Late Proterozoic. Such an evolution suggests that the São Francisco Craton underwent uplift and circumferal extension at this time (Fig. 6.13) and in particular the Sergipano Fold Belt evolved as an intracratonic basin on its western part, between what are now the Pernambuco-Alagoas Massif and the craton.

The opening and closure of the Sergipano Basin

A schematic model for the opening and closure of the Sergipano Basin is shown in Figure 6.14. This model incorporates the aspects of the geological evolution of the Sergipano Fold Belt (section 6.2), and also the relationships between the fold belt and the São Francisco Craton discussed above. Facies and thickness relationships (Chapter 3 & section 6.2 above) indicate that the area in the vicinity of the Itabaiana dome was the locus of the depocentre in the southern part of the Sergipano Basin.

The few formations and their small thicknesses in the cratonic and pericratonic parts of the Sergipano Fold Belt, to the west of the Tucano Basin (Gava et al. 1983, Conceição Filho & Sales 1988) and the passage from 1km of cratonic sediments to 4km of pericratonic sediments in the area of this thesis, point out to the Itabaiana Dome Area as the deepest depocentre in the southern part of the Sergipano Basin.

These data indicate an asymmetric basin that deepens eastward and northward of a hypothetical point in the western pan of the São Francisco Craton (Fig. 6.14 A), reaching maximum depths in the northeast, where the eugeoclinal Macururé Group was deposited. The data also suggest oblique extension (or a combination of extension along directions subparallel to N-S and E-W) and migration of the depocenter towards the ENE (Fig. 6.13). The extensional fault activity appears to have propagated westwards from the vicinity of the Itabaiana dome during the early Itabaiana Formation time, to the locality of the Simão Dias dome, by the late Itabaiana Formation time.

The model for the opening of the Sergipano Basin combines uplift of the central pan of the São Francisco Craton and oblique extensional delamination of its margins, along a low-angle basal detachment (Fig. 6.14 A). The lowest position of the detachment is speculative: by analogy with other areas (e.g. the Rhine Graben, Brun et al. 1991) it may have been within the upper-lower crust boundary, or alternatively the basal detachment may have gone to the base of the continental crust, as proposed for the Damara Fold Belt (Henri et al. 1990).

The closure of the Sergipano Basin (Fig. 6.14 B) assumes the inversion along the main extensional detachment, as a result of the collision between the southern pan of the Borborema Province and the São Francisco Craton. The inversion of the basin was initially accomplished by a southward movement of the Borborema Province into the São Francisco Craton developing the first phase of recumbent folding and low-angle thrusting toward south.

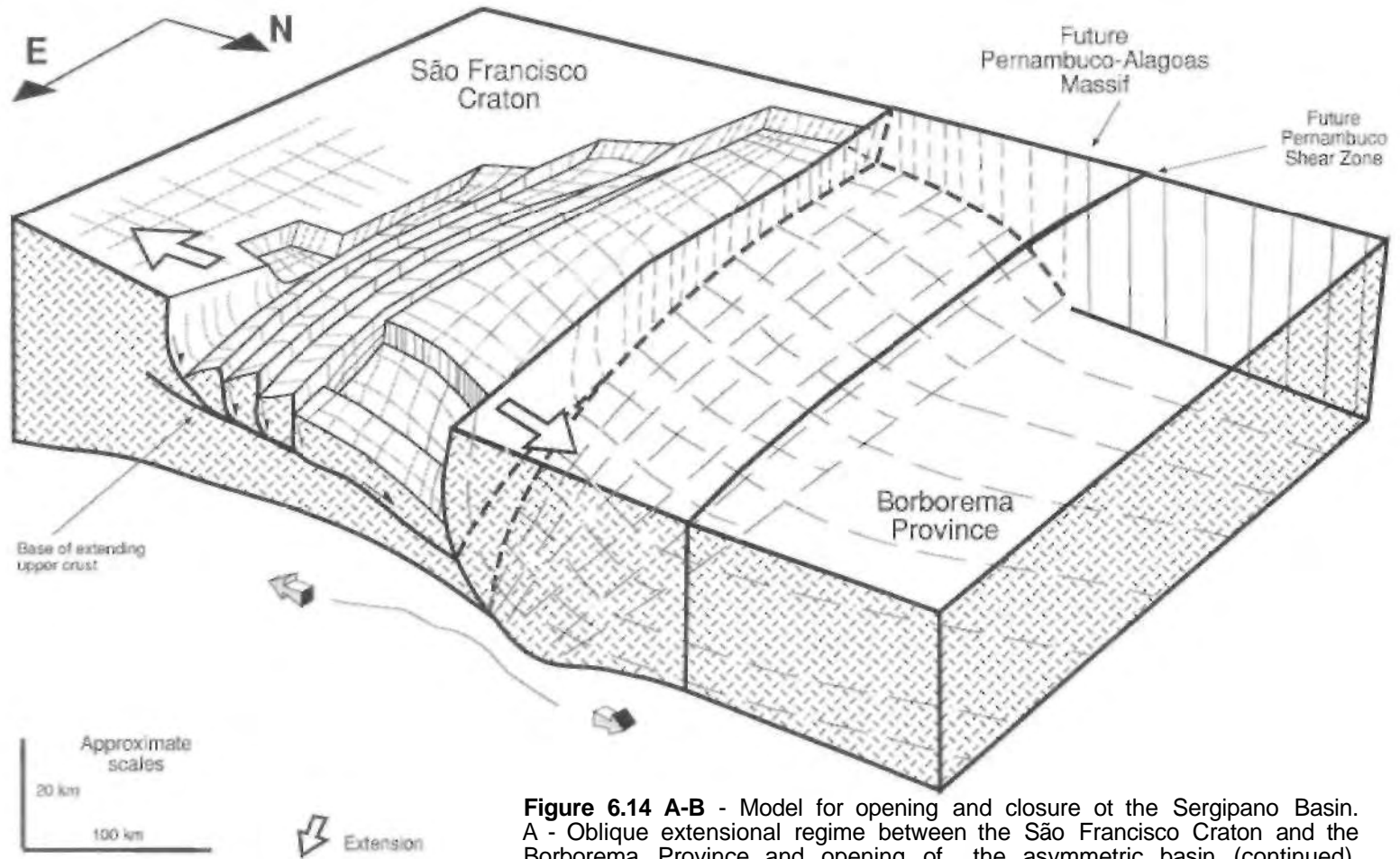


Figure 6.14 A-B - Model for opening and closure of the Sergipano Basin. A - Oblique extensional regime between the São Francisco Craton and the Borborema Province and opening of the asymmetric basin (continued).

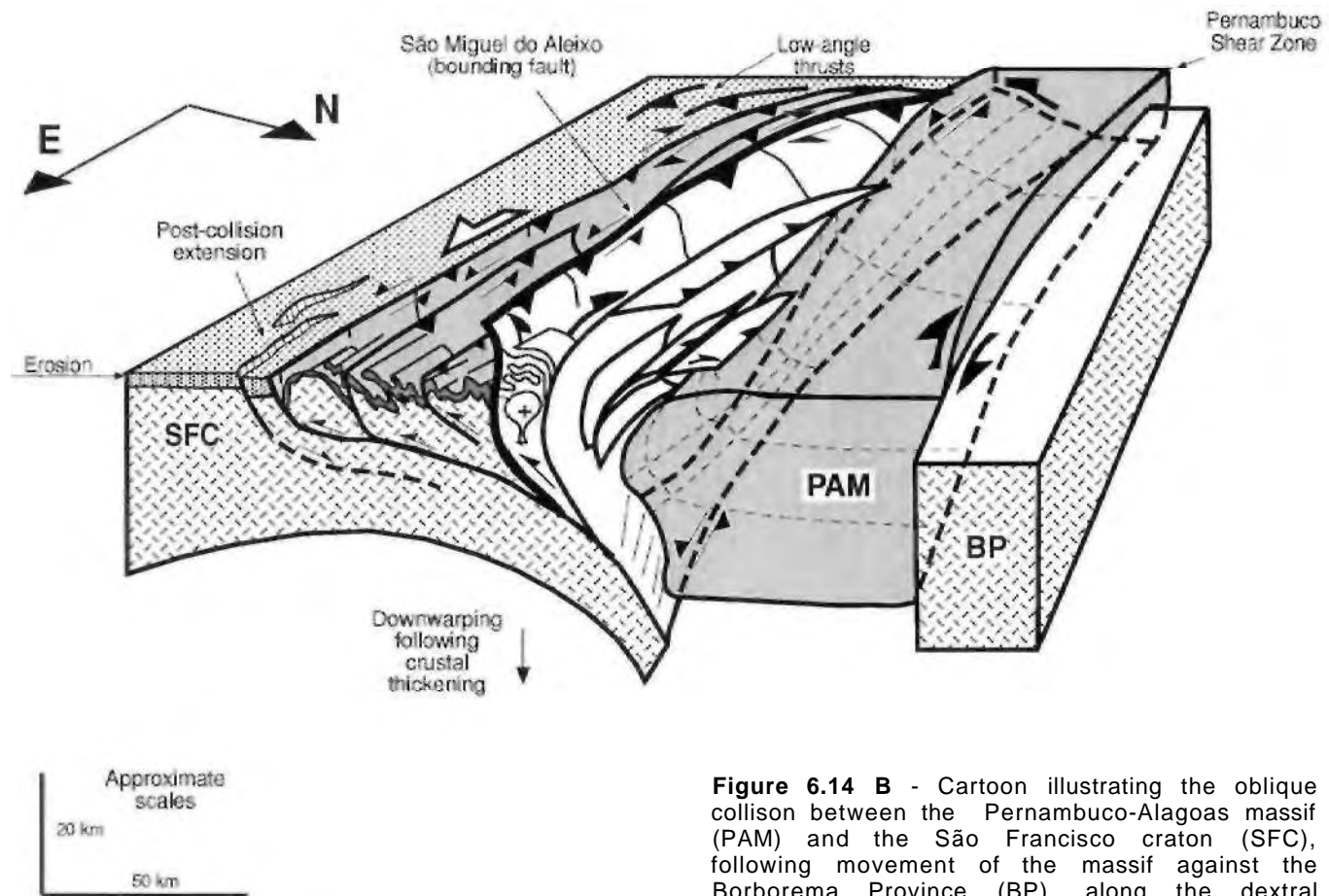


Figure 6.14 B - Cartoon illustrating the oblique collision between the Pernambuco-Alagoas massif (PAM) and the São Francisco craton (SFC), following movement of the massif against the Borborema Province (BP), along the dextral Pernambuco Shear Zone. See text for details.

Because the Sergipano Basin was probably narrower, and the detachment was probably shallower in the western part of the basin as opposed to its eastern part, basin sediments were thrust onto the western part of the São Francisco Craton but did not occur further east (Fig. 6.14 B).

In order to accommodate the continued convergence (probably oblique), the Pernambuco-Alagoas Massif started to move laterally toward the west, along the Pernambuco Shear Zone, creating a sinistral transpressive regime at the northern margin of the São Francisco Craton. This regime generated the asymmetric, SSW vergent F_2 folding and oblique slip thrust faults. High pore fluid pressures at this time facilitated the thrust emplacement (for example, as evidenced by the extensive quartz veining along the Pelada fault - Fig. 3.1, enclosure).

Climbing the inclined ramp (Fig. 6.14 B) the Pernambuco-Alagoas Massif possibly underwent uplift between the Sergipano Fold Belt and the Borborema Province, as a consequence of the curve of the Pernambuco Shear Zone to the south, combined with the resistance offered by the western margin of the craton. A slight change in the direction of the compressive field between the western parts of the Pernambuco-Alagoas Massif and the São Francisco Craton, combined with the tooth-shaped margin of the basin (Fig. 6.14 A) can explain the dominant dextral strike-slip movement associated with the regional faults, similarly as proposed by Moraes et al. (1987).

The faults are postulated to flatten at depth and merge into a basal detachment (Fig. 6.14b). The northward verging thrusts and folds of the northernmost part of the Sergipano Fold Belt are interpreted as a positive flower structure - a feature typical of transpressive regimes (Odonne & Vialon 1983; Christie-Blick & Biddle 1985). Thus, the legacy of the Brasiliano orogeny was a conjugate set of zones of crustal weakness in the Sergipano Fold Belt. They seem to have played a critical role in controlling the Mesozoic rift system which cross-cuts the Sergipano Fold Belt (Milani & Davison 1988).

6.4 - Implications for Proterozoic crustal evolution

6.4.1 - Introduction

The Sergipano Fold Belt can be described as a low to medium metamorphic grade, basement-involved, ductile fold and thrust belt. It is interpreted to have evolved by the inversion of an extensional half-graben fault system upon a low-angle basal detachment as a result of the oblique collision of the Pernambuco-Alagoas Massif with the São Francisco Craton during the 600 - 700Ma Brasiliano orogeny (Fig. 6.14).

The fold belt is characterised by south-vergent polyphase folding and thrusting with an oblique slip component of deformation. Basement gneiss domes (Fig. 6.11) show strong evidence of ductile reworking of the crystalline basement during the Brasiliano orogeny.

In the following sections the implications of this study for the understanding of Proterozoic stratigraphy, tectonic evolution, craton-mobile belt evolution and Proterozoic plate tectonics are discussed.

6.4.2 - Late Proterozoic sequence stratigraphy

Figure 6.15 highlights, in a pre-Mesozoic drift reconstruction of the South American and African continents, the Late Proterozoic Bambui Group sediments deposited in the center and margins of the São Francisco Craton, and the sediments equivalent to this group deposited in and around the Amazon, West African, Congo and Kalahari Cratons (Misi 1976).

Figure 6.16 is a summary geological map of the São Francisco Craton. It consists of Archean and Early Proterozoic high grade granite-gneiss and granulitic terranes, greenstone belts and supra-crustal sequences. Between 1800-1400Ma ago, the craton underwent intracratonic rifting, which resulted in the Espinhaço Fold Belt and sedimentary cover. The craton has also extensive Late Proterozoic sediments (the Bambui Group and Macaúbas supra-crustals) and a Phanerozoic cover, such as that in the Tucano Basin (Teixeira & Figueiredo 1991).

The Estância-Miaba Group is comprised of the lower siliciclastic megasequence (the Juetê-Itabaiana/Ribeirópolis Formations) and the lower carbonate megasequence (the Acauã-Jacoca Formation), and record the first sedimentary cycle (Cycle I) in the southern part of the Sergipano Fold Belt

Table 6.1 shows the part of the stratigraphy of the Sergipano Fold Belt and its equivalents - the Bambui Group around the São Francisco Craton. It can be seen that there are close correlations between the sequences in the Sergipano Fold Belt and strata in other fold belts around the craton. In the southern part of the Sergipano Fold Belt, the Bambui equivalent sediments have been divided into the Estância-Miaba Group, and the Lagarto Group (the Lagarto-Palmare Formation). Therefore the Bambui Group is here informally renamed Bambui Supergroup (Table 6.1).

The Estância-Miaba Group forms the lower siliciclastic megasequence and the lower carbonate megasequence of cycle I in the Sergipano Fold Belt (Fig. 6.3). In other fold belts around the São Francisco Craton (Table 6.1) only the basal equivalents of the siliciclastic megasequence of Cycle II of the Sergipano Fold Belt (Fig. 6.3) are found, and the overlying Palestina diamictites and Olhos D'Água carbonates have no stratigraphic correlatives.

The elastics of the Bambui Group and in particular the diamictites reflect the uplift and erosion of the craton. In the southern part of the Sergipano Fold Belt the diamictites contain clasts of gneiss, granite and quartz (Juetê Formation) and clasts of gneiss, granite, quartz and quartzites (Ribeirópolis diamictites). All the diamictite units in other fold belts around the craton have similar clast assemblages and in addition clasts of carbonates, metasilites, and metapelites (Karfunkell & Hoppe 1988; Egidio da Silva et al. 1989).

These assemblages indicate erosion of the cratonic basement and also Middle Proterozoic sediments (e.g. Rio Preto, Araçuaí, and Brasília Fold Belts). The Juetê diamictites therefore reflect the erosion of the basement, in an area where Middle Proterozoic sediments are not recorded (Fig. 6.16). The Ribeirópolis diamictites reflect the erosion of both the basement and Itabaiana quartzites.

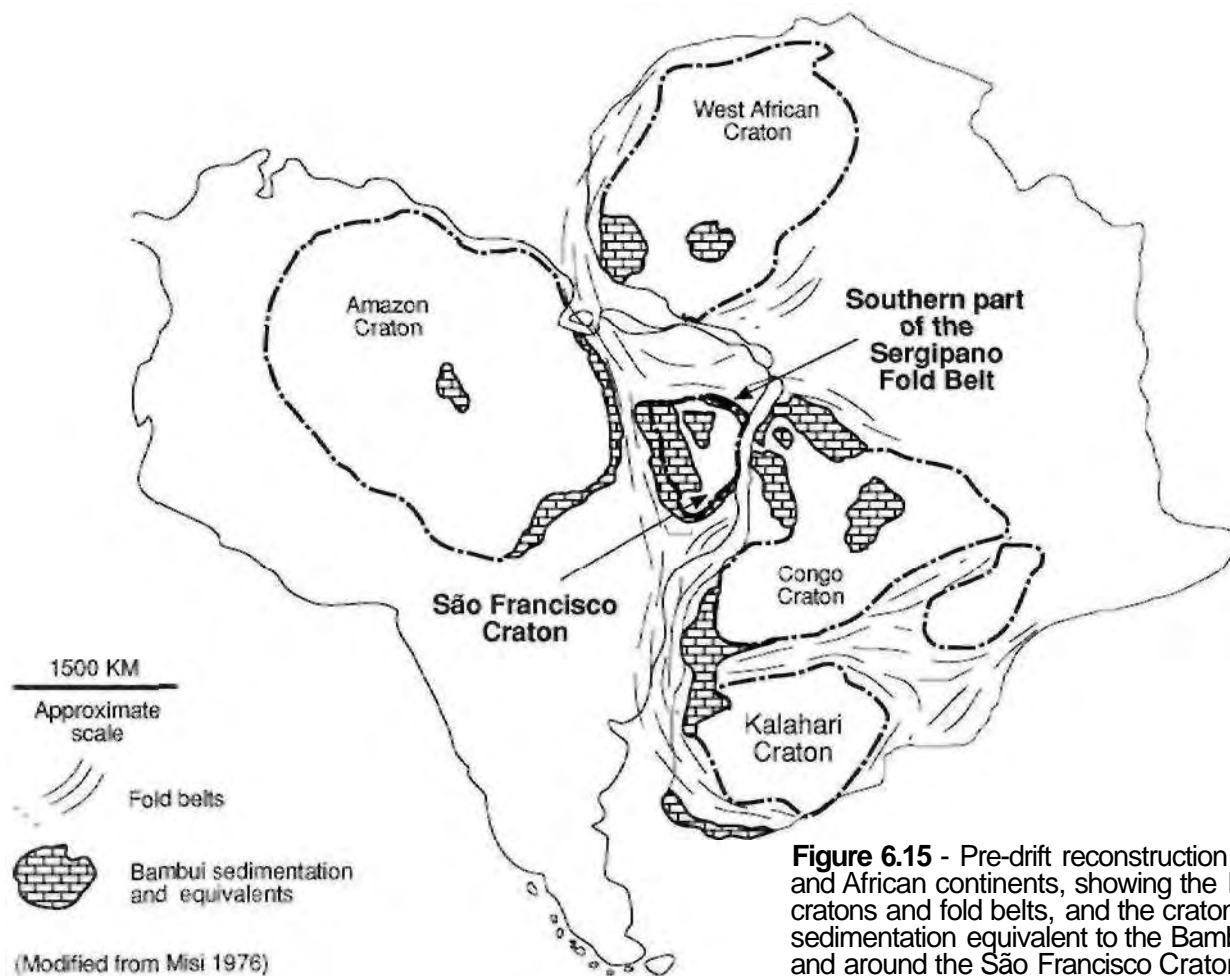


Figure 6.15 - Pre-drift reconstruction of the South American and African continents, showing the Pan-African-Brasiliano cratons and fold belts, and the cratonic-pericratonic sedimentation equivalent to the Bambui Group deposited in and around the São Francisco Craton.

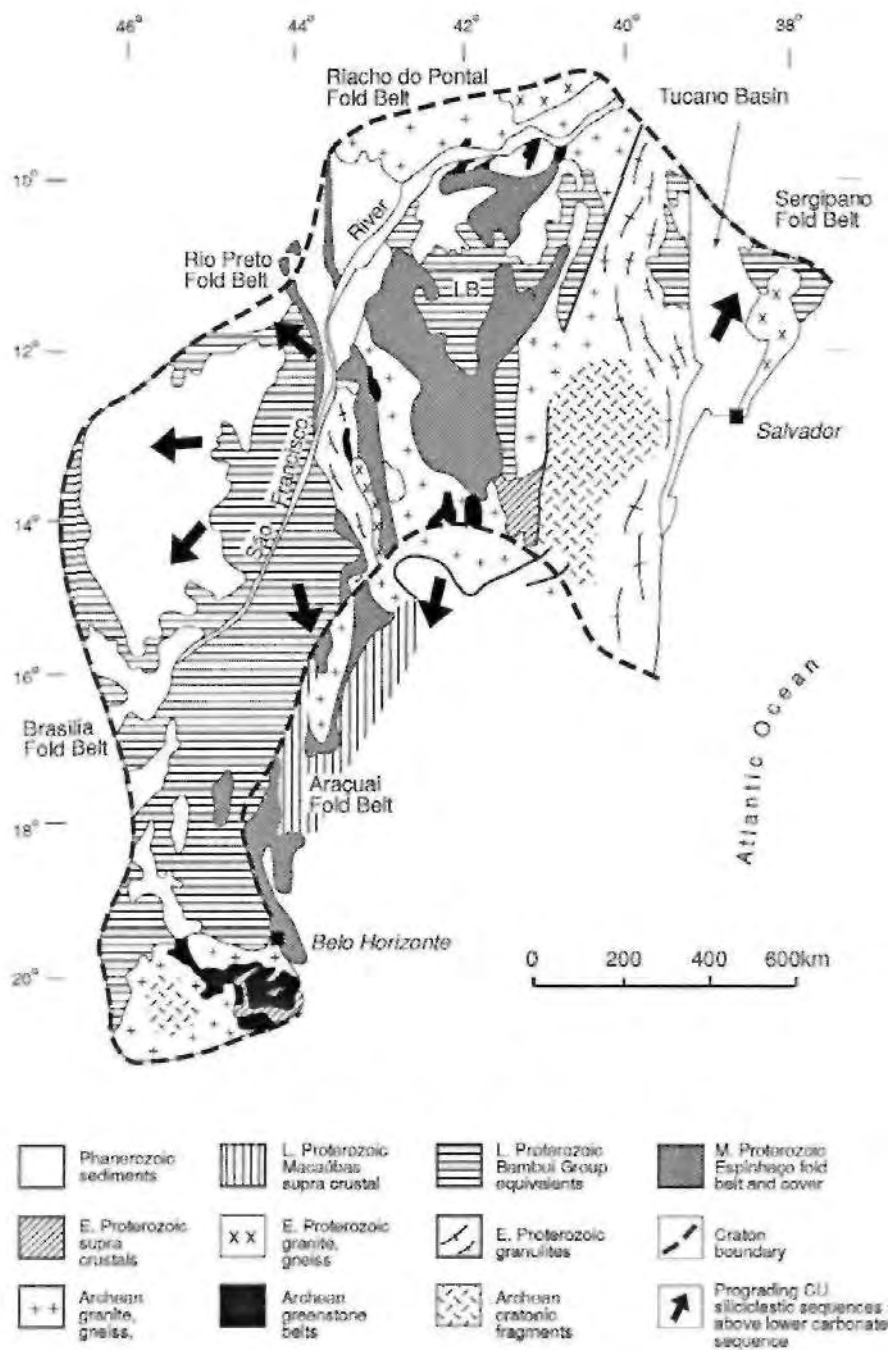


Figure 6.16 - Simplified geological map of the São Francisco Craton, showing the main lithotectonic units (Modified from Teixeira & Figueiredo 1991). The black arrows indicate progradation of coarsening-upwards siliciclastic sequences (equivalent to the Lagarto Group, this study) deposited on top of the Bambuí carbonates. LB=Lençóis Basin.

	Stratigraphic unit	Sergipano Fold Belt	Rio Preto Fold Belt	Brasília Fold Belt	Araçuaí Fold Belt	Lençóis Basin (centre of the craton)	Main Lithologies	Sequence stratigraphy
		<i>This study</i>	Egídio da Silva et al. (1989)	Egídio da Silva et al. (1989)	Uhlein et al. (1990)	Egídio da Silva et al. (1989)		
Late Proterozoic 900Ma	Bambuí	Lagarto Group Palmares Fm Lagarto Fm	Riachão das Neves Fm Serra da Mamona Fm	Três Marias Fm Serra da Saudade Fm	 Três Marias Fm	 No records	Fine- to medium-grained lithic sandstones, wackes, arkoses, Siltstones, mudstones, fine-grained sandstones	Upper siliciclastic megasequence
		Supergroup	Estância Group Acauã Fm Justê Fm	São Desidério Fm	Lagoa Jacaré Fm Serra de Santa Helena Fm Sete Lagoas Fm	lower carbonate sequence	Salitre Fm	
	Canabraninha Fm			Jequitai Fm (Ibiá Fm)	Jequitai Fm	Bebedouro Fm	Diamictites, quartzites, phyllites	Lower siliciclastic megasequence
1100Ma	<p>The basement of the Bambuí Supergroup consists of Archean-Early Proterozoic continental crust and/or postulated Middle Proterozoic sequences. These sequences are not recorded in the cratonic area of the southern part of the Sergipano Fold Belt.</p>							

Table 6.1 - Comparative stratigraphies for the sediments equivalent to the Bambuí Group deposited on the São Francisco Craton, within the cratonic-pericratonic areas of the Sergipano, Rio Preto, Brasília and Araçuaí Fold Belts, and in the Lençóis Basin.

It should also be noted that the carbonate megasequence (Acauã equivalent) of the Bambuí Group in all these belts is overlain by a coarsening-upward siliciclastic sequence equivalent to the Lagarto-Palmares Formation (Table 6.1). These siliciclastic sequences have similar petrographic characteristics (Saes 1984; Egidio da Silva et al. 1989; Uhlein et al. 1990), and may indicate progressively greater uplift in the centre of the craton (Figs. 6.13 & 6.16) by the time of the deposition of the Lagarto-Palmares Formation.

This discussion indicates that with more detailed stratigraphic and sedimentological analyses of the other fold belts surrounding the São Francisco Craton, may be possible to reconstruct the erosional history of the craton and hence to investigate in more detail the hypothesis of uplift and circumferal extension proposed here.

Palestina Diamictites

The Palestina diamictites and the overlying Olhos D'Água carbonates are important stratigraphic units of the Sergipano Fold Belt and can be closely matched with the stratigraphy of the West Congo and Damara Fold Belts (Table 6.2). The similarities in sedimentology and sequence stratigraphy of these belts implies a strong pre-Brasiliano linkage.

In particular the correlation of the Palestina diamictites with a major period of extension matches with similar interpretation for the Chuos diamictites of the Damara Fold Belt (Table 6.2) which have been interpreted as the record of continental break-up and opening of the Khomas Sea between the Congo and Kalahari Cratons (Fig. 6.17; Henri et al. 1990). The Pan-African South Atlantic ocean (Fig. 6.17) has been postulated in order to explain the incompleteness of the West Congo Fold Belt (another rift should have existed to the west but is now probably hidden by the Atlantic ocean). This probably existed 1100 to 750Ma ago, between the southern São Francisco Craton and the Congo Craton, but did not entirely separate the two continents (Porada 1989).

Therefore the Sergipano Basin may have evolved into a small, E-W trending ocean (here termed the Canindé sea) in the northeastern part of the Sergipano Fold Belt at this time. This hypothesis does not conflict with the concept of a Proterozoic supercontinent (Piper 1987) as the amount of craton separation would have been too small to be detected by paleomagnetic methods (Briden 1976; Shackleton 1986).

6.4.3 - Late Proterozoic tectonic evolution

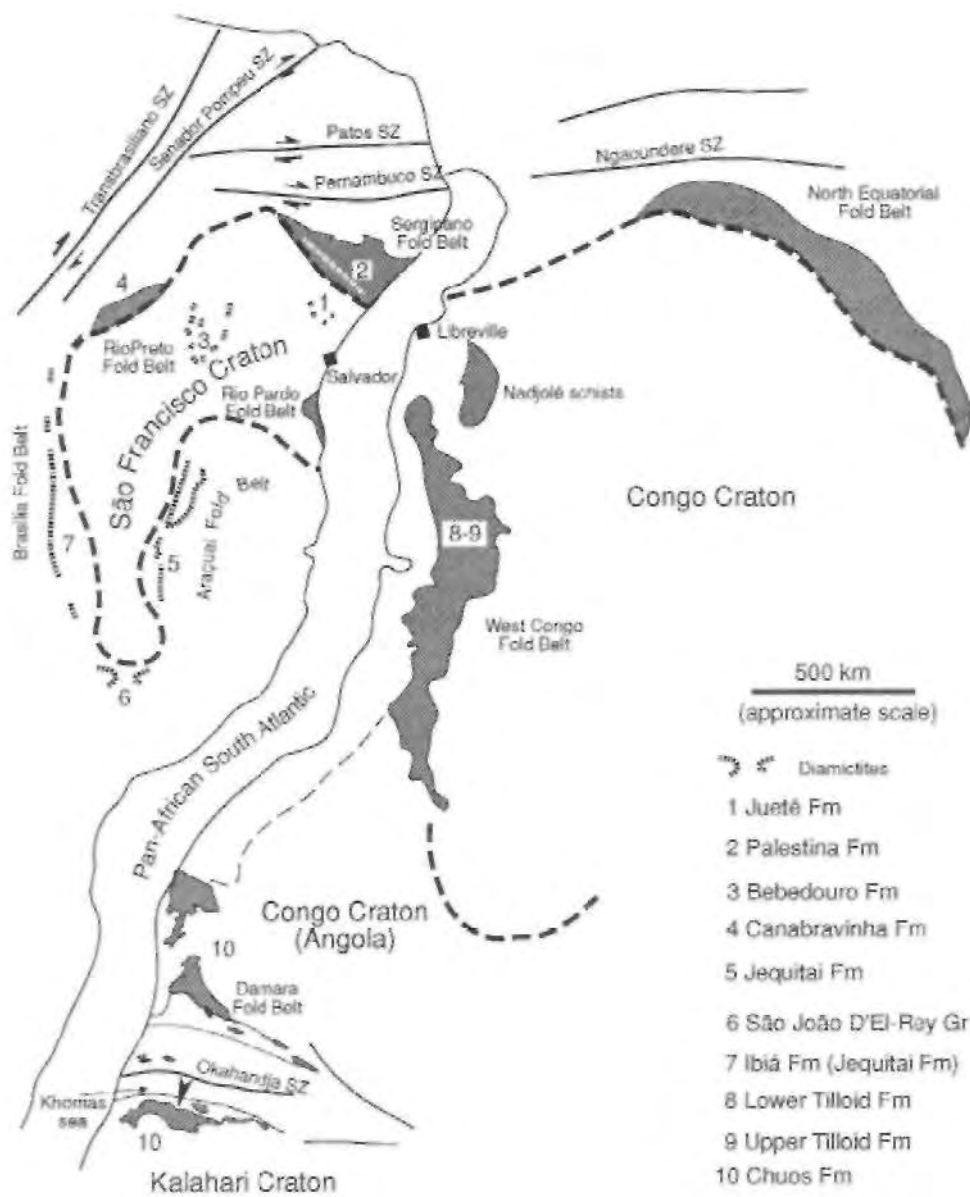
The Sergipano Fold Belt is characterised by ductile reworking of the crystalline basement and by south-southwest vergent folding and thrusting, with some north vergent folds and thrust in the Macurure Domain (Fig. 6.14 B).

Ductile reworking of crystalline basement is common in many other fold belts, such as the Early Proterozoic Aravalli of India (Nalia & Mohanty 1989), the Grenville Front of Canada (Brown et al. 1991), the Late Proterozoic Tuzo Mountains, USA (Williams 1991), and the Caledonian Fold-Thrust Belt of NW Scotland (Holdsworth 1989, 1990).

The internal structure of the Sergipano Fold Belt also compares well with other fold belts where progressive shortening by folding and thrusting has led to steepening of

		Sergipano Fold Belt		West Congo Fold Belt		Damara Fold Belt		Sequence stratigraphy			
		<i>This study</i>		Schermerhorn & Stanton (1973), Schermerhorn (1981)		Henri et al. (1990)					
Middle to Late Proterozoic	Vaza Barris Group	Olhos D'água Fm	Metacarbonates, mixed metacarbonates and metapelites	Schist Gréseux Group	Greywackes, quartzites, shales, local diamictites	Tsumeb Subgroup	Arenites, pelitic rocks	upper carbonate megasequence			
		Palestina Fm	Diamictites	Schist calcaire Group	Shallow water carbonates, limestone-shale turbidites		Carbonates				
	Bambuí Supergroup	Lagarto Group	Frei Paulo Fm	Phyllites, minor black shales, greywackes, minor metacarbonates, and volcanics	Haut Shiloango Group	Quartzites, mudstones, carbonaceous silty shales, local diamictites, and metacarbonates	Aberabe Subgroup	Carbonates, pelitic rocks, arenites	upper siliciclastic megasequence		
			Jacaré fm	Metasiltites				Arenites			
		Lagarto-Palmares Fm	Coarsening-upward sequence of mudstones, siltites, fine-grained sandstones, and medium-grained lithic sandstones and wackes	Carbonates, and metacarbonates				Pelitic rocks	lower carbonate megasequence		
		Acauã-Jacoca Fm	Carbonates, and metacarbonates	Diamictites (Lower Tilloid Fm)				Carbonates			
		Estância-Miaba Group	Ribeirópolis Fm	Phyllites, diamictites, volcanics				Quartzites, arkosic sandstones carbonaceous shales, volcanics	Nosib group	Arenites Local diamictites	lower siliciclastic megasequence
		Juetê-Itabaiana Fm	Quartzites, mudstones, phyllites, diamictites, conglomerates	Sansikwa Group						Arenites, local conglomerates, volcanics	
							<i>Break-up record</i>	Diamictites (Chuós Fm)			

Table 6.2 - Comparative stratigraphies of the Sergipano, West Congo and Damara Fold Belts. The Vaza Barris Group overlies the Lagarto Group (this study), and has no correspondent in the other belts surrounding the São Francisco Craton (see table 6.1).



Diamicrites data from this study, Egidio da Silva et al. (1990), Karfunkel & Hoppe (1988), Henri et al. (1990), Schermerhorn & Stanton (1963).

Fold belt data from Davison & Santos (1989), Forada (1989), Henri et al. (1990).

Figure 6.17 - Late Proterozoic diamicrites deposited around and in the São Francisco, Congo and Kalahari Cratons (Pre-drift reconstruction based on Fig. 2.12 A). The Phanerozoic sediments are not represented in this figure.

the thrusts together with locking-up of the system and transpressional deformation. A similar tectonic history has been interpreted for the Areachap Group of South Africa (Donker 1990.) and for the southeastern Australian Fold Belt (Wang & White 1990). The D₁-D₂ shortening of 75% across the fold belt (calculated in Fig. 6.9 A by line-length balance along bedding in the Olhos D'Água carbonates between the Itaporanga fault and point B) is comparable with other similar orogens that have resulted from collision (e.g. Daly 1986; Gray et al. 1991).

The tectonic characteristics of the Sergipano Fold Belt are very similar to those described for other Proterozoic fold belts in Brazil (Hasui & Costa 1990; Corsini et al. 1991), including those surrounding the São Francisco Craton (e.g. Campos Neto & Figueiredo 1990; Egidio da Silva et al. 1990; Gomes 1990; Schrank et al. 1990; Soares et al. 1990). The tectonic model of an inverted extensional half-graben (section 6.3 above) also agrees with similar models evoked to explain the sedimentary and structural asymmetry in Pan-African-Brasiliano fold belts and related basins (e.g. Henry et al. 1990; Krebs et al. 1990),

The majority of these fold belts have ductilely reworked crystalline basement, a high grade metamorphic axial zone, a double vergence of folds and thrusts both towards the foreland and towards the hinterland, and transpressive or strike-slip related deformation, as in the Damara Fold Belt (Henri et al. 1990)

6.4.4 - Craton - Mobile Belt evolution

The deposition of Late Proterozoic coarsening upwards siliciclastic sequences on top of the carbonates of the Bambui Group and equivalents indicate a radial dispersal pattern outwards from a central high within the São Francisco Craton (Fig. 6.16). This pattern may be interpreted to indicate domal uplift in the central part of the craton during the period of extensional tectonics that formed the precursor basins that surround the craton (Fig. 6.13).

The sedimentary basins which later formed the fold belts, appear to have been generated by circumferal extension at the margins of the updomed São Francisco Craton. Uplift of cratons, extension with onset of rift systems and continental break-up are being increasingly associated with the rising of mantle plumes in the asthenosphere (e.g. White & Mackenzie 1989; Kent 1991; Thompson & Gibson 1991). It can be postulated that the São Francisco Craton and its ring of marginal basins could be part of a long-lived, large-scale core complex-like evolution, which may have started following the Archean to Early Proterozoic periods of craton assembly.

The Middle-Late Proterozoic circumferal extension may be the end product of the uplift of the older mountain chains in the craton and exposure of their granulitic roots, similarly to the Basin and Range model of post-orogenic extension (Malavieille & Taboada 1991). This hypothesis agrees with predictions that the exposure of granules in Archean-Early Proterozoic terranes has probably required a faster denudation than just erosion could provide (Thompson & England 1984). The presence of voluminous granites in these terranes suggest deep crustal igneous activity increasing the heat supply and provoking uplift and erosion (Thompson & Ridley 1987). The Brasiliano-age

granites intruding the São Francisco Craton (Mascarenhas et al. 1984) may also be evidence of a deep seated heat source.

According to this model, the sedimentary cycle I of the Sergipano Fold Belt is associated with a progressive uplift of the centre of the São Francisco Craton and initial extension of its margins. In cycle II, the upper siliciclastic megasequence is associated with a progressively faster uplift of the centre of the craton coupled with a major rifting event in the basin, attributable to the unloading of the centre of the craton and opening of the Canindé sea. The upper carbonate megasequence records the post-rift sedimentation in the basin.

The applicability of this model to the other Pan-African-Brasiliano cratons and belts (Fig. 6.15) is strongly supported by the similarities of the tectonic evolution of the São Francisco and Congo Cratons (Teixeira & Figueiredo 1991) and by the correspondence between the Bambui Group with the craton-belt Late Proterozoic sediments deposited around the Amazon, West African, Congo, and Kalahary Cratons (Misi 1976).

The closure of the basins which are now (together with basement slices and gneiss domes) incorporated into the Brasiliano age fold belts that surround the São Francisco Craton, is generally accepted to have occurred by collisional tectonics (Couto 1984; Davison & Santos 1989; Jones 1989). In the case of the Sergipano Fold Belt collision between the Borborema Block - Pernambuco Alagoas Massif to the north and the São Francisco Craton to the south is believed to have generated the fold belt (section 6.3 above).

The models which have been invoked for the other fold belts that surround the São Francisco Craton assume the closure of intracratonic basins (Egidio da Silva et al. 1990), or episodes of A-subduction (Campos Neto et al. 1990; Heilbron 1990) or even the closure of small oceanic basins by collision of continental fragments or island arcs against the craton (Soares et al. 1990; Brito Neves & Cordani 1991).

In the cases of intracratonic basins, closure may have simply involved the return of extended continental crust to more normal thicknesses whereas in the case of small oceans subduction of oceanic lithosphere would have occurred. In the latter case identification of oceanic crustal rocks, high P / Low T metamorphism and melanges would be needed to identify paleosuture zones.

The characteristics of the Sergipano Fold Belt, such as the double vergence of folds and thrusts, an axial zone with intermediate pressure and temperature metamorphism, the slightly higher metamorphic pressures in its northernmost parts (Jardim de Sá et al. 1981), and the inferred suture along the line of the Canindé Complex (Fig. 6.11), are comparable with the Damara and North Equatorial Fold Belts, where the closure of small oceans and suture zones have also been interpreted (Henri et al. 1990; Kukla & Stanistreet 1991; Nzenti et al. 1988).

The probable characteristics of the Sergipano Basin (Fig. 6.14 A) and the unique combination of the Palestina diamictites with the Canindé, Marancó and Poço Redondo Domains implies that in, the Sergipano Fold Belt, the asymmetric basin passed along its axis from an western intracratonic setting into an eastern oceanic setting (Fig. 6.18).

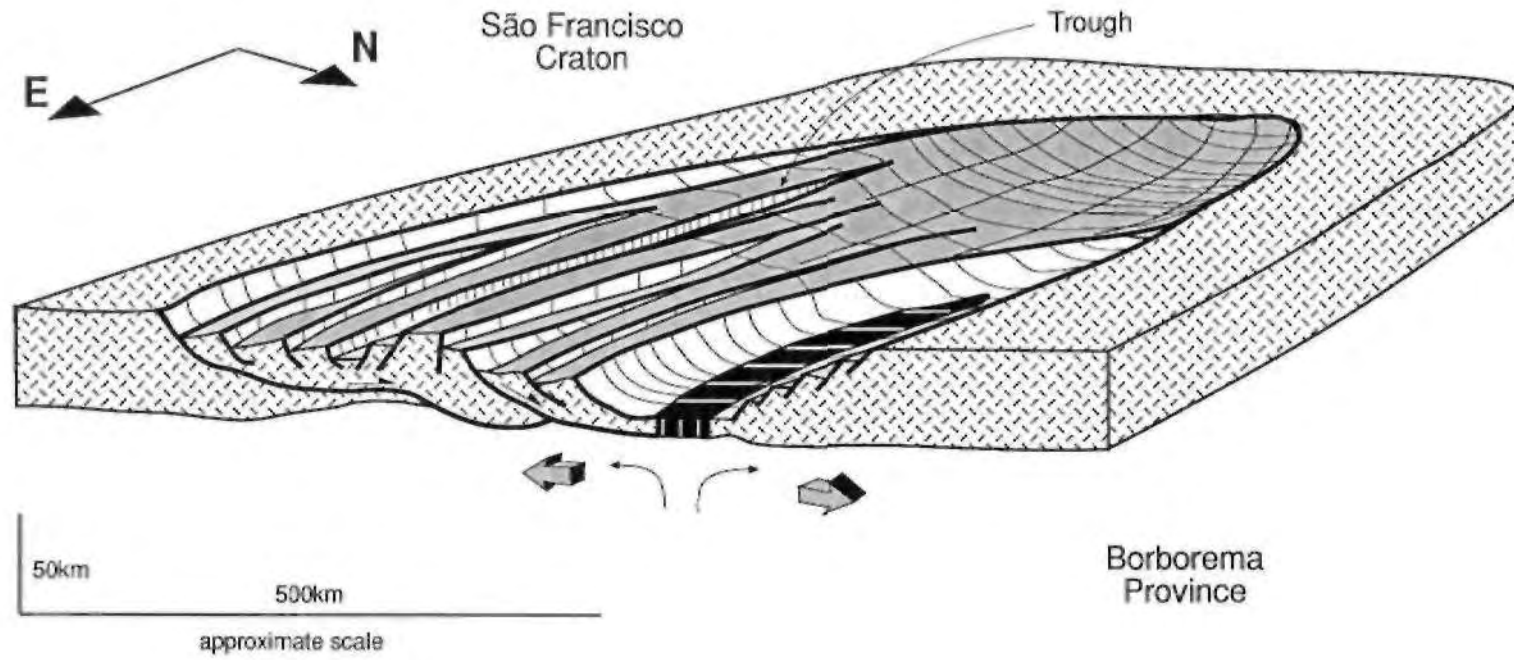


Figure 6.18 - Cartoon illustrating the opening of the Canindé sea, and its relationship with an asymmetric, continental crust-floored basin on its western end.

The consumption of the Canindé sea in the tectonic evolution of the Sergipano Fold Belt (Table 6.3) can explain the island arc signature and the emplacement of the major units of the Canindé complex, by subduction of oceanic crust underneath oceanic crust, and by collage of this arc onto the passive margin of the Pernambuco-Alagoas Massif. In a later stage, another arc (the Marancó Domain) possibly resulted from northward subduction of oceanic crust underneath the northern passive margin (Table 6.3) or under deforming continental crust. Hall (1987) and Wilson (1989) point out that although andesitic suites result from subduction of oceanic crust under continental or oceanic crusts, dacitic and rhyolitic suites (such as the Marancó Domain) are more common in the former than in the latter situation.

Both the Marancó and Poço Redondo Domains may have been emplaced at the beginning of the collisional stage (*sensu* of Shackleton 1986) and this may also explain the position of the Poço Redondo Domain within the Canindé and Marancó Domains in the map (Fig. 6.11). However, as Davison & Santos (1989) pointed out, the late stage transcurrent movement may have erased most of the evidence of movements other than the F-W sinistral shear, along the boundary between these domains.

The calcalkalic-alkaline granites intruded in the northern part of the Sergipano Fold Belt are co-genetic and can be explained by partial melting of the lower crust and upper mantle (Giuliani & Santos 1988). However, as the granodiorites of Coronel João Sá and most of the major bodies (Fig. 6.11) are late- to post-D₂ deformation (Santos et al. 1988; Davison & Santos 1989) they cannot have been part of pre-collisional arcs, as postulated by Fujimori (1989). Because the position of these granites within the Macururé Domain requires a southward subduction of oceanic crust underneath the São Francisco Craton, of which there is no evidence, a simple model of partial melting of a tectonically-thickened and garnet-rich lower crust (Table 6.3) is preferred here.

Although the tectonic evolution outlined above adds weight to the concept that the Canindé, Marancó and Poço Redondo Domains might be allocthonous (Davison & Santos 1989), the definite acceptance of such a terrane model requires detailed paleomagnetic and age studies of the three domains relative to the rest of the Sergipano Fold Belt.

6.4.5 - Implications for Proterozoic orogens and Plate Tectonic

The stratigraphic connections between the São Francisco Craton, Sergipano Fold Belt and the Congo and Kalahari Cratons are illustrated in Figure 6.17, Tables 6.1 and 6.2. In particular the outcrops of the diamictites of these areas are highlighted.

In the southern part of the Sergipano Fold Belt, diamictites occur in the cratonic Juetê Formation (Saes 1984), in the Ribeirópolis and Palestina Formations (Tables 6.1 & 6.2). Around the São Francisco Craton, diamictites have been described in the basal section of the Bambuí Group (Table 6.1 & Fig. 6.17); in the Canabravinha Formation of the Rio Preto Fold Belt (Egidio da Silva et al. 1989); in the Bebedouro Formation of the Lençóis Basin, in the Jequitai Formation of the Araçuaí Fold Belt, in the São João D'el-Rey Group at the southernmost end of the craton, and in the Ibií Formation (or Jequitai Formation) of the Brasília Fold Belt (Kaifunkel & Hoppe 1988).

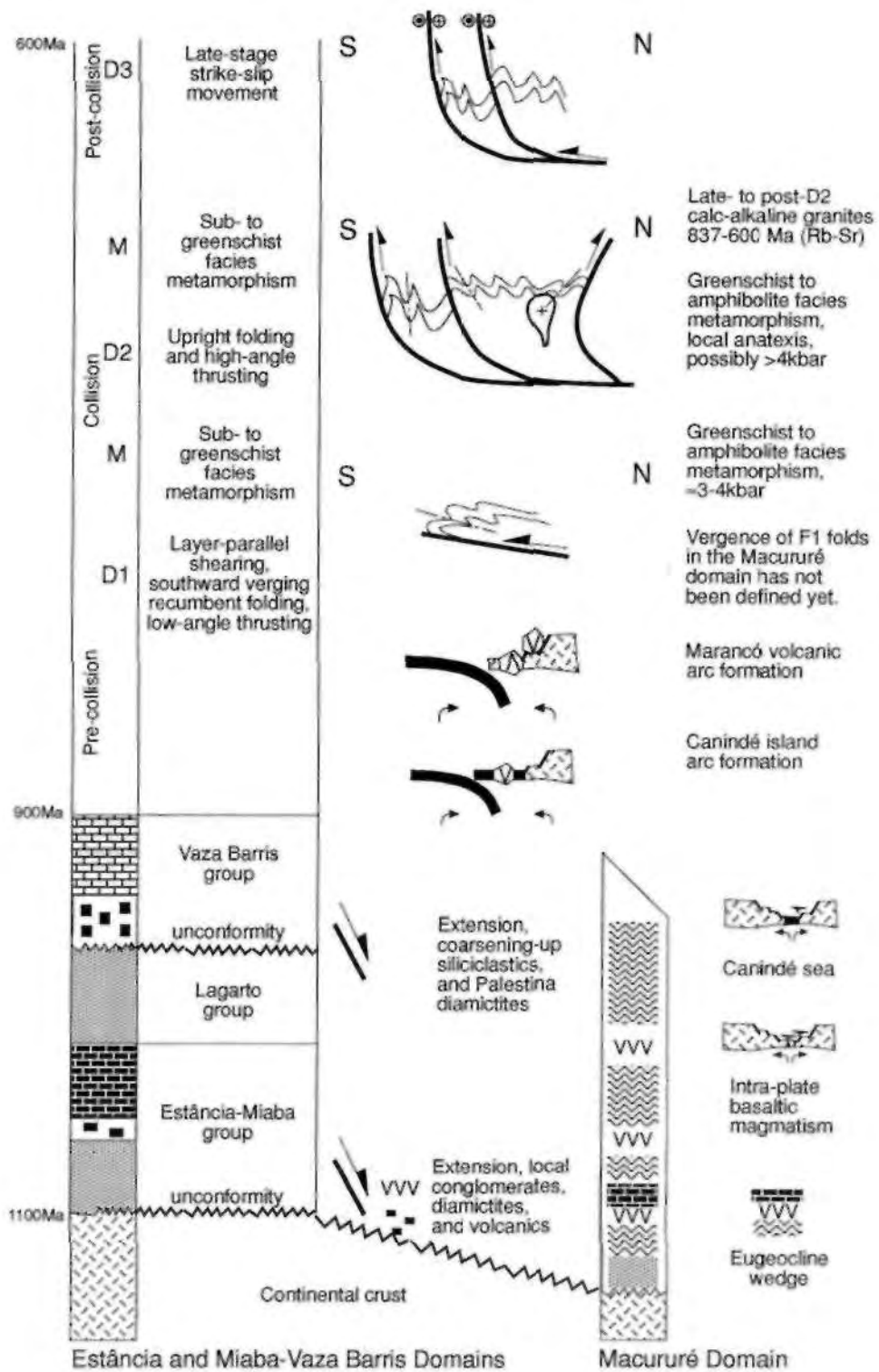


Table 6.3 - Summary of the tectonic evolution of the Sergipano Fold Belt.

In the West Congo and Damara Fold Belts (Fig. 6.17 & Tabic 6.2) diamictites are found in the Lower and Upper Tilloid Formations (Schermerhorn & Stanton 1963; Coward 1981a; Schermerhorn 1981) and in the Chuos Formation (Henri et al. 1990) respectively. The very similar stratigraphic relationships emphasised above therefore indicate similar tectonic histories of basin formation and extension.

There has been considerable debate as to whether the basins that are now incorporated into these Proterozoic fold belts were formed as intracratonic or oceanic basins (Kroner 1983; Windley 1987). For example the Proterozoic fold belts of Australia are thought to be largely intracratonic in nature (Preiss 1987; White 1989).

Porada (1989) and Brito Neves & Cordani (1991) consider that, although many of the Pan-African-Brasiliano belts are intracratonic, some may have formed from oceanic basins. Murphy & Nance (1990, 1991) considered the Late Proterozoic fold belts throughout the world as evidence of cnistal accretion and dispersal of a Proterozoic supercontinent. They classified the belts into internal and external orogens.

The interior orogens (e.g. Pan-African-Brasiliano fold belts), were related to the destruction of interior oceans and with supercontinent amalgamation. The external orogens (e.g. Avalonian-Cadomian belt of North America and western Europe, and the Arabian shield) were related to the destruction of wide oceans peripheral to the supercontinent. Subduction probably started everywhere by SOOMa ago, but each of the orogens evolved differently (Murphy & Nance 1990, 1991).

In this model the internal belts culminated in continent-continent collision 650-600Ma ago, producing abundant calcalkaline magmatism, crustal thickening, regional thrusting and nappe development, together with the erosion of the mountain chains and cratonic sedimentation (Murphy & Nance 1991). At the margins of the supercontinent, oblique subduction and closure of the wide oceans generated the peripheral fold belts, and produced widespread volcanism and synorogenic volcanoclastic sediments (=600Ma ago).

In the Proterozoic of South America, Brito Neves & Cordani (1991) recognised both marginal and 'internal fold belts. The marginal belts consist of probable passive margin sedimentary and volcanic sequences thrust onto large continental blocks during collisions events. The internal orogenies (e.g. the northern part of the Sergipano Fold Belt) consist of flysch-type volcano-sedimentary wedges, and occur within smaller blocks, and also in branching fold belt systems. They probably originated as continental rifts, small oceans, or back-arc basins.

In order to account for the architecture of the fold belts around the São Francisco Craton Couto (1984) proposed a model of radial cnistal extension that separated the São Francisco, Amazon, Paraná, Congo, West African and Kalahari Cratons (Fig. 2.11 B), followed by crustal shortening and convergence towards the São Francisco Craton.

The Pan-African-Brasiliano fold belts probably represent the closure of a basin system established within the Proterozoic supercontinent, about 1100-1000Ma ago and having an architecture very similar to the North Atlantic Mesozoic rift system (Fig. 6.19; Porada 1989). The evidence indicates that some of these basins were intracratonic

J.

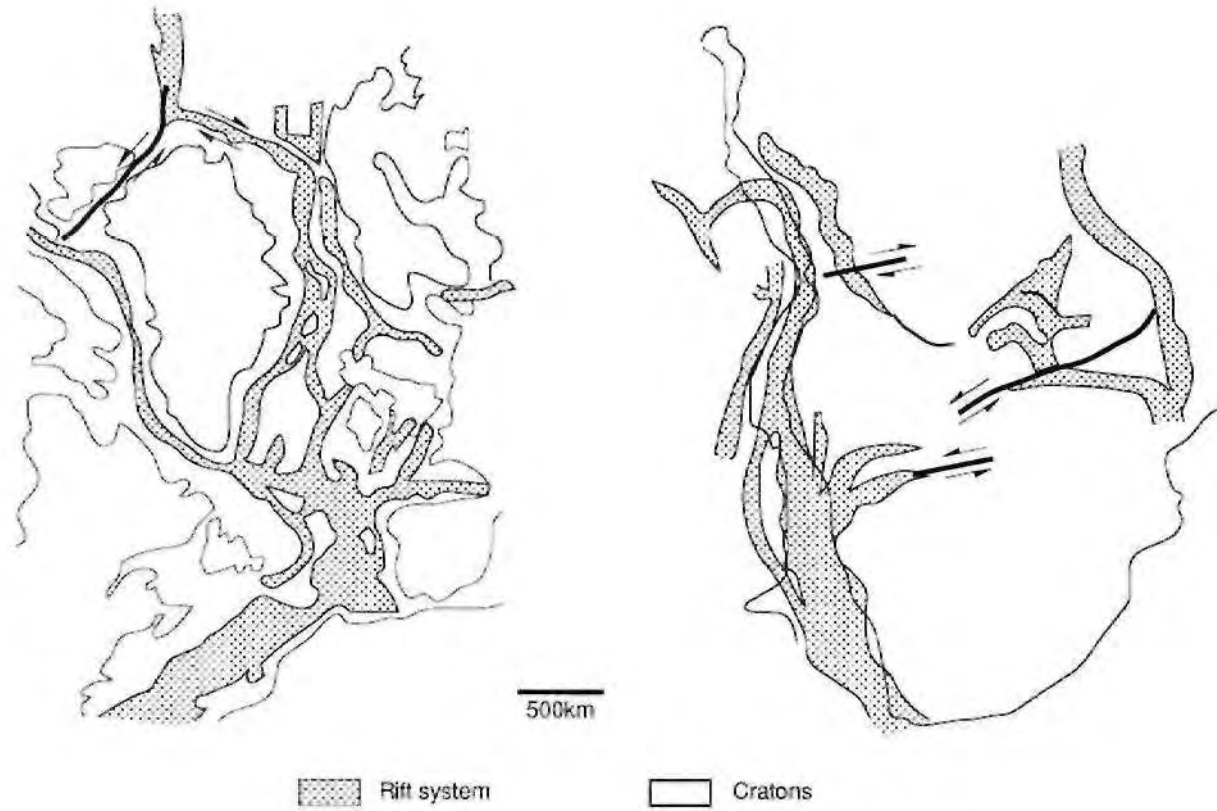


Figure 6.19 - Comparative maps of the Mesozoic rift system of North Atlantic (left) and the southern part of the Pan-African-Brasiliano rift system (right). Note the cratonic fragments within both systems. From Porada (1989).

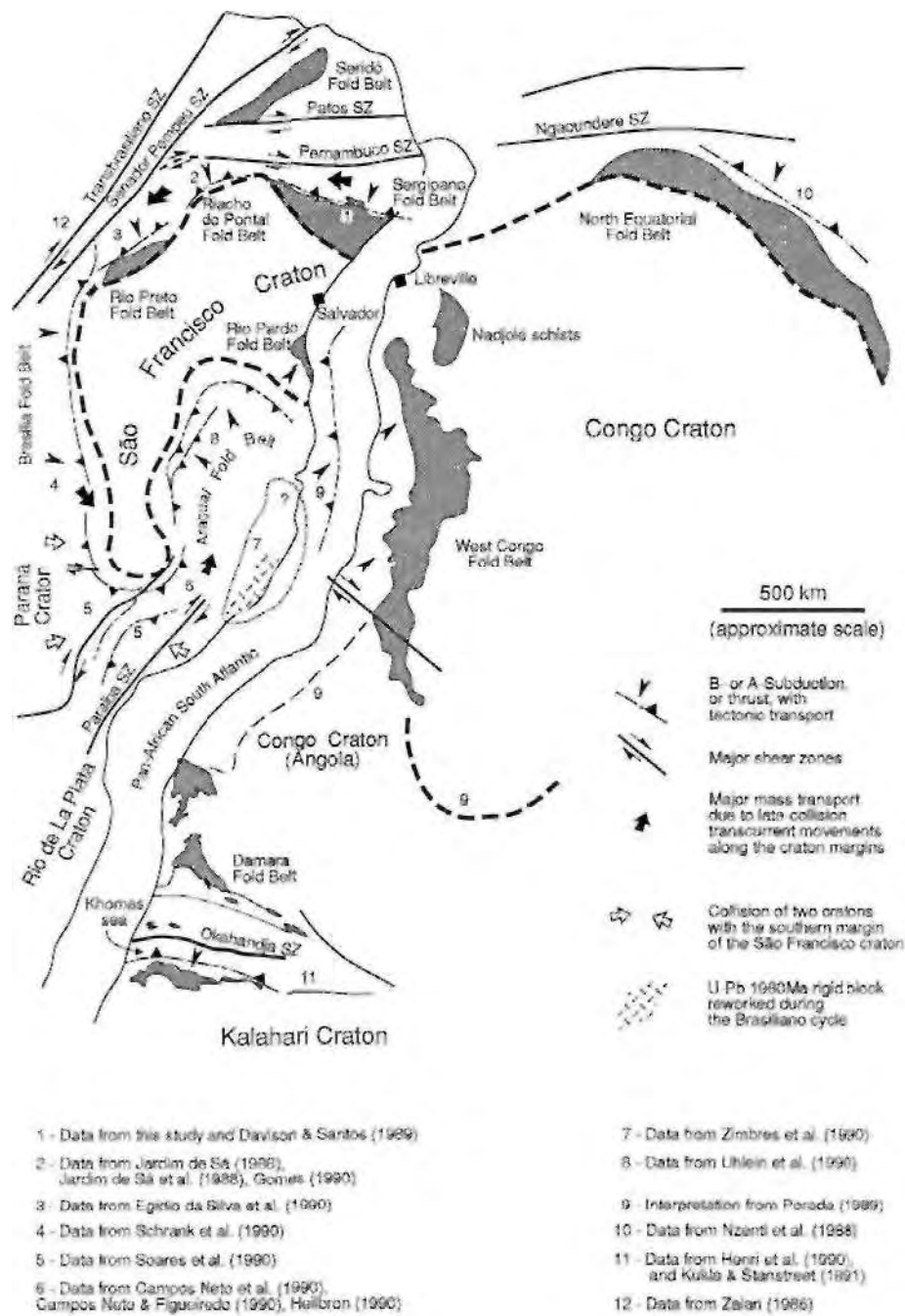


Figure 6.20 - The Late Proterozoic major tectonic elements around the São Francisco, Congo and Kalahari Cratons.

(Egidio da Silva et al. 1990; Uhlein et al. 1990). but some may have evolved into narrow internal oceans (e.g. this study; Henri et al. 1990; Soares et al. 1990).

The above suggests that in the closure of asymmetric basins similar to the Sergipano Basin (Fig. 6.18), subduction zones involving oceanic crust (B-subduction) passes axially into inverted extensional detachments of adjacent intracratonic basins, or alternatively into processes of A-subduction (Bally 1981). A modern analogue of this passage is postulated for the Tertiary evolution of the South China and Sulu seas (Howell 1989), whereas Shackleton (1986) argues that A-subduction settings are probably derivative from previous B-subduction processes.

Figure 6.20 shows some Late Proterozoic tectonic features which resulted from the closure of the original rift system. The combined result of many researches (see references in Fig. 6.20) is showing that the São Francisco Craton was probably subducted underneath the Pernambuco-Alagoas Massif and Paraná Craton, but overrides the West Congo Craton, which in turn overrides the Kalahari Craton to the south (Fig. 6.20).

This complex pattern of intracontinental deformation is further complicated if several smaller cratonic blocks which occur around the São Francisco Craton (as in Fig. 2 of Brito Neves & Cordani 1991) are considered. For example, the recently characterised Transamazonian-age rigid block described to the southeast of the São Francisco Craton (see 7, Fig. 6.20), could be either a continuation of the Angola Craton (Zimbres et al. 1990), or a continuation of the Rio de La Plata Craton.

Strike-slip movements along the Transbrasiliano, Senador Pompeu, Pernambuco and Paraíba crustal-scale shear zones, and other smaller faults to the south of the São Francisco Craton have further added to the tectonic complexity (Fig. 6.20).

Taken together, all of these movements strongly suggest a pattern of intracontinental deformation accommodated by rotation of crustal blocks and the development of widespread mylonitic zones. Such movement patterns are expected to be within the limits of the Proterozoic paleomagnetic data (Briden 1976), and have been incorporated in a model of a fluid-chanellised Proterozoic mega-mylonitic crust (Katz 1982). The connection of the Patos shear with the tectonic evolution of the Seridó Fold Belt (Fig. 6.20; Corsini et al. 1991) is an example possibly similar to this process.

The polycyclic evolution of many of these Brazilian and African Late Proterozoic Fold Belts (e.g. Ribeiro et al. 1990; Gomes 1990; Corsini et al. 1991) implies that these cyclic events occurred at essentially the same locations. Nance et al. (1988) postulated that Proterozoic plate tectonics was governed by a regular cyclical process of continuous disaggregation and amalgamation of a Proterozoic supercontinent along the same tectonic zones.

These authors consider heat as the primary engine of this process, and heat diffusion through the continental crust as the key for its understanding. Cox (1991) suggested a causal relationship between the upwelling of mantle plumes, continental break-up and the mechanisms which trigger subduction. If so, this process will have also to account for other complexities of the system, such as the anomalous tectonic transport of some fold belts, as the Rio Pardo (Fig. 6.19), the Australian Lachlan Fold

Belt (Gray et al. 1991) and the Paraguai Fold Belt (Alvarenga 1990) of the eastern margin of the Amazon Craton (see 8, Fig. 2.11 A).

Davison & Santos (1989) showed the difficulties in correlating mobile zones between Brazil and Africa (Fig. 6.20) because fold belts with very similar lithologies have different directions of tectonic transport, such that found for the Sergipano and West Congo Fold Belts (and Nadjolé schists) which may be part of a triple junction near Libreville. They also proposed the correlation between the Rio Preto, Sergipano and North Equatorial Fold Belts (Fig. 6.20). The correlation with the latter fold belt is reinforced because it shows sedimentation continuous from the craton to the mobile, and has a similar metamorphic zoning, although the axial zone contains granulites formed at $T=750^{\circ}\text{-}800^{\circ}$ and $P=10\text{-}12\text{kbar}$ (Nzenti et al. 1988).

Oldow et al. (1991) argued that transcurrent and thrust faults merge into the basal detachment, in virtually all fold belts, thus orogens float above subhorizontal zones of ductile flow in the lower crust (or above upper mantle detachments). They pointed out variations in the tectonic transport within an orogen may be due to relative motions of thrust sheets above the basal detachment. If so, different tectonic transport directions of Proterozoic fold belts (Fig. 6.20) may be due to the practically simultaneous collision of several continental blocks. An understanding of such a process may rest on the role mantle plumes (=heat) to govern the movement of fluids within the lithosphere.

If Late Proterozoic rifts and fold belts are governed by mantle plumes, triple and cusped junctions of fold belts should be common and fold belts associated with different cratons will have similar stratigraphic and tectonic histories, as a result of the similarity of the processes that control basin formation and closure. Understanding the stratigraphic and tectonic evolution of Sergipano Fold Belt is a key to unravelling the Proterozoic history of the São Francisco Craton and the Proterozoic supercontinent.

Chapter 7 - Conclusions

This chapter presents the conclusions of this PhD thesis together with recommendations for further research in the Sergipano Fold Belt and São Francisco Craton, of northeastern Brazil.

1. The Itabaiana Dome Area surrounds the Itabaiana and Simão Dias gneiss domes, in the southern pan of the Sergipano Fold Belt. This is where basement-contact stratigraphic and structural relationships are best preserved in the Pan-African-Brasiliano orogenic system in Brazil.

2. A new stratigraphy has been erected for the southern part of the Sergipano Fold Belt. Correlations can be made from the craton into the fold belt. Details of the stratigraphy are summarised below.

3. The sedimentary record of the Itabaiana Dome Area and the southern part of the Sergipano Fold Belt has been divided in two sedimentary cycles, each consisting of two megasequences. Cycle I consists of the laterally continuous Estância and Miaba Groups. Cycle II consists of the Lagarto and Vaza Barris Groups. The sedimentation is probably 1100-900Ma old.

4. The 300m-thick Estância Group is comprised of the Juetê and Acauã Formations. The 1000m-thick Miaba Group consists of the Itabaiana, Ribeirópolis and Jacoca Formations.

5. The Estância-Miaba Group consists of the Juetê-Itabaiana, Ribeirópolis and Acauã-Jacoca Formations. The Juetê-Itabaiana quartzites, mudstones, minor conglomerates and diamictites, together with the Ribeirópolis phyllites, pebbly phyllites, diamictites and metavolcanics, form the siliciclastic megasequence of cycle I. The Acauã-Jacoca carbonates form the carbonate megasequence of cycle I.

6. The 700m-3000m-thick Lagarto Group was deposited both on the craton and in the basin and consists of the Lagarto-Palmares, Jacaré and Frei Paulo Formations. The basinal, 2000m-thick Vaza Barris Group comprises the Palestina and Olhos D'água Formations. The Lagarto Group siliciclastics and the Palestina diamictites and pebbly phyllites, form the siliciclastic megasequence of cycle II. The Olhos D'água carbonates form the carbonate megasequence of cycle II.

7. These miogeoclinal sediments record a continental to shallow marine sedimentation, with fault-bounded and localised deep-water basins (Vaza Barris trough). The basins appear to have been controlled by syndepositional extensional faulting and uplift of cratonic blocks at their margins.

8. The structure of the Itabaiana Dome Area is dominated by SW vergent recumbent F_1 folds which are coaxially refolded by SW vergent, upright to reclined F_2 folds and cut by steep, oblique-slip D_2 thrust faults developed in a sinistral transpressive deformation. Late stage, small scale F_3 folds, kinks and the associated minor strike-slip faults indicate orogen-parallel contraction and extension. These three ductile to ductile-brittle deformational phases (D_1D_3) affected both the metasediments and the basement gneisses.

9. D_1 structures are a layer-parallel S_1 foliation and generally rootless, southward verging, WNW-ESE trending and up to 35km wavelength recumbent F_1 folds. These may be associated with low-angle thrusts and are coaxially refolded by F_2 folds.

10. D_2 structures are open to tight, gently inclined to upright, WNW-ESE trending, and generally southerly verging F_2 folds. These folds have a penetrative pressure solution-type S_2 axial planar foliation, and subhorizontal fold axes parallel to a penetrative stretching lineation. F_2 folds are associated with WNW-ESE trending, sinistral oblique, steeply dipping faults, many of which are probably inverted extensional faults.

11. D_3 structures are transversal, open to tight, generally upright, kink-style, subhorizontal to subvertical folds, crenulations and kink bands. The F_3 folds are generally associated with a steep-dipping, NE-SW trending, spaced cleavage.

12. The Itaporanga fault separates the almost undeformed and unmetamorphosed cratonic domain to the south, from the deformed area consisting of the regional, Simão Dias, Itabaiana, west and east structural domains.

13. In the deformed area, the WNW-ESE trend of the S_2 and L_2 features in the regional, Simão Dias and Itabaiana structural domains change to NNW-SSE trend in the west and east domains, respectively to the west and east of the Itabaiana dome. F_2 folds are generally more open in the Itabaiana, west and east structural domains, than in the regional and Simão Dias domains.

14. Deformation is attributed to a polyphase, progressive monocyclic event of basin inversion associated with sub-greenschist metamorphism and tectonic transport of the metasedimentary wedge of the southern part of the Sergipano Basin towards the São Francisco Craton.

15. D_1 records layer-parallel shearing and N-S shortening, with duplication of the stratigraphy. D_2 records ENE-SSW shortening together with upward and E-W, out-of-section movements in a transpressive tectonic regime. The D_1 - D_2 total shortening is estimated at around 75%. D_3 records a minor and late-stage event of orogen-parallel shortening and extension.

16. The Itabaiana and Simão Dias gneiss domes were progressively developed by superposition of D_1 and D_2 deformations and occupy the core of overturned F_2 folds.

17. The Itabaiana dome probably underwent a syn- D_2 , top down to the west extension, developing a phyllonitic zone sub-parallel to the basal unconformity in the western margin of the dome. It also probably underwent a late- D_2 counterclockwise rotation of 25° about a vertical axis.

18. The thick Itabaiana quartzites which surround the Itabaiana dome probably acted as a barrier to D_2 deformation. The quartzites of the eastern margin of the dome are affected by generally NW-SE trending and subvertical shear zones, whereas those in the western margin are affected by open F_2 folds.

19. The Sergipano Fold Belt comprises three WNW-ESE trending, fault-separated but probably lithologically and structurally continuous domains. These are from south to north - the cratonic Estância Domain, the miogeoclinal Miaba/Vaza Barris Domain, and the eugeoclinal Macururé Domain.

20. The evolution of the Sergipano Fold Belt is interpreted to have resulted from the inversion of a half graben above a low-angle detachment of a listric fault system within the continental crust. The original basin probably passed axially to a small oceanic setting on its northeastern side.

21. The architecture of the whole Sergipano Fold Belt can be interpreted as a positive flower structure formed by the oblique collision between the Borborema Province and the São Francisco Craton.

22. Thrust belt-foreland basin and post-orogenic sedimentation models do not explain the cratonic sedimentation of the southern part of the Sergipano Fold Belt. A model combining tectonic loading with downwarping of an attenuated cratonic margin is proposed in order to account for the lack of foreland basin in this part of the belt.

23. The sequence stratigraphy of the Sergipano Fold Belt compares well with the sedimentary record of the other Brasiliano belts surrounding the São Francisco Craton, and also with other Pan-African belts around the Congo and Kalahari Cratons of Africa.

24. The evolution of the Middle-Late Proterozoic basins developed around the São Francisco Craton may have been the expression of the rise of a mantle plume underneath the craton. This model may be extended to other Pan-African and Brasiliano cratons such as the Amazon, West African, Congo, and Kalahari Cratons.

25. Proterozoic crustal processes of basin opening and closure may be related to the evolution of mantle plumes. Proterozoic Plate Tectonics appears to have been governed by a cyclic process of supercontinent fragmentation and amalgamation along long-lived lines of lithospheric weakness.

Suggestions for further research in the Sergipano Fold Belt and the São Francisco Craton are as follows -

27. Field and/or geochronological evidence is required for the age of the Macambira phyllonites in the Itabaiana Dome Area. Such data may support the core complex hypothesis for the extension of the margin of the São Francisco Craton.

28. Detailed studies of the basement-cover relationships around the Jirau do Ponciano gneissic dome are recommended for definition of the tectonic transport during D_1 deformation in the Macururé Domain.

29. Detailed structural, metamorphic, paleomagnetic and age studies are recommended for the understanding of the affinities and mode of emplacement of the Canindé, Marancó and Poço Redondo Domains, as they may be suspect or allochthonous terranes.

30. Isotopic studies of the U-Pb and/or K-Ar systems across the Sergipano Fold Belt and its southern and northern cratonic margins, are recommended in order to understand the post-tectonic uplift of different segments of the belt.

31. More detailed studies are required on the syndepositional and possible extensional control of the sedimentation and lithofacies variations in the cratonic-pericratonic areas of the Rio Preto, Brasília and Araçuaí Fold Belts, in order to reconstruct the Pre-Brasiliano vertical movements of the São Francisco Craton.

32. An integrated tectono-stratigraphy is required for the marginal basins of the São Francisco Craton, in order to account for the stratigraphic evidence in the Sergipano Fold Belt. This could be a guide for similar studies around other cratons of the Pan-African-Brasiliano orogenic system.

33. Detailed structural analysis is required in key areas of the São Francisco Craton, in order to look for evidence of post-orogenic extension in the Early Proterozoic fold belts in the craton.

References

- Alkmin, F. F. de, Marshak, S. & Chemale Jr., F. 1990.** Evidências de uma tectônica extensional pré-inversão Brasileira, na porção sul do craton de São Francisco. XXXVI Congresso Brasileiro de Geologia, Anais SBG, Boletim de Resumos, p.249-250.
- Allard, G.O. 1969.** The Propria geosyncline, a key tectonic element in the continental drift puzzle of the South Atlantic. XXIII Congresso Brasileiro de Geologia, Salvador, Anais, SBG, p.47-59.
- Allard, G.O. & Hurst, V.J. 1969.** Brazil-Gabon geologic link supports continental drift. Science, Vol.163, p. 528-532.
- Almeida, F.F.M. de, Brito Neves, B.B. de, & Fuck, R.A. 1977.** Províncias estruturais brasileiras. VIII Simpósio de Geologia do Nordeste, Campina Grande, SBG, Atas, p.363-391.
- Almeida, F.F.M. & Hasui, Y. (coordenadores) 1984.** O pré-Cambriano do Brasil. Editora Edgard Blucher Ltda, p.378.
- Alvarenga, C.J.S. 1990.** Phenomenes sedimentaires, structuraux et circulation de fluides developpes a la transition chaine-craton: exemple de la chaine Paraguai d'age Proterozoic Superior, Mato Grosso, Bresil. PhD thesis, Universite de Droit, D'Economie et des Sciences D'Aix-Marseille, p. 170.
- Armin, K.A. & Mayer, L. 1983.** Subsidence analysis of Cordilleran Miogeocline: Implications for timing of Late Proterozoic rifting and amount of extension. Geology, vol.11, p.702-705.
- Auboin, J. 1965.** Geosynclines. Developments in Geotectonics, p.335, Elsevier-Amsterdam.
- Bally, A.W. 1981.** Thoughts on the tectonics of fold belts. In K.R. McClay & R.A. Price (eds), Thrust and Nappe Tectonics, Geological Society London Special Publication 9, p. 13-32.
- Barbosa, O. 1970.** Geologia econômica de parte da região do médio São Francisco. Boletim 140, Divisão de Fomento da Produção Mineral, DNPM, Rio de Janeiro.
- Barr, D. 1987.** Lithosphere stretching, detached normal faulting and footwall uplift. In M.P. Coward, J.F. Dewey & P.L.Hancock (eds), Continental Extensional Tectonics, Geological Society of London Special Publication 28, p.75-94.

- Barr, D. 1991.** Subsidence and sedimentation in semi-starved half-graben: a model based on North Sea data. In A.M. Roberts, G. Yielding, & B.Freeman (eds). *The Geometry of Normal Faults*, Geological Society of London Special Publication 56, p. 17-28.
- Beaumont, C. 1981.** Foreland basins. *Geophysical Journal Royal Astronomy Society*. Vol.65. p.291-329.
- Bechstadt, T. & Boni, M. 1989.** Tectonic control on the formation of a carbonate platform: the Cambrian of southwestern Sardinia. In P.D.Crevello, J.L.Wilson, J.F.Sarg & J.F.Read (eds), *Controls on Carbonate Platform and Basin Development*, SEPM Special Publication 44, p.107-120.
- Berthe, D., Choukroune, P. & Jegouzo, P. 1979.** Orthogneiss, mylonite and non-coaxial deformation of granites: the example of the South Armorican Shear Zone. *Journal of Structural Geology*, Vol.1, p.31-42.
- Blais, S., Jardim de Sá, E.F., Bezerra, F.G.R. & Nilson, A.A. 1989.** Preliminary data on the Canindé Complex, Sergipe Belt (northeast Brazil): a Brasiliano island arc?. *Terra Abstracts*, Vol.1, p.273.
- Bezerra, F.H.R., Nilson, A.A., Blais, S., & Jardim de Sá, E.F. 1989.** O Complexo Canindé do São Francisco e rochas encaixantes: resultados preliminares. XIII Simpósio de Geologia do Nordeste e II Simpósio Nacional de Estudos Tectônicos, Fortaleza. *Anais*, p.46-48.
- Bezerra, F.H.R., Nilson, A.A., Blais, S., & Jardim de Sá, E.F. 1990.** Contribuição à geologia e geoquímica do complexo Canindé do São Francisco e rochas encaixantes (Se-Al). XXXVI Congresso Brasileiro de Geologia, Natal, *Boletim de Resumos*, p.305.
- Borradaile, G.J. 1981.** Minimum strain from conglomerates with ductility contrast. *Journal of structural geology*, Vol.3, p.295-297.
- Bradley, D.C. & Kidd, W.S.F. 1991.** Flexural extension of the upper continental crust in collisional foredeeps. *Geological Society of America Bulletin*, Vol.103, p. 1416-1438.
- Briden, J.C. 1976.** Application of paleomagnetism of Proterozoic tectonics. *Philosophical Transactions Royal Society of London, Series A* 280, p.405-416.
- Brito Neves, B.B. de 1975.** Regionalização geotectônica do Precambriano nordestino. Tese de Doutorado, Inst, de Geociências-USP, São Paulo, 198p.

- Brito Neves, B.B. de 1986.** Tectonic regimes in the Proterozoic of Brazil. In 12°. Simpósio de Geologia do Nordeste, João Pessoa, Atas, SBG, p.235-251.
- Brito Neves, B.B. de & Cordani, U.G. 1973.** Problemas geocronológicos do "Geosinclinal Sergipano" e do seu embasamento. In XXVII Congresso Brasileiro de Geologia, Aracaju, Anais, SBG, p.67-76.
- Brito Neves, B.B. de, Sial, A.N. & Beurlen, H. 1977 a.** O sistema de Dobramentos Sergipano: análise do conhecimento. Atas Reunião Preparatória para o Simpósio sobre o Craton do São Francisco e suas faixas marginais. Salvador, Ba, Brazil, publicação SBG-SME-CPM, p.369-391.
- Brito Neves, B.B. de, Sial, A.N. & Albuquerque, J.P.T. 1977 b.** Vergência centrífuga residual no sistema de dobramentos Sergipano. Revista Brasileira de Geociências, Vol.7 (2) p.102-114.
- Brito Neves, B.B. de, Kawashita, K. & Mello, E.Z.V. de 1977 c •** Estudo geocronológico do Grupo Estância pelo método Rb-Sr. VIII Simpósio de Geologia do Nordeste, Campina Grande, Atas, p.311-321.
- Brito Neves, B.B. de, Campos Neto, M. da C. & Rangel, J.M. 1987.** Contribuição à análise estrutural do Sistema Sergipano. CNPq/SDC, Relatório do Processo 40.7211/84GL, 53p. Unpublished.
- Brito Neves, B.B. de & Cordani, U.G. 1991.** Tectonic evolution of South America during the Late Proterozoic. Precambrian Research, Vol.53, p.23-40.
- Brown, D., Van Gool, J., Calon, T. & Rivers, T. 1991.** The geometric and kinematic development of the Emma Lake Thrust stack, Grenville Front, southwestern Labrador. Canadian Journal of Earth Sciences, Vol.28, p. 136-144.
- Brumbaugh, D.S. 1984.** Compressive strains generated by normal faulting. Geology, Vol.12, p.491-494.
- Brun, J.P. 1983.** L'Origine des domes gneissiques: modeles et tests. Bulletin Société Géologique de France, Vol.7, Tome XXV, N. 2, p.219-228.
- Brun, J.P., Wenzel, F. & ECORS-DEKORP Team 1991.** Crustal-scale structure of the southern Rhine graben from ECORS-DEKORP seismic reflection data. Geology, Vol.19, 758-762.

Campos Neto, M. da C. & Brito Neves, B.B. de 1987. Considerações sobre a organização e geometria do Sistema de Dobramentos Sergipano. In I Simpósio Nacional de Estudos Tectônicos, Salvador, Ba, UFBA, Boletim de Resumos, p.90-93.

Campos Neto, M.C. & Figueiredo, M.C.H. 1990. Evolução geológica dos terrenos costeiro, Paraíba do Sul e Juiz de Fora (RJ-MG-ES). XXXVI Congresso Brasileiro de Geologia, Natal, Anais SBG, Vol.6, p.2631-2648.

Campos Neto, M.C, Perrota, M.M., Peloggia, A.U.G. & Figueiredo, M.C.H. 1990. A porção ocidental da faixa Alto Rio Grande. XXXVI Congresso Brasileiro de Geologia, Natal, Anais SBG, Vol.6, p.2615-2630.

Carl, B.S., Miller, CF. & Foster, D.A. 1991. Western Old Woman Mountains Shear Zone: Evidence for late ductile extension in the Cordilleran Orogenic Belt. *Geology*, Vol.19, p.893-896.

Cassedane, J.P. & Silva Filho, M.A. 1982. Stromatolites du Saco da Camisa (Sergipe). *Anais Academia Brasileira de Ciências*, Vol.54, p.429-439.

Castro, J. 1987. Short Course on Depositional Systems. UFRN, Natal, Brazil, leading field excursion to the Sergipano Fold Belt, September 1987.

Christie-Blick, N. & Biddle, K.T. 1985. Deformation and basin formation along strike-slip faults. *SEPM*, Vol.1, p.1-33.

Cliff, R.A., Drewery, S.E. & Leeder, M.R. 1991. Sourcelands for the Carboniferous Pennine river system: constraints from sedimentary evidence and U-Pb geochronology using zircon and monazite. In A.C. Morton, S.P. Todd & P.D.W. Haughton (eds) *Development in Sedimentary provenance Studies*. Geological Society, London, Special Publication 57, p.137-159.

Cloud, P.E. & Dardenne, M.A. 1973. Proterozoic age of the Bambui Group in Brazil. *Geological Society of America Bulletin*, Vol.84, p. 1673-1676.

Collier, R.E., LI. 1991. The Lower Carboniferous Stainmore Basin, N. England: extensional basin tectonics and sedimentation. *Journal of the Geological Society*, London, Vol.148, **Part 2**, p.379-390.

Collins, E.W. & Raney, J.A. 1991. Neotectonic history and geometric segmentation of the Campo Grande fault: A major structure bounding the Hueco basin, Trans-Pecos, Texas. *Geology*, Vol.19, p.493-496.

Conceição Filho, V.M. & Sales, J.C.S. de 1988. Projeto Faixa Sergipana. Relatório interno convênio SME/CBPM, Salvador, Brazil, 29p.

Coney, P.J. & Harms, T.A. 1984. Cordilleran metamorphic core complexes: Cenozoic extensional relics of Mesozoic compression. *Geology*, Vol. 12, p.550-554.

Cook, H.E. & Mullins, H.T. 1983. Basin Margin Environment. In P.A. Scholle, D.G. Bebout, C.H. Moore (eds). Carbonate Depositional Environments. The American Association of Petroleum Geologists, Memoir 33, p.540-617.

Cooper, M.A. & Trayner, P.M. 1986. Thrust-surface geometry. Implications for thrust-belt evolution and section balancing techniques. *Journal of Structural Geology*, Vol.8, p.305-312.

Corsini, M., Vauchez, A., Archanjo, C. & Jardim de Sá, E.F. 1991. Strain transfer at continental scale from a transcurrent shear zone to a transpressional fold belt: The Patos-Seridó system, northeastern Brazil. *Geology*, Vol.19, p.586-589.

Couto, J.G.P. 1984. Algumas considerações sobre a evolução tectônica/metagenética dos continentes sulamericano e africano no Proterozóico (formação de bacias rifeanas) e os efeitos de uma tríplice colisão cratônica na região sul do Estado de Minas Gerais e áreas adjacentes dos Estados do Rio de Janeiro e São Paulo (Brasil). XXXIII Congresso Brasileiro de Geologia, Rio de Janeiro, Anais, SBG, p.3044-3055.

Couto, J.G.P. & Bez, L. 1981. A glaciação Jequitaiá: um guia estratiográfico para o Precambriano Superior no Brasil. *Revista Brasileira de Geociências*, Vol.1 1, p. 17-21.

Cox, K.G. 1991. Tectonics and volcanism of the Karoo period in southern Africa and adjacent areas. Geological Society of London, International, Multidisciplinary Tectonic Studies Group meeting, 3-4/October, Programme with abstracts.

Coward, M.P. 1981 a. The Moaby Syncline: the West Congolian of Gabon and its tectonic significance. *Annales de La Société Géologique de Belgique*, T104, p. 102-104.

Coward, M.P. 1981 b. Diapirism and gravity tectonics: report of a Tectonic Studies Group conference, held at Leeds University, 25-26 March 1980. *Journal of Structural Geology*, Vol.3, 89-95.

Dahlstrom, C.D.A. 1969. Balanced cross-sections. *Canadian Journal of Earth Sciences*, Vol.6, p.743-757.

Daly, M.C. 1986. The intracratonic Irumide belt of Zambia and its bearing on collision orogeny during the Proterozoic of Africa. In M.P. Coward & A.C. Ries (eds) *Collision Tectonics*, Geological Society of London Special Publication 19, p.321-328.

Davis, G.A. & Lister, G.S. 1988. Detachment faulting in continental extension; Perspectives from the southwestern U.S. Cordillera. Geological Society of America Special Paper 218, p. 133-159.

Davis, G.A., Yu, H., Qian, X., Zheng, Y., Wang, C, Tong, H.M., Gehrels, G.E. & Shafidullah, M. 1991. A Mesozoic metamorphic core complex in the Yungmeng Shan north of Beijing, China-Variations on Cordilleran themes. Geological Society of America Abstracts with Program, 87th Annual Cordilleran Section, p. 17.

Davison, I. 1987. Acreção de terrenos e a colisão oblíqua do Proterozóico Superior na Faixa Sergipana. In I Simpósio Nacional de Estudos Tectônicos, Salvador, Ba, UFBA. Boletim de Resumos, p.87-89.

Davison, I. 1989. Extensional domino fault tectonics: kinematics and geometrical constraints. *Annales Tectonicae*, Vol. III, p .12-24.

Davison, I. & Santos, R.A. dos 1989. Tectonic Evolution of the Sergipano Fold Belt, NE Brazil, during the Brasiliano Orogeny. *Precambrian Research*, Vol.45, p. 319-342.

Dean, W.E. & Fouch, T.D. 1983. Lacustrine environments. In P.A. Scholle, D.G. Bebout, C.H. Moore (eds), *Carbonate Depositional Environments*. The American Association of Petroleum Geologists, Memoir 33, p.98-130.

D'el-Rey Silva, L.J.H. 1985. Geologia e controle estrutural do depósito cuprífero Caraíba, Vale do Curaçá, Bahia, Brasil. UFBA, Dissertação de Mestrado, 158p.

D'el-Rey Silva, L.J.H., Rocha da Rocha, A.M., Mota, E.R., Reis, J.G. & Cavalcante, P.R.B. 1988. Controle estrutural da Mina de Cobre Caraíba: Implicações na lavra e na tectônica das faixas móveis do Proterozóico Inferior. XXXV Congresso Brasileiro de Geologia, Belém, Anais SBG, Vbl.1, p16-29.

Dickinson, W.R. & Suczeck, CA. 1979. Plate Tectonics and sandstone composition. *American Association of Petroleum Geologists Bulletin*, Vol.63, p.2164-2182.

Dolan, J. & Ogawa, Y. 1989. Upslope deposition of extremely distal turbidites: an example from the Tiburon Rise, west-central Atlantic. *Geology*, Vol.17, p.990-994.

Donker, J.M. Van B. 1990. Fold interference and collision. Geological Society London, Tectonic Studies Group 21, Liverpool, Programme with Abstracts.

Egidio da Silva, M., Karmann, I. & Trompette, R. 1989. Litoestratigrafia do Supergrupo Espinhaço e Grupo Bambuí no Noroeste do Estado da Bahia. Revista Brasileira de Geociências, Vol. 19 (2), p. 141-152.

Egidio da Silva, M., Karmann, I. & Trompette, R. 1990. O sistema de dobramentos Rio Preto - Borda nordeste do craton do São Francisco. XXXVI Congresso Brasileiro de Geologia, Anais SBG, vol.6, p.2658-2671.

Ellis, M. & Watkinson, A.J. 1987. Orogen-parallel extension and oblique tectonics: the relation between stretching lineations and relative plate motions. *Geology*, vol.15, p.1022-1026.

Encal S.A. 1978. Projeto Baixo São Francisco: Levantamento Aeromagnetométrico e Aerogamaespectométrico. Relatório Final, p.35, CPRM, Rio de Janeiro.

England, P.C. & Richardson, S.W. 1977. The influence of erosion upon the mineral facies of rocks from different metamorphic environments. *Journal of the Geological Society, London*, vol.134, p.201-214.

England, P.C. & Thompson, A.B. 1984. Pressure-temperature-time paths of regional metamorphism, I: Heat transfer during the evolution of regions of thickened continental crust. *Journal of Petrology*, Vol.25, p.894-928.

Enos, P. 1983. Shelf Environment. In P.A. Scholle, D.G. Bebout, C.H. Moore (eds), Carbonate Depositional Environments. The American Association of Petroleum Geologists, Memoir 33, p.268-295.

Essene, E.J. 1989. The current status of thermobarometry in metamorphic rocks. In J.S. Daly, R.A. Cliff & B.W.D. Yardley (eds) Evolution of Metamorphic Belts, Geological Society of London Special Publication 43, p. 1-44.

Esteban, M. & Klappa, C.F, 1983. Sub-aerial exposure. In P.A. Scholle, D.G. Bebout, C.H. Moore (eds), Carbonate Depositional Environments. The American Association of Petroleum Geologists, Memoir 33, p. 1-54.

Eyles, N. & Miall, A.D. 1984. Glacial facies. In R.G.Walker (ed), Facies Model, 2nd edition. Geosciences Canada Reprint Series 1, p. 15-38.

Fleischer, V.D., Garlick, W.G. & Haldane, R. 1976. Geology of the Zambian Copperbelt. In K.H. Wolf (ed) Handbook of Stratabound and Stratiform Ore Deposits, vol.6, Chapter 6, p.223-352, Elsevier.

Flemming, B.W. 1981. Factors controlling shelf sediment dispersal along the southeast African continental margin. *Marine Geology*, Vol.42, p.259-277.

Flinn, D. 1962. On folding during three-dimensional progressive deformation. *Journal of the Geological Society London*, Vol.118, p.385-428.

Flinn, D. 1965. On the symmetry principle and the deformation ellipsoid. *Geological Magazine*, Vol.102, p.36-45.

Fry, N. 1979. Random points distributions and strain measurements in rocks. *Tectonophysics*, Vol.60, p.89-105.

Fujimori, S. 1989. Contribuição ao estudo dos granitóides do sistema de dobramentos Sergipano. *Revista Brasileira de Geociências*, Vol. 19 (2), p.241-247.

Gava, A., Nascimento, D.A. do, Vidal, J.L.B., Ghignone, J.I., Oliveira, E.P. de, Santiago Filho, A.L. & Teixeira, W. 1983. Projeto RADAMBRASIL, Geologia. Mapa geológico, Folhas SC.24/25, Aracaju/Recife, escala 1:1.000.000, Rio de Janeiro, Levantamento de Recursos Naturais 30.

Ghosh, S.K. 1982. The problem of shearing along axial plane foliation. *Journal of Structural Geology*, Vol.4, p.63-67.

Gibbs, A.D. 1984. Structural evolution of extensional basin margins. *Journal of the Geological Society, London*, Vol.141, p.609-620.

Gibbs, A.D. 1987. Development of extension and mixed-mode sedimentary basins. In M.P. Coward, J.F. Dewey & Hancock, P.L. (eds), *Continental Extensional Tectonics*, Geological Society of London Special Publication 28, p. 19-33.

Giuliani, G. & Santos, R.A. dos 1988. Geoquímica de alguns granitóides da Faixa de Dobramentos Sergipana. XXXV Congresso Brasileiro de Geologia, Belém, Anais, SBG, Vol.3, p.1037-1052.

Gomes, F.E.M. 1990. Relações litoestratigráfico-estruturais e evolução tectônica na faixa Riacho do Pontal - Região de Paulistana (Pi). XXXVI Congresso Brasileiro de Geologia, Natal, Anais, SBG, Vol.6 p.2843-2857.

Gray, D.R. 1977. Morphologic classification of crenulation cleavage. *Journal of Geology*, Vol.85, p.229-235.

Gray, D.R., Wilson, C.J.L. & Barton, T.J. 1991. Intracrustal detachments and implications for crustal evolution within the Lachlan fold belt, southeastern Australia. *Geology*, Vol.19, p.574-577.

Grotzinger, J.P. 1989. Facies and evolution of Precambrian carbonate depositional systems: emergence of modern platform archetype. In P.D.Crevello, J.L. Wilson, J.F. Sarg & J.F.Read (eds): *Controls on Carbonate Platform and Basin Development*, SEPM Special Publication 44, p.79-106.

Guimarães, J.G., Silva, R.W.S. & Toledo, L.A.A. de 1991. Relatório Final do Projeto Sulfetos da Faixa Sergipana. CBPM, Salvador, Brazil.

Gustavson, T.C. 1974. Sedimentation on gravel outwash fans, Malaspina Glacier foreland, Alaska. *Journal of Sedimentary Petrology*, Vol.44, p.374-389.

Hall, A. 1987. *Igneous Petrology*. Longman Scientific & Technical, 571 p.

Hanks, C.L. & Wallace, W.K. 1990. Cenozoic thrust emplacement of a Devonian batholith, northeastern Brooks Range: Involvement of crystalline rocks in a foreland fold-and-thrust belt. *Geology*, Vol.18, p.395-398.

Hanselman, D.H., Conolly, J.R. & Home, J.C. 1974. Carbonate environments in the Wilhite Formation of Central Eastern Tennessee. *Geological Society of America Bulletin*, Vol.85, p.45-50.

Hasui, Y. & Costa, J.B.S. 1990. O cinturão Araguaia: um novo enfoque estrutural-estratigráfico. XXXVI Congresso Brasileiro de Geologia, Natal, Anais SBG, vol.6, p.2535-2549.

Heilbron, M. 1990. O limite entre as faixas de dobramentos Alto Rio Grande e Ribeira, na seção geotransversal, Bom Jardim de Minas (MG) - Barra do Piraí (RJ). XXXVI Congresso Brasileiro de Geologia, Natal, Anais SBG, Vol.6, p.2813-2826.

Henry, G., Clendenin, C.W., Stanistreet, I.G. & Maiden, K.J. 1990. Multiple detachment model for the early rifting stage of the Late Proterozoic Damaran orogen in Namibia. *Geology*, Vol.18, p.67-71.

Herrington, P.M. & Fairchild, I.J. 1989. Carbonate shelf and slope facies evolution prior to Vendian glaciation, Central east Greenland. In R.A. Gayer (ed), *The Caledonide Geology of Scandinavia*, Graham & Trotman Publishers, p.263-273.

Hertz, N., Hasui, Y., Costa, J.B.S. & Matta, M.A. da S. 1989. The Araguaia Fold Belt, Brazil: a reactivated Brasiliano-Pan-African cycle (550Ma) geosuture. *Precambrian Research*, Vol.42, p.371-386.

Higgs, W.G., Williams, G.D. & Powell, C.M. 1991. Evidence for flexural shear folding associated with extensional faults. *Geological Society of America Bulletin*, Vol.103, p.710-717.

Hirst, J.P.P. & Nichols, G.J. 1986. Thrust tectonic controls on Miocene alluvial distribution patterns, southern Pyrenees. *Special Publications International Association Sedimentologists*, Vol.8, p.247-258.

Hoffman, P. 1974. Shallow and deep water stromatolites in Lower Proterozoic platform-to-basin facies change, Great Slave Lake, Canada. *American Association of Petroleum Geologists Bulletin*, Vol.58, p.856-867.

Holdsworth, R.E. 1989. The geology and evolution of a Caledonian fold and ductile thrust zone, Kyle of Tongue region, Sutherland, Northern Scotland. *Journal of the Geological Society*, Vol.146, p.809-823.

Holdsworth, R.E. 1990. Progressive deformation structures associated with ductile thrusts in the Moine Nappe, Sutherland, Northern Scotland. *Journal of Structural Geology*, Vol.12, p.443-452.

Holdsworth, R.E. & Strachan, R.A. 1991. Interlinked system of ductile strike-slip and thrusting formed by Caledonian sinistral transpression in northeastern Greenland. *Geology*, Vol.19, p.510-513.

Horbach, R. & Marimon, M.P.C. 1988. O depósito de Cobre do Serrote da Laje, em Arapiraca, Alagoas. XXXV Congresso Brasileiro de Geologia, Belém, Anais SBG, Vol.1, p.1-15.

Hossack, J.R. 1968. Pebble deformation and thrusting in the Bygdin area (southern Norway). *Tectonophysics*, Vol.5, p.315-339.

Hossack, J.R. 1979. The use of balance cross-sections in the calculation of orogenic contraction: a review. *Journal of the Geological Society, London*, Vol. 136, p.705-711.

Houseknecht, D.W. 1986. Evolution from passive margin to foreland basin: the Atoka Formation of the Arkoma basin, south-central U.S.A. *Special Publications International Association Sedimentologists*, Vol.8, p.327-346.

Howell, D.G. 1989. Tectonics of suspect terranes, Mountain building and continental growth. Chapman and Hall, Topics in the Earth Sciences 3, 232p.

Hsu, T.C. 1966. The characteristics of coaxial and non-coaxial strain paths. Journal of Strain Analysis, Vol.1, p.216-222.

Hubbard, R.J., Pape, J. & Roberts, D.G. 1985 a. Depositional sequence mapping as a technique to establish tectonic and stratigraphic framework and evaluate hydrocarbon potential on a passive continental margin. In O.R. Berg & D.G. Woolveiton (eds.): Seismic stratigraphy, Volume II. American Association of Petroleum Geologists, Memoir 39, p.79-92.

Hubbard, R.J., Pape, J. & Roberts, D.G. 1985 b. Depositional sequence mapping as a technique to establish tectonic and stratigraphic framework to illustrate the evolution of a passive continental margin. In O.R. Berg & D.G. Woolverton (eds.): Seismic stratigraphy. Volume II. American Association of Petroleum Geologists, Memoir 39, p.93-115.

Humphrey, F.L. & Allard, G.O. 1962. Reconnaissance of the Geology of Pre-Cretaceous Rocks in the State of Sergipe. Petrobrás, Salvador, Relatório 1625, 37p.

Humphrey, F.L. & Allard, G.O. 1967. O geosinclinal de Propria: província tectônica do Pré-Cambriano posterior, recém-descoberta no escudo brasileiro. Boletim Técnico da Petrobrás, Rio de Janeiro, Brazil, Vol. 10, p.409-430.

Humphrey, F.L. & Allard, G.O. 1968. The Propria geosyncline, a newly recognised tectonic element in the Brazilian shield. International Geology Congress 23, Praga, Vol.4, p. 123-139.

Humphrey, F.L. & Allard, G.O. 1969. Geologia do domo de Itabaiana (Sergipe) e sua relação com a geologia do geosinclinal de Propria, um elemento tectônico recém reconhecido no escudo brasileiro. Petrobrás, CENPES, Rio de Janeiro, p.104.

Hurley, P.M. 1966. Variations in isotopic abundances of strontium, calcium, and argon and related topics. M.I.T Fourteen Annual Progress Report for 1966.

Hurley, P.M., & 8 others 1967. Test of Continental Drift by Comparison of Radiometric ages. Science, Vol.157, p.495-500.

Inda, H.A.V. & Barbosa, J.F. 1982. Texto explicativo para o mapa geológico do Estado da Bahia, escala 1: 1,000,000. Salvador, SME-CPM, 137p.

- Inden, R.F. & Moore, C.H. 1983.** Beach environment. In P.A. Scholle, D.G. Bebout & C.H. Moore (eds), Carbonate Depositional Environments. The American Association of Petroleum Geologists, Memoir 33, p.212-265.
- Jamison, W.R. 1991.** Kinematics of compressional fold development in convergent wrench terranes. Tectonophysics, Vol.190, p.209-232.
- Jardim de Sá, E.F. 1986.** Análise geotectônica e avaliação do potencial mineral da Faixa Sergipana nos Estados da Bahia, Sergipe e Alagoas - Internal report, Mineração Caraiba, Bahia.
- Jardim de Sá, E.F. 1988.** An update of the Precambrian geology of Northeast Brazil. International meeting on Proterozoic geology and tectonics of high-grade terrains. LLe-Lfe, Nigeria, Program and Lecture Series, 23p.
- Jardim de Sá, E.F. & Calheiros, M.E.V. 1981.** Estruturas em nível profundo e o retrabalhamento do embasamento na Faixa Alagoana (Região de Palmeira dos índios). X Simpósio de Geologia do Nordeste, Atas, SBG, p.351-360.
- Jardim de Sá, E.F., Legrand, J.M. & Hackspacher, P.C. 1981.** Contraste de estilos estruturais e metamórficos na faixa dobrada Sergipana. Revista Brasileira de Geociências, Vol.11, p. 128-137.
- Jardim de Sá, E.F., Souza, Z.S., Fonseca, V.P. & Legrand, J.M. 1984.** Relações entre "greenstone belts" e terrenos de alto grau: o caso da faixa Rio Capim, NE da Bahia. In XXXIII Congresso Brasileiro de Geologia, Rio de Janeiro, Anais, SBG, Vol.6, p.2615-2629.
- Jardim de Sá, E.F., Moraes, J.A.C. de & D'El-Rey Silva, L.J.H. 1986.** Tectônica tangencial na Faixa Sergipana. Anais XXXIV Congresso Brasileiro de Geologia, Goiânia, Anais, SBG, Vol.3, p. 1246-1259.
- Jardim de Sá, E.F., Macedo, M.H.F., Torres, H.H.F. & Kawashita, K. 1988.** Geochronology of metaplutonics and the evolution of supracrustal belts in the Borborema province, NE Brazil. VII Congresso Latino-Americano de Geologia, Belém, Anais SBG, p.49-62.
- Jiang, Z., Zhao, C. & Menghuy, L. 1990.** The lake floor trench. 13TH International Sedimentology Congress, Abstracts, Papers, p.249.
- Johnson, H.D. & Baldwin, C.T. 1986.** Shallow siliciclastic seas. In H.G. Reading (ed), Sedimentary Environments and Facies, 2nd edition, Blackwell Scientific Publications, p.229-282.

Jones, J.P. 1989. Marginal fold belts of the Eastern Guaporé shield - Their Origins and related problems. *Revista Escola de Minas Ouro Preto* Vol.42, p.31-48.

Jordan, H. 1971. The Late Precambrian Synclinorium of Curaçá (Brazil). *Geologische Jb.* Vol.88, p.617-628.

Karfunkel, J. & Hoppe, A. 1988. Late Proterozoic glaciation in central-eastern Brazil: synthesis and model. *Palaeogeography, Palaeoclimatology, Palaeoecology*, vol.65, p.1-21.

Katz, M.B. 1982. Mobile belt-craton tectonic relationships in Precambrian Gondwanaland: Mega-analog of structural features found in shear and mylonite zones?. *International Symposium on Archean-Proterozoic Crustal Evolution, ISAP, Salvador-BA, SME/SBG/CNPq*, p.8-14.

Kent, R. 1991. Lithospheric uplift in Eastern Gondwana: evidence for a long-lived mantle plume system. *Geology*, Vol.19, p.19-23.

Knipe, R.J. 1989. Deformation Mechanisms - recognition from natural tectonites. *Journal of Structural Geology*, Vol.11, p.127-146.

Krebs, A.S.J., Silva, M.A.S., Dias, A.A., Lopes, R.C. & Camozzato, E. 1990. O Grupo Itajaí na folha de Botuverá (SC) - Modelo/Geométrico cinemático e relações com o cinturão granulítico e cinturão metavulcano-sedimentar Brusque-Instalação, preenchimento e inversão da bacia. XXXVI Congresso Brasileiro de Geologia, Natal, Anais SBG, Vol.6, p.2966-2975.

Kroner, A. 1977. Non-synchronicity of Late Precambrian glaciation in Africa. *Journal of Geology*, Vol.85, p.289-300.

Kroner, A. 1983. Proterozoic mobile belts compatible with the plate tectonics concept. In L.G. Medaris Jr., C.W. Byers, D.M. Michelson & W.C. Shanks (ed) *Proterozoic Geology: selected papers from an International Symposium*. Geological Society of America Memoir 161, p.59-74.

Kroner, A. & Rankama, K. 1973. Late Precambrian glaciogenic sedimentary rocks in southern Africa: a compilation with definition and correlation. *Geological Society of Finland Bulletin*, Vol.45, p.79-102.

Kukla, P.A. & Stanistreet, I.G. 1991. Record of Damaran Khomas Hochland accretionary prism in central Namibia: Refutation of an "ensialic" origin of a Late Proterozoic fold belt. *Geology*, Vol.19, p.473-476.

- Kusznir, N.J., Marsden, G. & Egan, S.S. 1991.** A flexural-cantilever simple-shear / pure-shear model of continental lithosphere extension: applications to the Jeanne d'Arc Basin, Grand Banks and Viking Graben, North Sea. In A.M. Roberts, G. Yielding & B.Freeman (eds). *The Geometry of Normal Faults*, Geological Society of London Special Publication 56, p.41-60.
- Lagarde, J.L. & Michard, L. 1986.** Stretching normal to the regional thrust displacement in a thrust-wrench shear zone, Rehamna Massif, Morocco. *Journal of Structural Geology*, Vol.8, p.483-492.
- Leite, W.A. 1969.** Geologia do Baixo São Francisco e depósitos de asbestos de Alagoas. SUDENE, Recife, Divisão de Geologia, unpublished internal report.
- Lindenmayer, Z.G. 1980.** Evolução geológica do Vale do Curaçá e dos corpos máficos/ultramáficos mineralizados a cobre. UFBA, Dissertação de Mestrado, 140p.
- Lisle, R.J. 1979.** Strain analysis using deformed pebbles: the influence of initial pebble shape. *Tectonophysics*, Vol.60, p.263-277.
- Lister, G.S. & Snoke, A.W. 1984.** S-C Mylonites. *Journal of Structural Geology*, Vol.5/6, p.617-638.
- Lister, G.S., Etheridge, M.A. & Symonds, P.A. 1986.** Detachment faulting and the evolution of passive continental margins. *Geology*, Vol.14, p.246-250.
- Lister, G.S. & Davis, G.A. 1989.** The origin of metamorphic core complexes and detachment faults formed during Tertiary continental extension in the northern Colorado River region, U.S.A. *Journal of Structural Geology*, Vol.12, p.65-94.
- Malavieille, J. & Taboada, A. 1991.** Kinematic model for post-orogenic Basin and Range extension. *Geology*, Vol.19, p.555-558.
- Markello, J.R. & Read, J.F. 1981.** Carbonate ramp-to-deeper shale shelf transitions of an upper Cambrian intrashelf basin, Nolinchucky Formation, southwest Virginia Appalachians. *Sedimentology*, Vol.28, p.573-597.
- Marsaglia, K.M. & Klein, G.D. 1983.** The paleogeography of Paleozoic and Mesozoic storm depositional systems. *Journal of Geology*, Vol.91, p. 117-142.
- Martin, D.McB., Stanistreet, I.G. & Camden-Smith, P.M. 1989.** The interaction between tectonics and mudflow deposits within the Main Conglomerate Formation in the 2.8-2.7 Ga Witwatersrand Basin. *Precambrian Research*, Vol.44, p. 19-38.

- Mascarenhas, J. de F., Misi, A., Motta, A.C. & Sá, J.H. da S. 1984.** Província São Francisco. In Almeida, FF.M. & Hasui, Y. (coordenadores), O pré-Cambriano do Brasil. Editora Edgard Blucher Ltda, p.46-122.
- McClay, K.R. 1977.** Pressure solution and cobble creep in rocks and minerals: a review. *Journal of the Geological Society London*, Vol.134, p.57-70.
- McClay, K.R. & Ellis, P.G. 1987.** Geometries of extensional fault systems developed in model experiments. *Geology*, Vol.15, p.341-344.
- McClay, K.R. & Buchanan, P.G. 1991.** Thrust faults in inverted extensional basins. In K.R. McClay (ed) *Thrust Tectonics*, Chapman & Hall, p.93-104.
- McKee, E.D. & Ward, W.C. 1983.** Eolian environment. In P.A. Scholle, D.G. Bebout, C.H. Moore (eds), *Carbonate Depositional Environments*. The American Association of Petroleum Geologists, Memoir 33, p. 132-170..
- McIlreath, I.A. & James, N.P. 1984.** Carbonate slopes. In R.G.Walker (ed), *Facies Model*, Geoscience Canada, Reprint Series 1, p.245-257.
- McPherson, J.G., Shanmugan, G. & Moiola, R.J. 1987.** Fan deltas and braid deltas: varieties of coarse-grained deltas. *Geological Society of America Bulletin*, Vol.99, p.331-340.
- Milani, E.J. & Davison, I. 1988.** Basement control and transfer tectonics in Recôncavo-Tucano-Jatobá rift. Northeast Brazil. *Tectonophysics*, Vol. 154(1), p.41-70.
- Miller, J.G.M. 1983.** Upper Precambrian unconformity within the Kingston Peak Formation, Panamint Range, eastern California. *Geological Society of America Abstracts with Program*, Vol.15, p.424.
- Misi, A. 1976.** As seqüências Bambuí no Estado da Bahia e as mineralizações de chumbo-zinco associadas. Tese para concurso de Livre Docência, UFBA, 80p.
- Mitchell, W.I & Owens, B. 1990.** The geology of the western part of the Fintona Block, Northern Ireland: evolution of Carboniferous basins. *Geological Magazine*, Vol.127, p.407-426, Cambridge University Press.
- Moraes, J.A.C. de, Rocha, A.M.R. da & Conceição Filho, V.M. 1987.** Tectônica rotacional na região de Bendengó (Ba): um caso de cisalhamento simples. In I Simpósio Nacional de Estudos Tectônicos, Salvador, Ba, UFBA, Boletim de Resumos, p.84-86.

- Motta, A. C. 1990.** Geofísica da área de Itabaiana. Relatório interno CPRM, Salvador, 20p.
- Muck, M.T. & Underwood, M.B. 1990.** Upslope flow turbidity currents: A comparison among field observation, Theory and laboratory models. *Geology*, Vol.18, p. 54-57.
- Murphy, D.C. 1990.** Basement involvement in Middle Jurassic west-vergent deformation, Omineca Belt hinterland, southeastern Canadian Cordillera: geometry and implications for crustal-scale cross-sections. In K.R. McClay (ed): Thrust Tectonics Conference 1990, p.35.
- Murphy, J.B. & Nance, R.D. 1990.** Interior and exterior Late Proterozoic orogenic belts: a record of supercontinent accretion and dispersal. Geological Society of London, Tectonic Studies Group, meeting 21, Liverpool, Programme with Abstracts.
- Murphy, J.B. & Nance, R.D. 1991.** Supercontinent model for the contrasting character of Late Proterozoic orogenic belts. *Geology*, Vol.19, p.469-472.
- Naha, K. & Mohanty, S. 1988.** Response of basement and cover rocks to multiple deformations: a study from the Precambrian of Rajasthan, Western India. *Precambrian Research*, Vol.42, p.77-96.
- Nance, R.D., Worsley, T.R. & Moody, J.B. 1988.** The Supercontinent Cycle. In E.M. Moores (ed) *Shaping the Earth: readings from the Scientific American Magazine*, p.177-187.
- Nichols, G.J. 1987.** Syntectonic alluvial fan sedimentation, southern Pyrenees. *Geological Magazine*, Vol.124, p.121-133.
- Nio, S-D, Van der Berg, J.H., Goesten, M. & Smulders, F. 1980.** Dynamics and sequential analysis of a mesotidal shoal and intershoal channel complex in the eastern Scheldt (southwestern Netherlands), *Sedimentary Geology*, Vol.26, p.263-279.
- Nzenti, J.P., Barbey, P., Macaudiere, J. & Soba, D. 1988.** Origin and evolution of the Late Precambrian high-grade Yaounde gneisses (Cameroon). *Precambrian Research*, Vol.38, p.91-109.
- Odonne, F. & Vialon, P. 1983.** Analogue models of folds above a wrench fault. *Tectonophysics*, Vol.99, p.31-46.

- Oldov, J.S., Bally, A.W. & Ave Lallemand, H.G. 1990.** Transpression, orogenic float, and lithospheric balance. *Geology*, Vol.18, p.991-994.
- Oliveira, E.P. & Tarney, J. 1990.** Petrogenesis of the Canindé de São Francisco Complex: a major Late Proterozoic gabbroic body in the Sergipe Fold Belt, NE Brazil. *Journal of South American Earth Sciences*, Vol.3, p. 125-140.
- Passchier, C.W. 1984.** The generation of ductile and brittle shear bands in a low-angle mylonite zone. *Journal of Structural Geology*, Vol.6, p.273-281.
- Passchier, C.W. & Simpson C. 1986.** Porphyroblast systems as kinematic indicators. *Journal of Structural Geology*, Vol.8, p.831-844.
- Pimentel, M.M., Heaman, L. & Fuck, R.A. 1992.** Idade do Meta-Riolito da Seqüência Maratá, Grupo Araxá, Goiás: Estudo Geocronológico pelos métodos U-Pb em Zircão, Rb-Sr Sm-Nd. *Anais da Academia Brasileira de Ciências*, Vol.64, p. 19-28.
- Piper, J.D.A. 1976.** Paleomagnetic evidence for a Proterozoic supercontinent. *Philosophical Transactions Royal Society London, Series A*, Vol.280, p.469-490.
- Piper, J.D.A. 1987.** Paleomagnetism and the continental crust. Open University Press, UK, 434 p.
- Piatt, J.P. & Vissers, R.L.M. 1980.** Extensional structures in anisotropic rocks. *Journal of Structural Geology*, Vol.2, p.397-410.
- Preiss, W. V. 1987 (compiler).** The Adelaide Geosyncline: Late Proterozoic stratigraphy, sedimentation and tectonics. *Geological Society of South Australia, Bulletin* 53, 450p.
- Pope, A.J. 1989.** The tectonics and Mineralisation of the Toby Horsethief Creek area, Purcell Mountains, southeast British Columbia, Canada. University of London, RHBNC, PhD Thesis, 350p.
- Porada, H. 1989.** Pan-African Rifting and Orogenesis in Southern to Equatorial Africa and Eastern Brazil. *Precambrian Research*, Vol.44, p. 103-136.
- Ramberg, H. 1981.** Gravity, Deformation and the Earth's Crust (2nd Edition). Academic Press, 452p.
- Ramsay, J.G. 1967.** Folding and fracturing of rocks. McGraw Hill, N.Y., 568p.

Ramsay, J.G. & Huber, M.I. 1987. The Techniques of Modern Structural Geology, Volumes 1 and II. Academic Press, 1007p.

Rand, H., Sial, A.N., Brito Neves, B.B. de & Manso, V.V. 1980. Gravimetric and magnetometric study of the Late Precambrian Sergipe Folding System, Northeast Brazil. In XXXI Congresso Brasileiro de Geologia, Camboriú, Anais, SBG, vol.5 p.2700-2708.

Ribeiro, A., Paciullo, F.V.P., Andreis, R.R., Trouw, R.A.J. & Heilbron, M. 1990. Evolução policíclica Proterozóica no sul da craton de São Francisco: análise da região de São João D'E1-Rey e Andrelândia, MG. XXXVI Congresso Brasileiro de Geologia, Natal, Anais SBG, Vol.6, p.2605-2614.

Ridley, J. 1986. Parallel stretching lineations and fold axes oblique to a shear displacement direction - a model and observations. Journal of Structural geology, Vol.8, p.647-653.

Roberts, A.M. & Yielding, G. 1991. Deformation around basin-margin faults in the North Sea / mid-Norway rift. In A.M. Roberts, G. Yielding., & B.Freeman (eds), The Geometry of Normal Faults, Geological Society of London Special Publication 56, p.61-78.

Royden, L. & Burchfiel, B.C. 1989. Are systematic variations in thrust belt style related to plate boundary processes? (The western Alps versus the Carpatian). Tectonics, Vol.8, p51-61.

Rudolph, K.W. & Lehmann, P.J. 1989. Platform evolution and sequence stratigraphy of the Natuna Platform, South China Sea. In PA. Scholle, D.G. Bebout, C.H. Moore (eds), Carbonate Depositional Environments. The American Association of Petroleum Geologists, Memoir 33, p.620-691.

Saes, G.S. 1984. Estratigrafia e sedimentologia do Grupo Estância na região nordeste do Estado da Bahia. UFBa, Dissertação de Mestrado, IOOp.

Santos, E.J. dos & Silva Filho, M.A. 1975. Ensaio interpretativo sobre a evolução da geosinclinal de Propria, Nordeste do Brasil. Mineração e Metalurgia, ano XXXIX, N. 367, p.3-22.

Santos, E.J. dos & Brito Neves, B.B. de 1984. Província Borborema. In Almeida, F.F.M. & Hasui, Y. (coordenadores), O pré-Cambriano do Brasil. Editora Edgard Blucher Ltda, p.123 - 186.

Santos, E.L., Azevedo, G.C., Maciel, L.A.C., Mossmann, R. & Remus, M.V.D. 1990. Mapeamento geológico de seqüências metavulcano-sedimentares do oeste do escudo sul Rio-Grandense, RS. XXXVI Congresso Brasileiro de Geologia, Natal, Anais SBG, Vol.6, p.2976-2990.

Santos, R.A., Menezes Filho, N.R. & Souza, J.D. de 1988. Programa Levantamentos Geológicos Básicos; carta geológica, carta metalogenética/previsional - escala 1:100.000, Projeto Carira. DNPM/CPRM, 4 volumes. Folha Carira.

Shackleton, R.M. 1986. Precambrian collision tectonics in Africa. In M.P. Coward & A.C. Ries (eds) Collision Tectonics, Geological Society of London Special Publication 19, p.329-349.

Schermerhorn, L.J.G. 1974. Late Precambrian mixtites: glacial and/or nonglacial?. American Journal of Science, Vol.274, p.673-824.

Schermerhorn, L.J.G. 1981. The West Congo Orogen: A key to Pan-African thermotectonism. Geologische Rundschau, Vol.70, p.850-867.

Schermerhorn, L.J.G. & Stanton, W.I. 1963. Tilloids in West Congo geosyncline. Quarterly Journal of Geological Society of London, Vol.119, p.201-241.

Schinn, E.A. 1983. Tidal Flat Environment. In P.A. Scholle, D.G. Bebout, C.H. Moore (eds). Carbonate Depositional Environments. The American Association of Petroleum Geologists, Memoir 33, p.172-210.

Scholle, P.A., Arthur, M.A. & Ekdale, A.A. 1983. Pelagic Environment. In P.A. Scholle, D.G. Bebout, C.H. Moore (eds). Carbonate Depositional Environments. The American Association of Petroleum Geologists, Memoir 33, p.620-691.

Schrank, A., Abreu, F.R. de, Roig, H.L., Chouduri, A., Szabó, G.J.A. & Carvalho, E.D.R. 1990. Determinação dos vetores de transporte tectônico na borda sudoeste do craton do São Francisco. XXXVI Congresso Brasileiro de Geologia, Natal, Boletim de Resumos, p.250.

Sellwood, B.W. 1986. Shallow marine carbonate environments. In H.G. Reading (ed), Sedimentary Environments and Facies. Blackwell Scientific Publications, p.283-342.

Shimamoto, T. 1989. The origin of S-C mylonites and a new fault-zone model. Journal of Structural Geology, Vol.11, p.51-64.

Silva Filho, M.A. 1976. A suíte ofiolítica da Geosinclinal de Propria. XXIX Congresso Brasileiro de Geologia, Ouro Preto, Anais SBG, p.51-58.

Silva Filho, M.A., Bonfim, L.F.C. & Santos, R.A. dos 1978 a. A geosinclinal Sergipana: estrutura e evolução. XXX Congresso Brasileiro de Geologia, Recife, Anais, SBG, Vol.6, p.2464-2477.

Silva Filho, M.A., Santana, A.C. & Bonfim, L.F.C. 1978 b. Evolução tectono-sedimentar do Grupo Estância: suas correlações. XXX Congresso Brasileiro de Geologia, Recife, Anais, SBG, Vol.2, p.685-699.

Silva Filho, M.A. & Brito Neves, B.B. de 1979. O Sistema de dobramentos Sergipano no nordeste da Bahia. SME/SGM, Série Geologia e Recursos Minerais da Bahia, Textos Básicos, p.203-214.

Silva Filho, M.A. 1982. A evolução da porção marginal do cinturão Sergipano e sua metalogenia. XXXII Congresso Brasileiro de Geologia, Salvador, Anais, SBG, Vol. 1, p.316-324.

Simões, L.S.A. & Valeriano, C.M. 1990. Porção meridional da faixa de dobramentos Brasília: estágio atual do conhecimento e problemas de correlação tectono-estratigráfica. XXXVI Congresso Brasileiro de Geologia, Natal, Anais SBG, Vol.6, p.2564-2575.

Simpson, C. 1985. Deformation of granites across the brittle-ductile transition. *Journal of Structural Geology*, Vol.7, p.503-511.

Sliter, W.V., Murchey, B.L., McLaughlin, R.J. & Kistler, R.W. 1991. Permanente Terrane: history of early Cretaceous seamount formation in the eastern Pacific. Geological Society of America Abstracts with Program, 87th Annual Cordilleran Section, abstract 1217.

Soares, P.C., Fiori, A.P. & Carvalho, S.G. 1990. Tectônica colisional oblíqua entre o bloco Paraná e a margem sul do craton de São Francisco, no maciço Guaxupé. XXXVI Congresso Brasileiro de Geologia, Natal, Anais SBG, Vol.6, p.2723-2734.

Souza, Z.S., Medeiros, H., Althoff, F.J. & Dall'Agnol, R. 1990. Geologia do terreno granito-greenstone Arqueano da região de Rio Maria, Sudeste do Pará. XXXVI Congresso Brasileiro de Geologia, Natal, Anais SBG, Vol.6, p.2913-2928.

Stewart, J.H. 1972. Initial deposits in the Cordilleran Geosyncline: evidence of a Late Precambrian (<850 m.y.) continental separation. Geological Society of America Bulletin, Vol.83, p.1345-1360.

Tankard, A.J. 1986. On the depositional response to thrusting and lithospheric flexure. Special Publications International Association Sedimentologists, Vol.8, p.369-394.

Teixeira, W. & Figueiredo, M.C.H. 1991. An outline of Early Proterozoic crustal evolution in the São Francisco craton, Brazil: a review. Precambrian Research, Vol.53, p.1-22.

Thompson, A.B. & England, P.C. 1984 - Pressure-temperature-time paths of regional metamorphism, II: Their inference and interpretation using mineral assemblages in metamorphic rocks. Journal of Petrology, Vol.25, p.929-955.

Thompson, A.B. & Ridley, J.R. 1987. Pressure-temperature-time (P-T-t) histories in orogenic belts. In E.R. Oxburgh, B.W.D. Yardley & P.C. England (eds), Tectonic Settings of Regional Metamorphism. Philosophical Transactions of the Royal Society, London, A321, p.27-45.

Thompson, R.N. & Gibson, S.A. 1991. Subcontinental mantle plumes, hotspots and pre-existing thin spots. Journal of the Geological Society London, Vol.148, p.973-978.

Tillman, R.W. 1985 a. A spectrum of shelf sands and sandstones. In R.W. Tillman, D.J.P. Swift & R.G. Walker (eds), Shelf sands and sandstone reservoirs. SEPM Short Courses 13, p.1-46.

Tillman, R.W. 1985 b. The Tocito and Gallup sandstones, New Mexico: A comparison. In R.W. Tillman, D.J.P. Swift & R.G. Walker (eds). Shelf sands and sandstone reservoirs. SEPM Short Courses 13, p.403-463.

Torquato, J.R. 1974. Geologia do sudoeste de Moçamedes e suas relações com a evolução tectônica de Angola. Tese Livre Docência, IG/USP, São Paulo, 234 p.

Torquato, J.R. & Cordani, U.G. 1981. Brazil-Africa geological links. Earth-Science Reviews, Vol. 17, p.155-176.

Trexler Jr., J.H. & Nitchman, S.P. 1990. Sequence stratigraphy and evolution of the Antler basin, east-central Nevada. Geology, Vol.18, p.422-425.

Trompette, R. 1982. Brasil e a margem Atlântica da África no Proterozóico Superior. Importância do Fraturamento Espinhaço (Kibariano). XXXII Congresso Brasileiro de Geologia, Salvador, Anais, SBG, Vol.1, p.386-394.

Uhlein, A., Egidio da Silva, M. & Trompette, R. 1990. A faixa de dobramentos Araçuaí, no Estado de Minas Gerais: uma cadeia monocíclica de idade Brasileira. XXXVI Congresso Brasileiro de Geologia, Natal, Anais SBG, Vol.6, p.2576-2588.

Unrug, R. 1990. Modes of Kibaran basement recycling in the Pan-African Lufilian and Zambezi Fold Belts, and the Mwembeshi-Ciiimaliro dislocation zone, Zambia. XXXVI Congresso Brasileiro de Geologia, Natal, Anais SBG, Vol.6, p.2672-2682.

Vauchez, A., Maillet D. & Sougy, J. 1987. Strain and deformation mechanisms in the Variscan nappes of Vendee, South Brittany, France. *Journal of Structural Geology*, vol.9, p.31-40.

Vernon, R.H. 1989 - Porphyroblast-matrix microstructural relationships: recent approaches and problems. In J.S. Daly, R.A. Cliff & B.W.D. Yardley (eds) *Evolution of Metamorphic Belts*, Geological Society of London Special Publication 43, p.83-102.

Visser, M.J. 1980. Neap-spring cycles reflected in Holocene subtidal large-scale bedform deposits: a preliminar note. *Geology*, Vol.10, p.135-140.

Young, G.M. 1981. The Amundsen Embayment, Northwest Territories: relevance to the upper Proterozoic of North America. In F.H.A. Campbell (ed), *Proterozoic Basins of Canada*. Geological Survey of Canada, Paper 81-10, p.203-218.

Zalan, P. V. 1986. A tectônica transcorrente na exploração de petróleo: uma revisão. *Revista Brasileira de Geociências*, Vol. 16, p.245-257.

Zimbres, E.A., Kawashita, K. & Van Schmus, W.R. 1990. Evidências de um núcleo Transamazônico na região de Cabo Frio, RJ e sua correlação com o craton de Angola, África. XXXVI Congresso Brasileiro de Geologia, Natal, Anais SBG, Vol.6, p.2735-2743.

Wagoner, J.C., Mitchum Jr., R.M., Posamentier, H.W. & Vail, P.R. 1987. Seismic stratigraphy interpretation using sequence stratigraphy, part 2: key definition of sequence stratigraphy. In A.W. Bally (ed.). *Atlas of Seismic Stratigraphy*. American Association of Petroleum geologists, *Studies in Geology, Memoir 27*, p.11-14.

Walker, R.G. 1985 a. Comparison of shelf environments and deep basin turbidite systems. In R.W. Tillman, D.J.P. Swift & R.G. Walker (eds). Shelf sands and sandstone reservoirs. SEPM Short Courses 13, p.465-503.

Walker, R.G. 1985 b. Ancient examples of tidal sand bodies formed in open, shallow seas. In R.W. Tillman, D.J.P. Swift & R.G. Walker (eds), Shelf sands and sandstone reservoirs. SEPM Short Courses 13, p.303-342.

Walker, R.G. 1985 c. Geological evidences for storm transportation and deposition on ancient shelves. In R.W. Tillman, D.J.P. Swift & R.G. Walker (eds), Shelf sands and sandstone reservoirs. SEPM Short Courses 13, p.243-303.

Wang, G.M. & White, S.H. 1990. Tectonic setting of shear zone hosted gold mineralisation, Central Victoria, SE Australia. Geological Society London, Tectonic Studies Group 21, Liverpool, Programme with Abstracts.

Wardle, R.J. & Bailey, D.G. 1981, Early Proterozoic sequences in Labrador. In F.H.A. Campbell (ed), Proterozoic Basins of Canada. Geological Survey of Canada, Paper 81-10, p.331-359.

Waters, D. 1991. Active tectonics of Epirus, Northwest Greece. Tectonic Studies Group, Geological Society of London, Meeting 22, Edinburgh-Scotland, Programme with Abstracts.

Wernicke, B. 1985. Uniform-sense normal simple shear of the continental lithosphere. Canadian Journal of Earth Sciences, Vol.22, p. 108-125.

Wernicke, B. & Burchfiel, B.C. 1982. Modes of extensional tectonics. Journal of Structural Geology, Vol.4, p.105-115.

Wernicke, E., Hasui, Y. & Brito Neves, B.B. de 1978. As regiões de dobramentos Nordeste e Sudeste. XXX Congresso Brasileiro de Geologia, Recife, Anais, SBG, Vol.6, p.2493-2507.

Wescott, W.A. 1990. The Yallahs Fan Delta: A coastal fan in a humid tropical climate. In A.H.Rachocki & M. Church (eds), Alluvial Fans: a field approach, Chapter 11, p.213-225, John Wiley & Sons **Ltd.**

Wescott, W.A. & Ethridge, F.G. 1990. Fan Deltas - Alluvial Fans in coastal settings. In A.H.Rachocki & M. Church (eds). Alluvial Fans: a field approach. Chapter 10, p. 195-212, John Wiley & Sons Ltd.

- White, S.H. 1989.** Quo Vadis?. Geological Society of London, Tectonic Studies Group, 20th annual meeting, London.
- White, R. & McKenzie, D. 1989.** Magmatism at rift zones: the generation of volcanic continental margins and flood basalts. *Journal of Geophysical Research* Vol.94, p.7685-7729.
- Williams, M.X. 1991.** Heterogeneous deformation in a ductile fold-thrust belt: The Proterozoic structural history of the Tusas Mountains, New Mexico, *Geological Society of America Bulletins*, vol. 103, p.171-188.
- Williams, P.L. 1985.** Multiply deformed terrains - problems of correlation. *Journal of Structural Geology*, vol.7, p.269-280.
- Williams, G.D. & Chapman, T.J. 1979.** The geometrical classification of non-cylindrical folds. *Journal of Structural Geology*, Vol. 1, p. 181 -185.
- Wilson, M. 1989.** *Igneous Petrogenesis*. HarperCollins Academic, 466p.
- Windley, B.F. 1984,** *The evolving Continents*. 2nd edition. John Wiley & Sons, Chichester, 399p.
- Windley, B.F. 1987.** Tectonic framework of Precambrian Belts. In J.P. Schaer & J. Rogers (eds.), *The anatomy of Mountain Ranges*. Princeton University Press, Chapter 3, p. 19-27.
- Woodward, N.B. Boyer, S.E, & Suppe, J. 1985.** An outline of balanced cross-sections. Notes for the short course held in Orlando, Florida, USA, November, 1985, University of Tennessee.

Appendix

This appendix is comprised of three parts (A1-A3):

Appendix **A1** contains additional information on the stratigraphy of the Itabaiana Dome Area (Chapter 3). It includes a reduced geological map with location of the **12** stratigraphic section constructed around the Itabaiana and Simão Dias domes (A1.1) and seven of these stratigraphic sections (A1.2-A1.8).

Appendix A2 contains measurement of axis of clasts and clasts **+ tail** from Palestina Formation rocks in outcrops and thin sections. These data (A2.1-A2.3) form the base for the strain analysis of section 4.4.4 .

Appendix A3 contains observed and calculated gravity and magnetometric data, as well as density data of rocks in the Itabaiana Dome area. These data (A3.1-A3.4) form the base **for the** geophysical interpretations of section 5.5 .

LITHOLOGY		TOTAL THICK (M)	THICKNESS M	SYMBOL	FORMATION
		1500			
		1000	>1000	PC OA	OLHOS D'AGUA : Finely laminated, fine grained, dark grey to black or purple, dolitic limestones, with subordinated, cm-thick, variegated silty phyllites, and local intercalations of light grey dolomites and brown to black metachert.
		500	100	PC P	PALESTINA : Green-brown diamictites.
			150	PC FP	FREI PAULO : Finely laminated, variegated, silty phyllites, with intercalations of yellow to grey, generally <5m thick lenses of quartzite nearby the upper contact.
			70	PC Je	JACARE : Light brown to yellow, micaceous metasilites.
			60	PC LP	LAGARTO-PALMARES : Micaceous, wave-rippled, and parallel laminated metasandstones.
			100	PC R	RIBEIROPOLIS : Well-laminated, dark brown to black metaconglomerates and blue to green-brown phyllites.
			50	PC I	ITABAIANA : White arkosid quartzites, sheared at the basal contact.
		0		SDG	SIMAO DIAS GNEISS : Quartz (s)idapar biotite-chlorite gneiss, sheared at the contact with the Itabaiana Formation.

From B to B' includes outcrops 290, 1190, 285, 284, 241, 240, 242, 1141, 1147, 239, 1139, and 251.

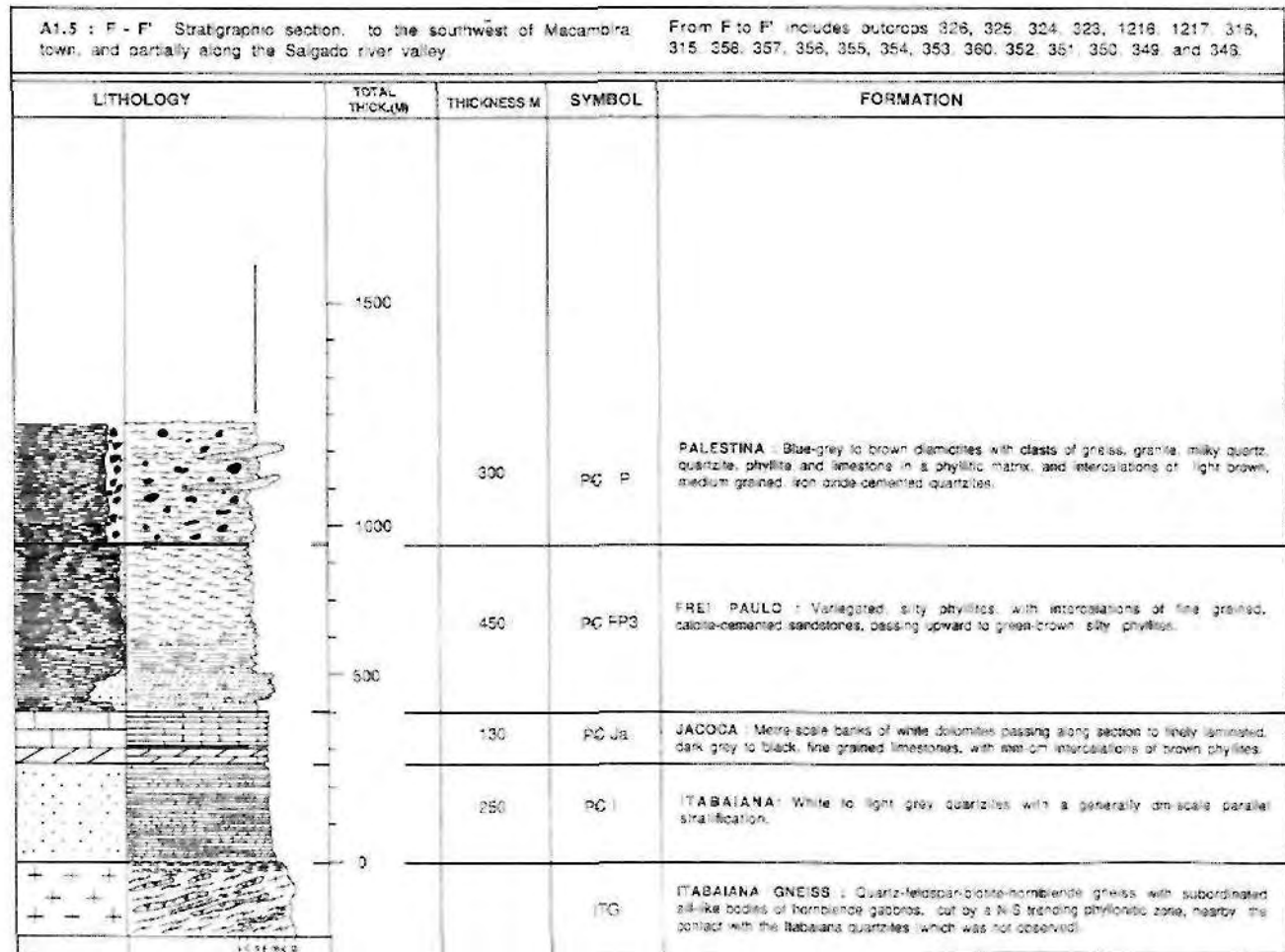
A1.2 : B - B' stratigraphic section, across the Anão da'n, west of Simão Dias.

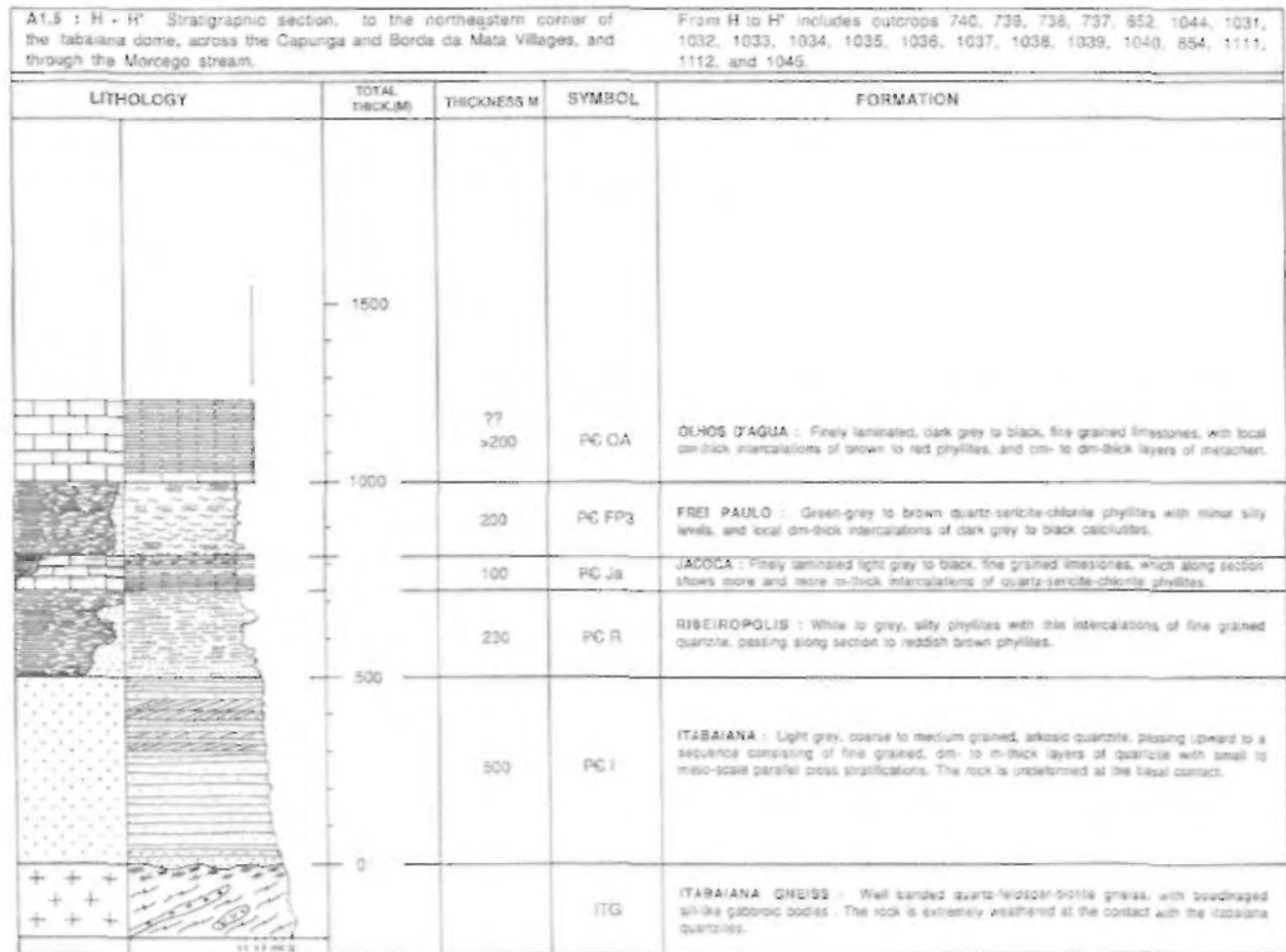
LITHOLOGY		TOTAL THICK (M)	THICKNESS M	SYMBOL	FORMATION
<p>A1.3 : C - C' stratigraphic section, west of Simão Dias. From C to C' includes outcrops 98, 99, 100, 101, 202, 203, 204, 1179, 1149, 1150, 1151, 226, 227, 228, 229, 230, 231, 232, 233, 234, 235, 1138, 1139, and 1140.</p>					
			>1000	PC OA	OLHOS D'ÁGUA : Finely laminated, black to dark grey, fine grained limestones intercalated with mm to dm thick layers of brown phyllites.
		100	100	PC P	PALESTINA : Green-brown diamicrites, with intrabasinal, generally <10cm clasts.
		200	200	PC FP	FREI PAULO : Light brown and silty phyllites and local dark grey to black phyllites, with intercalation of a <5m thick lens of medium to coarse grained, dark grey quartzite, nearby the upper contact.
		100	100	PC Ja	JACOCA : Light brown and silty phyllites with discontinuous (generally <10m thick) lenses of white dolomite.
		<150	<150	PC R	RIBEIROPOLIS : Grey to light brown pebbly phyllites with a silty matrix and cm size clasts of basement rocks, passing along section to phyllites and minor pebbly phyllites.
		<50	<50	PC I	ITABAIANA : Arkose metabasaltites and wackes intercalated with red-brown phyllites.
				SDG	SIMÃO DIAS GNEISS : Quartz-feldspar-biotite gneiss. Both the gneisses and the Itabaiana quartzites are strongly sheared nearby their contact, which however is not directly observed.

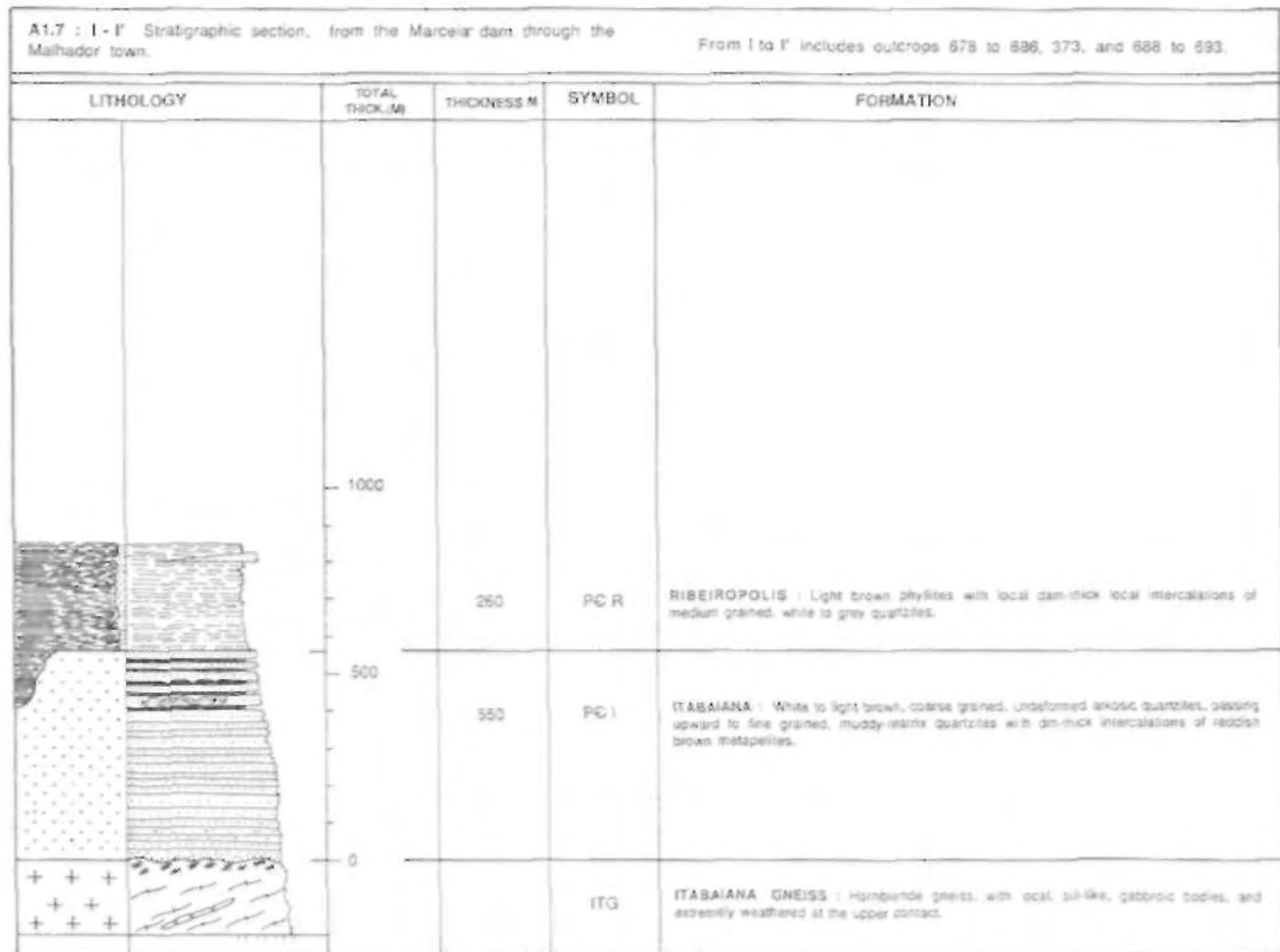
LITHOLOGY		TOTAL THICK. (M)	THICKNESS M	SYMBOL	FORMATION
		1500			
		1000	500	PC P	PALESTINA : Grey-green diamicrites, green-brown pebbly phyllites and subordinated phyllites. The clasts are mostly from gneiss and milky quartz, and are generally $\le 15\text{ cm}$.
		500	450	PC FP	FREI PAULO : Finely interbedded, dark grey to black (locally carbonaceous) phyllites, metasilites and minor psilulites, passing along the section to white to grey silty phyllites and then to green-brown to blue-grey quartz-sericite-chlorite phyllites, with locally intercalated m-thick lenses of generally iron oxide-cemented quartzites.
			100	PC Ja	JACCOCA : White to grey dolomites and finely laminated, fine grained, dark grey to black limestones.
			50	PC R	RIBEIRÓPOLIS : White, silty and pebbly phyllites, with clasts of gneiss and quartzites.
	200	PC I	ITABAIANA : Grey to light yellow basal arkosic quartzites and white quartzites.		
				ITG	ITABAIANA GNEISS : Quartz-feldspar-biotite gneiss in the inner dome. Both the basement and cover are highly sheared nearby the contact, which is not observed directly.

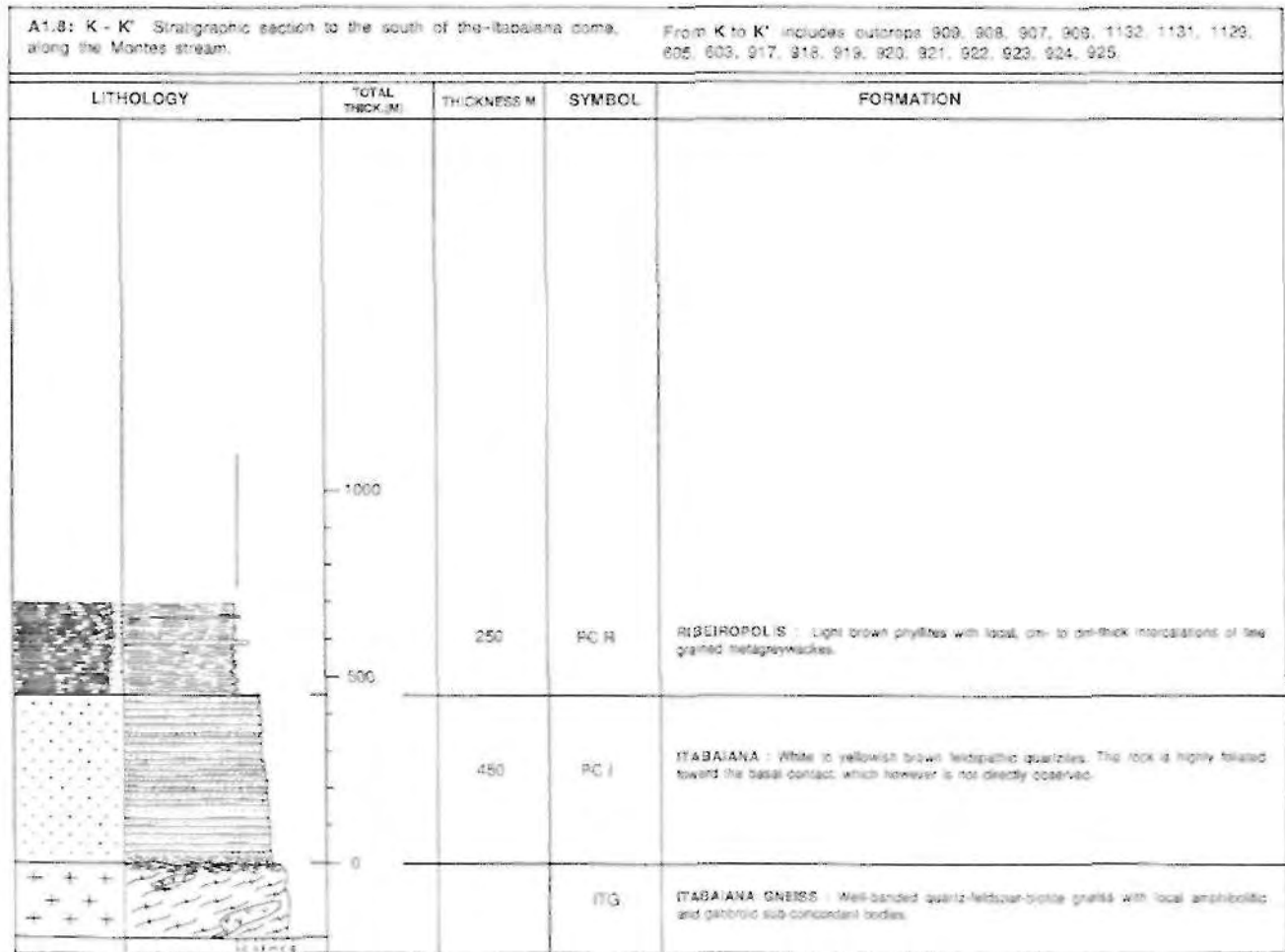
A1.4 : D - D' Stratigraphic section, across the southwestern corner of the Itabaiana dome.

From D to D' includes outcrops 583, 582, 581, 479, 480, 471, 470, 469, 468, 467, 466, 465, 877, 873, 422, 421, 402, and 401.









Outcrop 36. road Simão Dias - Pinhão					
	Face XY			Face YZ	
X (cm)	Y (cm)	X/Y	Y (cm)	Z (cm)	Y/Z
0.6	0.1	6.0	22.0	9.0	2.4
1.0	0.3	3.3	12.0	5.0	2.4
0.8	0.3	2.7	8.5	5.0	1.7
2.5	0.9	2.8	3.0	3.0	1.0
1.3	0.4	3.3	3.0	2.0	1.5
1.9	0.6	3.2	5.0	4.0	1.3
1,2	0.5	2.4	6.0	4.C	1.5
10.0	3.0	3.3	1.5	1.5	1.0
5.0	1.4	3.6	7.0	3.5	2.0
10.0	3.0	2.3	10.5	7.0	1.5
1.5	0.5	3.0	7.0	6.0	1.2
2.1	0.3	7.0	6.5	2.7	2.4
1.1	0.3	3.7	6.0	2.2	2.7
'-±	0.4	3.5	4.0	2.8	1.4
1.6	0.4	4.0	11.0	7.0	1.6
3.6	1.6	2.3	3.0	2.5	1.2
2.6	0.4	6.5	-	-	-
3.2	0.0	3.S	-	-	-
Outcrop 90, road Paripiranga-Simão Dias					
	FaceXY			FaceYZ	
X (cm)	Y <cm)	X/Y	Y (cm)	Z (cm)	Y/Z
14.0	3.6	3.9	0./	0.7	1.0
4.1	0.3	13.7	2.9	2.9	1.0
2.2	0.5	4.4	1.1	0.5	2.2
3.5	0.5	7.0	0.7	0.7	1.0
8.8	1.0	8.8	1.2	1.2	1.0
9.5	3.0	3.2	1.0	0.7	1.4
2.0	0,7	2.9	1.0	1.0	1.0
3.3	0.3	11.0	3.3	3.3	1.0
5.3	1.2	4.4	0.7	0.7	1.0
24.5	2.0	12.3	0.9	0.9	1.0
6.0	1.8	3.3	1.6	1.4	1.1
2.7	0.5	5.4	1.2	0.8	1.5
			2.8	1.7	1.6
			2.3	2.3	1.0
			1.8	1.8	1.0
			1.0	0.4	2.5
			1.1	1.1	1.0
			1.5	1.2	1.3
-	-	-	-	-	-

A2.1 - Length of the axis of clasts measured in surfaces nearly parallel to XY and YZ in Palestina diamictites. The X/Y and Y/Z ratios are shown. The ratios in bold were taken for the estimative of the strain ellipse using the methods derived by Flynn (1962, 1965) and Hsu (1966). The results are shown in Figure 4.12 A-B.

(Continued)

Outcrop 107. road Paripiranga Manta					
FaceXY			FaceYZ		
X (cm)	Y (cm)	X / Y	Y ;cm)	Z (cm)	Y /Z
15.5	4.0	3.9	2.3	1.2	1.9
3.5	0.9	3.9	4.0	2.6	1.5
2.1	0.7	3.0	1.3	0.6	2.2
1.7	0.7	2.4	2.6	2.5	1.0
4.6	0.7	6.6	4.0	4.0	1.0
2.4	0.11	2.7	35.0	28.0	1.3
5.5	2.5	2.2	5.5	5.5	1.0
4.4	2.0	2.2	2.8	2.8	1.0
7.0	2.8	2.5	1.0	0.4	2.5
2.0	0.3	6.7	2.0	0.7	2.9
1.3	0.5	2.6	1.6	1.1	1.5
0.8	0.7	4.0	7.0	5.5	1.3
2.6	0.3	8.7	11.5	6.5	1.8
1.9	0.3	6.3	5.2	3.0	1.7
			21.0	9.0	2.3
			1.3	1.3	1.0
-	-	-	-	-	-
Outcrop 10 3, road Paripiranga-Maritã					
Face XY			Face YZ		
X (cm)	Y (cm)	X / Y	Y (cm)	Z (cm)	Y/Z
5.0	2.7	1.9	16.5	12.0	1.4
5.2	1.5	3.5	14.7	6.5	2.3
12.0	5.5	2.2	2.7	2.5	1.1
2.2	0.5	4.4	5.5	5.2	1.1
4.0	1.3	3.1	18.5	14.7	1.1
			3.0	2.5	1.2
-	-	-	-	-	-

A2.1 (final) -See plot of the strain ellipsoids in Figure 4.12 A-B.

Face XZ Face xz (outcrop 44, Simão Dias Pinhão)

X (on)	Z=D (cm)	X/Z	X-tailXt	Xr/Z	S	S/D	(S-ü)/D
2.5	1.5	1.7	6.0	4.0	0.3	0.20	0.80
14,0	4.5	3.1	23.0	5.1	2.0	0.44	0,56
1.5	0.7	2,1	3.0	4.3	0.3	0.43	-0.57
1.3	1.0	1.3	3.5	3.5	0.5	0.50	0.50
3.5	0,7	5.0	7.0	10.0	0.2	0.29	0.71
2.5	1.3	1.9	4.5	3.5	0.4	0.31	0.69
1.5	1.0	1.5	3,5	3.5	0.3	0.30	0.70
3.5	5.0	0.7	12.0	2.4	1.6	0.32	-0.68
15.C	9.0	1.7	9.0	-	0.0	0.00	-1.00
6.5	4.0	1.6	14.0	3.5	1.2	0.30	-0.70
4.0	2.0	2.0	8.0	4.0	1.0	0.50	-0.50
4.5	4.2	1.1	10.0	2.4	2.0	0.48	0.52
Harmonic	mean	1.57		2.99		0.34	•0.64

Face xz (outcrop 107, Road Paripiranga-Maritá)

X [cm]	z=0 (cm)	X/Z	X.taN-Xt	Kt/2	S	S/B	(S-D)/D
6.7	2.9	2.3	10.5	3.6	1.3	0.45	-0.55
5.5	2.0	2.6	10.5	5.3	1.2	0.60	-0.40
4.0	2.0	2.0	9.0	4.5	1.0	0.50	0.50
2,3	1.6	1.4	5.5	3.4	0.4	0.25	-0.75
1.4	1.0	1.4	7.0	7.0	0.2	0.20	-0.80
5.3	3.0	1.8	12.0	4.0	0.4	0.13	0.87
3 0	0.6	5.0	0.6	-	0.0	0.00	-1.00
2.0	2.3	0.9	7.5	3.3	0 4	0.17	-0.83
Harmonic	mean	1.73		2.99		0.25	-0.65

Face xz (outcrop 108, Road Paripiranga-Maritá)

X (cm)	Z-D (cm)	X/Z	X4tail-Xt	Xl/Z	S	S/D	(S-D)/D
9.3	4.Ç	2.0	36.0	7.8	1.2	0.26	-0.74
2.1	1.1	1.9	7.0	6.4	0.2	0.18	-0.82
5.3	2.0	2.7	17 0	8.5	0.5	0.25	0.75
9.0	4.2	2.1	26 0	6.2	1.5	0.36	064
7.2	3.2	2.3	16.5	5.2	0.8	0.25	-0.75
1.3	1.6	0.8	15.0	0.4	0.3	0.19	0.81
9.5	2.2	4.3	28.0	12.7	1.0	0.45	0.55
3.4	3.2	1.1	17.0	5.3	0.9	0.28	-0.72
1.5	1.5	1.0	6.5	4.3	1.0	0.67	0.33
6.5	2.5	2.6	16.0	6.4	0.3	0.12	-0.83
4.5	3.0	1.5	13.0	4.3	1.3	0.43	-0.57
3.5	2.5	1.4	11.0	4.4	0 4	0.16	-0 84
Harmonic	mean	1.61		6.07		0.25	-0.05

A2.2 - Axial ratio of clasts and clasts+tail (surface nearly parallel to XZ) with their harmonic means (method of Lisle 1979). S, D and S/D were obtained by the method of Borradaile (1981). The negative values are the calculated amount of shortening of the matrix. (Continued)

Face XZ (Outcrop			405. north of Olhos D'água)				
X (cm)	Z-D (cm)	X/Z	X+taikXt	Xt/Z	S	S/D	(S-D)/D
12.0	3.0	4.0	40.0	13.3	2.0	0.67	-D.33
12.0	3.S	3.8	30.0	9.4	1.0	0.31	-0.69
3.2	1.1	2.9	8.0	7.3	1.0	0.91	-0.09
5.5	1.7	3.2	14.0	8.2	0.8	0.47	-0.53
8.3	4.0	2.1	65.0	16.3	0.7	0.18	-0.83
15.5	2.5	6.2	32.0	12.8	0.0	0.00	-1.00
18.0	14.0	1.3	80.0	5.7	3.5	0.25	-0.75
11.5	5.2	2.2	40.0	7.7	1.0	0.19	0.81
13.0	6.5	2.0	44.0	6.8	2.0	0.31	-0.69
10.0	1.7	5.9	28.0	16.5	0.7	0.41	-0.59
4.7	2.7	1.7	16.0	5.9	0.2	0.07	-0.93
14.0	2.2	6.4	28.0	12.7	0.1	0.05	-0.95
9.0	2.3	3.9	28.0	12.2	0.2	0.09	-0.91
8.0	2.0	4.0	16.0	8.0	0.1	0.05	-0.95
9.0	1.8	5.0	18.0	10.0	0.1	0.06	-0.94
9.0	5.5	1.6	35.0	6.4	1.5	0.27	-0.73
7.0	3.5	2.0	25.0	7.1	0.6	0.17	-0.83
6.2	3.4	1.8	25.0	7.4	1.0	0.29	-D.71
1G.0	7.0	2.3	66.0	9.4	1.5	0.21	-0.79
12.5	4.5	2.8	40.0	8.9	0.3	0.07	-0.93
29.5	7.0	4.2	60.0	8.6	0.5	0.07	-3.93
31.0	5.5	5.6	66.0	12.0	0.2	0.04	-3.96
18.0	12.0	1.5	60.0	5.0	0.1	0.01	-0.99
5.0	2.1	2.4	13.0	6.2	0.2	0.10	-0.90
4.5	2.5	1.8	16.0	6.4	0.2	0.08	-0.92
27.0	5.5	4.9	40.0	7.3	0.2	0.04	-0.96
5.5	3.5	1.6	20.0	5.7	0.7	0.20	0.80
7.4	2.5	3.0	20.0	8.0	0.3	0.12	-3.88
7.3	2.3	3.?	26.0	11.3	0.3	0.13	-0.87
10.5	7.2	1.5	40.0	5.6	2.0	0.28	-0.72
14.2	4.5	3.2	50.0	11.1	1.2	0.27	-3.73
14.5	4.5	3.2	40.0	8.9	0.5	0.11	0.89
10.5	1.5	7.0	24.0	16.0	0.2	0.13	3.87
10.2	2.9	3.5	30.0	10.3	0.5	0.17	-3.83
21.0	8.2	2.6	50.0	6.1	2.0	0.24	-3.76
7.3	2.4	3.0	18.0	7.5	1.0	0.42	-3.58
5.7	1.9	3.0	19.0	10.0	0.2	0.11	-3.89
5.4	1.9	2.8	14.0	7.4	0.1	0.05	-3.95
7.2	2.7	2.7	22.0	8.1	0.2	0.07	-0.93
7.5	3.6	2.1	27.0	7.5	0.7	0.19	0.81
Harmonic	mean	2.71		8.39		0.09	3.66

A2.2 - Axial ratio of clasts and clasts+tail (surface nearly parallel to XZ) with their harmonic means (method of Lisle 1979). S, D and S/D were obtained by the method of Borradaile (1981). The negative values are the calculated amount of shortening of the matrix.

(continued)

Face YZ (Outcrop 107)

Y (cm)	Z-D (cm)	Y/Z	Y+tail=Yt	Yt/Z	S	S/D	(S-D)/D
10.5	8.5	1.2	22.0	2.6	2.5	0.29	-0.71
12.C	8.0	1.5	21.0	2.6	3.0	0.38	-0.63
3.5	2.5	1.4	7.0	2.8	0.5	0.20	0.80
5.5	4.7	1.2	13.0	2.8	1.5	0.32	0.68
15.0	6.0	2.5	6.0	1.0	0.0		1.00
21.5	9.0	2.4	37.0	4.1	1.5	0.17	-0.83
4.0	2.7	1.5	9.0	3.3	1.5	0.56	-0.44
7.5	5.0	1.5	5.0	1.0	0.0	0.00	-1.00
3.3	2.5	1.3	8.0	3.2	1.3	0.52	-0.48
2.2	1.5	1.5	5.0	3.3	0.6	0.40	-0.60
7.0	3.0	2.3	13.0	4.3	1.5	0.50	-0.50
9.0	5.4	1.7	16.0	3.0	2.0	0.3/	-0.53
Harmonic mean		1.56		2.30		0.32	-0.65

v (cm)	Z=D (cm)	Y/Z	Y+tail=Yt	Yt/Z	S	S/D	(S-D)/D
4.0	2.6	1.5	10.0	3.8	1.0	0.38	-0.62
2.6	2.5	1.0	9.5	3.9	0.5	0.20	-0.80
2.3	1.2	1.9	2.3	1.9	0.0	0.00	-1.00
1.3	0.6	2.2	1.3	2.2	0.0	0.00	-1.00
4.0	4.0	1.0	15.0	3.8	2.0	0.50	-0.50
35.0	28.0	1.3	35.0		0.0	0.00	-1.00
5.5	6.0	0.9	35.0	5.8	2.0	0.33	-0.67
2.0	2.8	0.7	2.0	0.7	0.0	0.00	-1.00
1.0	0.4	2.5	1.0	2.5	0.0	0.00	-1.00
2.0	0.7	2.9	2.0	2.9	0.0	0.00	-1.00
7.9	1.2	6.6	1.6	1.3	1.1	0.92	-0.08
1.6	1.1	1.5	1.6	1.5	0.0	0.00	-1.00
7.0	5.5	1.3	23.0	5.1	3.0	0.55	-0.45
11.5	6.5	1.8	31.0	4.8	2.0	0.31	-0.69
13.0	3.5	3.7	13.0	3.7	0.0	0.00	-1.00
21.0	9.0	2.3	21.0	2.2	0.0	0.00	1.00
5.2	3.0	1.7	15.0	5.0	1.4	0.47	-0.53
21.0	9.0	2.3	21.0	2.3	0.0	0.00	-1.00
1.3	1.3	1.0	1.3	1.0	0.0	-	-1.00
0.7	0.6	1.2	0.7	1.2	0.0	-	-1.00
5.2	3.8	1.4	5.2	1.4	0.0	-	-1.00
Harmonic mean		1.49		1.97		0.45	-0.57

A2.2 - Axial ratio of clasts and clasts+tail (surface nearly parallel to YZ) with their harmonic means (method of Lisle 1979). S, D and S/D were obtained by the method of Borradaile (1981). The negative values are the calculated amount of shortening of the matrix.

(continued)

Faci YZ (Outcrop 10B)

Y(cm)	Z-D (cm)	Y/Z	Y+tail/Yt	Yt/Z	S	S/D	(S-D)/D
16.5	12.0	1.4	70.0	5.8	0.0		-1.00
14.7	6.5	2.3	40.0	6.2	1.5	0.23	-0.77
2.7	2.7	1.0	2.7	1.0	0.0	0.00	1.00
5.5	5.2	1.1	18.0	3.5	1.5	0.29	0.71
1f;b	14.7	1.1	52.0	3.5	5.5	0.37	-0.63
3.0	2.5	1.2	11.5	4.6	1.2		0.52
Harmonic	mean	1.22		2.83		0.29	0.73

Face YZ (Outcrop 405)

Y (cm)	Z=D (cm)	Y/Z	Y ^{tail} -Yt	Yt/Z	S	S/D	(S-D)/D
9.5	9.5	1.0	50.0	5.3	5.5	0.58	-0.42
5.5	1.6	3.4	5.5	3.4	0.0	0.00	-1.00
5.5	3.5	1.6	5.5	1.6	0.0	0.00	-1.00
9.5	3.8	2.5	42.0	11.1	0.5	0.13	-0.87
5,5	2.0	2.8	12.0	6.0	0.5	0.25	-0.75
4.2	4.6	0.9	18.0	3.9	3.0	0.65	-0.35
3.5	1.1	3.2	10.0	9.1	0.1	0.09	-0.91
11.5	5.0	2.3	38.0	/6	1.5	0.30	-0.70
2.7	2.1	1.3	10.0	4.8	1.2	0.57	-0.43
2.0	1.7	1.2	14.0	8?	1.0	0.59	0.41
11.0	4.5	2,4	11.0	2.4	0.0	0.00	-1.00
17.0	10.0	1.7	54.C	5.4	3.0	0.30	0.70
4.0	1.2	3.3	11.0	9.?	0.3	0.25	0.75
18.0	17.5	1.0	80.0	4.6	1.4	0.08	-0.92
4.0	4.7	0.8	20.0	4.3	3.0	0.64	-0.36
5.5	3.7	1.5	18.0	4,9	1.0	0.77	-0.73
11.0	3.2	3.4	26.0	8.1	1.0	0.31	-0.69
8.5	1.5	5.7	8.5	5.7	0.0	0.00	-1.00
3.3	1.3	2.5	11.0	3.5	0.1	0.08	-0.92
10.0	10.0	1.0	46.0	4.6	5.0	0.50	-0.50
3.5	2.5	1.4	3,5	1.4	0.0	0.00	-1.00
14.5	9.0	1.6	42.0	4.7	1.5	0.17	-0.83
12.0	7.5	1.6	44.0	5.9	1.0	0.13	0.87
5.0	3.0	1.7	5.0	1.7	0.0	0.00	-1.00
Harmonic	mean	1.63		4.07		0.21	-0.67

A2.2 - Axial ratio of clasts and clasts+tail (surface nearly parallel to YZ) with their harmonic means (method of Lisle 1979). S, D and S/D were obtained by the method of Borradaile (1981). The negative values are the calculated amount of shortening of the matrix.

(Final).

Thin section on face XZ (Outcrop 33, road Simão Dias-Pi nhão)

X (mm)	Z (mm)	X/Z	X+tail-U-Xt	Xt/Z
7.0	4.0	1.8	19.0	4,8
10.0	4.0	2.5	18.0	4,5
14.0	6.0	2.3	21.0	3.5
14.0	5.0	2.8	25.0	5.0
20.0	7.0	2.9	35.0	5.0
15.0	10.0	1.5	30.0	3.0
9.0	4.0	2.3	19.0	4.8
7.0	3.0	2.3	14.0	4.7
12.0	5.0	2.4	20.0	4.0
7.0	3.0	2.3	17.0	5.7
Harmonic mean		2.3		4.4

Thin section on face YZ (outcrop 33)

Y (mm)	Z (mm)	Y/Z	Y+tail-Yt	Yt/Z
13.0	5.0	2.6	17.0	3.4
11.0	9.0	1.2	22.0	9.4
14.0	8.0	1.8	25.0	3.1
15.0	5.0	3.0	18.0	3.6
6.0	4.0	1.5	10.0	2.5
9.0	4.0	2.3	14.0	3.5
14.0	6.0	2.3	20.0	3.3
10.0	4.0	2.5	15.0	3.8
6.0	4.0	1.5	8.0	2.0
8.0	5.0	1.6	12.0	2.4
Harmonic mean		1.8		2.7

Thin section on face XZ (Outcrop 36, road Simão Dias Pi nhão)

X (mm)	Z (mm)	X/Z	X + tail-U-Xt	Xt/Z
10.0	7.0	1.4	24.0	3.4
11.0	8.0	1.4	31.0	3.9
19.0	11.0	1.7	32.0	2.9
21.0	7.0	3.0	45.0	6.4
8.0	8.0	1.0	35.0	4.4
8.0	6.0	1.3	24.0	4.0
9.0	5.0	1.8	24.0	4.8
8.0	8.0	1.0	21.0	2.6
5.0	6.0	0.8	16.0	2.7
9.0	4.0	2.3	19.0	4.5
Harmonic mean		1.4		3.8

- A2.3** - Length of clasts and clasts + tail, measured in thin sections cut parallel to XZ and YZ, in the Palestina diamictites and pebbly phyllites. Compare the harmonic mean of the ratios in the XZ and YZ planes. See text.

(Continued)

Thin section on face YZ (outcrop 36)

Y (mm)	Z (mm)	Y/Z	Ytail-Vt	Yt/Z
10.0	9.0	1.1	18.0	2.0
9.0	4.0	2.3	9.0	2.3
8.0	6.0	1.3	15.0	2.5
7.0	6.0	1.2	7.0	1.2
9.0	6.0	1.5	12.0	2.0
5.0	4.0	1.3	5.0	1.3
8.0	5.0	1.6	8.0	1.6
9.0	9.0	1.0	9.0	1.0
4.0	3.0	1.3	6.0	2.0
8.0	4.0	2.0	10.0	2.5
Harmonic mean		1.5		1.7

Thin sect on on face XZ (Outcrop 42, road S mao Dias-Pinhão)

X (mm)	Z (mm)	X/Z	Xtail- Xt	xt/z
22.0	10.0	2.2	36.0	3.6
20.0	8.0	2.5	30.0	3.8
12.0	7.0	1.7	29.0	4.1
12.0	7.0	1.7	23.0	3.3
10.0	4.0	2.5	22.0	5.5
8.0	4.0	2.0	21.0	5.3
13.0	5.0	2.6	20.0	4.0
4.0	2.0	2.0	13.0	6.5
11.0	6.0	1.8	21.0	3.5
9.0	4.0	2.3	19.0	4.8
Harmonic mean		2.1		4.4

Thin section on face YZ (outcrop 42)

Y (mm)	Z (mm)	Y/Z	Ytail-Vt	Yt/Z
13.0	8.0	1.6	17.0	2.1
9.0	4.0	2.3	20.0	5.0
15.0	18.0	0.8	32.0	1.8
7.0	6.0	1.2	14.0	2.3
M.O	6.0	1.8	22.0	3.7
8.0	5.0	1.6	12.0	2.4
9.0	4.0	2.3	14.0	3.5
13.0	13.0	1.0	20.0	1.5
40.0	20.0	2.0	55.0	2.3
13.0	10.0	1.3	22.0	2.2
Harmonic mean		1.4		2.5

A2.3 - Length of clasts and clasts + tail, measured in thin sections cut parallel to XZ and YZ, in the Palestina diamictites and pebbly phyllites. Compare the harmonic mean of the ratios in the XZ and YZ planes. See text.

(continued)

Thin section on face XZ (Outcrop 84. road Simão Dias Sao Domingos)

X (mm)	Z (mm)	X/Z	X+tail-Xt	xt/Z
10.0	9.0	1.2	37.0	3.3
4.0	4.0	1.0	20.0	5.0
7.0	7.0	1.0	32.0	4.6
4.0	3.0	1.3	16.0	5.3
5.0	6.0	0.8	18.0	3.0
6.0	4.0	1.5	18.0	4.5
5.0	4.0	1.3	15.0	3.8
7.0	3.0	2.3	15.0	5.0
5.0	3.0	1.7	15.0	5.0
3.0	4.0	0.8	20.0	5.0
Harmonic mean		1.1		4.5

Thin section on face YZ (outcrop 84)

Y (mm)	Z (mm)	Y/Z	Y+tail-Yt	Yt/Z
15.0	20.0	0.8	30.0	1.5
5.0	5.0	1.0	5.0	1.0
7.0	6.0	1.2	10.0	1.7
8.0	3.0	2.7	10.0	3.3
5.0	4.0	1.3	8.0	2.0
87.0	25.0	3.5	170.0	6.8
17.0	12.0	1.4	32.0	2.7
5.0	3.0	1.7	12.0	4.0
9.0	8.0	1.1	9.0	1.1
6.0	4.0	1.5	10.0	2.5
Harmonic mean		1.5		2.1

Thin section on face YZ (outcrop 42)

X (mm)	Z (mm)	X/Z	X+tail-Xt	Xt/Z
G.O	3.0	2.0	15.0	5.0
22.0	10.0	2.2	32.0	3.2
17.0	6.0	2.8	45.0	7.5
16.0	12.0	1.3	45.0	3.8
8.0	6.0	1.3	20.0	3.3
7.0	5.0	1.4	15.0	3.0
9.0	7.0	1.3	20.0	2.9
44.0	16.0	2.8	80.0	5.0
6.0	4.0	1.5	14.0	3.5
18.0	12.0	1.5	43.0	3.6
Harmonic mean		1.6		3.7

- A2.3 - Length of clasts and clasts + tail, measured in thin sections cut parallel to XZ and YZ, in the Palestina diamictites and pebbly phyllites. Compare the harmonic mean of the ratios in the XZ and YZ planes. See text. (continued)

Thin section on face YZ (outcrop 90)

Y (mm)	Z (mm)	Y/Z	Y+tail-Yt	Yt/Z
9.0	7.0	1.3	9.0	1.3
14.0	15.0	0.9	14.0	0.9
11.0	8.0	1.4	11.0	1.4
7.0	6.0	1.2	7.0	1.2
5.0	4.0	1.3	5.0	1.3
12.0	9.0	1.3	12.0	1.3
8.0	4.0	2.0	8.0	2.0
12.0	7.0	1.7	12.0	1.7
6.0	5.0	1.2	6.0	1.2
9.0	9.0	1.0	9.0	1.0
Harmonic mean		1.2		1.2

Thin section on face XZ (Outcrop 107, road Paripitanga- Maritá)

X (mm)	Z (mm)	X/Z	X+tail=Xt	Xt/Z
23.0	10.0	2.3	90.0	9.0
17.0	7.0	2.4	31.0	4.4
11.0	4.0	2.8	20.0	5.0
9.0	6.0	1.5	24.0	4.0
10.0	7.0	1.4	25.0	3.6
14.0	8.0	1.8	40.0	5.0
8.0	4.0	2.0	16.0	4.0
28.0	15.0	1.9	60.0	4.0
7.0	5.0	1.4	20.0	4.0
12.0	8.0	1.5	35.0	4.4
Harmonic mean		1.7		4.2

Thin section on face YZ (outcrop 107)

Y (mm)	Z (mm)	Y/Z	Y+tail=Yt	Yt/Z
9.0	7.0	1.3	9.0	1.3
14.0	15.0	0.9	14.0	0.9
11.0	8.0	1.4	11.0	1.4
7.0	6.0	1.2	7.0	1.2
5.0	4.0	1.3	5.0	1.3
12.0	9.0	1.3	12.0	1.3
8.0	4.0	2.0	8.0	2.0
12.0	7.0	1.7	12.0	1.7
6.0	5.0	1.2	6.0	1.2
9.0	9.0	1.0	9.0	1.0
Harmonic mean		1.2		1.2

- A2.3 - Length of clasts and clasts + tail, measured in thin sections cut parallel to XZ and YZ, in the Palestina diamictites and pebbly phyllites. Compare the harmonic mean of the ratios in the XZ and YZ planes. See text. (continued)

Thin section on face XZ (Outcrop 111, road Paripitinga-Maritá)

X (mm)	Z (mm)	X/Z	X+tail=Xt	Xt/Z
12.0	7.0	1.7	30.0	4.3
9.0	10.0	0.9	27.0	2.7
12.0	6.0	2.0	25.0	4.2
14.0	14.0	1.0	49.0	3.5
7.0	6.0	1.2	15.0	2.5
16.0	9.0	1.8	30.0	3.3
14.0	7.0	2.0	28.0	4.0
7.0	5.0	1.4	13.0	2.6
7.0	3.0	2.3	17.0	5.7
9.0	5.0	1.8	18.0	3.6
Harmonic mean		1.5		3.4

Thin section on face YZ (outcrop 111)

Y (mm)	Z (mm)	Y/Z	Y+tail=Yt	Yt/Z
16.0	15.0	1.1	25.0	1.7
12.0	9.0	1.3	18.0	2.0
11.0	7.0	1.6	20.0	2.9
13.0	11.0	1.2	22.0	2.0
6.0	6.0	1.0	6.0	1.0
9.0	6.0	1.5	12.0	2.0
3.0	8.0	1.0	17.0	2.1
10.0	8.0	1.3	17.0	2.1
16.0	15.0	1.1	25.0	1.7
7.0	4.0	1.8	12.0	3.0
Harmonic mean		1.3		2.0

Thin section on face XZ (Outcrop 140. road Panpranga-Arapiraca farm)

X (mm)	Z (mm)	X/Z	X+tail=Xt	Xt/Z
9.0	5.0	1.8	23.0	4.6
11.0	9.0	1.2	30.0	3.3
12.0	7.0	1.7	29.0	4.1
8.0	5.0	1.6	27.0	5.4
15.0	9.0	1.7	24.0	2.7
20.0	15.0	1.3	47.0	3.1
6.0	6.0	1.0	17.0	2.8
17.0	9.0	1.3	24.0	2.7
23.0	10.0	2.3	60.0	6.0
10.0	7.0	1.4	22.0	3.1
Harmonic mean		1.4		3.4

A2.3 - Length of clasts and clasts + tail, measured in thin sections **cut** parallel to XZ and YZ, in the Palestina diamictites and pebbly phyllites. Compare the harmonic mean of the ratios in the XZ and YZ planes. See text.

(continued)

Thin section on 'aco Y7 (outcrop 140)

V (mm)	Z (mm)	Y / Z	Y+tail-Yt	Yt/Z
10.0	8.0	1.3	10.0	1.3
7.0	4.0	1.8	7.0	1.8
8.0	6.0	1.3	12.0	2.0
8.0	6.0	1.3	10.0	1.7
6.0	6.0	1.0	9.0	1.5
11.0	7.0	1.6	11.0	1.6
9.0	12.0	0.8	25.0	2.1
10.0	7.0	1.4	10.0	1.4
7.0	5.0	1.4	7.0	1.4
4.0	2.7	1.5	5.1	1.9
Harmonic mean		1.3		1.6

Thin Section on face xz outcrop 142, road Piripiranga-Arapica farm

X (mm)	Z (mm)	X / Z	X+tail-Xt	Xt / Z
13.0	5.0	2.6	37.0	6.2
9.0	4.0	2.3	26.0	6.5
11.0	8.0	1.4	28.0	3.5
3.0	4.0	2.0	13.0	4.8
9.0	4.0	2.3	25.0	6.3
6.0	9.0	0.7	34.0	3.8
5.0	3.0	1.7	12.0	4.0
9.0	6.0	1.5	24.0	4.0
9.0	5.0	1.8	21.0	4.2
8.0	7.0	1.1	22.0	3.1
Harmonic mean		1.5		4.2

Thin Section on face xz outcrop 142

Y (mm)	Z (mm)	Y / Z	Y+tail=yt	Yt/Z
12.0	10.0	1.2	12.0	1.2
8.0	6.0	1.3	15.0	2.5
12.0	7.0	1.7	15.0	2.1
10.0	6.0	1.7	10.0	1.7
8.0	8.0	1.0	8.0	1.0
10.0	10.0	1.0	10.0	1.0
8.0	6.0	1.3	8.0	1.3
21.0	15.0	1.4	40.0	2.7
14.0	10.0	1.4	24.0	2.4
9.0	7.0	1.3	10.0	1.4
Harmonic mean		1.3		1.6

A2.3 - Length of clasts and clasts + tail, measured in thin sections cut parallel to xz and YZ, in the Palestina diamictites and pebbly phyllites. Compare the harmonic mean of the ratios in the XZ and YZ planes. See text. (continued)

Thin section on face XZ (Outcrop 185, SW of Podra Mole)

X (mm)	Z (mm)	X/Z	X+tail-Xt	Xt/Z
11.0	7.0	1.6	27.0	3.9
6.0	8.0	0.8	33.0	4.1
25.0	7.0	3.6	42.0	6.0
8.0	4.0	2.0	27.0	6.8
9.0	5.0	1.8	30.0	6.0
14.0	8.0	1.8	32.0	4.0
11.0	6.0	1.8	33.0	5.5
10.0	8.0	1.3	34.0	4.3
12.0	5.0	2.4	35.0	7.0
14.0	6.0	2.3	26.0	4.3
Harmonic mean		1.7		5.2

Thin section on face YZ (outcrop 186)

Y (mm)	Z (mm)	Y/Z	Y+tail-Yt	Yt/Z
20.0	16.0	1.3	35.0	2.2
19.0	15.0	1.3	30.0	2.0
20.0	8.0	2.5	27.0	3.4
23.0	13.0	1.8	40.0	3.1
13.0	14.0	0.9	22.0	1.6
15.0	9.0	1.7	27.0	3.0
20.0	10.0	2.0	30.0	3.0
14.0	9.0	1.6	25.0	2.8
15.0	8.0	1.5	30.0	3.8
10.0	10.0	1.0	20.0	2.0
Harmonic mean		1.5		2.6

Thin section on face XZ (Outcrop 188, SW of Podra Mole)

X (mm)	Z (mm)	X/Z	X+tail-Xt	Xt/Z
15.0	8.0	1.9	40.0	5.0
10.0	7.0	1.4	23.0	3.3
14.0	5.0	2.8	31.0	6.2
17.0	7.0	2.4	53.0	7.6
17.0	14.0	1.2	83.0	4.5
13.0	9.0	1.4	38.0	4.2
10.0	7.0	1.4	27.0	3.9
10.0	7.0	1.4	25.0	3.6
23.0	11.0	2.1	48.0	4.4
33.0	10.0	3.3	80.0	8.0
Harmonic mean		1.8		4.6

A2.3 - Length of clasts and clasts + tail, measured in thin sections cut parallel to XZ and YZ, in the Palestina diamictites and pebbly phyllites. Compare the harmonic mean of the ratios in the XZ and YZ planes. See text.

(continued)

Thin section on face YZ (outcrop188)

Y (mm)	Z (mm)	Y / Z	Y+tailYt	Yt.Z
10.0	5.0	2.0	15.0	3.0
15.0	7.0	2.1	30.0	4.3
7.0	4.C	1.8	13.0	3.3
15.0	7.0	2.1	21.0	3.0
13.0	10.0	1.3	27.0	2.7
10.0	7.0	1.4	30.0	4.3
10.0	6.0	1.7	21.0	3.5
18.0	9.0	2.0	36.0	4.0
13.0	11.0	1.2	40.0	3.6
13.0	3.0	4.3	22.0	7.3
Harmonic mean		1.7		3.7

Thin section on face XZ (Outcrop T8S, SW of Pedra Mole)

X (mm)	Z (mm)	X / Z	X-tailXt	Xt/Z
25.0	15.0	1.7	65.0	4.3
11.0	4.0	2.8	26.0	6.5
27.0	20.0	1.4	56.0	2.8
25.0	27.0	0.9	80.0	3.0
9.0	6.0	1.5	27.0	4.5
8.0	6.0	1.3	21.0	3.5
11.0	5.0	2.2	29.0	5.8
12.0	12.0	1.0	32.0	2.7
21.0	11.0	1.9	40.0	3.6
15.0	17.0	0.9	60.0	3.5
Harmonic mean		1.4		3.7

Thin section on face YZ (outcrop 192)

Y (mm)	Z (mm)	Y/Z	Y+tail-Yt	Yt/2
8.0	3.0	2.7	11.0	3.7
11.0	6.0	1.8	11.0	1.8
11.0	6.0	1.8	15.0	2.5
12.0	7.0	1.7	15.0	2.1
25.0	14.0	1.8	37.0	2.6
25.0	15.0	1.7	40.0	2.7
11.0	9.0	1.2	20.0	2.2
11.0	5.0	2.2	17.0	?.. 4
18.0	13.0	1.4	23.0	2.2
7.0	6.0	1.2	13.0	2.2
Harmonic mean		1.6		2.3

- A2.3 • Length of clasts and clasts + tail, measured in thin sections cut parallel to XZ and YZ, in the Palestina diamictites and pebbly phyllites. Compare the harmonic mean of the ratios in the XZ and YZ planes. See text. (continued)

Thin section on face XZ (Outcrop 193, SW of Pedra Mole)

X (mm)	Z (mm)	X/Z	X+tailXt	xt/Z
14.0	9.0	1.6	40.0	4.4
16.0	12.0	1.3	52.0	4.3
9.0	6.0	1.5	30.0	5.0
16.0	7.0	2.3	42.0	6.0
8.0	5.0	1.6	21.0	4.2
10.0	3.0	3.3	23.0	7.7
10.0	6.0	1.7	25.0	4.2
12.0	5.0	2.4	25.0	fc.G
7.0	6.0	1.2	23.0	3.8
10.0	6.0	1.7	33.0	5.5
Harmonic mean		1.6		4.8

Thin section on face YZ (outcrop 193)

Y (mm)	Z (mm)	Y/Z	Y+tailYt	Yt/Z
10.0	10.0	1.0	21.0	2.1
7.0	7.0	1.0	16.0	2.3
10.0	6.0	1.7	19.0	3.2
14.0	7.0	2.0	20.0	2.9
18.0	7.0	2.6	18.0	2.6
8.0	5.0	1.6	16.0	3.2
7.0	8.0	0.9	16.0	2.0
9.0	10.0	0.9	21.0	2.1
15.0	6.0	2.5	23.0	&§
12.0	8.0	1.5	23.0	2.9
Harmonic mean		1.5		2.7

Thin section on face XZ (Outcrop 239 south of Pariplranqa)

X (mm)	Z (mm)	X/Z	X+tailXt	Xt/Z
8.0	8.0	1.0	22.0	2.8
11.0	5.0	2.2	27.0	5.4
10.0	8.0	1.3	33.0	4.1
13.0	16.0	0.8	70.0	4.4
12.0	4.0	3.0	25.0	6.3
18.0	13.0	1.4	60.0	4.6
15.0	7.0	2.1	32.0	4.6
25.0	18.0	1.4	60.0	3.3
12.Cl	9.0	1.3	25.0	2.8
11.0	6.0	1.8	32.0	5.3
Harmonic mean		1.5		4.1

- A2.3 - Length of clasts and clasts + tail, measured in thin sections cut parallel to XZ and YZ, in the Palestina diamictites and pebbly phyllites. Compare the harmonic mean of the ratios in the XZ and YZ planes. See text. (continued)

Thin section on face YZ (outcrop 239)

Y (mm)	Z (mm)	Y/Z	Y+tail=Yt	Yt/Z
8.0	8.0	1.0	11.0	1.4
15.0	3.0	1.2	25.0	1.9
12.0	7.0	1.7	20.0	2.9
8.0	6.0	1.3	13.0	2.2
16.0	13.0	1.3	23.0	1.9
16.0	13.0	1.2	23.0	1.8
50.0	35.0	1.4	70.0	2.0
13.0	7.0	1.9	20.0	2.9
100.0	50.0	2.0	130.0	3.6
80.0	45.0	1.8	140.0	3.1
Harmonic mean		1.5		2.3

Thin section on face XZ (Outcrop 246, WSW of Paripiranga)

X (mm)	Z (mm)	X/Z	X+tail=Xt	Xt/Z
6.0	4.0	1.5	22.0	5.5
8.0	5.0	1.6	18.0	3.6
15.0	5.0	3.0	25.0	5.0
7.0	7.0	1.0	28.0	4.0
18.0	13.0	1.4	50.0	3.8
12.0	13.0	0.9	48.0	3.7
19.0	10.0	1.9	40.0	4.0
15.0	9.0	1.7	31.0	3.4
11.0	8.0	1.4	21.0	2.6
14.0	10.0	1.4	33.0	3.3
Harmonic mean		1.4		3.5

Thin section on face YZ (outcrop 246)

Y (mm)	Z (mm)	Y/Z	Y+tail=Yt	Yt/Z
10.0	6.0	1.7	15.0	2.5
22.0	13.0	1.7	30.0	2.3
13.0	11.0	1.2	23.0	2.1
12.0	8.0	1.5	25.0	3.1
8.0	7.0	1.1	20.0	2.9
10.0	7.0	1.4	16.0	2.3
11.0	7.0	1.6	15.0	2.1
13.0	8.0	1.6	21.0	2.6
9.0	7.0	1.3	18.0	2.6
12.0	6.0	2.0	20.0	3.3
Harmonic mean		1.4		2.5

- A2.3 - Length of clasts and clasts + tail, measured in thin sections cut parallel to XZ and YZ, in the Palestina diamictites and pebbly phyllites. Compare the harmonic mean of the ratios in the XZ and YZ planes. See text. (continued)

Thin section on face XZ (Outcrop 246, SW of Paripiranga)

X (mm)	Z (mm)	X/Z	X+tail-Xt	Xt/Z
7.0	5.0	1.4	19.0	3.8
4.0	2.0	2.0	13.0	6.5
5.0	3.0	1.7	22.0	7.3
4.0	3.0	1.3	13.0	4.3
8.0	6.0	1.3	25.0	4.2
12.0	8.0	1.5	33.0	4.1
25.0	15.0	1.7	90.0	R.O
8.0	4.0	2.0	27.0	6.8
5.0	4.0	1.3	20.0	5.0
7.0	4.0	1.8	17.0	4.3
Harmonic mean		1.5		5.1

Thin section on face YZ (outcrop 249)

Y (mm)	Z (mm)	Y/Z	Y-tail-Yt	Yt/Z
6.0	3.0	2.0	9.0	3.0
7.0	5.0	1.4	11.0	2.2
10.0	6.0	1.7	15.0	2.5
8.0	6.0	1.3	11.0	1.8
10.0	5.0	2.0	14.0	2.8
9.0	7.0	1.3	12.0	1.7
8.0	5.0	1.6	13.0	2.6
8.0	6.0	1.3	10.0	1.7
10.0	7.0	1.4	10.0	1.4
8.0	5.0	1.6	15.0	3.0
Harmonic mean		1.5		2.0

Thin section on face XZ (Outcrop 341. NW of Macambira)

X (mm)	Z (mm)	X/Z	X+tail-Xt	Xt/Z
13.0	8.0	1.6	32.0	4.0
12.0	8.0	1.5	35.0	4.4
12.0	6.0	2.0	30.0	5.0
20.0	5.0	4.0	40.0	8.0
13.0	7.0	1.9	32.0	4.6
8.0	5.0	1.6	22.0	4.4
20.0	10.0	2.0	42.0	4.2
10.0	7.0	1.4	26.0	3.7
20.0	15.0	1.3	46.0	3.1
15.0	10.0	1.6	47.0	4.7
Harmonic mean		1.7		4.2

A2.3 - Length of clasts and clasts + tail, measured in thin sections cut parallel to XZ and YZ, in the Palestina diamictites and pebbly phyllites. Compare the harmonic mean of the ratios in the XZ and YZ planes. See text. (continued)

Thin section on face YZ (outcrop 341)

Y (mm)	Z (mm)	Y/Z	Y+tail-Yt	Yt/Z
1.0	6.0	1.8	17.0	2.8
12.0	6.0	2.0	22.0	3.7
20.0	10.0	2.0	33.0	3.3
10.0	14.0	0.7	25.0	1.8
9.0	8.0	1.1	15.0	1.9
15.0	20.0	0.8	43.0	2.2
50.0	42.0	1.2	130.0	3.1
60.0	40.0	1.5	136.0	3.4
28.0	50.0	0.6	50.0	1.0
9.0	8.0	1.1	22.0	2.8
Harmonic mean		0.9		2.0

Thin section on face XZ (Outcrop 406. NNE of Oihos D' água)

X (mm)	Z (mm)	x/z	X+tail-Xt	Xt/Z
9.0	9.0	1.0	30.0	3.3
6.0	4.0	1.5	17.0	4.3
8.0	6.0	1.3	17.0	2.8
8.0	4.0	2.0	30.0	7.5
9.0	3.0	3.0	23.0	7.7
15.0	10.0	1.5	37.0	3.7
9.0	6.0	1.5	38.0	5.3
9.0	5.0	1.8	33.0	6.6
14.0	9.0	1.6	40.0	4.4
20.0	11.0	1.8	50.0	4.5
Harmonic mean		1.7		4.8

Thin section on face YZ (outcrop 405)

Y (mm)	Z (mm)	Y/Z	X+tail=xt	Yt/Z
8.0	5.0	1.6	12.0	2.4
10.0	5.0	2.0	13.0	2.6
7.0	5.0	1.4	13.0	2.6
14.0	10.0	1.4	23.0	2.3
15.0	9.0	1.7	27.0	3.0
13.0	8.0	1.6	20.0	2.5
10.0	8.0	1.3	14.0	1.8
8.0	5.0	1.6	10.0	2.0
12.0	10.0	1.2	20.0	2.0
12.0	9.0	1.3	18.0	2.0
Harmonic mean		1.4		2.2

- A2.3** - Length of clasts and clasts + tail, measured in thin sections cut parallel to XZ and YZ, in the Palestina diamictites and pebbly phyllites. Compare the harmonic mean of the ratios in the XZ and YZ planes. See text.

(continued)

Thin section on face XZ (Outcrop 997, road Road Simão Dias-Piã)

X (mm)	Z (mm)	x/z	X+ta:Wt	XtZ
16.0	20.0	0.8	70.0	3.5
11.0	7.0	1.6	34.0	4.9
11.0	8.0	1.4	38.0	4.8
15.0	9.0	1.7	37.0	4.1
12.0	8.0	1.5	33.0	4.1
12.0	6.0	2.0	35.0	5.8
7.0	6.0	1.2	26.0	4.3
9.0	6.0	1.5	23.0	3.8
9.0	5.0	1.8	24.0	4.8
8.0	5.0	1.6	26.0	5.2
Harmonic mean		1.6		4.6

Thin section on face YZ

Y (mm)	Z (mm)	Y/Z	Y+ta:UYt	YtZ
8.0	5.0	1.6	8.0	1.6
8.0	6.0	1.3	10.0	1.7
20.0	15.0	1.3	25.0	1.7
17.0	12.0	1.4	30.0	2.5
15.0	12.0	1.3	26.0	2.2
17.0	10.0	1.7	26.0	2.6
32.0	30.0	1.1	70.0	2.3
10.0	7.0	1.4	20.0	2.0
8.0	7.0	1.1	8.0	1.1
9.0	14.0	0.6	9.0	0.6
Harmonic mean		1.2		1.5

A2.3 - Length of clasts and clasts + tail, measured in thin sections cut parallel to XZ and YZ, in the Palestina diamictites and pebbly phyllites. Compare the harmonic mean of the ratios in the XZ and YZ planes. See text.

(final)

GRAVITY			MAGNETOMETRY		
STATION	OBSERVED	CALCULATED	STATION	OBSERVED	CALCULATED
(km)	(mGals)	(mGals)	!km)	(nT)	
0.0	-3.00	-2.04	0.0	0.0	16.0
09	1.80	-1.47	3.0	00	22.0
1.8	-1.60	-0.86	6.0	25.0	290
2.6	070	-0.21	90	30.0	38.0
3.5	0.00	0.53	12.0	84.0	490
4.6	030	1.34	150	75.0	-100.0
5.2	1.00	2.19	1B 0	25.0	11S.0
6.0	1.70	3.00	21 0	-75.0	-62.0
7.0	350	3.95	24.0	-150.0	1230
7.3	500	468	27.0	-187.0	-163.0
8.7	6.20	5.50	30.0	-200.0	-192.0
9.6	7.10	6.42	33.0	-186.0	-201.0
10.4	9.10	748	33.0	-150.0	-121.0
11.3	10.30	9.53	39 0	-115.0	104.0
122	! J SO	11.01	42 0	-80.0	-880
13.0	12.40	12.03	43 0	-74.0	74 0
14.C	13.60	1310	-	-	-
14.8	14.20	1383			
15.7	14.80	14.49			
16.5	15.60	14.84			
17.4	1600	15.35			
18.3	16.70	15.87			
19.1	1710	15.31			
20.0	1G20	16.74			
20.9	17.00	16.98			
?1.8	6.90	16.85			
22.6	16.80	16.97			
235	1730	17.17			
24.4	17.80	17.36			
252	17.50	17.53			
261	16.90	17.82			
27.0	16.40	16.00			
27.8	16.20	15.28			
28.7	15.60	1481			
29.5	15.20	14.88			
30.5	13.70	14.95			
31.3	13.50	14.83			
32.2	13.40	14.58			
33.1	13.10	14.31			
33.9	13.60	14.18			
34.8	14.50	14.72			
35.7	15.10	14.89			
-	-	-			

A3.1 - Observed and calculated gravity and aeromagnetic data along the XX' section line.

G RAVI- Y			M A G I M E T O M E T R Y		
STATION	OBSERVED	CALCULATED	STATION	OBSERVED	CALCULATED
(km)	(mGals)	(mGals)	(km)	(nT)	(nT)
0.0	19.40	17.29	0.0		
1.0	15.CO	16.26	1.5	12.0	
2.0	18.30	15.21	3.0	25.0	-
3.0	17.10	14.11	4.5	50.0	-
4.0	15.50	12.91	5.5	-75.0	-
5.0	13.50	11.33	6.4	-75.0	-
6.0	11.60	9.12	7.5	60.0	-55.0
7.0	10.10	8.42	8.4	-76.0	-55.0
8.0	8.20	7.84	9.5	100.0	-90.0
S.O	6.90	8.32	10.0	-100.0	-96.0
10.0	7.80	8.90	10.6	-126.0	-103.0
11.0	8.80	8.65	13.0	-127.0	-114.0
12.0	8.10	8.11	14.5	-124.0	-96.0
13.0	7.60	7.37	15.4	-100.0	-80.0
14.0	6.90	6.44	16.0	-125.0	-80.0
15.0	6.20	5.26	16.5	-150.0	-103.0
16.0	4.80	3.55	17.0	-150.0	-150.0
17.0	1.70	1.77	13.2	-175.0	-158.0
18.0	0.60	0.40	19.0	-200.0	-166.0
15.0	-0.10	-0.80	20.0	190.0	-174.0
26.6	-1.30	-1.86	21.0	-200.0	-200.0
21.0	-2.00	-2.73	22.5	215.0	-198.0
22.0	-2.60	3.10	23.0	200.0	-192.0
23.0	-3.50	-3.06	24.0	-195.0	-183.0
24.0	5.00	3.49	25.0	-187.0	-176.0
25.0	-5.30	-4.06	25.5	185.0	-175.0
26.0	-7.70	-4.71	26.0	185.0	-173.0
27.0	-5.60	-5.37	27.0	-180.0	168.0
28.0	-6.50	5.54	28.2	-180.0	164.0
23.0	-6.60	5.70	29.3	-180.0	-160.0
30.0	-7.70	6.20	30.0	-175.0	-156.0
31.0	-9.20	7.20	31.5	151.0	-140.0
32.0	-11.90	-9.10	33.0	150.0	150.0
33.0	12.80	-11.93	34.2	-150.0	-162.0
34.0	-13.90	-13.79	34.6	-150.0	-165.0
35.0	-15.10	-15.21	36.5	-175.0	-185.0
36.0	16.40	16.55	37.7	200.0	-213.0
37.0	-17.70	-17.37	39.0	226.0	265.0
38.0	-18.60	-18.21	42.0	-200.0	-172.0
39.0	-15.50	18.99	46.5	-100.0	-112.0
40.0	20.20	-19.82	47.0	88.0	-104.0
41.0	20.30	-20.25	50.0	-76.0	-90.0
42.0	20.00	-20.40	-	-	-
43.0	-20.30	20.31			
44.0	-20.30	-20.06			
45.0	19.10	-19.69			
46.0	-18.00	19.28			
47.0	-17.10	18.86			
48.0	15.60	-18.47			
49.0	-15.00	-18.13			
50.0	-14.70	17.86			

A3.2 - Observed and calculated gravity and aeromagnetic data along the YY' section line.

G R A V I T Y			MAGNETOMETRY		
STATION	OBSERVED	CALCULATED	STATION	OBSERVED	CALCULATED
(km)	(mGals)	(mGals)	(km)	(nT)	(nT)
0.0	3.90	0.41	-2.0	-30.0	-100.0
2.0	2.50	1.12	-1.3	-75.0	-
4.0	2.40	2.02	-0.8	-100.0	-126.0
6.0	0.80	0.90	-0.2	-125.0	-130.0
8.0	-2.20	-2.07	0.6	-125.0	-116.0
10.0	7.80	-5.10	1.0	-100.0	-110.0
12.0	-9.00	-4.00	2.0	-100.0	-88.0
14.0	-7.00	-7.00	3.0	-125.0	-84.0
16.0	-11.40	-8.40	4.0	-125.0	-114.0
18.0	-9.50	-9.10	5.0	-208.0	-215.0
20.0	-10.30	-10.20	5.5	-300.0	-254.0
22.0	-12.10	-11.00	6.0	-300.0	-290.0
24.0	-12.00	-11.90	6.3	-275.0	-300.0
26.0	-15.10	-12.70	6.7	-300.0	-340.0
28.0	-14.90	-14.20	7.0	-325.0	-366.0
30.0	-16.70	-15.60	7.5	-325.0	-364.0
32.0	-17.90	-16.20	7.7	-300.0	-318.0
34.0	-18.00	-16.00	8.3	-200.0	-200.0
36.0	-15.70	-16.09	9.0	-150.0	-144.0
38.0	-14.20	-15.86	10.0	-125.0	-98.0
40.0	-15.21	-15.38	10.8	-125.0	94.0
42.0	-12.39	-14.84	11.5	-125.0	-110.0
44.0	-13.43	-14.37	12.3	-150.0	-134.0
46.0	-12.68	-14.01	13.3	-200.0	-188.0
48.0	-13.06	-13.73	14.0	-225.0	-240.0
50.0	-13.90	-13.51	14.8	-200.0	-183.0
52.0	-13.00	-13.32	15.5	-175.0	-150.0
54.0	-13.13	-13.17	16.8	-150.0	-120.0
56.0	-12.69	-13.03	17.7	-135.0	-104.0
58.0	-11.84	-12.89	19.7	-95.0	-85.0
60.0	-14.23	-12.76	22.7	-50.0	-73.0
62.0	-11.47	-12.59	23.0	70.0	-72.0
64.0	-10.03	-12.36	25.0	-65.0	-65.0
66.0	-9.96	-12.02	-	-	-
68.0	-10.50	-11.37			
70.0	-10.29	-9.66			
72.0	-10.92	-9.07			
74.0	-12.60	-10.47			
76.0	-10.35	-11.18			
78.0	-8.72	-11.24			
80.0	-9.01	-11.41			
82.0	-10.21	-11.67			
84.0	-11.16	-12.08			
86.0	-12.79	-12.79			
88.0	-14.78	-13.80			
90.0	-15.67	-15.07			
92.0	-16.82	-16.78			
94.0	-19.02	-19.96			
96.0	-25.70	-23.50			
98.0	-28.00	-28.00			
100.0	-27.40	-29.00			
102.0	-26.30	-27.30			
104.0	-29.00	-26.30			

A3.3 -
gravity and
the "ZZ" se
256

Observed and calculated
aeromagnetic data along
ction line.